LOSS OF BASIGIN EXPRESSION IN THE UTERUS REDUCES FERTILITY IN FEMALE MICE

BY

KAILIANG LI

DISSERTATION

Submitted in partial fulfillment of the requirements
for the degree of Doctor of Philosophy in Animal Sciences
in the Graduate College of the
University of Illinois at Urbana-Champaign, 2020

Urbana, Illinois

Doctoral Committee:

Professor Romana Nowak, Chair and Director of Research
Professor Jodi Flaws
Professor David Miller
Assistant Professor Matthew Dean
Research Associate Professor Quanxi Li

ABSTRACT

Basigin (BSG), a member of the immunoglobulin superfamily, is a transmembrane glycoprotein expressed in many cell types. It is involved in neurological processes, lymphocyte migration, angiogenesis, tissue remodeling and lactate transport. Our data show that *Bsg* is expressed in the reproductive tract and is important for fertility in both males and females. I hypothesized that loss of *Bsg* expression in the uterus reduces fertility in female mice by altering implantation, decidualization, lactate transporters and angiogenesis. In mice, global ablation of *Bsg* is embryonic lethal, which complicates the studies on the role of BSG in reproduction. To overcome the embryonic lethality, we generated a progesterone receptor (PR)-Cre *Bsg* conditional knockout (cKO) mouse model and used this animal model to test this hypothesis. The aims of the present study were 1) to validate the *Bsg* cKO animal model and investigate the fertility phenotype associated with this animal model; 2) to investigate whether BSG is required for luminal epithelial cell and basement membrane integrity at the time of implantation; 3) to examine whether BSG regulates decidualization process *in vivo* and *in vitro*; and 4) to investigate whether loss of BSG affects angiogenesis and lactate transport.

Successful deletion of uterine *Bsg* was confirmed by quantitative real-time PCR (qRT-PCR), immunohistochemistry (IHC) and immunofluorescence (IF) staining. qRT-PCR indicated much lower *Bsg* mRNA levels in the cKO uteri compared to the controls. BSG was expressed in the luminal epithelial and stromal cells in the control mouse uteri. In the cKO mouse uteri, *Bsg* expression was lost in these PR positive cells, and only presented in PR negative cells such as immune cells and endothelial cells. BSG expression in the kidney was not affected, indicating it was PR-positive cell specific. Breeding study results showed that the cKO females had significantly reduced fertility about 40% compared to the controls. They had much smaller litter

size and litter frequency. The fertility of the cKO mice decreased more severely as they aged compared to the controls. Ovulation, progesterone production, fertilization and early embryo development were not affected in the cKO mice, suggesting that dysfunction occurred primarily in the uterus.

Day 5 pregnant uteri were collected to analyze implantation. The results showed that about 70% cKO mice did not show signs of implantation. In these animals the luminal epithelial cells still showed E-cadherin and cytokeratin at the site of implantation, indicating an intact luminal epithelial cell layer. In contrast, E-cadherin and cytokeratin in the control uteri were lost at the site of implantation, and only presented at the regions of luminal epithelium far from the embryo. The luminal epithelium basement membrane in the cKO mice was intact, not disrupted as in the controls. Many embryos in the cKO mice were restrained in a continuous layer of luminal epithelium, not able to break down the epithelium and penetrate the basement membrane.

To investigate whether BSG regulates decidualization, an artificially induced decidualization experiment was performed. I found that the cKO mice had reduced response to the artificial stimulus compared to a robust response in the controls. The decidua size was also significantly smaller in the cKO mice. qRT-PCR results showed that decidual genes *Cebpβ* and *Bmp2* were significantly downregulated in the cKO decidua. IHC results showed that CEBPβ and HAND2 protein expression were lower in the induced decidua and day 5 pregnant uteri in the cKO mice. Mouse endometrial stromal cell (MESC) culture experiments showed there was no difference in cell proliferation, but qRT-PCR results showed that *Prl8a2*, *Cebpβ*, *Bmp2* and *Hand2* were significantly downregulated in the cKO MESCs. These results suggest that BSG is required for proper decidualization *in vivo* and *in vitro*.

BSG is involved in angiogenesis. To test whether loss of BSG leads to abnormal angiogenesis, day 6 pregnant uteri were stained with the angiogenic marker CD31. There was significantly lower abundance of CD31 in the cKO mouse uteri compared to the controls. BSG is a chaperone protein for the lactate transporter MCT1/4. The abundance and localization of MCT1 were altered in the cKO mouse uteri *in vivo*. A lactate assay of medium from MESCs collected from both genotypes showed that the cKO MESCs secreted less lactate than the controls. These data indicate that loss of BSG leads to reduction in angiogenesis and lactate transport. Collectively, data in this dissertation suggest that uterine expression of BSG is required for proper implantation, decidualization, angiogenesis and lactate transport and loss of BSG results in severe subfertility in female mice.

ACKNOWLEDGEMENTS

I would never have been able to complete my dissertation without the generous help, support, guidance and encouragement from many wonderful people.

First I would like to express my sincere thanks and appreciation to my research advisor, Dr. Romana Nowak, for believing in me and giving me endless care, support and encouragement. Dr. Nowak took me in when I was in a bad situation and provided me with a friendly atmosphere to learn science and conduct research. She has always been patient with me, especially with my English and writing. She encouraged me to teach lectures and discussions, which not only prepared me to become a better speaker, but also explored my passion for teaching. This dissertation would never have been possible without her timely feedback, generous support and insightful mentorship.

My appreciations also go to my committee members, Dr. Jodi Flaws, Dr. David Miller, Dr. Quanxi Li and Dr. Matt Dean for their support and guidance. I am grateful for all the meetings we had, the questions you asked, the suggestions and advice you gave towards my project. I am grateful for the new ideas and inspirations.

I wish to thank many collaborators and colleagues who have given me much technical support and help. Dr. Arti Kannan improved my IHC and IF techniques. Ms. Karen Doty was very generous to let me use her embedding center and answer so many histology questions from me. Dr. Brent Bany helped to modify my artificial decidualization experiment protocol, with which I struggled for a long time. I would also like to acknowledge the IGB Core and the Functional Genomic Center for their fantastic equipment and resources.

I am also very thankful to all the past and present members of the Nowak laboratory. There have been so many times that we work late together and help each other's experiment. You all helped to critic my presentations and writings, troubleshoot when experiments failed, encourage

me when I was feeling low. I will always remember the laughter we shared and the cherish the good times we spend together during this journey.

Finally yet importantly, I would like to thank my family members: my wife, my parents, and my late grandfather for their love, understanding, support and faith in me.

Table of Contents

CHAPTER ONE Introduction and Rationale 1

References 5

CHAPTER TWO Literature Review 6

A. Basigin 6
B. Implantation 23
Figures 38
References 42

CHAPTER THREE Basigin Conditional Knockout Mouse Model and Fertility Phenotypes 66

Abstract 66
Introduction 67
Material and Methods 69
Results 75
Discussion 79
Tables and Figures 85
References 95

CHAPTER FOUR Basigin Expression in the Uterus is Required for Proper Implantation and Decidualization *in vivo* 99

Abstract 99
Introduction 100
Material and Methods 103
Results 109
Discussion 115
Tables and Figures 123
References 142

CHAPTER FIVE Loss of Basigin in the Mouse Endometrial Stromal Cells Leads to Impaired Decidualization and Lactate Transport *in vitro* 150

Abstract 150
Introduction 151
Material and Methods 153
Results 158
Discussion 162
Table and Figures 167
References 173

CHAPTER SIX Summary and Future Directions 178

Summary 178
Future Directions 184
Figure 187

Appendix 188

Acronyms and Abbreviations 188
Supplementary Figures 191
Antibody List 197
Genes and Primer Sequences 198
Protocols 199

CHAPTER ONE

Introduction and Rationale

Infertility is one of the most common reproductive health diseases in humans and affects about 10-15% of reproductive aged couples worldwide (Ramathal et al. 2010). Only 50-60% of all conceptions advance beyond 20 weeks of gestation and implantation failure is the major cause of early pregnancy loss, reaching about 75% (Norwitz, Schust, and Fisher 2001). Assisted reproductive technologies (ART) have helped millions of couples with fertility issues (Sharkey and Smith 2003). Despite the significant developments in culture medium and embryo quality, the success rate of ART remains very low mainly due to implantation failure (H. Wang et al. 2013). Therefore, it is imperative to gain a comprehensive understanding of the mechanism underlying implantation in order to address this global clinical issue. Many studies have identified molecules and proteins that are critical during embryo implantation, but the mechanisms regulating implantation are not fully understood. Thus, it is important to further investigate this process to advance the field of reproduction and fertility.

Basigin (BSG), a member of the immunoglobulin superfamily encoded by *Bsg* gene, has been identified as one of the key molecule regulating early pregnancy by our laboratory and others (L. Chen et al. 2007; T Igakura et al. 1998). BSG is a highly glycosylated transmembrane protein expressed in many cell and tissue types including the reproductive organs in both human and mice (K. Li and Nowak 2019). In mice, BSG is expressed in the luminal and glandular epithelium on day 1 and 2 of pregnancy, and starting on day 3 and 4, its expression appears in the stromal cells. After implantation, BSG is expressed in the secondary decidual zone on day 5, then in the deep undifferentiated stromal zone (L. Chen, Belton, and Nowak 2009). Previous studies using human

cell lines have suggested BSG plays a role in implantation and decidualization and *Bsg* null females are profoundly infertile (T Igakura et al. 1998). However, global deletion of *Bsg* in mice results in high embryonic lethality, making it impractical as an animal model to study *Bsg* (Muramatsu and Miyauchi 2003). Thus, we generated a uterine tissue *Bsg* conditional knockout (cKO) mouse model to help us investigate its role in early pregnancy. **My central hypothesis is that cKO of *Bsg* in the uterus reduces fertility in female mice. The overall goal of this project is to elucidate the roles of BSG in implantation and early pregnancy.** To complete my dissertation work and test this hypothesis, I completed the following specific aims:

Specific Aim 1: Validating the uterine specific *Bsg* cKO animal model and investigating the fertility phenotype in the cKO animals.

To complete this aim, I crossed our *Bsg* floxed mice with a progesterone receptor (PR)-Cre mouse line to generate the cKO mice and their littermate controls. The mice were euthanized on day 1, day 4, and day 6 of gestation for tissue collection. Tissue samples were subjected to immunohistochemistry (IHC) and immunofluorescence (IF) staining for BSG and quantitative real-time PCR (qRT-PCR) to confirm successful deletion of BSG in the uterus. Then, a six-month fertility study was carried out to determine whether the cKO females experienced subfertility or infertility. The timing of pregnancy loss was investigated by euthanizing mice at different gestational stages. The location of pregnancy issues was limited to the uterus after assessing ovulation, fertilization, ovarian hormone levels and embryo development. These data are presented in Chapter 3.

Specific Aim 2: Investigating luminal epithelial cell status and basement membrane integrity in the *Bsg* cKO females.

To complete this aim, mice of both genotypes were euthanized on day 5 of pregnancy at different times. Uterine tissues were collected and processed for histological analysis. Slides of cross sections of the implantation sites from both genotypes were stained for epithelial marker E-cadherin and cytokeratin by IHC and IF. Additional slides were stained with Jones' silver stain to evaluate basement membrane integrity on day 5 evening of pregnancy. These data are presented in Chapter 4.

Specific Aim 3: Investigating post-implantation defects in decidualization, angiogenesis and lactate transporter expression in the *Bsg* cKO females *in vivo*.

To complete this aim, animals of both genotypes were euthanized and collected at different days of pregnancy post-implantation. Samples were subjected to RNA isolation and histology. IHC and IF staining against Monocarboxylate transport 1 (MCT1) and CD31 were carried out to investigate lactate transporter expression and angiogenesis. Animals of both genotypes were ovariectomized to artificially induce decidualization. Uterine samples were collected and analyzed for decidualization. qRT-PCR on several decidualization-marker genes were analyzed. IHC and IF staining for CCAAT enhancer-binding protein beta (CEBPβ) and Heart and neural crest derivatives-expressed protein 2 (HAND2) were performed on the decidual tissue from artificial decidualization as well as day 5 evening pregnant uteri from both genotypes. These data are presented in Chapter 4 as well.

Specific Aim 4: Investigating *in vitro* decidualization and lactate secretion in the primary endometrial stromal cells of the cKO females.

To complete this aim, primary mouse endometrial stromal cells (MESC) of both genotypes were isolated and cultured to induce decidualization *in vitro*. Cells were cultured for 3-5 days under either normoxic or hypoxic conditions. Culture medium was collected to quantify lactate concentration secreted by the cells using a lactate assay. The cells were harvested to isolate RNA for qRT-PCR for expression of decidualization markers. These data are presented in Chapter 5.

In summary, Chapter 1 describes the overview of this dissertation. Chapter 2 provides a detailed review of A) BSG and B) implantation and decidualization in the current literature. Chapter 3 presents the data on validation of the cKO mouse model as well as the fertility phenotype associated with the cKO females. In Chapter 4, I describe the data on altered implantation, decidualization, lactate transporter localization and angiogenesis in the cKO females *in vivo*. Chapter 5 presents the *in vitro* data on decidualization and lactate assay under either normoxic or hypoxic conditions. Finally, Chapter 6 summarizes the findings presented in the entire dissertation work and suggests directions for future study. The appendix contains lists of abbreviations, antibodies used, primer sequences for all the genes analyzed, as well as detailed protocols on the materials and techniques used in all experimental studies.

References

Chen, Li, Robert J. Belton, and Romana a. Nowak. 2009. "Basigin-Mediated Gene Expression Changes in Mouse Uterine Stromal Cells during Implantation." *Endocrinology* 150 (2): 966–76. https://doi.org/10.1210/en.2008-0571.

Chen, Li, Masaaki Nakai, Robert J. Belton, and Romana A. Nowak. 2007. "Expression of Extracellular Matrix Metalloproteinase Inducer and Matrix Metalloproteinases during Mouse Embryonic Development." *Reproduction (Cambridge, England)* 133 (2): 405–14. https://doi.org/10.1530/rep.1.01020.

Igakura, T, K Kadomatsu, T Kaname, H Muramatsu, Q W Fan, T Miyauchi, Y Toyama, et al. 1998. "A Null Mutation in Basigin, an Immunoglobulin Superfamily Member, Indicates Its Important Roles in Peri-Implantation Development and Spermatogenesis." *Developmental Biology* 194 (2): 152–65. https://doi.org/10.1006/dbio.1997.8819.

Li, Kailiang, and Romana A Nowak. 2019. "The Role of Basigin in Reproduction." *Reproduction (Cambridge, England)*, September. https://doi.org/10.1530/REP-19-0268.

Muramatsu, Takashi, and T. Miyauchi. 2003. "Basigin (CD147): A Multifunctional Transmembrane Protien Involved in Reproduction, Neural Function, Inflammation and Tumor Invasion." *Histology and Histopathology* 18 (3): 981–87.

Norwitz, Errol, Danny Schust, and Susan Fisher. 2001. "Implantation and the Survival of Early Pregnancy." *The New England Journal of Medicine* 345 (19): 1400–1408.

Ramathal, Cyril, Indrani Bagchi, Robert Taylor, and Milan Bagchi. 2010. "ENDOMETRIAL DECIDUALIZATION: OF MICE AND MEN." *Semin Reprod Med* 28 (1): 17–26. https://doi.org/10.1055/s-0029-1242989.ENDOMETRIAL.

Sharkey, Andrew M., and Stephen K. Smith. 2003. "The Endometrium as a Cause of Implantation Failure." *Best Practice and Research: Clinical Obstetrics and Gynaecology* 17 (2): 289–307. https://doi.org/10.1016/S1521-6934(02)00130-X.

Wang, Haibin, Shuang Zhang, Haiyan Lin, Shuangbo Kong, Shumin Wang, Hongmei Wang, and D. Randall Armant. 2013. "Physiological and Molecular Determinants of Embryo Implantation." *Molecular Aspects of Medicine* 34 (5): 939–80. https://doi.org/10.1016/j.mam.2012.12.011.

CHAPTER TWO

Literature Review

A. Basigin

Background on basigin, a member of the Ig superfamily

Basigin was discovered in the 1980s in the laboratory of Dr. C. Biswas, where investigators co-cultured rabbit fibroblasts with mouse tumor cells of epithelial origin and found that these showed increased collagenase production when compared to fibroblasts cultured alone (C Biswas 1982). The tumor cell lines were found to secrete a protein(s) that stimulates collagenase production by human fibroblasts (C Biswas 1984; Chitra Biswas and Nugent 1987) This protein was purified from human lung carcinoma cells and first named tumor cell collagenase-stimulatory factor (TCSF). TCSF was later renamed extracellular matrix metalloproteinase inducer (EMMPRIN) to indicate its role in extracellular matrix metalloproteinase induction in normal, as well as pathological, cellular interactions (Ellis, Nabeshima, and Biswas 1989; Kataoka et al. 1993; C. Biswas et al. 1995). Several different labs independently identified this protein in a number of different species. Thus EMMPRIN is also known as CD147 and M6 in human, basigin and GP42 in mice, HT7 and neurothelin in chicken and OX-47, MC31 and CE9 in the rat (Nehme, Fayost, and Bartlest 1995; Sameshima et al. 2000; Schlosshauer and Herzog 1990; Seulberger, Unger, and Risau 1992; Wakayama et al. 2000; Ellis, Nabeshima, and Biswas 1989; Kataoka et al. 1993). In this review, the protein will be referred to as basigin.

Basigin is a highly glycosylated, type-1 transmembrane protein belonging to the immunoglobulin (Ig) superfamily (Fossum, Mallett, and Neil Barclay 1991) as shown in **Figure 2.1**. The molecular weight of basigin ranges from 43-66 kDa depending on different glycosylation

status and the non-glycosylated molecular weight is 27 kDa (Bai et al. 2014). Different glycosylation patterns are found in different cell types and contribute to its multiple physiological functions (J. Sun and Hemler 2001). The full length form of human basigin is 269 amino acids (Agrawal and Yong 2011) and its structure consists of a heavily glycosylated extracellular domain, a transmembrane domain, and a short cytoplasmic domain (J. N. Hahn, Kaushik, and Yong 2015). The most abundant isoform is basigin-2, where the extracellular domain is 176 amino acids in length, with 77 amino acids forming the extracellular Ig-like domain 1 (EC1) and 95 residues forming the extracellular Ig-like domain 2 (EC2) (Hiraishi et al. 2003). These two Ig-like loops are held together by disulfide bonds. The extracellular region contains three N-linked glycosylation sites at Asn residues and is important for metalloproteinase (MMP) stimulation (H. M. Guo et al. 1997; Hanna et al. 2003; wei Tang et al. 2004; Ku et al. 2007). The single transmembrane domain is highly conserved among species, as human, mouse, rat and chicken show almost identical amino acid sequence in this region. It contains a glutamic acid residue and a leucine zipper in the middle, which is important for association with other transmembrane molecules (Muramatsu and Miyauchi 2003; Miyauchi, Masuzawa, and Muramatsu 1991). The short cytoplasmic tail is about 40 amino acid residues in length and has been shown to be involved in the initiation of various signaling pathways (Muramatsu 2016).

There are four different isoforms of basigin in humans, namely basigin-1, -2, -3,and -4, resulting from alternative splicing. The only difference among them is in the extracellular domain (Grass and Bryan 2016). Basigin isoform 1 has three Ig-like domains in its extracellular portion and is specifically expressed in the retinal epithelium (Redzic et al. 2011; Hanna et al. 2003). Basigin-2 is the most predominant splice variant, encoding two Ig like extracellular domains. It is expressed in most tumor and fibroblast cells and is the only isoform that is secreted. It is also

expressed in the reproductive tissues and is the isoform we are focusing on in this review. Basigin-3 and basigin-4 are short isoforms encoding only one Ig-like domain in the extracellular domain. These two isoforms are less abundant and were originally identified in human endometrial stromal cells and cervical carcinoma cells (L. Chen, Belton, and Nowak 2009). Basigin-3 serves as an endogenous inhibitor of basigin-2 via hetero-oligomerization (Liao et al. 2011). Basigin-4 is overexpressed in cervical cancer and promote proliferation of cervical cancer cells (Zhao et al. 2013).

Basigin is unusual compared with other plasma membrane glycoproteins in terms of its relative level of glycosylation as basigin contains 15-25 kDa of glycans, which is far greater than what is typically observed in a plasma membrane glycoprotein with three N-glycosylation sites. (wei Tang et al. 2004). Highly glycosylated forms of basigin have frequently been reported and are functionally relevant (J. Sun and Hemler 2001). The first Ig domain of basigin (ECI) and the N-glycosylation of its extracellular domains are critical for the MMP-stimulating activity of basigin (Nabeshima et al. 2006). Evidence to support this comes from several studies. Recombinant basigin produced in a bacteria expression system is not glycosylated and of much smaller molecular weight. This non-glycosylated form was unable to stimulate MMP production whereas a highly glycosylated form of basigin isolated from Chinese hamster ovary cells did stimulate production of MMPs-1, -2, and -3 from fibroblasts (H. M. Guo et al. 1997). Belton and colleagues reported that a soluble, non-glycosylated form of recombinant basigin, expressed in the periplasm of bacteria was able to increase MMP-1, -2 and -3 expression in uterine fibroblasts by binding in a homophilic manner to basigin-2 in the cell membrane and activating the ERK1/2 signaling pathway (Belton et al. 2008). Periplasmic expression of the protein exposes the protein to an oxidative environment allowing for the formation of intramolecular disulfide bonds during

translocation into the periplasm, suggesting that the biological activity of basigin depends on the tertiary and quaternary structure of the protein. A third study demonstrated that a synthetic ECI of basigin carrying $GlcNAc_{1-2}$ was able to stimulate MMP-2 production from fibroblasts but the basigin ECI alone had no such activity (Hojo et al. 2003).

One mechanism of regulation of basigin glycosylation status is through caveolin-1, which is a central component of plasma membrane caveolae (wei Tang et al. 2004). Mutagenesis experiments demonstrated that the basigin extra cellular domain II (ECII), but not glycosylation, was required for caveolin-1 interaction (W. Tang and Hemler 2004). Caveolin-1 inhibits the conversion of the low glycosylated form of basigin into the highly glycosylated form and also blocks the MMP inducing activity of basigin (wei Tang et al. 2004; W. Tang and Hemler 2004).

In addition to the plasma membrane-bound form, basigin also exists in a soluble form (Guindolet and Gabison Eric 2019), a conclusion supported by the finding that basigin-expressing tumor cells upregulate MMP production by stromal cells located in or around the tumor (Nabeshima et al. 2004). Two main mechanisms for generating a soluble form of basigin have been reported. Soluble basigin is generated by proteolysis of basigin, removing the carboxyl terminus. (Y. Tang et al. 2004). Second is the release of full-length basigin through microvesicle shedding reported in tumor cells and uterine cells (Sukhvinder S. Sidhu et al. 2004; Braundmeier et al. 2012; Burnett et al. 2012; Grass and Bryan 2016). The shedding of basigin within microvesicles is a regulated process (Emilova 2012). These soluble forms of basigin retain the ability to induce MMP production and stimulate angiogenesis, suggesting that basigin can exert its effect on cells in a paracrine manner or at distant sites (Sukhvinder S. Sidhu et al. 2004; Millimaggi et al. 2007; Gabison et al. 2005).

Role of basigin in cancer: major functions in angiogenesis, energy metabolism and immune function.

Basigin has many physiological functions but is best known for its 1) involvement in tissue remodeling through regulation of matrix metalloproteinases (MMPs) (Seulberger, Unger, and Risau 1992; Wakayama et al. 2000; Saxena and Toshimori 2004; Naruhashi et al. 1997; Schlosshauer and Herzog 1990; Zhou et al. 2005; Ochrietor and Linser 2004); 2) stimulation of angiogenesis (Alcazar et al. 2009; Kirk et al. 2000; Halestrap and Price 1999; Philp et al. 2003; Pistol et al. 2007; Koch et al. 1999); 3) role in glycolytic energy metabolism through shuttling of monocarboxylate transporters (MCTs) to the cell surface membrane (Woodhead et al. 2000; Y. Tang et al. 2004; Amit-Cohen, Rahat, and Rahat 2013; Faten Bougatef et al. 2010; F. Bougatef et al. 2009); and 4) stimulatory effects on lymphocyte and macrophage activation (Ke et al. 2012; Su, Chen, and Kanekura 2009; Renaud Le Floch et al. 2011). (**Figure 2.2**)

Since its discovery three decades ago, basigin has been shown by many investigators to be a major inducer of MMPs in a variety of cell types (Grass and Bryan 2016). Its ECI domain interacts with MMPs and it has been shown to mediate the expression and activity of MMP-1, -2, -3 and -9, and MT1-MMP and MT2-MMP (J. Sun and Hemler 2001; Weidle et al. 2010; Xiong, Edwards, and Zhou 2014; Nabeshima et al. 2006; Braundmeier et al. 2006; L. Chen, Belton, and Nowak 2009). Studies in breast cancer cell lines have indicated that homophilic basigin interactions play a pivotal role in MMP-1 and MMP-2 production and facilitate tumor invasion. This induction of MMP-1 and MMP-2 by basigin is dependent on proper glycosylation of the core protein since deglycosylated basigin fails to stimulate their production (J. Sun and Hemler 2001). A study on squamous cell carcinomas of the uterine cervix in humans reported that MMP-9

expression is stimulated by basigin and is strongly correlated to tumor invasion and metastasis (Weiwei et al. 2009).

Studies have also shown that basigin is important in promoting tumor progression by stimulating angiogenesis (Muramatsu 2016). Changes in basigin expression affect vascular endothelial growth factor (VEGF) production at both the protein and RNA levels in human breast cancer cells. VEGF expression is increased when basigin is over-expressed and is inhibited when basigin is suppressed. *In vivo*, basigin overexpression promotes tumor angiogenesis and growth by inducing VEGF and MMPs expression in both human and mouse (Y. Tang et al. 2005). In another study, investigators showed that increased expression of basigin may enhance angiogenesis in both stromal fibroblasts and gastric carcinoma cells by upregulating MMPs and VEGF (H.-C. Zheng et al. 2006).

In human glioblastoma U251 cells, downregulation of basigin resulted in reducing secretions of MMP2, MMP9 as well as VEGF, indicating a role of basigin in cancer cell angiogenesis and invasion (Liang et al. 2005). In human umbilical vein endothelial cells (HUVEC), basigin acts on stromal and tumor cell MMP production to stimulate angiogenesis (Caudroy et al. 2002). Studies also show that in endothelial cells, basigin upregulate hypoxia inducible factor-2α, VEGF2-2 and soluble forms of VEGF to directly regulate angiogenic process (F. Bougatef et al. 2009). Szubert et al also showed in the epithelial ovarian cancer patients, basigin and VEGF expression are both higher than the benign ovarian tumors and normal ovaries (Szubert et al. 2014).

Another class of binding partners of basigin are the monocarboxylate transporters (MCTs). MCTs are a family of transporters involved in shuttling lactate, pyruvate and ketone across the plasma membrane and play an important role in metabolic homeostasis in diverse tissue and cell

types (Halestrap 2012). There are four isoforms of MCTs (MCT1-MCT4), each with distinct affinities for basigin. Studies have confirmed that basigin is a chaperone protein for MCT1 and MCT4 and is responsible for shuttling these MCTs to the cell membrane where they remain tightly bound to one another (Woodhead et al. 2000; Amit-Cohen, Rahat, and Rahat 2013; Gallagher et al. 2007). MCT1 and basigin co-localize and likely form a heterodimer. MCT1 preferentially binds to basigin; however, when basigin is absent, MCT1 can also bind to embigin, the founding member of this immunoglobulin family (Halestrap 2012). The association of basigin and MCT through the transmembrane domain is important in cells with a high glycolytic rate under hypoxic conditions, which leads to excessive lactic acid production such as in highly invasive tumors (F. Bougatef et al. 2009; L. Chen, Belton, and Nowak 2009). Such increase in glycolytic flux are also critical for rapidly proliferating cells in normal physiological processes such as embryo implantation and placental development.

In addition to the MCTs, basigin also interacts with CD98 through its heavy chain. CD98 directly associates with large neutral amino acid transporter 1 (LAT1) (K. Mori et al. 2004). Together with basigin, it forms a basigin-CD98-LAT1 supercomplex and is involved in regulating adhesion, amino acid transport and energy metabolism (D. Xu and Hemler 2005). Furthermore, the structure of basigin allows it to interact with other proteins for signal transduction and regulation of physiological functions. These proteins include integrin α3-β1 (Xin et al. 2016) and α6-β1 (J. Dai et al. 2009), caveolin-1 (wei Tang et al. 2004) and cyclophilin A (Seizer, Gawaz, and May 2014).

Mechanism of action of basigin

Basigin acts through several different signaling pathways that tend to be cell type specific. Several studies have demonstrated that basigin acts through the MAP kinase pathway to activated

extracellular signal-regulated kinase (ERK)1/2 signaling (Boulos et al. 2006; Q.-Q. Li et al. 2007). For example, Belton et al. reported that basigin activated the ERK1/2 signaling pathway in uterine fibroblast cells leading to increased expression of MMPs-1, -2, and -3. Knockdown of basigin expression using siRNA markedly reduced ERK signaling (Belton et al. 2008). The ERK signaling pathway is also involved in basigin mediated proliferation and invasion of gastric cancers (Xiong, Edwards, and Zhou 2014).

Basigin also serves as a cell surface receptor for cyclophilin A (CyP-A) and is an essential component in the CyP-A-initiated signaling cascade that culminates in ERK activation (Vyacheslav Yurchenko et al. 2002). CyP-A is a ubiquitously expressed intracellular protein of the immunophilin family and plays a role in protein folding. Although initially discovered as a intracellular protein, CyP-A recently is found to be secreted from cells and functions in chemotaxis and cell signaling through its cellular receptor basigin (M. Li et al. 2006). Binding of CyP-A to basigin results in a pro-inflammatory response and agents targeting either basigin or CyP-A reduce the inflammation. Extracellular CyP-A and CyP-B stimulate ERK1/2 phosphorylation (Vyacheslav Yurchenko et al. 2001; V. Yurchenko et al. 2010).

In addition, studies show that basigin is involved in the mitogen-activated protein kinases (MAPK) pathway (Sukhvinder S. Sidhu et al. 2004; Huang et al. 2008). Davidson et al reported that in metastatic serous ovarian carcinoma patients, basigin expression correlate strongly with MMP-1,-2, and -9 as well as p38, suggesting a link between MAPK signaling, MMP expression and basigin expression *in vivo* (Davidson, Givant-Horwitz, et al. 2003; Davidson, Goldberg, et al. 2003). Basigin shed from lung carcinoma cell microvesicles utilizes the MAPK pathway to promote extracellular matrix degradation (Sukhvinder S. Sidhu et al. 2004). Studies have shown that basigin stimulates the production of MMP-1 through p38 MAP kinase in human lung

fibroblasts. Blocking p38 with an inhibitor significantly decreased the production of MMP-1 induced by basigin (M. Lim et al. 1998).

A number of reports have also confirmed that basigin may act via the phosphoinositide 3-kinase (PI3K)-Akt signaling pathway (Yuan Wang et al. 2015; Y. Tang et al. 2006). In Kaposi's sarcoma (KS), basigin is induced when treated with KS herpesvirus, which activates PI3K/Akt dependent secretion of VEGF (L. Dai et al. 2012). Overexpression of basigin in breast cancer cells stimulated phosphorylation of Akt and inhibition of basigin expression resulted in suppressed Akt phosphorylation (Y. Tang et al. 2006). Treatment of lung fibroblast cells with recombinant basigin (rBASIGIN) resulted in phosphorylation of Akt kinase and an increase in VEGF production (J. Tang et al. 2008; Y. Tang et al. 2006). Both the activation of Akt kinase and the induction of VEGF were specifically inhibited with a neutralizing antibody to basigin. The PI3K-specific inhibitors Wortmannin and LY294002 also inhibited VEGF production by basigin-overexpressing cells in a dose- and time-dependent manner (J. Tang et al. 2008; L. Dai et al. 2012).

Basigin also forms complexes with α3β1 and α6β1 integrins promoting cell-cell interactions (Berditchevski et al. 1997). In cancer cells, this basigin-integrin interaction activates the focal adhesion kinase (FAK)-PI3K signaling pathway. This cooperates with Src family kinase activation and stimulates production of MMPs which promote cancer invasiveness (J. Tang et al. 2008; Yuan Wang et al. 2015). β1 integrins also form complexes with basigin and CD98 and play a role in MMP production (Grass and Bryan 2016).

Several studies have also shown that basigin is involved in the Wnt/β-catenin signaling pathway (Hasaneen et al. 2016; Knutti, Huber, and Friedrich 2019). Increasing basigin levels in lung tumor epithelial cells led to an increase in the metastatic potential of lung cancer cells through upregulation of Wnt/β-catenin signaling (S S Sidhu et al. 2010). Moreover, silencing of basigin

using shRNA significantly blocked this signaling pathway and inhibited cell migration, proliferation and tumor growth (S S Sidhu et al. 2010). Furthermore, overexpression of basigin also increases cell proliferation and migration in lung fibroblasts and promotes resistance to apoptosis by activating β-catenin/canonical Wnt signaling pathway (Hasaneen et al. 2016). In MCF-7 breast carcinoma cells, basigin promotes cancer cells proliferation by stimulating the Wnt/β-catenin target protein MMP-14 (Knutti, Kuepper, and Friedrich 2015). Basigin also influences the malignancy-related properties of the breast cancer cells through both Wnt/β-catenin and JAK/STAT pathways (Knutti, Huber, and Friedrich 2019).

Basigin also regulates nuclear factor kappa-light-chain-enhancer of activated B cells (NFκB) pathways (C. Wang et al. 2017; R. Jin et al. 2017). In mouse testis and spermatocyte cell line, basigin reduces apoptosis in spermatocytes by modulating the NFκB pathway. Knockout of basigin leads to apoptosis through extrinsic apoptotic pathway, suppression of canonical NFκB signaling and downregulation of TRAF2 and results in infertility in mice (C. Wang et al. 2016). In human cytomegalovirus infection, knockdown of basigin significantly downregulate NFκB and IFN-β pathways (J. Chen et al. 2017).

Overall, basigin plays important roles in inducing production of MMPs and VEGF, which promotes cell proliferation and survival, stimulate tissue remodeling and angiogenesis through the PI3K, ERK/AKT, FAK, Wnt/β-catenin and NFκB pathways.

Role in Female Reproduction

a) Basigin in the ovary

Expression of basigin in the ovary was confirmed in several earlier papers with somewhat conflicting findings. *Kuno et al.* (1998) determined that expression of *Bsg* mRNA was present in the cumulus granulosa cells and at a low level in the corpora lutea and ovarian stroma in mice. We

observed similar expression patterns in cycling mice, with basigin being expressed only in the endothelial cells of the corpora lutea (L. Chen et al. 2010b). Chang and coworkers (2004) reported that basigin was expressed in the corpora lutea during early gestation (days 1-3) but subsequently disappeared thereafter in Kunming White outbred mice. Smedts and colleagues (2006) carried out a more detailed analysis of expression patterns in the rat ovary during specific functional stages of follicular development, follicular rupture and corpus luteum formation. They reported that *Bsg* expression was present in developing follicles from 1-48 hours after eCG stimulation in the theca and granulosa cells. Expression persisted following ovulation in the pseudopregnant females in the functional corpora lutea but declined as luteal regression occurred. In cycling rats, *Bsg* mRNA was localized to the theca cells of preovulatory follicles and newly forming corpora lutea in cycling rats. Expression of basigin was also assessed in human ovaries (Smedts et al. 2006). Basigin mRNA and protein were detected in granulosa cells in follicles at all stages of development and in the corpora lutea. Basigin expression does not appear to be estrogen dependent in the mouse ovary as expression is not altered in estrogen receptor-α or estrogen receptor-β knockout mice (L. Chen et al. 2010b).

While expression of basigin has been confirmed in the ovaries of several species, a specific function for basigin in the ovary has not yet been identified. The original publications reporting the phenotypic effects of loss of basigin expression on reproductive function in female mice noted that although loss of basigin appeared to greatly impact embryo implantation, ovarian morphology and function appeared to be normal (Tadahiko Igakura et al. 1998; Kuno et al. 1998) Similar conclusions were reached by Smedts and colleagues (2005).

b) Basigin in the endometrium: importance in implantation

Basigin is expressed in the uterus and appears to play an important role during embryo implantation. Very interestingly, both embryonic and uterine expression of basigin are needed for successful implantation. *Igakura et al.* (1998) and *Kuno et al.* (1998) first reported that *Bsg* null mutant embryos develop normally to the blastocyst stage, but very few of these blastocysts implant successfully in the uterus of heterozygous mothers. The vast majority of null mutant embryos are lost between days 4.5 and 7.5 of gestation with only 1-3% of *Bsg* null embryos born as viable pups. *In vitro* trophoblast outgrowth assays with *Bsg* null mutant blastocysts determined that these blastocysts undergo outgrowth comparable to wild type blastocysts (Tadahiko Igakura et al. 1998). This suggests that *Bsg* null embryos may have defects in activation or attachment.

Adult female *Bsg* null mice are infertile, and the cause of the infertility appears to be a uterine endometrium that is not permissive for embryo implantation (Tadahiko Igakura et al. 1998; Kuno et al. 1998). Embryo transfer experiments in wild type and *Bsg* null mutant adult female mice demonstrated that when wild type embryos were transferred into the uteri of *Bsg* null mutant females, less than 5% were successfully born as pups, compared to over 40% for embryos transferred into wild type females. Due to the high rate of embryonic lethality in *Bsg* null mutant embryos, very few reach adulthood and are available for fertility studies. This has made investigation of the role of basigin in endometrial remodeling and decidualization quite difficult.

Studies in the mouse have shown that basigin is expressed in the uterus during the estrous cycle and early pregnancy and expression is regulated by ovarian steroid hormones (Xiao et al. 2002; L. Chen, Belton, and Nowak 2009). Basigin expression in the uterine epithelium is dependent on estrogen and estrogen receptor α (L. Chen et al. 2010b). Basigin is strongly expressed within the luminal and glandular epithelial cells on days 1 and 2 of gestation, but levels decline

over the following two days. Expression in the uterine stromal cells is upregulated by progesterone, becoming detectable on day 3 of gestation and rapidly increasing at day 4 (Tadahiko Igakura et al. 1998; Xiao et al. 2002; L. Chen, Belton, and Nowak 2009). On day 5, when the stromal cells surrounding the invading embryo begin to undergo decidualization, intense basigin expression is evident. On day 6, basigin expression disappears in the secondary decidual zone, but strong basigin expression is still detected in the deep undifferentiated stromal cells. By days 7 and 8, as the number of decidual cells increases, basigin expression is reduced (L. Chen, Belton, and Nowak 2009).

Basigin is also present in the human endometrium where its expression is menstrual-cycle dependent (Noguchi et al. 2003; Braundmeier, Fazleabas, and Nowak 2010). Immunohistochemical analysis of basigin protein expression showed that uterine epithelial cells and stromal fibroblasts display significantly different patterns of expression throughout the menstrual cycle. Basigin protein levels in uterine epithelial cells was strongest during the proliferative phase, when estrogen and progesterone receptors are maximally expressed in these cells. Basigin expression then decreased in epithelial cells during the secretory and menstrual phases in parallel with a loss of estrogen and progesterone receptor expression. The expression pattern in stromal fibroblast cells was more complicated, showing a slow spread of basigin expression from the luminal toward the basal layers of the endometrium during the secretory phase. At menstruation, there was a high level of immunoreactivity for basigin throughout the entire endometrial stroma. Thus, in contrast to uterine epithelial cells, fibroblasts show increased expression of basigin during the secretory phase when progesterone and progesterone receptor levels are high (Braundmeier et al. 2006). Noguchi et al. (Noguchi et al. 2003) did not detect any immunoreactivity for basigin in luminal epithelial cells at any time throughout the menstrual cycle

but this may be due to differences in antibody sensitivity between the different studies. Basigin expression has also been confirmed in the endometrium of baboons (Braundmeier, Fazleabas, and Nowak 2010) and in both the caruncular and intercaruncular endometrium of pregnant cows (Mishra et al. 2012). A recent report from Turgut et al. (Turgut et al. 2014) determined that expression of basigin was significantly lower during the luteal phase in the uterine endometrium of women experiencing multiple implantation failures after IVF in comparison to women with normal fertility. These results also support an important role for basigin during embryonic implantation.

Several *in vitro* studies have investigated the functional role of basigin in endometrial cells. Treatment of human uterine stromal cell cultures with recombinant basigin protein stimulated production of specific MMPs, including MMPs-1, -2, and-3 in human cells (Braundmeier et al. 2006; Belton et al. 2008; Braundmeier et al. 2012) and MMPs-3 and -9 in mouse stromal cells (L. Chen, Belton, and Nowak 2009). Belton et al. (Belton et al. 2008) reported that basigin stimulated secretion of MMPs by human uterine stromal cells through homophilic binding of recombinant basigin protein with basigin protein in the plasma membrane. This homophilic binding led to activation of the ERK1/2 signaling pathway. Basigin is shed by human uterine epithelial cells in microvesicles (Braundmeier et al. 2012) and thus one can envision local regulation of MMP production within the endometrium through paracrine communication between endometrial epithelial and stromal cells (Braundmeier et al. 2012).

c) Basigin in the developing conceptus and placenta

Basigin is expressed in preimplantation mouse and human embryos as early as the 2-cell stage of development and is expressed in both the inner cell mass and trophectoderm of mouse blastocysts (Tadahiko Igakura et al. 1998; Ding, He, and Yang 2002; L. Chen et al. 2007; Hérubel

et al. 2002). Expression of basigin mRNA is highest in the oocyte, morula and blastocyst stages (Ding, He, and Yang 2002). A very recent study by Lindgren et al. (Lindgren et al. 2018) reported that human preimplantation embryos secrete basigin and that embryos that developed into blastocysts secreted more basigin than arrested embryos. Most *Bsg* KO mouse embryos are lost before day 6 of gestation with only about 1-2% of null mutant embryos surviving to birth (Kuno et al. 1998; Tadahiko Igakura et al. 1998). Basigin expression in the embryo is therefore critical for successful implantation and may play a role in embryo metabolism through its effects on MCTs or on embryo attachment to the uterine epithelium.

Basigin expression in placental trophoblast cells was first confirmed in human term placenta (W. Li, Alfaidy, and Challis 2004; Yong-qing Wang et al. 2006) and expression was found to be lower in placentas of patients with preeclampsia (Yong-qing Wang et al. 2006). More recent studies reported that basigin is expressed in placental trophoblast and endothelial cells throughout gestation in the mouse (Nagai et al. 2010) and rat (Dang et al. 2013). An elegant study by Lee et al. (C. L. Lee et al. 2013) examined expression of basigin in the human placenta during the first trimester and performed a number of functional studies using human primary cytotrophoblast cells and the BeWo choriocarcinoma cell line to investigate the function of basigin in the placenta. Basigin expression was evident in all the first trimester placental samples. Functional studies using a siRNA knockdown approach determined that loss of basigin expression reduced trophoblast-endometrial cell interaction, trophoblast cell invasion and syncytialization, and suppressed production of MMPs -2 and -9 and urokinase plasminogen activator by trophoblast cells. Thus basigin regulates several important physiological functions during placental development and differentiation.

Trophoblast cells as well as other cells of the placenta are known to shed microparticles (now referred to as extracellular vesicles or EVs) that consist of both microvesicles and exosomes throughout pregnancy (VanWijk, Svedas, et al. 2002; VanWijk, Boer, et al. 2002; Meziani et al. 2006; Shomer et al. 2013). These EVs, isolated from the blood of pregnant women, are increased in women with preeclampsia (VanWijk, Svedas, et al. 2002; Meziani et al. 2006). Several groups have reported that EVs from blood plasma of pregnant women with preeclampsia have marked negative impacts on vascular endothelial cells and trophoblast cell function when compared to EVs isolated from plasma of women with normal healthy pregnancies (VanWijk, Svedas, et al. 2002; VanWijk, Boer, et al. 2002; Meziani et al. 2006; Shomer et al. 2013). EVs from preeclamptic pregnancies increased trophoblast cell apoptosis and inhibited migration, suppressed endothelial cell migration and tube formation, and negatively affected vascular contractility (VanWijk, Boer, et al. 2002; Meziani et al. 2006; Shomer et al. 2013). Romao et al. recently reported that basigin levels were higher in the blood of women diagnosed with preeclampsia compared to women with normal healthy pregnancies (Romão et al. 2014). Basigin is shed in microvesicles by tumor cells (Sukhvinder S. Sidhu et al. 2004) and uterine cells (Braundmeier et al. 2012; Burnett et al. 2012). Whether basigin is shed in EVs by cell of the placenta and how it may contribute to the regulation of trophoblast cell and vascular function during pregnancy is not currently known but deserves further investigation.

Basigin is also expressed in the extraembryonic membranes particularly in the amniotic epithelium. Significantly elevated expression of basigin was noted in the amnion of patients with premature rupture of membranes at term labor along with higher levels of MMPs (Sukhikh et al. 2016).

d) Basigin in uterine reproductive diseases

In the normal, healthy uterus basigin is expressed both in the endometrium and in the myometrium. Several studies have investigated whether basigin expression is altered in two common uterine diseases in women, uterine leiomyomas and endometriosis. Reports from Ozler et al., (Ozler et al. 2014) and Kefeli et al. (Kefeli et al. 2016) confirmed that basigin is expressed in the smooth muscle cells of most leiomyoma tumors and expression is positively correlated with Ki67 expression and mitotic index. Interestingly, malignant leiomyosarcomas showed much higher expression than leiomyomas suggesting that basigin may be a useful prognostic marker for patients with leiomyosarcoma. Cell culture studies using primary cultures of leiomyoma-derived smooth muscle cells showed that the progesterone receptor modulator asoprisnil (CDB-2914) induced expression of basigin in smooth muscle cells leading to increased production of MMPs and a reduction in collagen synthesis (Q. Xu et al. 2008; Akira et al. 2008). These effects of asoprisnil were not observed in cultured myometrial smooth muscle cells but may be due to the differential responsiveness of the two smooth muscle cell types to progesterone receptor modulators.

Expression of basigin is upregulated in endometriotic lesions in women (Braundmeier et al. 2006; Smedts et al. 2006; A. Jin et al. 2014) and also in baboons (Braundmeier, Fazleabas, and Nowak 2010). Levels of expression were highest in lesions of baboons at early stages of the disease (1-3 months) and decreased in later stages of disease progression (9-15 months). Cell culture studies with immortalized endometriotic cell lines determined that basigin is an important anti-apoptotic factor, protecting endometriotic cells from apoptosis through upregulation of Bcl-2 via the ERK signaling pathway (A. Jin et al. 2014; C. Wang et al. 2015). Inhibition of basigin expression in endometriotic cells markedly reduced migration as well. The increased levels of

basigin expression in endometriotic lesions appear to be regulated through increases in prostaglandin E2 production. Treatment of cultured immortalized endometriotic cells with specific inhibitors of the prostaglandin E receptors EP2 and EP4 reduced basigin expression in these cells and also led to reduced cell migration (Je Hoon Lee et al. 2011).

B. Implantation

Introduction

In mammalian species, a new life begins at fertilization when an egg meets a sperm (Wassarman 1999). The zygote then undergoes a few rounds of cell division to form a blastocyst, which is composed of two cell types: the trophectoderm and the inner cell mass (Rossant 2016). After hatching from the zona pellucida, the blastocyst will attach to the uterine endometrium, then invade into the stroma and establish the placenta. This process is known as implantation and it is a dynamic event that involves a series of physical and physiological interactions between the implanting blastocyst and the receptive uterus (H. Wang and Dey 2006). Implantation requires a complex two-way cross talk between the embryo and the maternal endometrium, and a variety of genes and molecules have been identified to play a role in this process. These genes and molecules include steroid hormones, cytokines, homeobox transcription factors and developmental genes (Tranguch et al. 2005; Dimitriadis et al. 2005a; Benson and et al. 1996; B C Paria et al. 2001). There are three processes during implantation: **uterine receptivity**, **blastocyst attachment and invasion**, and **decidualization** (H. Wang et al. 2013). In this chapter, a detailed literature review on these three processes, as well as hormonal profile in early pregnancy and important signaling pathways will be provided. Proper implantation is critical for successful pregnancy, and

perturbations can generate adverse outcomes for subsequent development and lead to loss of the pregnancy (Q. Chen et al. 2011).

Hormonal Profile in Early Pregnancy and Uterine Receptivity

In most mammals, implantation occurs in a fixed interval of time after ovulation (Finn and Martin 1974). In humans, it is during the luteal phases; in mice, it is in the diestrus of the estrous cycle. It is well known that estrogen and progesterone are the main hormones in this process (Hantak, Bagchi, and Bagchi 2014). Similar to humans, the uterine tissue of mice consists of three major layers, the outer myometrial layer, the inner luminal epithelium and the stromal layer in between (H. Wang and Dey 2006). During the pre-implantation period, the uterus needs to undergo a series of changes to prepare for the attaching embryo. The hormonal profile of both species has been well studied and the estrogen and progesterone act in concert to orchestrate these changes (Pawar et al. 2014).

The hormonal profile and the physiological changes in the uterus in early pregnancy in mice are shown in **Figure 2.3**. Estrogen levels increase in mice starting on day 1 of pregnancy and stimulate extensive proliferation of the luminal epithelium. This is mediated by stromal estrogen receptor α (ERα) (Winuthayanon et al. 2010). As pregnancy progresses, progesterone levels begin to rise and lead to a cessation of epithelial proliferation. On day 4 of pregnancy, the uterus enters the pre-receptive stage, where the uterine epithelial cells lose polarity and the plasma membranes of the epithelial cells become smooth and flattened to be receptive to the blastocyst (Tranguch et al. 2005). In mice, nidatory estrogen activation of uterine receptivity opens the implantation window and starts the implantation process (Yamada et al. 2014). Without this estrogen surge, the embryo will be dormant and free-floating in the uterus. At the same time, the underlying stromal

cells begin to proliferate under the influence of rising progesterone produced by the newly formed corpora lutea under a hypoxic condition (Harvey 2007). The uterus is only receptive to the blastocyst during a restricted period when its environment is favorable for implantation. This narrow receptive time is referred to as the implantation window. In mice, it is limited to the afternoon of day 4 of pregnancy (H. Wang and Dey 2006). In the pre-receptive stage (day 1-3), the uterus cannot initiate implantation before this time. After the receptive stage (day 5 and onward), the uterus enters a refractory stage spontaneously and the uterine environment is not receptive for blastocyst attachment (Carson et al. 2000b). In humans, the proliferative phase is under the influence of rising estrogen from growing antral follicles, resulting in proliferation of the epithelium, stroma and vascular endothelium to regenerate the endometrium. At midcycle, a surge of luteinizing hormone leads to ovulation on day 14. In secretory phase, the endometrium thickens and the corpus luteum forms and secretes progesterone in preparation for implantation. At this time, glands become secretory and stromal cells differentiate to decidual cells (Cha, Sun, and Dey 2012). In humans, the implantation window is between days 6 to 10 after ovulation (Bruce A. Lessey 2011). To some extent, the implantation window is flexible and can be modified by hormones. In mice, for example, with progesterone supplementation, blastocysts are able to initiate the attachment reaction in the non-receptive uterus when transferred on day 5 of pseudo-pregnancy (Song, Han, and Lim 2007)

In addition to steroid hormones, many genes are required for normal implantation, such as cytokines, homeobox transcription factors and developmental genes. The IL-6 family of cytokines is of great importance during embryo implantation (Dimitriadis et al. 2005a). The IL-6 family includes cytokines such as LIF, IL-6, and IL-11 that all signal through gp130 and mediate the activation of STAT3 (Pawar et al. 2013). LIF deficient mice experience implantation failure and

supplementation with LIF rescues this defect (J. R. Chen et al. 2000). The importance of LIF signaling in implantation is supported by studies that blocking its downstream targets gp130 and STAT3 also leads to implantation failure (Menkhorst et al. 2011). IL-6 is also required for normal implantation as studies show mice lacking IL-6 failed to undergo implantation (Dimitriadis et al. 2005b).

Homeobox genes are a group of conserved transcription regulators that are important for embryonic morphogenesis and development (Kwon and Taylor 2004). Homeobox A genes Hoxa10 and Hoxa 11 are expressed in uterine stromal cells during receptivity and decidualization in mice (Bagot, Kliman, and Taylor 2001). Studies have shown that both Hoxa10 and Hoxa11 mutant mice are infertile due to failed implantation (Rahman et al. 2006; HS Taylor 1999). Non-classical Hox genes may also play a role during implantation as deletion of H6 homeobox in mice causes implantation defects (Weidong Wang, Van De Water, and Lufkin 1998). Another homeobox gene, Msx1, is transiently expressed in the luminal and glandular epithelium during the implantation window but is downregulated after the completion of receptivity. Conditional knocking out of uterine Msx1 leads to compromised implantation and the double knockout of Msx1 and Msx2 leads to complete implantation failure and infertility (Nallasamy et al. 2012; Daikoku 2011).

There are also developmental genes that are critical for uterine receptivity and implantation, and some examples are Indian hedgehog (IHH), bone morphogenetic proteins (BMPs), Wingless-type MMTV integration site family members (WNTs) and their receptors (B C Paria et al. 2001). IHH is part of the hedgehog family which controls cell proliferation, differentiation and cell to cell interactions in many biological processes (Q Wei 2010). In the uterus, IHH is expressed in the luminal epithelium under the influence of progesterone, and its

effectors are expressed in the stroma (H Matsumoto 2002). Conditional deletion of IHH in the uterus results in failed implantation because the mice lack progesterone-facilitated stromal cell proliferation (Franco et al. 2010). BMPs are morphogens belonging to the transforming growth factor-β (TGF-β) superfamily and several BMPs are expressed in the uteri of mice (Ying and Zhao 2000; Zamani and Brown 2011). BMP2 is responsive to progesterone and knockout out of BMP2 or its mediator proprotein convertase 6 (PC6) leads to infertility in mice due to defects in implantation and decidualization (K. Y. Lee et al. 2007; Q. Li et al. 2007). WNT4, a downstream target of BMP2, is expressed mainly in the luminal epithelium before implantation and in the stromal cells later surrounding the implanting embryo (Hayashi et al. 2009). Conditional knockout of WNT4 in the uterus causes subfertility in mice due to compromised implantation and subsequently impaired decidualization (Franco et al. n.d.).

Blastocyst Attachment and Invasion

During embryo implantation, a series of physical and physiological interactions happen between the blastocyst trophectoderm and endometrial cells such as luminal and glandular epithelial cells and stromal cells (H. J. Lim, Dey, and Lim 2009). The embryo goes through three stages during implantation: apposition, adhesion/attachment, and penetration (Schlafke, Welsh, and Enders 1985). During apposition, the trophectoderm comes into close proximity with the luminal epithelium. Upon uterine lumen closure, firm attachment between the trophectoderm and luminal epithelium is initiated through adhesion molecules. After the attachment reaction, the embryo initiates penetration through the luminal epithelium and invades into the underlying stromal cells (Carson et al. 2000a). This process also involves breakdown of the epithelium and the basement membrane, which is mediated by MMPs (Rashid et al. 2011).

In mice, uterine luminal fluid serves as a medium for transporting the preimplantation embryos into the uterine horn, and then on day 4 of pregnancy, the uterine luminal fluid is absorbed. This leads to luminal closure, which assists the blastocyst to position in the uterine cavity in intimate contact with the luminal epithelium (H. Wang et al. 2013). Ovarian estrogen stimulates fluid secretion, while progesterone triggers fluid absorption before implantation, and these actions occur through two ion channels, the cystic fibrosis transmembrane conductance regulator (CFTR) and the epithelial Na^+ channel (ENaC) (Salleh et al. 2005). CFTR is a cAMP-activated Cl^- channel expressed in the apical membrane of endometrial epithelial cells. ENaC is expressed in the stromal cells (Chan et al. 2002). Estrogen stimulates CFTR expression and represses ENaC expression, which leads to fluid accumulation in the uterine lumen. On the other hand, progesterone induces ENaC expression and inhibits CFTR expression, which results in absorption of the luminal fluid and luminal closure (Nobuzane, Tashiro, and Kudo 2008; X.-Y. Zheng, Chen, and Wang 2004). Studies have shown that in mice, inflammation-induced upregulated expression of CFTR results in abnormal uterine fluid accumulation and implantation failure (He et al. 2010). The blastocyst at the time of invasion can release trypsin to activate ENaC and a study found activation of ENaC is required for normal uterine fluid absorption and implantation (Ruan et al. 2012). Thus CFTR and ENaC provide a mechanism explaining how uterine fluid absorption is achieved to assist in uterine closure and blastocyst apposition.

Blastocyst attachment is essentially the interaction between the trophectoderm and the uterine epithelium, and adhesion molecules are involved in this process. Studies have identified that certain adhesion molecules, such as integrins, selectins and cadherins play important roles in blastocyst attachment (Armant 2011; Kimber and Spanswick 2000; H. Singh and Aplin 2009a). Integrins are a group of adhesion molecules that bind to the arginine-glycine-aspartic acid (RGD)

sequences of the extracellular matrix components such as fibronectin, osteopontin and vitronectin (Campbell et al. 1995). Many integrins play a role in implantation, including α1β1, α3β1, α6β1, αvβ1, αvβ3, αvβ5 and αvβ6 (H. Singh and Aplin 2009b). Among these integrins, the β3 subunit is most broadly studied in mice and human. Integrin αvβ3 is expressed in mice in luminal epithelium during implantation, and injection of neutralizing antibody against the αv or β3 subunit reduces the implantation rate, suggesting its role in facilitating trophectoderm and luminal epithelium interaction (Illera et al. 2000). Similarly in human, the β3 subunit is strongly expressed in the luminal and glandular epithelium during the mid-secretory phase and abnormal expression of β3 integrins leads to recurrent pregnancy loss and infertility (B. A. Lessey et al. 1995).

L-selectin is a carbohydrate-binding protein and is thought to mediate the adhesion of the blastocyst to the luminal epithelium in human (B. Wang et al. 2008). L-selectin is expressed in the human trophoblast and blocking of L-selectin with specific neutralizing antibodies results in defective adhesion of trophoblasts to the epithelium (Genbacev 2003). The expression of L-selectin ligand in the endometrium is significantly lower in infertile patients compared to fertile women, and reduced expression of L-selectin ligands lowers implantation success rates (Margarit et al. 2009; Shamonki et al. 2006). E-cadherin is a Ca^{2+}-dependent transmembrane protein that forms adhesion junctions between cells (Wesseling, Van Der Valk, and Hilkens 1996). On the embryo side, E-cadherin is required for blastocyst formation as blastocysts deficient in E-cadherin fail to form adhesion junctions in the trophectoderm and die before implantation (de Vries et al. 2004). On the maternal side, E-cadherin is expressed in the luminal epithelium prior to implantation, but expression is lost during implantation and transiently appears in the stromal cells, suggesting the importance of luminal epithelial cell remodeling to assist in blastocyst attachment and invasion into the stroma (Bibhash C. Paria et al. 1999; Q. Li et al. 2002). Persistent expression

of E-cadherin results in implantation failure due to impaired epithelial cell remodeling to support the blastocyst (Nallasamy et al. 2012). Mice lacking E-cadherin in the uterus also have failed implantation and decidualization because they cannot form adhesion junctions and tight junctions in the luminal epithelium (Reardon et al. 2012). Together, these data suggest embryonic and endometrial E-cadherin is critical for normal implantation.

Decidualization and Associated Signals

Decidualization is a unique process in human and rodents. During decidualization, the uterine stromal cells surrounding the implanting blastocyst undergo a dramatic transformation to form decidua to support embryo growth and maintain early pregnancy (Ramathal et al. 2010). Similar to humans, the stromal cells at the implantation site undergo extensive proliferation and then differentiation into large, multinucleated decidual cells in response to implantation in mice (Ramathal et al. 2010; H. J. Lim and Wang 2010). The differentiating stromal cells form an avascular primary decidual zone (PDZ) that first encases the embryo on day 5 of pregnancy (X. Wang et al. 2004). Then the adjacent stromal cells continue to proliferate and differentiate into a well-vascularized secondary decidual zone (SDZ). Decidualization is precisely controlled by hormones, epithelial cell secreted factors, cell cycle regulators and immune cells (Conneely, Mulac-Jericevic, and Lydon 2003; Wetendorf and DeMayo 2012; Das 2009; Croy et al. 2012). Studies have suggested important functions of decidualization including providing nutrition to the developing embryo, establishing a barrier for uncontrolled trophoblast invasion, protecting the embryo from the maternal immune system, and synthesizing hormones prior to the formation of a functional placenta. It is widely accepted that a fully developed decidua is a prerequisite for successful implantation (Peng et al. 2008; X. Wang et al. 2004; Welsh and Enders 1987).

During implantation, luminal epithelial cells undergo apoptosis at the site of embryo attachment and assist embryo invasion to access the maternal blood supply (Pampfer and Donnay 1999). At the same time, the luminal epithelial cells also secrete signals to facilitate decidualization. For example, KLF5 is a transcription factor containing a zinc finger that is expressed in the luminal epithelium during implantation (Ema et al. 2008). Knockout of KLF5 in mice leads to implantation failure and defective decidualization (X. Sun et al. 2012). IHH is expressed in the luminal epithelium and IHH null mice are infertile due to failed implantation as well as failed decidualization in response to an artificial stimulus (K. Lee et al. 2006). Mice with deletion of IHH's receptor Ptch1 and downstream effector Gli1-3 and COUP-TFII in the stromal cells also have decidualization failure (K. Lee et al. 2006; Kurihara et al. 2007). These data suggest the epithelial cells produce important paracrine factors to act on the stromal cells for normal implantation and decidualization.

One of the characteristics of decidualization is the formation of polyploid cells and this requires the action of cell cycle regulators (Dey et al. 2004). Cyclin D3 is important for stromal cells proliferation, differentiation and polyploidy and knockout of cyclin D3 leads to failed decidualization in mice (Das 2009). Moreover, mice deficient in Hoxa10, a cyclin D3 effector, exhibits defective decidualization (Rahman et al. 2006). Knocking out of the upstream regulator of Hoxa10, basic transcription element-binding protein 1 (BTEB1), also results in decidualization failure and subfertility in mice (Simmen et al. 2004). Death effector domain-containing protein (DEDD) stabilizes cyclin D3 and ablation of DEDD leads to attenuated polyploidy and impaired decidualization (M. Mori et al. 2011). These results together support cyclin D3's central role in the process of decidualization. In addition to cyclin D3, other cell cycle related genes have been shown to regulate the decidual response. For instance, stromal cells in mice lacking hepatoma

upregulated protein (Hurp) are unable to decidualize and this results in infertility (Tsou et al. 2003). Transcription factor CCAAT enhancer-binding protein beta (CEBPβ) is expressed at high levels in the stromal cells surrounding the implanted blastocyst during decidualization and is involved in the Cyclin E-cdk2 and STAT3 pathway. When CEBPβ is ablated in the uterus, mice completely fail decidualization and are infertile (Bagchi et al. 2006; Ramathal et al. 2011).

The decidua serves as an immune privileged site for the implanted blastocyst because it is genetically foreign to the maternal immune system. The primary decidual zone is avascular and composed of layers of semi-epithelialized stromal cells to set a physical barrier for the maternal immune components (X. Wang et al. 2004). A number of genes have been identified to participate in immune tolerance during decidualization to protect the embryo (Yoshinaga 2012; Taglauer, Adams Waldorf, and Petroff 2010). For instance, programmed death ligand 1 (PDL1) is an inhibitory T cell costimulatory protein that is important in regulating the immune response in many systems (Khoury and Sayegh 2004). Expression of PDL1 is restricted to the decidua basalis, suggesting PDL1's role in the maternal alloimmune response (Guleria et al. 2005). Blocking of PDL1 signaling with antibody results in significantly higher T cell-dependent fetal rejection. Female mice with PDL1 ablation also have a much lower rate of allogeneic fetal survival (Guleria and Sayegh 2007). Galectins (Gal) are a member of the β-galactoside-binding lectin family and play a role in immune response by regulating the proliferation and survival of T cells (Rabinovich et al. 2007). Gal1 is expressed in the mouse uterus during implantation and can induce cell death of T cells (Hirota et al. 2012). Female mice that lack Gal1 have a higher rate of fetal loss on gestational day 13 when mated with allogeneic males (Blois et al. 2007). Ablation of Gal1's upstream regulator FK506 binding protein 4 (Fkbp52) in mice also results in a higher rate of fetal

resorption (Hirota et al. 2012). Collectively, these results suggest the importance of immune-regulating genes in supporting normal decidualization and pregnancy.

Steroid Hormones, Receptors and Related Signaling Pathways

Ovarian estradiol and progesterone are the principal hormones regulating implantation. Progesterone is essential for implantation and maintenance of pregnancy in all mammals studied, thus it is also called the "pregnancy hormone", whereas the requirement for estrogen is species specific (Dey et al. 2004). The uterine effects of estrogen and progesterone are carried out though their nuclear receptors ERα, ERβ, PRα and PRβ. Many studies have focused on the role of these receptors in implantation and have revealed that ERα null uteri are unable to support implantation, whereas ERβ null uteri still allow normal implantation to occur (Red-Horse et al. 2004). Progesterone administration is sufficient to induce decidualization in ERα null mice, indicating that ERα may be essential for blastocyst attachment, but not for later decidualization (Curtis et al. 1999). Mice that lack PRα and PRβ have shown many defects in reproductive functions, but these functions are all normal in mice lacking only PRβ, which indicates that progesterone actions are primarily mediated by PRα (Mulac-Jericevic et al. 2000). Mice lacking PR exclusively in the epithelium are infertile and show persistent proliferation of the luminal epithelium (Franco et al. 2012). Another study demonstrated a role of PR in the transition of the uterine epithelium from a proliferative to receptive state (Hamatani et al. 2004). Estrogen and progesterone coordinate uterine functions through multiple paracrine, juxtacrine and autocrine factors in a spatiotemporal manner (Cha, Sun, and Dey 2012). This requires a signaling network that involves cytokines, homeotic proteins, morphogens and transcription factors (Xie 2007). Some examples of signals communicating between the epithelial cells and stromal cells are reviewed here.

Leukemia inhibitory factor (LIF) is a very well characterized paracrine factor of epithelial cell origin that regulates implantation (Hamatani et al. 2004). It is a secreted cytokine belonging to the interleukin (IL-6) family. LIF binds to cell surface LIF receptor, triggers its interaction with the signal transducer glycoprotein 130 (GP130, which then activates Janus Kinase (JAK), and mediates the phosphorylation and activation of the transcription factor signal transducer and activator of transcription 3 (STAT3) (Yang et al. 1995). LIF is expressed predominantly in the glandular epithelium on day 4 of pregnancy and LIF null mice are infertile due to impaired implantation and decidualization (Bhatt, Brunet, and Stewart 1991). In the absence of LIF, the transactivation and nuclear localization of STAT3 is lost, which is required for implantation (Catalano et al. 2005). Loss of LIF-STAT3 signaling leads to undifferentiated uterine luminal epithelium that is not receptive to the embryo (Pawar et al. 2013). Studies have shown that PR interacts directly with STAT3 during the peri-implantation phase and PR and STAT3 act in concert to regulate a subset of progesterone responsive genes that are critical for decidualization (Jae Hee Lee et al. 2013). In summary, LIF is produced by the glandular epithelium under estrogen stimulation, and acts on luminal epithelium to activate JAK-STAT signaling pathway to mediate the shift from the proliferative state to differentiated state. LIF also drives stromal proliferation through regulation of the EGF signaling pathway.

Indian hedgehog (IHH) is a member of the hedgehog family and once it binds to its receptor, it recruits and activates downstream transducer to activate the transcription factors Gli and chicken ovalbumin upstream promoter transcription factor II (COUP-TFII) which regulates cell proliferation and differentiation (McMahon 2000). IHH is expressed in the uterus on day3 and day4, and then declines on day 5. Deletion of IHH in the uterus leads to infertility due to implantation defects and failure of progesterone –induced decidualization (K. Lee et al. 2006;

Takamoto et al. 2002). PRKO mouse model studies have shown that IHH is a progesterone regulated genes (H Matsumoto 2002). IHH-COUP-TFII signaling controls luminal epithelium remodeling necessary for implantation and IHH is also important for decidualization through COUP-TFII mediated induction of BMP2 (D. K. Lee et al. 2010). Bone morphogenetic protein 2 (BMP2) is a member of the BMP family of morphogens. Its expression is observed in the uterine stroma near the site of attachment and persists through early phases of decidualization (B C Paria et al. 2001). BMP2 is downstream of the IHH-COUP-TFII signaling pathway and BMP2 expression is lost in the stroma of COUP-TFII knockout uteri (Ying and Zhao 2000). BMP2 knockout studies have shown that the blastocysts are able to attach to the luminal epithelium, but not able to penetrate the uterine epithelium and induce decidualization (K. Y. Lee et al. 2007). In vitro studies have shown that knock down of Bmp2 expression in human endometrial stromal cells prevents hormone induced decidualization (Q. Li et al. 2007).

Wingless-type MMTV integration site family member 4 belongs to the WNT family and expresses in the adult uterus under regulation of progesterone (J. W. Jeong et al. 2009). Its primary expression appears in the uterine stroma at day 4.5 in primary decidual zone and persists into the secondary decidual zone (Hayashi et al. 2009). Wnt4 conditional knockout studies reported normal attachment of the blastocyst, but failed invasion through the epithelium and failed induction of the decidual response. Wnt4 is an important regulator of decidualization by mediating progesterone actions to promote both stromal cell differentiation and survival.

Insulin-like growth factor 1 (IGF1) is a peptide hormone that promotes cell growth (Baker et al. 1996). Studies have shown that IGF1 expression is detected in both uterine epithelial cells and stromal cells on day 4 of pregnancy and is limited to the stroma underlying the implanting embryo on day 5. IGF receptors are expressed in all uterine cell types (Kapur et al. 1992). Estrogen

stimulates IGF1 expression in the uterine stroma and more modestly in the luminal epithelium (L. Zhu and Pollard 2007). IGF1 also appears to be a direct target of ERα. There are several proposed mechanisms of action and one of them is that IGF1 acts through IGF1 receptor in the epithelium to stimulate activation of the PI3K/AKT pathway, that phosphorylates and inactivates GSK3β to allow cell cycle progression (Walker et al. 2010). These studies indicate the important role of IGF1 in executing estrogen-induced epithelial proliferation in a paracrine manner.

Heart and neural crest derivatives-expressed protein 2 (HAND2) is a basic helix-loop-helix transcription factor and has a critical role in the uterine stroma to regulate epithelial function (Wu and Howard 2002). Progesterone regulates HAND2 because HAND2 expression is induced by progesterone administration in ovariectomized mice and blocked by the PR antagonist RU486 (Q. Li, Yamagishi, et al. 2011). Beginning at day 3 of pregnancy, HAND2 expression is robust in the uterine stroma but not evident in the epithelium. Stromal expression persists through implantation and is present until day 8.5, suggesting a role for HAND2 during decidualization (DV Huyen 2011). Deletion of HAND2 in the uterus results in infertility due to a defect in implantation and Hand2 conditional knockout mice show persistent epithelial proliferation on day 4 of pregnancy, which indicates that HAND is important for uterine receptivity (Q. Li, Yamagishi, et al. 2011). HAND2 also inhibits the expression of stromal FGFs that induce luminal epithelial proliferation through the ERK1/2 pathway. Thus, progesterone induces stromal expression of HAND2 and inhibits epithelial proliferation to promote implantation.

Other transcription factors regulated by progesterone that play an important role in implantation and decidualization include but are not limited to Homeobox 10 (Hoxa10), CCAAT/Enhancer binding protein β (C/EBP β), and muscle segment homeobox gene 1 and 2 (MSX1 and MSX2). Ablation of these genes leads to failed implantation and decidualization

(Bagchi et al. 2006; H Lim 1999; Daikoku 2011). A model figure adopted from S.K. Dey's review (Cha, Sun, and Dey 2012) on signaling network in decidualization is illustrated in **Figure 2.4**.

In summary, implantation is a complex process that requires synchronized development of the maternal endometrium and the mature blastocyst. There is constant communication between the mother and the embryo. Steroid hormones play vital roles during this crosstalk. Other important genes involved in implantation include cytokines, homeobox transcription factors, developmental genes, cell cycle regulators, and adhesion molecules. Although studies in the past have established the role of various signaling pathways, we are not clear whether theses pathways function independently or converge into a larger network that need to be explored. Mouse models are still important as functional tools to study embryo-uterine interaction, as more Cre models need to be made to study the role of novel genes, such as basigin, in a specific cell type. It is clear that basigin is a critically important protein for successful reproduction in both males and females. While much has been learned regarding the specific functions of basigin in uterus, many questions regarding the role of basigin in implantation remain. Progress has been hampered by the lack of availability of conditional KO mouse models and the lack of a reliable commercial source of the recombinant protein. Basigin is a glycosylated plasma membrane protein that serves as the center of a molecular hub within the cell membrane, interacting with a number of other proteins that are important for adhesion, cell metabolism, and angiogenesis. A better understanding of the physiological and molecular functions of basigin in implantation will improve reproductive health and infertility treatments.

Figures

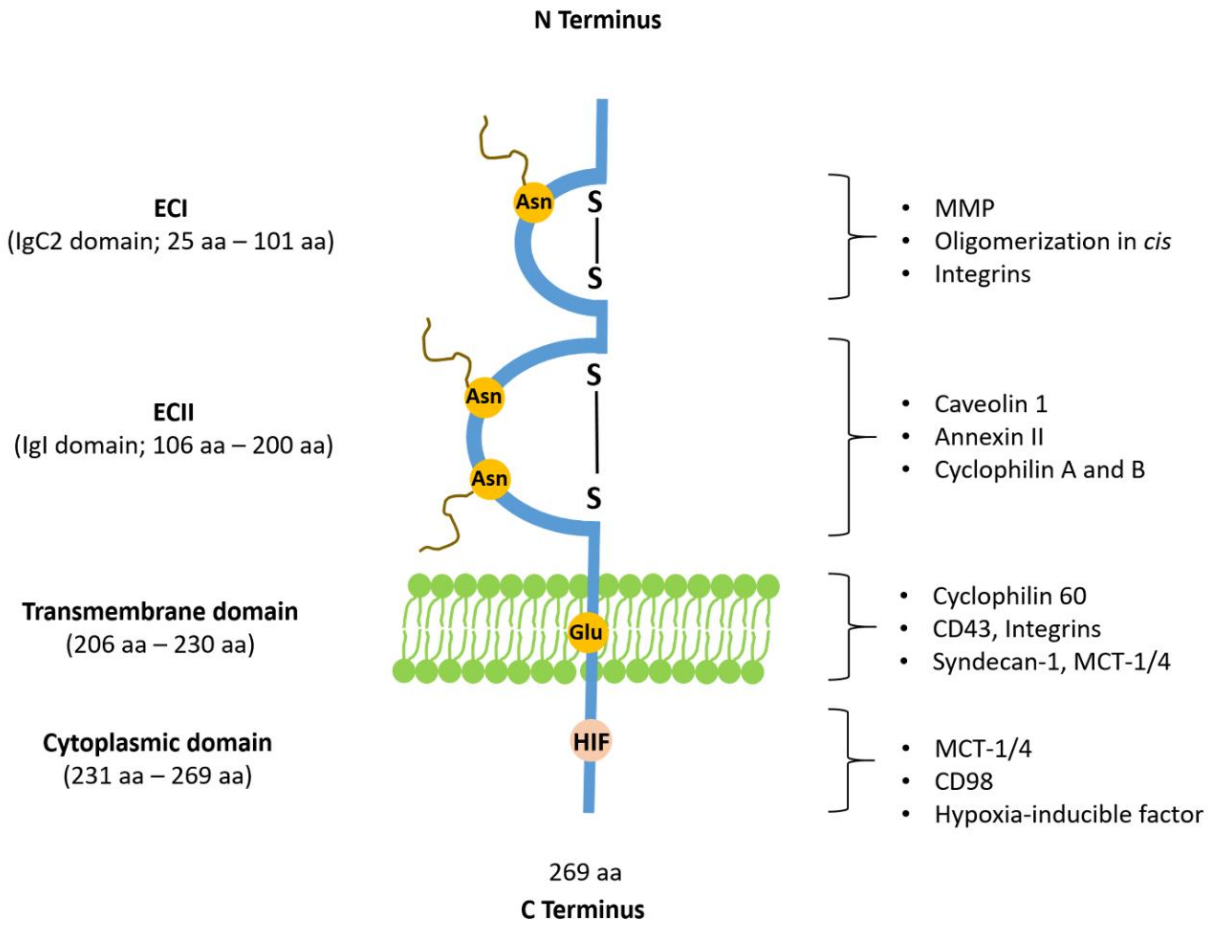

Figure 2.1 Schematic representation of basigin structure and binding partners.
Basigin is composed of two Ig-like extracellular domains (ECI and ECII), a transmembrane domain and a short cytoplasmic domain. Each EC is held together by disulfide bonds. Three conserved Asparagine residues serve as glycosylation sites. Glycosylation is marked by curved lines on ECI and ECII. A conserved Glutamic Acid residue in the transmembrane domain is thought to be important for interacting with certain molecules. A hypoxia inducible factor binding site is in the cytoplasmic domain. MMP: matrix metalloproteinases; MCT: monocarboxylate transporter.

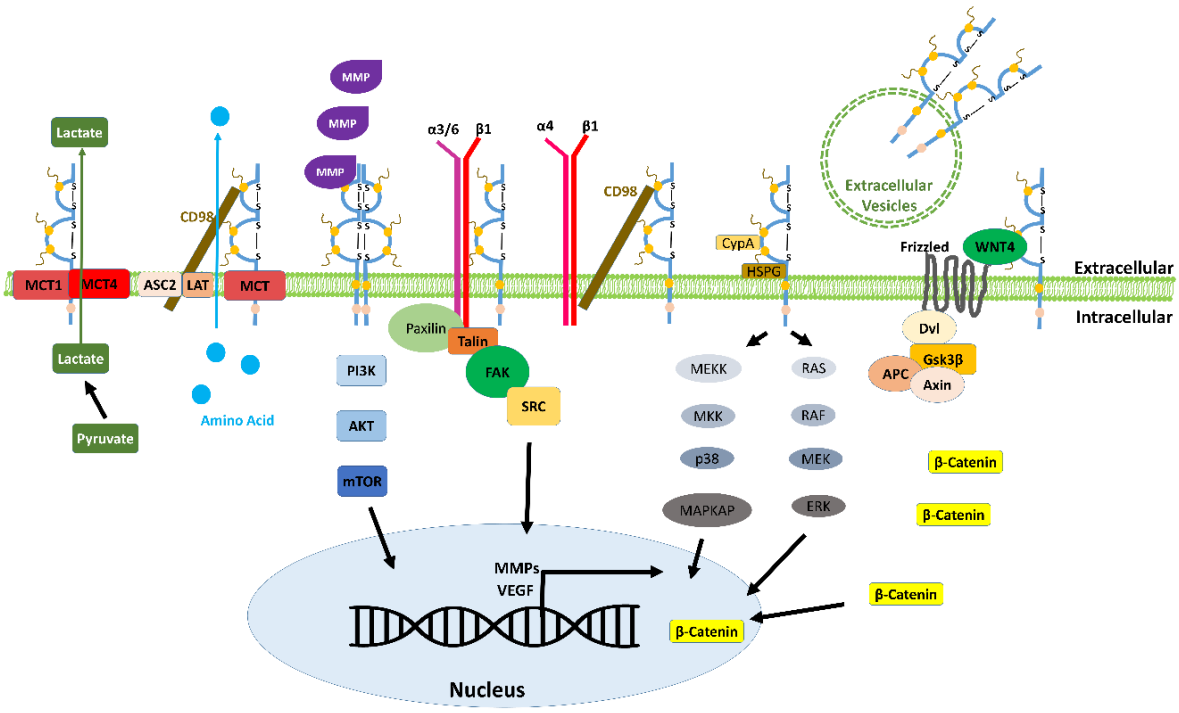

Figure 2.2 Schematic overview of basigin-associated proteins and the signaling pathways involved. From left to right: Basigin binds MCT1/4 and shuttles them to the cell membrane for lactate transport across the cell; Basigin forms a supercomplex by interacting with MCT, CD98, ASC2 and LAT to aid amino acid transport; Basigin forms a homodimer to induce MMP production and activates PI3K/AKT pathway; Basigin binds to α3/6-β1 integrins and activates FAK pathway; Basigin binds CD98 and α4β1 integrin for cell adhesion; Basigin binds cyclophilin A in the ECII to activate MAPK and ERK pathways; Basigin binds WNT4 and Frizzled to activate the Wnt/β-catenin pathway; Basigin is also present and shed in extracellular vesicles. In the nucleus, these interactions lead to upregulation of MMPs and VEGF transcription.

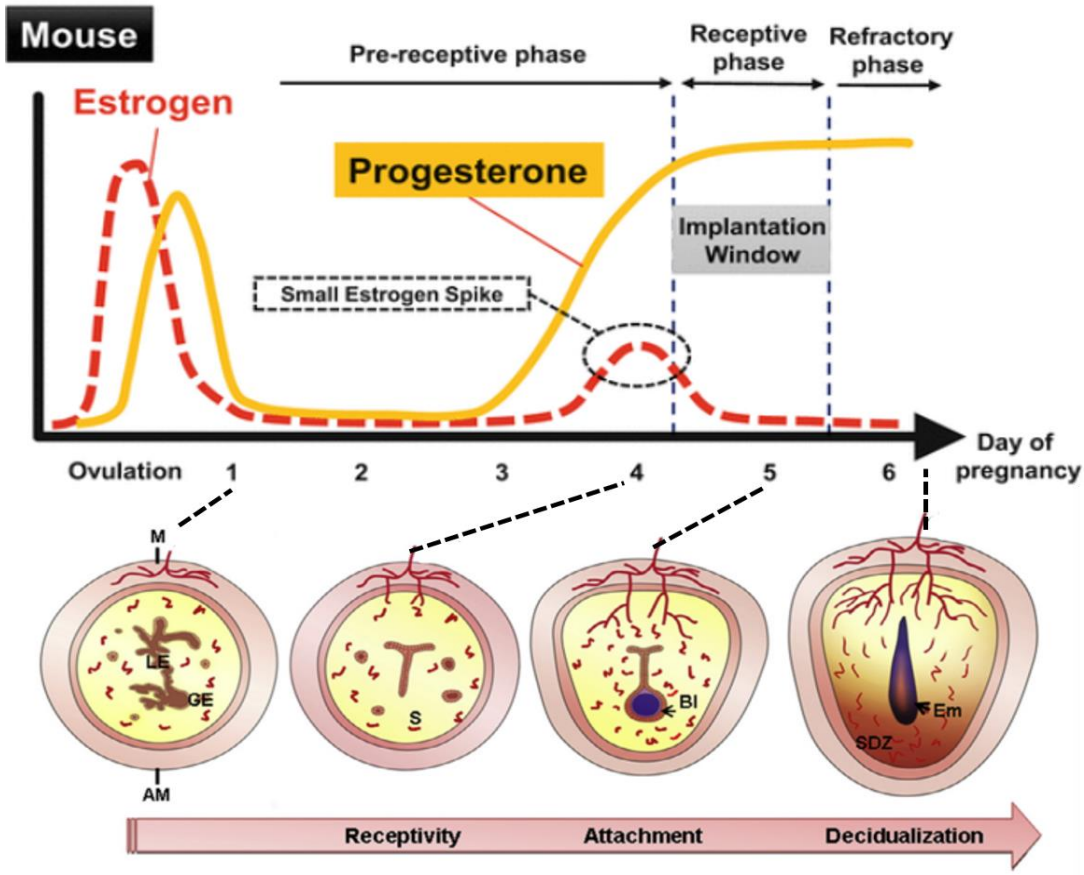

Figure 2.3 Hormonal profile and uterine changes during early pregnancy in mice. Top panel: Steroid hormone patterns are illustrated during indicated days of pregnancy. Estrogen (red dotted line) secretion is high after ovulation. Progesterone (yellow solid line) starts to rise from day 3 and onward due to secretion from newly formed corpora luteum after mating. On day 4, a small spike of nidatory estrogen opens implantation window. Embryo implantation occurs at midnight of day 4. After implantation, high level of progesterone is required for proper decidualization, placentation and completion of pregnancy. Bottom panel: Diagrams of cross-sections of the preimplantation uterus (day1, day4) and implantation sites (day5, day8). On day 1, the luminal epithelium of the non-receptive uterus is highly proliferative and branched. On day 4, the luminal epithelium ceases proliferation and is receptive to the incoming blastocyst. The stroma starts to proliferate. On day 5, the trophectoderm of the blastocyst attaches to the antimesometrial luminal epithelium. The stromal cells at the implantation site undergo proliferation and differentiation to form an avascular primary decidual zone on day 5. The stromal cells next to the PDZ continues to proliferate and differentiate into a vascularized secondary decidual zone (SDZ) by day 8. M, mesometrial side; AM, antimesometrial side; LE, luminal epithelium; GE, glandular epithelium; S, stroma; Bl, blastocyst; SDZ, secondary decidual zone; Em, embryo.

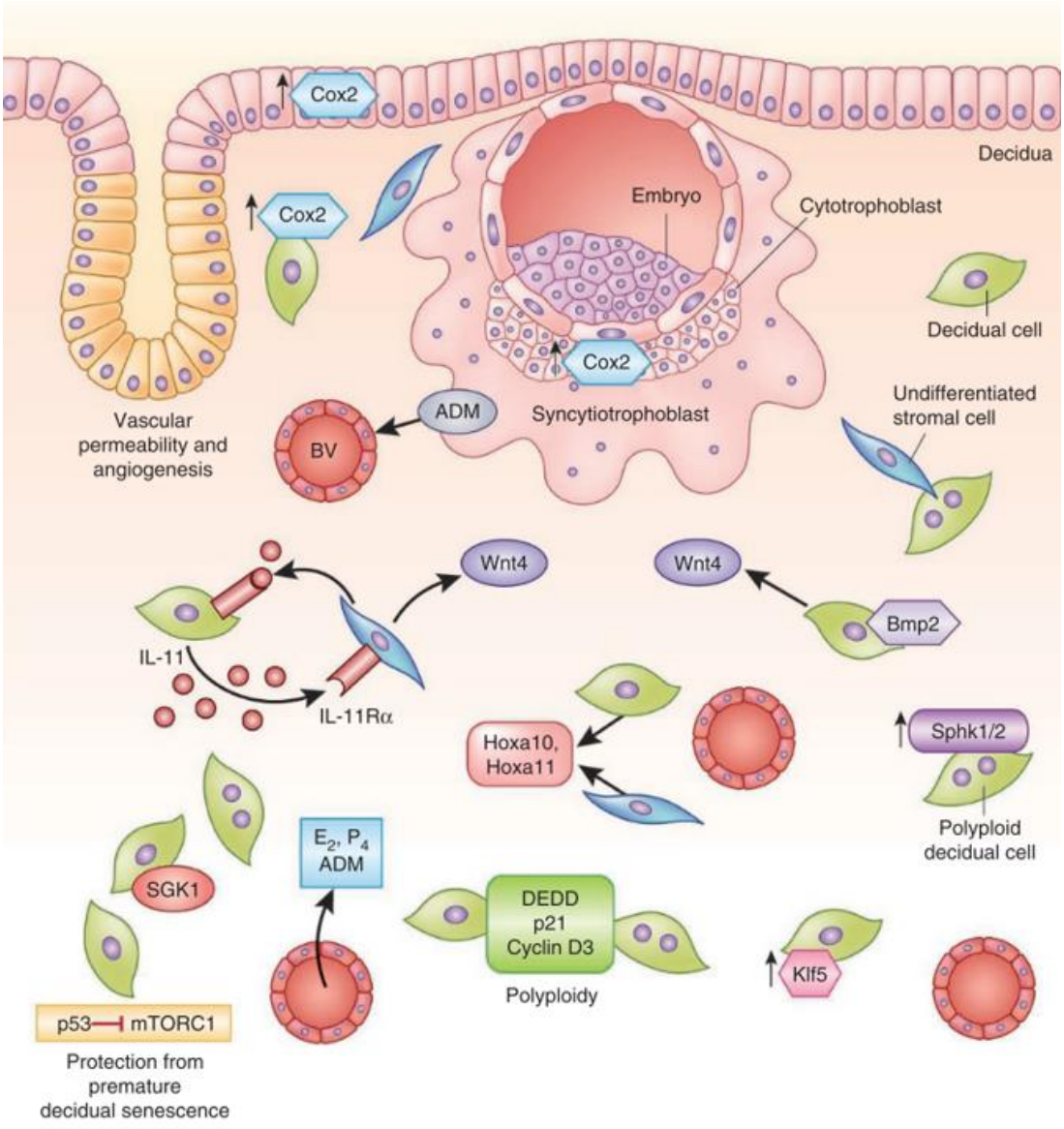

Figure 2.4 Signaling networks in decidualization. Key molecules for decidualization are depicted in this hybrid cartoon as gathered from mouse and human studies. The decidua is composed of differentiated stromal (decidual) cells, many of which are terminally differentiated (polyploid). Decidualization involves coordination of several processes, including polyploidy, and several types of molecules, such as cytokine receptors, enzymes, morphogens, hormones and transcription factors. ADM, adrenomedullin; BV, blood vessel; DEDD, death effector domain–containing protein; IL-11Rα, interleukin 11 receptor α; mTORC1, mammalian target of rapamycin complex 1; SGK1, serum- and glucocorticoid-inducible kinase 1; Sphk1/2, sphingosine kinase 1/2. *Adopted from Cha, Sun and Dey, 2012.*

References

Agrawal, Smriti M., and V. Wee Yong. 2011. "The Many Faces of EMMPRIN-Roles in Neuroinflammation." *Biochimica et Biophysica Acta - Molecular Basis of Disease* 1812 (2): 213–19. https://doi.org/10.1016/j.bbadis.2010.07.018.

Akira, Morikawa, Ohara Noriyuki, Xu Qin, Nakabayashi Koji, DeManno D.A., Chwalisz K., Shigeki Yoshida, and Takeshi Maruo. 2008. "Selective Progesterone Receptor Modulator Asoprisnil Down-Regulates Collagen Synthesis in Cultured Human Uterine Leiomyoma Cells through up-Regulating Extracellular Matrix Metalloproteinase Inducer." *Human Reproduction (Oxford, England)* 23 (4): 944–51. http://ovidsp.ovid.com/ovidweb.cgi?T=JS&PAGE=reference&D=emed8&NEWS=N&AN=18281245.

Alcazar, Oscar, Adam M. Hawkridge, Timothy S. Collier, Scott W. Cousins, Sanjoy K. Bhattacharya, David C. Muddiman, and Maria E. Marin-Castano. 2009. "Proteomics Characterization of Cell Membrane Blebs in Human Retinal Pigment Epithelium Cells." *Molecular & Cellular Proteomics* 8 (10): 2201–11. https://doi.org/10.1074/mcp.M900203-MCP200.

Amit-Cohen, Bat-Chen, Michal A. Maya M. Rahat, and Michal A. Maya M. Rahat. 2013. "Tumor Cell-Macrophage Interactions Increase Angiogenesis through Secretion of EMMPRIN." *Frontiers in Physiology* 4: 178. https://doi.org/10.3389/fphys.2013.00178.

Armant, D Randall. 2011. "Life and Death Responses to Trophinin-Mediated Adhesion during Blastocyst Implantation." *Cell Cycle (Georgetown, Tex.)* 10 (4): 574–75. http://www.ncbi.nlm.nih.gov/pubmed/21311237.

Bagchi, Milan K., Srinivasa R. Mantena, Athilakshmi Kannan, and Indrani C. Bagchi. 2006. "Control of Uterine Cell Proliferation and Differentiation by C/EBPβ: Functional Implications for Establishment of Early Pregnancy." *Cell Cycle*. Taylor and Francis Inc. https://doi.org/10.4161/cc.5.9.2712.

Bagot, Catherine N., Harvey J. Kliman, and Hugh S. Taylor. 2001. "Maternal Hoxa10 Is Required for Pinopod Formation in the Development of Mouse Uterine Receptivity to Embryo Implantation." *Developmental Dynamics* 222 (3): 538–44. https://doi.org/10.1002/dvdy.1209.

Bai, Yang, Wan Huang, Li-tian Ma, Jian-li Jiang, and Zhi-nan Chen. 2014. "Importance of N-Glycosylation on CD147 for Its Biological Functions." *International Journal of Molecular Sciences* 15 (5): 6356–77. https://doi.org/10.1248/bpb.32.780.

Baker, J, M P Hardy, J Zhou, C Bondy, F Lupu, A R Bellvé, and A Efstratiadis. 1996. "Effects of an Igf1 Gene Null Mutation on Mouse Reproduction." *Molecular Endocrinology* 10 (7): 903–18. https://doi.org/10.1210/mend.10.7.8813730.

Belton, Robert J., Li Chen, Fernando S. Mesquita, and Romana a. Nowak. 2008. "Basigin-2 Is a Cell Surface Receptor for Soluble Basigin Ligand." *Journal of Biological Chemistry* 283 (26):

17805–14. https://doi.org/10.1074/jbc.M801876200.

Benson, G. V., and et al. 1996. “Mechanisms of Reduced Fertility in Hoxa-10 Mutant Mice: Uterine Homeosis and Loss of Maternal Hoxa-10 Expression.” *Development (Cambridge, England)* 122 (9): 2687–96. https://doi.org/10.1002/jez.1402660610.

Berditchevski, Fedor, Sharon Chang, Jana Bodorova, and Martin E Hemler. 1997. “Generation of Monoclonal Antibodies to Integrin-Associated Proteins EVIDENCE THAT 3 1 COMPLEXES WITH EMMPRIN/BASIGIN/OX47/M6*.” http://www.jbc.org/.

Bhatt, Harshida, Lisa J. Brunet, and Colin L. Stewart. 1991. “Uterine Expression of Leukemia Inhibitory Factor Coincides with the Onset of Blastocyst Implantation.” *Proceedings of the National Academy of Sciences of the United States of America* 88 (24): 11408–12. https://doi.org/10.1073/pnas.88.24.11408.

Biswas, C., Y. Zhang, R. DeCastro, H. Guo, T. Nakamura, H. Kataoka, and K. Nabeshima. 1995. “The Human Tumor Cell-Derived Collagenase Stimulatory Factor (Renamed EMMPRIN) Is a Member of the Immunoglobulin Superfamily.” *Cancer Research* 55 (2): 434–39. https://doi.org/10.1002/ijc.10390.

Biswas, C. 1982. “Tumor Cell Stimulation of Collagenase Production by Fibroblasts.” *Biochemical and Biophysical Research Communications* 109 (3): 1026–34. http://www.ncbi.nlm.nih.gov/pubmed/6297481.

Biswas,C. 1984. “Collagenase Stimulation in Cocultures of Human Fibroblasts and Human Tumor Cells.” *Cancer Letters* 24 (2): 201–7. http://www.ncbi.nlm.nih.gov/pubmed/6090011.

Biswas, Chitra, and Matthew A. Nugent. 1987. “Membrane Association of Collagenase Stimulatory Factor(s) from B-16 Melanoma Cells.” *Journal of Cellular Biochemistry* 35 (3): 247–58. https://doi.org/10.1002/jcb.240350307.

Blois, Sandra M., Juan M. Ilarregui, Mareike Tometten, Mariana Garcia, Arif S. Orsal, Rosalia Cordo-Russo, Marta A. Toscano, et al. 2007. “A Pivotal Role for Galectin-1 in Fetomaternal Tolerance.” *Nature Medicine* 13 (12): 1450–57. https://doi.org/10.1038/nm1680.

Bougatef, F., C. Quemener, S. Kellouche, B. Naimi, M.-P. Podgorniak, G. Millot, E. E. Gabison, et al. 2009. “EMMPRIN Promotes Angiogenesis through Hypoxia-Inducible Factor-2 - Mediated Regulation of Soluble VEGF Isoforms and Their Receptor VEGFR-2.” *Blood* 114 (27): 5547–56. https://doi.org/10.1182/blood-2009-04-217380.

Bougatef, Faten, Suzanne Menashi, Farah Khayati, Benyoussef Naïmi, Raphaël Porcher, Marie-Pierre Podgorniak, Guy Millot, et al. 2010. “EMMPRIN Promotes Melanoma Cells Malignant Properties through a HIF-2alpha Mediated Up-Regulation of VEGF-Receptor-2.” Edited by Ludovic Tailleux. *PLoS ONE* 5 (8): e12265. https://doi.org/10.1371/journal.pone.0012265.

Boulos, Sherif, Bruno P Meloni, Peter G Arthur, Bernadette Majda, Christina Bojarski, and Neville W Knuckey. 2006. “Evidence That Intracellular Cyclophilin A and Cyclophilin A/CD147 Receptor-Mediated ERK1/2 Signalling Can Protect Neurons against in Vitro Oxidative and

Ischemic Injury.” https://doi.org/10.1016/j.nbd.2006.08.012.

Braundmeier, A. G., C. A. Dayger, P. Mehrotra, R. J. Belton, and R. A. Nowak. 2012. “EMMPRIN Is Secreted by Human Uterine Epithelial Cells in Microvesicles and Stimulates Metalloproteinase Production by Human Uterine Fibroblast Cells.” *Reproductive Sciences* 19 (12): 1292–1301. https://doi.org/10.1177/1933719112450332.

Braundmeier, A. G., A. T. Fazleabas, B. A. Lessey, H. Guo, B. P. Toole, and R. A. Nowak. 2006. “Extracellular Matrix Metalloproteinase Inducer Regulates Metalloproteinases in Human Uterine Endometrium.” *Journal of Clinical Endocrinology and Metabolism* 91 (6): 2358–65. https://doi.org/10.1210/jc.2005-0601.

Braundmeier, A. G., A. T. Fazleabas, and R. A. Nowak. 2010. “Extracellular Matrix Metalloproteinase Inducer Expression in the Baboon Endometrium: Mestrual Cycle and Endometriosis.” *Reproduction* 140 (6): 911–20. https://doi.org/10.1530/REP-09-0481.

Burnett, Lindsey A., Mallory M. Light, Pavni Mehrotra, and Romana A. Nowak. 2012. “Stimulation of GPR30 Increases Release of EMMPRIN-Containing Microvesicles in Human Uterine Epithelial Cells.” *Journal of Clinical Endocrinology and Metabolism* 97 (12): 4613–22. https://doi.org/10.1210/jc.2012-2098.

Campbell, S., H. R. Swann, M. W. Seif, S. J. Kimber, and J. D. Aplin. 1995. “Integrins and Adhesion Mlecules: Cell Adhesion Molecules on the Oocyte and Preimplantation Human Embryo.” *Human Reproduction* 10 (6): 1571–78. https://doi.org/10.1093/HUMREP/10.6.1571.

Carson, Daniel D., Indrani Bagchi, Sudhandsu K. Dey, Allen C. Enders, Asgerally T. Fazleabas, Bruce A. Lessey, and Koji Yoshinaga. 2000a. “Embryo Implantation.” *Developmental Biology* 223 (2): 217–37. https://doi.org/10.1006/dbio.2000.9767.

Catalano, Rob D., Martin H. Johnson, Elizabeth A. Campbell, D. Stephen Charnock-Jones, Stephen K. Smith, and Andrew M. Sharkey. 2005. “Inhibition of Stat3 Activation in the Endometrium Prevents Implantation: A Nonsteroidal Approach to Contraception.” *Proceedings of the National Academy of Sciences of the United States of America* 102 (24): 8585–90. https://doi.org/10.1073/pnas.0502343102.

Caudroy, Stéphanie, Myriam Polette, Béatrice Nawrocki-Raby, Jian Cao, Bryan P Toole, Stanley Zucker, and Philippe Birembaut. 2002. “EMMPRIN-Mediated MMP Regulation in Tumor and Endothelial Cells.” *Clinical & Experimental Metastasis*. Vol. 19. https://link.springer.com/content/pdf/10.1023%2FA%3A1021350718226.pdf.

Cha, Jeeyeon, Xiaofei Sun, and Sudhansu K. Dey. 2012. “Mechanisms of Implantation: Strategies for Successful Pregnancy.” *Nature Medicine*. Nature Publishing Group. https://doi.org/10.1038/nm.3012.

Chan, L. N., L. L. Tsang, D. K. Rowlands, L. G. Rochelle, R. C. Boucher, C. Q. Liu, and H. C. Chan. 2002. “Distribution and Regulation of ENaC Subunit and CFTR MRNA Expression in Murine Female Reproductive Tract.” *Journal of Membrane Biology* 185 (2): 165–76. https://doi.org/10.1007/s00232-001-0117-y.

Chang, Hong, Hua Ni, Xing Hong Ma, Li Bin Xu, Kenji Kadomatsu, Takashi Muramatsu, and Zeng Ming Yang. 2004. "Basigin Expression and Regulation in Mouse Ovary During the Sexual Maturation and Development of Corpus Luteum." *Molecular Reproduction and Development* 68 (2): 135–41. https://doi.org/10.1002/mrd.20060.

Chen, J. R., Jr Gang Cheng, T. Shatzer, L. Sewell, L. Hernandez, and C. L. Stewart. 2000. "Leukemia Inhibitory Factor Can Substitute for Nidatory Estrogen and Is Essential to Inducing a Receptive Uterus for Implantation but Is Not Essential for Subsequent Embryogenesis." *Endocrinology* 141 (12): 4365–72. https://doi.org/10.1210/endo.141.12.7855.

Chen, Jun, Sisi Xia, Xiangmin Yang, Huizi Chen, Fanni Li, Fenyong Liu, Zhinan Chen, et al. 2017. "Human Cytomegalovirus Encoded MiR-US25-1-5p Attenuates CD147/EMMPRIN-Mediated Early Antiviral Response." *Viruses* 9 (12): 365. https://doi.org/10.3390/v9120365.

Chen, Li, Robert J. Belton, and Romana a. Nowak. 2009. "Basigin-Mediated Gene Expression Changes in Mouse Uterine Stromal Cells during Implantation." *Endocrinology* 150 (2): 966–76. https://doi.org/10.1210/en.2008-0571.

Chen, Li, Jiajia Bi, Masaaki Nakai, David Bunick, John F. Couse, Kenneth S. Korach, and Romana A. Nowak. 2010. "Expression of Basigin in Reproductive Tissues of Estrogen Receptor-?? Or -?? Null Mice." *Reproduction* 139 (6): 1057–66. https://doi.org/10.1530/REP-10-0069.

Chen, Li, Masaaki Nakai, Robert J. Belton, and Romana A. Nowak. 2007. "Expression of Extracellular Matrix Metalloproteinase Inducer and Matrix Metalloproteinases during Mouse Embryonic Development." *Reproduction (Cambridge, England)* 133 (2): 405–14. https://doi.org/10.1530/rep.1.01020.

Chen, Qi, Ying Zhang, Hongying Peng, Li Lei, Haibin Kuang, Li Zhang, Lina Ning, Yujing Cao, and Enkui Duan. 2011. "Transient B2-Adrenoceptor Activation Confers Pregnancy Loss by Disrupting Embryo Spacing at Implantation." *Journal of Biological Chemistry* 286 (6): 4349–56. https://doi.org/10.1074/jbc.M110.197202.

Conneely, Orla M., Biserka Mulac-Jericevic, and John P. Lydon. 2003. "Progesterone-Dependent Regulation of Female Reproductive Activity by Two Distinct Progesterone Receptor Isoforms." *Steroids* 68 (10–13): 771–78. https://doi.org/10.1016/S0039-128X(03)00126-0.

Croy, B. Anne, Zhilin Chen, Alexander P. Hofmann, Edith M. Lord, Abigail L. Sedlacek, and Scott A. Gerber. 2012. "Imaging of Vascular Development in Early Mouse Decidua and Its Association with Leukocytes and Trophoblasts1." *Biology of Reproduction* 87 (5): 1–11. https://doi.org/10.1095/biolreprod.112.102830.

Curtis, Sylvia W., James Clark, Page Myers, and Kenneth S. Korach. 1999. "Disruption of Estrogen Signaling Does Not Prevent Progesterone Action in the Estrogen Receptor α Knockout Mouse Uterus." *Proceedings of the National Academy of Sciences of the United States of America* 96 (7): 3646–51. https://doi.org/10.1073/pnas.96.7.3646.

Dai, Jing-yao, Ke-feng Dou, Cong-hua Wang, Pu Zhao, Wayne Bond Lau, Ling Tao, Ya-mei Wu, Juan Tang, Jian-li Jiang, and Zhi-nan Chen. 2009. "The Interaction of HAb18G/CD147 with

Integrin Alpha6beta1 and Its Implications for the Invasion Potential of Human Hepatoma Cells." *BMC Cancer* 9 (1): 337. https://doi.org/10.1186/1471-2407-9-337.

Dai, Lu, Momka Bratoeva, Bryan P. Toole, Zhiqiang Qin, and Chris Parsons. 2012. "KSHV Activation of VEGF Secretion and Invasion for Endothelial Cells Is Mediated through Viral Upregulation of Emmprin-Induced Signal Transduction." *International Journal of Cancer* 131 (4): 834–43. https://doi.org/10.1002/ijc.26428.

Daikoku, T. 2011. "Conditional Deletion of MSX Homeobox Genes in the Uterus Inhibits Blastocyst Implantation by Altering Uterine Receptivity." *Dev. Cell* 21: 1014–24.

Dang, Yiping, Wei Li, Victoria Tran, and raouf a. Khalil. 2013. "EMMPRIN-Mediated Induction of Uterine and Vascular Matrix Metalloproteinases during Pregnancy and in Response to Estrogen and Progesterone." *Biochem Pharmacology* 86 (6). https://doi.org/10.1177/1098300712437042.Improving.

Das, Sanjoy K. 2009. "Cell Cycle Regulatory Control for Uterine Stromal Cell Decidualization in Implantation." *Reproduction* 137 (6): 889–99. https://doi.org/10.1530/REP-08-0539.

Davidson, Ben, Vered Givant-Horwitz, Philip Lazarovici, Björn Risberg, Jahn M. Nesland, Claes G. Trope, Erik Schaefer, and Reuven Reich. 2003. "Matrix Metalloproteinases (MMP), EMMPRIN (Extracellular Matrix Metalloproteinase Inducer) and Mitogen-Activated Protein Kinases (MAPK): Co-Expression in Metastatic Serous Ovarian Carcinoma." *Clinical and Experimental Metastasis* 20 (7): 621–31. https://doi.org/10.1023/A:1027347932543.

Davidson, Ben, Iris Goldberg, Aasmund Berner, Gunnar B Kristensen, and Reuven Reich. 2003. "EMMPRIN (Extracellular Matrix Metalloproteinase Inducer) Is a Novel Marker of Poor Outcome in Serous Ovarian Carcinoma." *Clinical & Experimental Metastasis*. Vol. 20. https://link.springer.com/content/pdf/10.1023%2FA%3A1022696012668.pdf.

Dey, S. K., H. Lim, Sanjoy K. Das, Jeff Reese, B. C. Paria, Takiko Daikoku, and Haibin Wang. 2004. "Molecular Cues to Implantation." *Endocrine Reviews* 25 (3): 341–73. https://doi.org/10.1210/er.2003-0020.

Dimitriadis, Evdokia, C. A. White, R. L. Jones, and L. A. Salamonsen. 2005a. "Cytokines, Chemokines and Growth Factors in Endometrium Related to Implantation." *Human Reproduction Update* 11 (6): 613–30. https://doi.org/10.1093/humupd/dmi023.

Dimitriadis, E, White, R., Jones, R et al. 2005b. "Cytokines, Chemokines and Growth Factors in Endometrium Related to Implantation." *Human Reproduction Update*. Oxford Academic. https://doi.org/10.1093/humupd/dmi023.

Ding, Nai-Zheng, Cheng-Qiang He, and Zeng-Ming Yang. 2002. "Quantification of Basigin MRNA in Mouse Oocytes and Preimplantation Embryos by Competitive RT-PCR." *Zygote (Cambridge, England)* 10 (3): 239–43. http://www.ncbi.nlm.nih.gov/pubmed/12214805.

DV Huyen, BM Bany. 2011. "Evidence for a Conserved Function of Heart and Neural Crest Derivatives Expressed Transcript 2 in Mouse and Human Decidualization." *Reproduction* 142: 353–68.

Ellis, Steven M, Kazuki Nabeshima, and Chitra Biswas. 1989. “Monoclonal Antibody Preparation and Purification of a Tumor Cell Collagenase-Stimulatory Factor1.” *CANCER RESEARCH*. Vol. 49. http://cancerres.aacrjournals.org/content/canres/49/12/3385.full.pdf.

Ema, Masatsugu, Daisuke Mori, Hitoshi Niwa, Yoshikazu Hasegawa, Yojiro Yamanaka, Seiji Hitoshi, Junsei Mimura, et al. 2008. “Krüppel-like Factor 5 Is Essential for Blastocyst Development and the Normal Self-Renewal of Mouse ESCs.” *Cell Stem Cell* 3 (5): 555–67. https://doi.org/10.1016/j.stem.2008.09.003.

Emilova, Viktoriya. 2012. “BASIGIN in TROPHOBLAST CELLS VIA MICROVESICLE SHEDDING Viktoriya Thesis.”

Finn, C. A., and L. Martin. 1974. “The Control of Implantation.” *Journal of Reproduction and Fertility*. https://doi.org/10.1530/jrf.0.0390195.

Floch, Renaud Le, Johanna Chiche, Ibtissam Marchiq, Tanesha Naiken, Tanesha Naïken, Karine Ilc, Karine Ilk, et al. 2011. “CD147 Subunit of Lactate/H+ Symporters MCT1 and Hypoxia-Inducible MCT4 Is Critical for Energetics and Growth of Glycolytic Tumors.” *Proceedings of the National Academy of Sciences of the United States of America* 108 (40): 16663–68. https://doi.org/10.1073/pnas.1106123108.

Fossum, Sigbj∅Rn, Susan Mallett, and A. Neil Barclay. 1991. “The MRC OX-47 Antigen Is a Member of the Immunoglobulin Superfamily with an Unusual Transmembrane Sequence.” *European Journal of Immunology* 21 (3): 671–79. https://doi.org/10.1002/eji.1830210320.

Franco, Heather L., Kevin Y. Lee, Russell R. Broaddus, Lisa D. White, Beate Lanske, John P. Lydon, Jae-Wook Jeong, and Francesco J. DeMayo. 2010. “Ablation of Indian Hedgehog in the Murine Uterus Results in Decreased Cell Cycle Progression, Aberrant Epidermal Growth Factor Signaling, and Increased Estrogen Signaling1.” *Biology of Reproduction* 82 (4): 783–90. https://doi.org/10.1095/biolreprod.109.080259.

Franco, Heather L., Cory A. Rubel, Michael J. Large, Margeaux Wetendorf, Rodrigo Fernandez-Valdivia, Jae-Wook Jeong, Thomas E. Spencer, Richard R. Behringer, John P. Lydon, and Francesco J. DeMayo. 2012. “Epithelial Progesterone Receptor Exhibits Pleiotropic Roles in Uterine Development and Function.” *The FASEB Journal* 26 (3): 1218–27. https://doi.org/10.1096/fj.11-193334.

Franco, Heather L, Daisy Dai, Kevin Y Lee, Cory A Rubel, Dennis Roop, Derek Boerboom, Jae-Wook Jeong, et al. n.d. “WNT4 Is a Key Regulator of Normal Postnatal Uterine Development and Progesterone Signaling during Embryo Implantation and Decidualization in the Mouse.” *The FASEB Journal • Research Communication*. Accessed April 20, 2020. https://doi.org/10.1096/fj.10-175349.

Gabison, Eric E, Thanh Hoang-Xuan, Alain Mauviel, and Suzanne Menashi. 2005. “EMMPRIN/CD147, an MMP Modulator in Cancer, Development and Tissue Repair.” *Biochimie* 87: 361–68. https://doi.org/10.1016/j.biochi.2004.09.023.

Gallagher, Shannon M., John J. Castorino, Dian Wang, and Nancy J. Philp. 2007. “Monocarboxylate Transporter 4 Regulates Maturation and Trafficking of CD147 to the

Plasma Membrane in the Metastatic Breast Cancer Cell Line MDA-MB-231." *Cancer Research* 67 (9): 4182–89. https://doi.org/10.1158/0008-5472.CAN-06-3184.

Genbacev, OD. 2003. "Trophoblast L-Selectin–Mediated Adhesion at the Maternal-Fetal Interface." *Science* 299: 405–8.

Grass, G Daniel, and P Bryan. 2016. "How , with Whom and When : An Overview of CD147-Mediated Regulatory Networks Influencing Matrix Metalloproteinase Activity." *Biosci. Rep.*, 1–16. https://doi.org/10.1042/BSR20150256.

Guindolet, Damien, and Gabison Eric. 2019. "Role of CD147 (EMMPRIN/Basigin) in Tissue Remodeling." *The Anatomical Record*. https://onlinelibrary.wiley.com/doi/pdf/10.1002/ar.24089.

Guleria, Indira, Arezou Khosroshahi, Mohammed Javeed Ansari, Antje Habicht, Miyuki Azuma, Hideo Yagita, Randolph J. Noelle, et al. 2005. "A Critical Role for the Programmed Death Ligand 1 in Fetomaternal Tolerance." *Journal of Experimental Medicine* 202 (2): 231–37. https://doi.org/10.1084/jem.20050019.

Guleria, Indira, and Mohamed H. Sayegh. 2007. "Maternal Acceptance of the Fetus: True Human Tolerance." *The Journal of Immunology* 178 (6): 3345–51. https://doi.org/10.4049/jimmunol.178.6.3345.

Guo, H M, S Zucker, M K Gordon, B P Toole, and C Biswas. 1997. "Stimulation of Matrix Metalloproteinase Production by Recombinant Extracellular-Matrix Metalloproteinase Inducer from Transfected Chinese-Hamster Ovary Cells." *Journal of Biological Chemistry* Vol 272 (Iss 1): 24–27.

H Lim, L Ma, WG Ma, RL Maas, SK Dey. 1999. "Hoxa-10 Regulates Uterine Stromal Cell Responsiveness to Progesterone during Implantation and Decidualization in the Mouse." *Mol. Endocrinol.* 13: 1005–17.

H Matsumoto, X Zhao, SK Das, BL Hogan, SK Dey. 2002. "Indian Hedgehog as a Progesterone-Responsive Factor Mediating Epithelial-Mesenchymal Interactions in the Mouse Uterus." *Dev. Biol.* 245: 280–90.

Hahn, J. N., D. K. Kaushik, and V. W. Yong. 2015. "The Role of EMMPRIN in T Cell Biology and Immunological Diseases." *Journal of Leukocyte Biology* 98 (1): 33–48. https://doi.org/10.1189/jlb.3RU0215-045R.

Halestrap, Andrew P. 2012. "The Monocarboxylate Transporter Family-Structure and Functional Characterization." *IUBMB Life* 64 (1): 1–9. https://doi.org/10.1002/iub.573.

Halestrap, Andrew P, and Nigel T Price. 1999. "The Proton-Linked Monocarboxylate Transporter (MCT) Family : Structure, Function and Regulation." *Biochem. J.* Vol. 343. https://www.ncbi.nlm.nih.gov/pmc/articles/PMC1220552/pdf/10510291.pdf.

Hamatani, Toshio, Mark G. Carter, Alexei A. Sharov, and Minoru S.H. Ko. 2004. "Dynamics of Global Gene Expression Changes during Mouse Preimplantation Development." *Developmental Cell* 6 (1): 117–31. https://doi.org/10.1016/S1534-5807(03)00373-3.

Hanna, S. Melanie, Peter Kirk, Oliver J. Holt, Michael J. Puklavec, Marion H. Brown, and A. Neil Barclay. 2003. "A Novel Form of the Membrane Protein CD147 That Contains an Extra Ig-like Domain and Interacts Homophilically." *BMC Biochemistry* 4: 1–9. https://doi.org/10.1186/1471-2091-4-17.

Hantak, Alison, Indrani Bagchi, and Milan Bagchi. 2014. "Role of Uterine Stromal-Epithelial Crosstalk in Embryo Implantation." *International Journal of Developmental Biology* 58 (0): 139–46. https://doi.org/10.1126/science.1249098.Sleep.

Harvey, A. J. 2007. "The Role of Oxygen in Ruminant Preimplantation Embryo Development and Metabolism." *Animal Reproduction Science* 98 (1–2): 113–28. https://doi.org/10.1016/j.anireprosci.2006.10.008.

Hasaneen, Nadia A., Jian Cao, Ashleigh Pulkoski-Gross, Stanley Zucker, and Hussein D. Foda. 2016. "Extracellular Matrix Metalloproteinase Inducer (EMMPRIN) Promotes Lung Fibroblast Proliferation, Survival and Differentiation to Myofibroblasts." *Respiratory Research* 17 (1): 17. https://doi.org/10.1186/s12931-016-0334-7.

Hayashi, Kanako, David W. Erikson, Sarah A. Tilford, Brent M. Bany, James A. Maclean, Edmund B. Rucker, Greg A. Johnson, and Thomas E. Spencer. 2009. "Wnt Genes in the Mouse Uterus: Potential Regulation of Implantation1." *Biology of Reproduction* 80 (5): 989–1000. https://doi.org/10.1095/biolreprod.108.075416.

He, Qiong, Lai Ling Tsang, Louis Chukwuemeka Ajonuma, and Hsiao Chang Chan. 2010. "Abnormally Up-Regulated Cystic Fibrosis Transmembrane Conductance Regulator Expression and Uterine Fluid Accumulation Contribute to Chlamydia Trachomatis-Induced Female Infertility." *Fertility and Sterility* 93 (8): 2608–14. https://doi.org/10.1016/j.fertnstert.2010.01.040.

Hérubel, François, Said El Mouatassim, Pierre Guérin, René Frydman, and Yves Ménézo. 2002. "Genetic Expression of Monocarboxylate Transporters during Human and Murine Oocyte Maturation and Early Embryonic Development." *Zygote (Cambridge, England)* 10 (2): 175–81. http://www.ncbi.nlm.nih.gov/pubmed/12056458.

Hiraishi, Katsuya, Tatsuo Ide, Fumie Jimma, Hiroshi Ohi, Fumiko Inokuchi, Teruo Miyauchi, and Keiji Suzuki. 2003. "Immunohistochemical Distribution of Human Basigin by Using a Novel Monoclonal Antibody." *Acta Histochemica Et Cytochemica* 36 (2): 135–44. https://doi.org/10.1267/ahc.36.135.

Hirota, Yasushi, Kristin E. Burnum, Nuray Acar, Gabriel A. Rabinovich, Takiko Daikoku, and Sudhansu K. Dey. 2012. "Galectin-1 Markedly Reduces the Incidence of Resorptions in Mice Missing Immunophilin FKBP52." *Endocrinology* 153 (5): 2486–93. https://doi.org/10.1210/en.2012-1035.

Hojo, Hironobu, Eiichiro Haginoya, Yoshiyuki Matsumoto, Yoshiaki Nakahara, Kazuki Nabeshima, Bryan P. Toole, and Yasushi Watanabe. 2003. "The First Synthesis of Peptide Thioester Carrying N-Linked Core Pentasaccharide through Modified Fmoc Thioester Preparation: Synthesis of an N-Glycosylated Ig Domain of Emmprin." *Tetrahedron Letters* 44 (14): 2961–64. https://doi.org/10.1016/S0040-4039(03)00394-0.

HS Taylor, P Igarashi, DL Olive, A Arici. 1999. “Sex Steroids Mediate HOXA11 Expression in the Human Peri-Implantation Endometrium.” *J. Clin. Endocrinol. Metab.* 84: 1129–35.

Huang, Zhouqing, Changqian Wang, Li Wei, Jun Wang, Yuqi Fan, Liansheng Wang, Yue Wang, and Ting Chen. 2008. “Resveratrol Inhibits EMMPRIN Expression via P38 and ERK1/2 Pathways in PMA-Induced THP-1 Cells.” *Biochemical and Biophysical Research Communications* 374 (3): 517–21. https://doi.org/10.1016/J.BBRC.2008.07.058.

Igakura, Tadahiko, Kenji Kadomatsu, Tadashi Kaname, Hisako Muramatsu, Qi Wen Fan, Teruo Miyauchi, Yoshiro Toyama, et al. 1998. “A Null Mutation in Basigin, an Immunoglobulin Superfamily Member, Indicates Its Important Roles in Peri-Implantation Development and Spermatogenesis.” *Developmental Biology* 194 (2): 152–65. https://doi.org/10.1006/dbio.1997.8819.

Illera, Maria J., Emily Cullinan, Yaoting Gui, Lingwen Yuan, Stan A. Beyler, and Bruce A. Lessey. 2000. “Blockade of the Avβ3 Integrin Adversely Affects Implantation in the Mouse1.” *Biology of Reproduction* 62 (5): 1285–90. https://doi.org/10.1095/biolreprod62.5.1285.

Jeong, J. W., H. S. Lee, H. L. Franco, R. R. Broaddus, M. M. Taketo, S. Y. Tsai, J. P. Lydon, and F. J. DeMayo. 2009. “β-Catenin Mediates Glandular Formation and Dysregulation of β-Catenin Induces Hyperplasia Formation in the Murine Uterus.” *Oncogene* 28 (1): 31–40. https://doi.org/10.1038/onc.2008.363.

Jin, Aihong, Hao Chen, Chaoqun Wang, Lai Ling Tsang, Xiaohua Jiang, Zhiming Cai, Hsiao Chang Chan, and Xiaping Zhou. 2014. “Elevated Expression of CD147 in Patients with Endometriosis and Its Role in Regulating Apoptosis and Migration of Human Endometrial Cells.” *Fertility and Sterility* 101 (6): 1681-1687.e1. https://doi.org/10.1016/j.fertnstert.2014.02.007.

Jin, Rong, Adam Y. Xiao, Rui Chen, D. Neil Granger, and Guohong Li. 2017. “Inhibition of CD147 (Cluster of Differentiation 147) Ameliorates Acute Ischemic Stroke in Mice by Reducing Thromboinflammation.” *Stroke* 48 (12): 3356–65. https://doi.org/10.1161/STROKEAHA.117.018839.

Kapur, Suman, Hiromichi Tamada, Sudhansu K. Dey, and Glen K. Andrews. 1992. “Expression of Insulin-Like Growth Factor-I (IGF-l) and Its Receptor in the Peri-Implantation Mouse Uterus, and Cell-Specific Regulation of IGF-l Gene Expression by Estradiol and Progesterone1.” *Biology of Reproduction* 46 (2): 208–19. https://doi.org/10.1095/biolreprod46.2.208.

Kataoka, Hiroaki, Rosana Decastro, Stanley Zucker, and Chitra Biswas3. 1993. “Tumor Cell-Derived Collagenase-Stimulatory Factor Increases Expression of Interstitial Collagenase, Stromelysin, and 72-KDa Gelatinase1.” *CANCER RESEARCH*. Vol. 53. http://cancerres.aacrjournals.org/content/canres/53/13/3154.full.pdf.

Ke, Xia, Fei Fei, Yanke Chen, Li Xu, Zheng Zhang, Qichao Huang, Hongxin Zhang, Hushan Yang, Zhinan Chen, and Jinliang Xing. 2012. “Hypoxia Upregulates CD147 through a Combined Effect of HIF-1?? And Sp1 to Promote Glycolysis and Tumor Progression in

Epithelial Solid Tumors." *Carcinogenesis* 33 (8): 1598–1607. https://doi.org/10.1093/carcin/bgs196.

Kefeli, Mehmet, Levent Yildiz, Seda Gun, Fatma Z. Ozen, and Filiz Karagoz. 2016. "EMMPRIN (CD147) Expression in Smooth Muscle Tumors of the Uterus." *International Journal of Gynecological Pathology* 35 (1): 1–7. https://doi.org/10.1097/PGP.0000000000000216.

Khoury, Samia J, and Mohamed H Sayegh. 2004. "The Roles of the New Negative T Cell Costimulatory Pathways in Regulating Autoimmunity." *Immunity* 20 (5): 529–38. https://doi.org/10.1016/s1074-7613(04)00116-5.

Kimber, Susan J., and Catherine Spanswick. 2000. "Blastocyst Implantation: The Adhesion Cascade." *Seminars in Cell and Developmental Biology* 11 (2): 77–92. https://doi.org/10.1006/scdb.2000.0154.

Kirk, P, M C Wilson, C Heddle, M H Brown, a N Barclay, and a P Halestrap. 2000. "CD147 Is Tightly Associated with Lactate Transporters MCT1 and MCT4 and Facilitates Their Cell Surface Expression." *The EMBO Journal* 19 (15): 3896–3904. https://doi.org/10.1093/emboj/19.15.3896.

Knutti, Nadine, Otmar Huber, and Karlheinz Friedrich. 2019. "CD147 (EMMPRIN) Controls Malignant Properties of Breast Cancer Cells by Interdependent Signaling of Wnt and JAK/STAT Pathways." *Molecular and Cellular Biochemistry* 451 (1–2): 197–209. https://doi.org/10.1007/s11010-018-3406-9.

Knutti, Nadine, Michael Kuepper, and Karlheinz Friedrich. 2015. "Soluble Extracellular Matrix Metalloproteinase Inducer (EMMPRIN, EMN) Regulates Cancer-Related Cellular Functions by Homotypic Interactions with Surface CD147." *FEBS Journal* 282 (21): 4187–4200. https://doi.org/10.1111/febs.13414.

Koch, C, G Staffler, R Hüttinger, I Hilgert, E Prager, J Cerný, P Steinlein, O Majdic, V Horejsí, and H Stockinger. 1999. "T Cell Activation-Associated Epitopes of CD147 in Regulation of the T Cell Response, and Their Definition by Antibody Affinity and Antigen Density." *International Immunology* 11 (5): 777–86. http://www.ncbi.nlm.nih.gov/pubmed/10330283.

Ku, X. M., C. G. Liao, Y. Li, X. M. Yang, B. Yang, X. Y. Yao, L. Wang, L. M. Kong, P. Zhao, and Z. N. Chen. 2007. "Epitope Mapping of Series of Monoclonal Antibodies against the Hepatocellular Carcinoma-Associated Antigen HAb18G/CD147." *Scandinavian Journal of Immunology* 65 (5): 435–43. https://doi.org/10.1111/j.1365-3083.2007.01930.x.

Kuno, Naohiko, Kenji Kadomatsu, Qi Wen Fan, Masako Hagihara, Takao Senda, Shigehiko Mizutani, and Takashi Muramatsu. 1998. "Female Sterility in Mice Lacking the Basigin Gene, Which Encodes a Transmembrane Glycoprotein Belonging to the Immunoglobulin Superfamily." *FEBS Letters* 425 (2): 191–94. https://doi.org/10.1016/S0014-5793(98)00213-0.

Kurihara, Isao, Dong Kee Lee, Fabrice G. Petit, Jaewook Jeong, Kevin Lee, John P. Lydon, Francesco J. DeMayo, Ming Jer Tsai, and Sophia Y. Tsai. 2007. "COUP-TFII Mediates Progesterone Regulation of Uterine Implantation by Controlling ER Activity." *PLoS Genetics*

3 (6): 1053–64. https://doi.org/10.1371/journal.pgen.0030102.

Kwon, Hye Eun, and Hugh S. Taylor. 2004. “The Role of HOX Genes in Human Implantation.” In *Annals of the New York Academy of Sciences*, 1034:1–18. New York Academy of Sciences. https://doi.org/10.1196/annals.1335.001.

Lee, Cheuk Lun, Maggie P.Y. Y Lam, Kevin K.W. W Lam, Carmen O.N. N Leung, Ronald T.K. K Pang, Ivan K. Chu, Tiffany H.L. L Wan, Joyce Chai, William S.B. B Yeung, and Philip C.N. N Chiu. 2013. “Identification of CD147 (Basigin) as a Mediator of Trophoblast Functions.” *Human Reproduction* 28 (11): 2920–29. https://doi.org/10.1093/humrep/det355.

Lee, Dong Kee, Isao Kurihara, Jae Wook Jeong, John P. Lydon, Francesco J. DeMayo, Ming Jer Tsai, and Sophia Y. Tsai. 2010. “Suppression of ERα Activity by COUP-TFII Is Essential for Successful Implantation and Decidualization.” *Molecular Endocrinology* 24 (5): 930–40. https://doi.org/10.1210/me.2009-0531.

Lee, Jae Hee, Tae Hoon Kim, Seo Jin Oh, Jung Yoon Yoo, Shizuo Akira, Bon Jeong Ku, John P. Lydon, and Jae Wook Jeong. 2013. “Signal Transducer and Activator of Transcription-3 (Stat3) Plays a Critical Role in Implantation via Progesterone Receptor in Uterus.” *FASEB Journal* 27 (7): 2553–63. https://doi.org/10.1096/fj.12-225664.

Lee, Je Hoon, Sakhila K. Banu, Thenmozhi Subbarao, Anna Starzinski-Powitz, and Joe A. Arosh. 2011. “Selective Inhibition of Prostaglandin E2 Receptors EP2 and EP4 Inhibits Invasion of Human Immortalized Endometriotic Epithelial and Stromal Cells through Suppression of Metalloproteinases.” *Molecular and Cellular Endocrinology* 332 (1–2): 306–13. https://doi.org/10.1016/j.mce.2010.11.022.

Lee, K. Y., J.-W. Jeong, J. Wang, L. Ma, J. F. Martin, S. Y. Tsai, J. P. Lydon, and F. J. DeMayo. 2007. “Bmp2 Is Critical for the Murine Uterine Decidual Response.” *Molecular and Cellular Biology* 27 (15): 5468–78. https://doi.org/10.1128/mcb.00342-07.

Lee, Kevin, Jae Wook Jeong, Inseok Kwak, Cheng Tai Yu, Beate Lanske, Desi W. Soegiarto, Rune Toftgard, et al. 2006. “Indian Hedgehog Is a Major Mediator of Progesterone Signaling in the Mouse Uterus.” *Nature Genetics* 38 (10): 1204–9. https://doi.org/10.1038/ng1874.

Lessey, B. A., A. J. Castelbaum, S. W. Sawin, and J. Sun. 1995. “Integrins as Markers of Uterine Receptivity in Women with Primary Unexplained Infertility.” *Fertility and Sterility* 63 (3): 535–42. https://doi.org/10.1016/S0015-0282(16)57422-6.

Lessey, Bruce A. 2011. “Assessment of Endometrial Receptivity.” *Fertility and Sterility* 96 (3): 522–29. https://doi.org/10.1016/j.fertnstert.2011.07.1095.

Li, Min, Qihui Zhai, Uddalak Bharadwaj, Hao Wang, Fei Li, William E. Fisher, Changyi Chen, et al. 2006. “Cyclophilin A Is Overexpressed in Human Pancreatic Cancer Cells and Stimulates Cell Proliferation through CD147.” *Cancer* 106 (10): 2284–94. https://doi.org/10.1002/cncr.21862.

Li, Qing-Quan, Wen-Juan Wang, Jing-Da XU, Xi-Xi Cao, Qi Chen, Jin-Ming Yang, and Zu-De Xu. 2007. “Involvement of CD147 in Regulation of Multidrug Resistance to P-Gp Substrate

Drugs and in Vitro Invasion in Breast Cancer Cells." *Cancer Science* 98 (7): 1064–69. https://doi.org/10.1111/j.1349-7006.2007.00487.x.

Li, Quanxi, Athilakshmi Kannan, Wei Wang, Francesco J. DeMayo, Robert N. Taylor, Milan K. Bagchi, and Indrani C. Bagchi. 2007. "Bone Morphogenetic Protein 2 Functions via a Conserved Signaling Pathway Involving Wnt4 to Regulate Uterine Decidualization in the Mouse and the Human." *Journal of Biological Chemistry* 282 (43): 31725–32. https://doi.org/10.1074/jbc.M704723200.

Li, Quanxi, Jun Wang, D. Randall Armant, Milan K. Bagchi, and Indrani C. Bagchi. 2002. "Calcitonin Down-Regulates E-Cadherin Expression in Rodent Uterine Epithelium during Implantation." *Journal of Biological Chemistry* 277 (48): 46447–55. https://doi.org/10.1074/jbc.M203555200.

Li, Quanxi, Hiroyuki Yamagishi, Deepak Srivastava, Milan K Bagchi, and Indrani C Bagchi. 2011. "The Antiproliferative Action of Progesterone in Uterine Epithelium Is Mediated by Hand2." *Science* 331 (February): 912–17.

Li, Wei, Nadia Alfaidy, and John R.G. Challis. 2004. "Expression of Extracellular Matrix Metalloproteinase Inducer in Human Placenta and Fetal Membranes at Term Labor." *Journal of Clinical Endocrinology and Metabolism* 89 (6): 2897–2904. https://doi.org/10.1210/jc.2003-032048.

Liang, Qinchuan, Hua Xiong, Guodong Gao, Kanghui Xiong, Xuelian Wang, Zhenwei Zhao, Hua Zhang, and Yonglin Li. 2005. "Inhibition of Basigin Expression in Glioblastoma Cell Line via Antisense RNA Reduces Tumor Cell Invasion and Angiogenesis." *Cancer Biology & Therapy* 4 (7): 759–62. https://doi.org/10.4161/cbt.4.7.1828.

Liao, C.-G., L.-M. Kong, F. Song, J.-L. Xing, L.-X. Wang, Z.-J. Sun, H. Tang, et al. 2011. "Characterization of Basigin Isoforms and the Inhibitory Function of Basigin-3 in Human Hepatocellular Carcinoma Proliferation and Invasion." *Molecular and Cellular Biology* 31 (13): 2591–2604. https://doi.org/10.1128/MCB.05160-11.

Lim, Hyunjung Jade, S K Dey, and H Jade Lim. 2009. "HB-EGF: A Unique Mediator of Embryo-Uterine Interactions during Implantation." *Exp Cell Res* 315 (4): 619–26. https://doi.org/10.1016/j.yexcr.2008.07.025.

Lim, Hyunjung Jade, and Haibin Wang. 2010. "Review Series Uterine Disorders and Pregnancy Complications : Insights from Mouse Models." *The Journal of Clinical Investigation* 120 (4): 1004–15. https://doi.org/10.1172/JCI41210.1004.

Lim, Melissa, Tom Martinez, David Jablons, Robert Cameron, Huiming Guo, Bryan Toole, Jian-dong Li, and Carol Basbaum. 1998. "Tumor-Derived EMMPRIN (Extracellular Matrix Metalloproteinase Inducer) Stimulates Collagenase Transcription through MAPK P38." *FEBS Letters* 441 (1): 88–92. https://doi.org/10.1016/S0014-5793(98)01474-4.

Lindgren, Karin E., Fatma Gülen Yaldir, Julius Hreinsson, Jan Holte, Karin Kårehed, Inger Sundström-Poromaa, Helena Kaihola, and Helena Åkerud. 2018. "Differences in Secretome in Culture Media When Comparing Blastocysts and Arrested Embryos Using Multiplex

Proximity Assay." *Upsala Journal of Medical Sciences* 123 (3): 143–52. https://doi.org/10.1080/03009734.2018.1490830.

Margarit, L, D Gonzalez, P D Lewis, L Hopkins, C Davies, R S Conlan, L Joels, and J O White. 2009. "L-Selectin Ligands in Human Endometrium: Comparison of Fertile and Infertile Subjects." *Human Reproduction* 24 (11): 2767–77. https://doi.org/10.1093/humrep/dep247.

McDonnel Smedts, A., and T.E. Curry. 2005. "Expression of Basigin, an Inducer of Matrix Metalloproteinases, in the Rat Ovary1." *Biology of Reproduction* 73 (1): 80–87. https://doi.org/10.1095/biolreprod.104.036145.

McMahon, Andrew P. 2000. "More Surprises in the Hedgehog Signaling Pathway." *Cell*. Cell Press. https://doi.org/10.1016/S0092-8674(00)81555-X.

Menkhorst, Ellen, Jian-Guo Zhang, Natalie A. Sims, Phillip O. Morgan, Priscilla Soo, Ingrid J. Poulton, Donald Metcalf, et al. 2011. "Vaginally Administered PEGylated LIF Antagonist Blocked Embryo Implantation and Eliminated Non-Target Effects on Bone in Mice." Edited by Lisa Ng Fong Poh. *PLoS ONE* 6 (5): e19665. https://doi.org/10.1371/journal.pone.0019665.

Meziani, Ferhat, Angela Tesse, Eric David, M. Carmen Martinez, Rosemarie Wangesteen, Francis Schneider, and Ramaroson Andriantsitohaina. 2006. "Shed Membrane Particles from Preeclamptic Women Generate Vascular Wall Inflammation and Blunt Vascular Contractility." *American Journal of Pathology* 169 (4): 1473–83. https://doi.org/10.2353/ajpath.2006.051304.

Millimaggi, Danilo, Marianna Mari, Sandra D'Ascenzo, Eleonora Carosa, Emmanuele Angelo Jannini, Stanley Zucker, Gaspare Carta, Antonio Pavan, and Vincenza Dolo. 2007. "Tumor Vesicle—Associated CD147 Modulates the Angiogenic Capability of Endothelial Cells." *Neoplasia* 9 (4): 349–57. https://doi.org/10.1593/neo.07133.

Mishra, B., K. Kizaki, T. Sato, a. Ito, and K. Hashizume. 2012. "The Role of Extracellular Matrix Metalloproteinase Inducer (EMMPRIN) in the Regulation of Bovine Endometrial Cell Functions." *Biology of Reproduction* 87 (October): 1–8. https://doi.org/10.1095/biolreprod.112.102152.

Miyauchi, Teruo, Yasushi Masuzawa, and Takashi Muramatsu. 1991. "The Basigin Group of the Immunoglobulin Superfamily: Complete Conservation of a Segment in and around Transmembrane Domains of Human and Mouse Basigin and Chicken HT7 Antigen." *Journal of Biochemistry* 110 (5): 770–74. https://doi.org/10.1093/oxfordjournals.jbchem.a123657.

Mori, Kouki, Makoto Nishimura, Masato Tsurudome, Morihiro Ito, Machiko Nishio, Mitsuo Kawano, Yuuji Kozuka, et al. 2004. "The Functional Interaction between CD98 and CD147 in Regulation of Virus-Induced Cell Fusion and Osteoclast Formation." *Medical Microbiology and Immunology* 193 (4): 155–62. https://doi.org/10.1007/s00430-003-0191-0.

Mori, Mayumi, Miwako Kitazume, Rui Ose, Jun Kurokawa, Kaori Koga, Yutaka Osuga, Satoko Arai, and Toru Miyazaki. 2011. "Death Effector Domain-Containing Protein (DEDD) Is Required for Uterine Decidualization during Early Pregnancy in Mice." *Journal of Clinical*

Investigation 121 (1): 318–27. https://doi.org/10.1172/JCI44723.

Mulac-Jericevic, B., R. A. Mullinax, F. J. DeMayo, J. P. Lydon, and O. M. Conneely. 2000. "Subgroup of Reproductive Functions of Progesterone Mediated by Progesterone Receptor-B Isoform." *Science* 289 (5485): 1751–54. https://doi.org/10.1126/science.289.5485.1751.

Muramatsu, Takashi. 2016. "Basigin (CD147), a Multifunctional Transmembrane Glycoprotein with Various Binding Partners." *Journal of Biochemistry* 159 (5): 481–90. https://doi.org/10.1093/jb/mvv127.

Muramatsu, Takashi, and T. Miyauchi. 2003. "Basigin (CD147): A Multifunctional Transmembrane Protien Involved in Reproduction, Neural Function, Inflammation and Tumor Invasion." *Histology and Histopathology* 18 (3): 981–87.

Nabeshima, Kazuki, Hiroshi Iwasaki, Kaori Koga, Hironobu Hojo, Junji Suzumiya, and Masahiro Kikuchi. 2006. "Emmprin (Basigin/CD147): Matrix Metalloproteinase Modulator and Multifunctional Cell Recognition Molecule That Plays a Critical Role in Cancer Progression." *Pathology International* 56 (7): 359–67. https://doi.org/10.1111/j.1440-1827.2006.01972.x.

Nabeshima, Kazuki, Junji Suzumiya, Mitsuyuki Nagano, Koichi Ohshima, Bryan P. Toole, Kazuo Tamura, Hiroshi Iwasaki, and Masahiro Kikuchi. 2004. "Emmprin, a Cell Surface Inducer of Matrix Metalloproteinases (MMPs), Is Expressed in T-Cell Lymphomas." *Journal of Pathology* 202 (3): 341–51. https://doi.org/10.1002/path.1518.

Nagai, A., K. Takebe, J. Nio-Kobayashi, H. Takahashi-Iwanaga, and T. Iwanaga. 2010. "Cellular Expression of the Monocarboxylate Transporter (MCT) Family in the Placenta of Mice." *Placenta* 31 (2): 126–33. https://doi.org/10.1016/j.placenta.2009.11.013.

Nallasamy, Shanmugasundaram, Quanxi Li, Milan K. Bagchi, and Indrani C. Bagchi. 2012. "Msx Homeobox Genes Critically Regulate Embryo Implantation by Controlling Paracrine Signaling between Uterine Stroma and Epithelium." *PLoS Genetics* 8 (2): e1002500. https://doi.org/10.1371/journal.pgen.1002500.

Naruhashi, Kazumasa, Kenji Kadomatsu, Tadahiko Igakura, Qi Wen Fan, Naohiko Kuno, Hisako Muramatsu, Teruo Miyauchi, et al. 1997. "Abnormalities of Sensory and Memory Functions in Mice Lacking Bsg Gene." *Biochemical and Biophysical Research Communications* 236 (3): 733–37. https://doi.org/10.1006/bbrc.1997.6993.

Nehme, Cheryl L, Barbara E Fayost, and James R Bartlest. 1995. "Distribution of the Integral Plasma Membrane Glycoprotein CE9 (MRC OX-47) among Rat Tissues and Its Induction by Diverse Stimuli of Metabolic Activation." *Biochem. J.* Vol. 310. https://www.ncbi.nlm.nih.gov/pmc/articles/PMC1135951/pdf/biochemj00056-0321.pdf.

Nobuzane, Takahiro, Satoshi Tashiro, and Yoshiki Kudo. 2008. "Morphologic Effects of Epithelial Ion Channels on the Mouse Uterus: Differences between Raloxifene Analog (LY117018) and Estradiol Treatments." *American Journal of Obstetrics and Gynecology* 199 (4): 363.e1-363.e6. https://doi.org/10.1016/j.ajog.2008.03.047.

Noguchi, Yutaka, Takashi Sato, Michiko Hirata, Tetsuaki Hara, Koso Ohama, and Akira Ito. 2003. "Identification and Characterization of Extracellular Matrix Metalloproteinase Inducer in Human Endometrium during the Menstrual Cycle in Vivo and in Vitro." *The Journal of Clinical Endocrinology and Metabolism* 88 (12): 6063–72. https://doi.org/10.1210/jc.2003-030457.

Ochrietor, Judith D., and Paul J. Linser. 2004. "5A11/Basigin Gene Products Are Necessary for Proper Maturation and Function of the Retina." *Developmental Neuroscience* 26 (5–6): 380–87. https://doi.org/10.1159/000082280.

Ozler, Ali, Mehmet Sıddık Evsen, Abdulkadir Turgut, Muhammet Erdal Sak, Senem Yaman Tunc, Elif Agacayak, Ulas Alabalik, Serdar Basaranoglu, Ayse Nur Keles, and Talip Gul. 2014. "CD147 Expression in Uterine Smooth Muscle Tumors, and Its Potential Role as a Diagnostic and Prognostic Marker in Patients with Leiomyosarcoma." *Journal of Experimental Therapeutics & Oncology* 10 (4): 325–30. http://www.ncbi.nlm.nih.gov/pubmed/25509988.

Pampfer, Serge, and Isabelle Donnay. 1999. "Apoptosis at the Time of Embryo Implantation in Mouse and Rat." *Cell Death and Differentiation* 6 (6): 533–45. https://doi.org/10.1038/sj.cdd.4400516.

Paria, B C, W Ma, J Tan, S Raja, S K Das, S K Dey, and B L Hogan. 2001. "Cellular and Molecular Responses of the Uterus to Embryo Implantation Can Be Elicited by Locally Applied Growth Factors." *Proceedings of the National Academy of Sciences of the United States of America* 98 (3): 1047–52. https://doi.org/10.1073/pnas.98.3.1047.

Paria, Bibhash C., Xuemei Zhao, Sanjoy K. Das, Sudhansu K. Dey, and Koji Yoshinaga. 1999. "Zonula Occludens-1 and E-Cadherin Are Coordinately Expressed in the Mouse Uterus with the Initiation of Implantation and Decidualization." *Developmental Biology* 208 (2): 488–501. https://doi.org/10.1006/dbio.1999.9206.

Pawar, Sandeep, Alison M. Hantak, Indrani C. Bagchi, and Milan K. Bagchi. 2014. "Minireview: Steroid-Regulated Paracrine Mechanisms Controlling Implantation." *Molecular Endocrinology* 28 (9): 1408–22. https://doi.org/10.1210/me.2014-1074.

Pawar, Sandeep, Elina Starosvetsky, Grant D. Orvis, Richard R. Behringer, Indrani C. Bagchi, and Milan K. Bagchi. 2013. "STAT3 Regulates Uterine Epithelial Remodeling and Epithelial-Stromal Crosstalk During Implantation." *Molecular Endocrinology* 27 (12): 1996–2012. https://doi.org/10.1210/me.2013-1206.

Peng, Sha, Jing Li, Chenglin Miao, Liwei Jia, Zeng Hu, Ping Zhao, Juxue Li, Ying Zhang, Qi Chen, and Enkui Duan. 2008. "Dickkopf-1 Secreted by Decidual Cells Promotes Trophoblast Cell Invasion during Murine Placentation." *Reproduction* 135 (3): 367–75. https://doi.org/10.1530/REP-07-0191.

Philp, Nancy J., Judith D. Ochrietor, Carla Rudoy, Takashi Muramatsu, and Paul J. Linser. 2003. "Loss of MCT1, MCT3, and MCT4 Expression in the Retinal Pigment Epithelium and Neural Retina of the 5A11/Basigin-Null Mouse." *Investigative Opthalmology & Visual Science* 44 (3): 1305. https://doi.org/10.1167/iovs.02-0552.

Pistol, Gina, Cristiana Matache, Ana Calugaru, Crina Stavaru, Stefanita Tanaseanu, Ruxandra Ionescu, Sergiu Dumitrache, and Maria Stefanescu. 2007. “Roles of CD147 on T Lymphocytes Activation and MMP-9 Secretion in Systemic Lupus Erythematosus.” *Journal of Cellular and Molecular Medicine* 11 (2): 339–48. https://doi.org/10.1111/j.1582-4934.2007.00022.x.

Q Wei, ED Levens, L Stefansson, LK Nieman. 2010. “Indian Hedgehog and Its Targets in Human Endometrium: Menstrual Cycle Expression and Response to CDB-2914.” *J. Clin. Endocrinol. Metab.* 95: 5330–37.

Rabinovich, G. A., F. T. Liu, M. Hirashima, and A. Anderson. 2007. “An Emerging Role for Galectins in Tuning the Immune Response: Lessons from Experimental Models of Inflammatory Disease, Autoimmunity and Cancer.” *Scandinavian Journal of Immunology*. https://doi.org/10.1111/j.1365-3083.2007.01986.x.

Rahman, Mohammad A., Meiling Li, Ping Li, Haibin Wang, Sudhansu K. Dey, and Sanjoy K. Das. 2006. “Hoxa-10 Deficiency Alters Region-Specific Gene Expression and Perturbs Differentiation of Natural Killer Cells during Decidualization.” *Developmental Biology* 290 (1): 105–17. https://doi.org/10.1016/j.ydbio.2005.11.016.

Ramathal, Cyril, Indrani Bagchi, Robert Taylor, and Milan Bagchi. 2010. “ENDOMETRIAL DECIDUALIZATION: OF MICE AND MEN.” *Semin Reprod Med* 28 (1): 17–26. https://doi.org/10.1055/s-0029-1242989.ENDOMETRIAL.

Ramathal, Cyril, Wei Wang, Elizabeth Hunt, Indrani C. Bagchi, and Milan K. Bagchi. 2011. “Transcription Factor CCAAT Enhancer-Binding Protein β (C/EBPβ) Regulates the Formation of a Unique Extracellular Matrix That Controls Uterine Stromal Differentiation and Embryo Implantation.” *Journal of Biological Chemistry* 286 (22): 19860–71. https://doi.org/10.1074/jbc.M110.191759.

Rashid, Najwa A., Sujata Lalitkumar, Parameswaran G. Lalitkumar, and Kristina Gemzell-Danielsson. 2011. “Endometrial Receptivity and Human Embryo Implantation.” *American Journal of Reproductive Immunology* 66 (SUPPL. 1): 23–30. https://doi.org/10.1111/j.1600-0897.2011.01048.x.

Reardon, Sarah N., Mandy L. King, James A. MacLean, Jordan L. Mann, Francesco J. DeMayo, John P. Lydon, and Kanako Hayashi. 2012. “Cdh1 Is Essential for Endometrial Differentiation, Gland Development, and Adult Function in the Mouse Uterus1.” *Biology of Reproduction* 86 (5). https://doi.org/10.1095/biolreprod.112.098871.

Red-Horse, Kristy, Yan Zhou, Olga Genbacev, Akraporn Prakobphol, Russell Foulk, Michael McMaster, and Susan J. Fisher. 2004. “Trophoblast Differentiation during Embryo Implantation and Formation of the Maternal-Fetal Interface.” *Journal of Clinical Investigation* 114 (6): 744–54. https://doi.org/10.1172/jci22991.

Redzic, Jasmina S., Geoffrey S. Armstrong, Nancy G. Isern, David N M Jones, Jeffrey S. Kieft, and Elan Zohar Eisenmesser. 2011. “The Retinal Specific CD147 Ig0 Domain: From Molecular Structure to Biological Activity.” *Journal of Molecular Biology* 411 (1): 68–82. https://doi.org/10.1016/j.jmb.2011.04.060.

Romão, Mariana, Ingrid Cristina Weel, Shirlee Jaffe Lifshitz, Maria Terezinha Serrão Peraçoli, and Steven S. Witkin. 2014. "Elevated Hyaluronan and Extracellular Matrix Metalloproteinase Inducer Levels in Women with Preeclampsia." *Archives of Gynecology and Obstetrics* 289 (3): 575–79. https://doi.org/10.1007/s00404-013-3021-7.

Rossant, Janet. 2016. "Making the Mouse Blastocyst: Past, Present, and Future." In *Current Topics in Developmental Biology*, 117:275–88. Academic Press Inc. https://doi.org/10.1016/bs.ctdb.2015.11.015.

Ruan, Ye Chun, Jing Hui Guo, Xinmei Liu, Runju Zhang, Lai Ling Tsang, Jian Da Dong, Hui Chen, et al. 2012. "Activation of the Epithelial Na+ Channel Triggers Prostaglandin E2 Release and Production Required for Embryo Implantation." *Nature Medicine* 18 (7): 1112–17. https://doi.org/10.1038/nm.2771.

Salleh, N., D. L. Baines, R. J. Naftalin, and S. R. Milligan. 2005. "The Hormonal Control of Uterine Luminal Fluid Secretion and Absorption." *Journal of Membrane Biology* 206 (1): 17–28. https://doi.org/10.1007/s00232-005-0770-7.

Sameshima, T, K Nabeshima, B P Toole, K Yokogami, Y Okada, T Goya, M Koono, and S Wakisaka. 2000. "Glioma Cell Extracellular Matrix Metalloproteinase Inducer (EMMPRIN) (CD147) Stimulates Production of Membrane-Type Matrix Metalloproteinases and Activated Gelatinase A in Co-Cultures with Brain-Derived Fibroblasts." *Cancer Letters* 157 (2): 177–84. http://www.ncbi.nlm.nih.gov/pubmed/10936678.

Saxena, Dinesh K., and Kiyotaka Toshimori. 2004. "Molecular Modifications of MC31/CE9, a Sperm Surface Molecule, During Sperm Capacitation and the Acrosome Reaction in the Rat: Is MC31/CE9 Required for Fertilization?1." *Biology of Reproduction* 70 (4): 993–1000. https://doi.org/10.1095/biolreprod.103.021667.

Schlafke, S., A. O. Welsh, and A. C. Enders. 1985. "Penetration of the Basal Lamina of the Uterine Luminal Epithelium during Implantation in the Rat." *The Anatomical Record* 212 (1): 47–56. https://doi.org/10.1002/ar.1092120107.

Schlosshauer, B, and K H Herzog. 1990. "Neurothelin: An Inducible Cell Surface Glycoprotein of Blood-Brain Barrier-Specific Endothelial Cells and Distinct Neurons." *The Journal of Cell Biology* 110 (4): 1261–74. http://www.ncbi.nlm.nih.gov/pubmed/2324198.

Seizer, Peter, Meinrad Gawaz, and Andreas E. May. 2014. "Cyclophilin A and EMMPRIN (CD147) in Cardiovascular Diseases." *Cardiovascular Research* 102 (1): 17–23. https://doi.org/10.1093/cvr/cvu035.

Seulberger, Harald, Carolin M. Unger, and Werner Risau. 1992. "HT7, Neurothelin, Basigin, Gp42 and OX-47 - Many Names for One Developmentally Regulated Immuno-Globulin-like Surface Glycoprotein on Blood-Brain Barrier Endothelium, Epithelial Tissue Barriers and Neurons." *Neuroscience Letters* 140 (1): 93–97. https://doi.org/10.1016/0304-3940(92)90690-9.

Shamonki, Mousa I., Isaac Kligman, Jaime M. Shamonki, Glenn L. Schattman, Elizabeth Hyjek, Steven D. Spandorfer, Nikica Zaninovic, and Zev Rosenwaks. 2006. "Immunohistochemical

Expression of Endometrial L-Selectin Ligand Is Higher in Donor Egg Recipients with Embryonic Implantation." *Fertility and Sterility* 86 (5): 1365–75. https://doi.org/10.1016/j.fertnstert.2006.04.035.

Shomer, Einat, Sarah Katzenell, Yaniv Zipori, Rami N. Sammour, Berend Isermann, Benjamin Brenner, and Anat Aharon. 2013. "Microvesicles of Women with Gestational Hypertension and Preeclampsia Affect Human Trophoblast Fate and Endothelial Function." *Hypertension* 62 (5): 893–98. https://doi.org/10.1161/HYPERTENSIONAHA.113.01494.

Sidhu, S S, R Nawroth, M Retz, H Lemjabbar-Alaoui, V Dasari, and C Basbaum. 2010. "EMMPRIN Regulates the Canonical Wnt/Beta-Catenin Signaling Pathway, a Potential Role in Accelerating Lung Tumorigenesis." *Oncogene* 29 (29): 4145–56. https://doi.org/10.1038/onc.2010.166.

Sidhu, Sukhvinder S., Aklilu T. Mengistab, Andrew N. Tauscher, Jennifer LaVail, and Carol Basbaum. 2004. "The Microvesicle as a Vehicle for EMMPRin in Tumor-Stromal Interactions." *Oncogene* 23 (4): 956–63. https://doi.org/10.1038/sj.onc.1207070.

Simmen, Rosalia C.M., Renea R. Eason, Jennelle R. McQuown, Amanda L. Linz, Tae Jung Kang, Leon Chatman, S. Reneé Till, Yoshiaki Fujii-Kuriyama, Frank A. Simmen, and S. Paul Oh. 2004. "Subfertility, Uterine Hypoplasia, and Partial Progesterone Resistance in Mice Lacking the Krüppel-like Factor 9/Basic Transcription Element-Binding Protein-1 (Bteb1) Gene." *Journal of Biological Chemistry* 279 (28): 29286–94. https://doi.org/10.1074/jbc.M403139200.

Singh, Harmeet, and John D. Aplin. 2009a. "Adhesion Molecules in Endometrial Epithelium: Tissue Integrity and Embryo Implantation." In *Journal of Anatomy*, 215:3–13. Wiley-Blackwell. https://doi.org/10.1111/j.1469-7580.2008.01034.x.

Smedts, Anna M., Subodh M. Lele, Susan C. Modesitt, and Thomas E. Curry. 2006. "Expression of an Extracellular Matrix Metalloproteinase Inducer (Basigin) in the Human Ovary and Ovarian Endometriosis." *Fertility and Sterility* 86 (3): 535–42. https://doi.org/10.1016/j.fertnstert.2006.01.042.

Song, Haengseok, Kyuyong Han, and Hyunjung Lim. 2007. "Progesterone Supplementation Extends Uterine Receptivity for Blastocyst Implantation in Mice." *Reproduction* 133 (2): 487–93. https://doi.org/10.1530/REP-06-0330.

Su, Juan, Xiang Chen, and Takuro Kanekura. 2009. "A CD147-Targeting SiRNA Inhibits the Proliferation, Invasiveness, and VEGF Production of Human Malignant Melanoma Cells by down-Regulating Glycolysis." *Cancer Letters* 273 (1): 140–47. https://doi.org/10.1016/j.canlet.2008.07.034.

Sukhikh, Gennady T., Natalia E. Kan, Victor L. Tyutyunnik, Maya V. Sannikova, Elena A. Dubova, Konstantin A. Pavlov, Elrad Y. Amiraslanov, and Nataliya V. Dolgushina. 2016. "The Role of Extracellular Inducer of Matrix Metalloproteinases in Premature Rupture of Membranes." *The Journal of Maternal-Fetal & Neonatal Medicine* 29 (4): 656–59. https://doi.org/10.3109/14767058.2015.1015416.

Sun, Jianxin, and Martin E Hemler. 2001. “Regulation of MMP-1 and MMP-2 Production through CD147 / Extracellular Matrix Metalloproteinase Inducer Interactions Regulation of MMP-1 and MMP-2 Production through CD147 / Extracellular Matrix.” *Cancer Research* 61: 2276–81.

Sun, Xiaofei, Liqian Zhang, Huirong Xie, Huajing Wan, Bliss Magella, Jeffrey A. Whitsett, and Sudhansu K. Dey. 2012. “Kruppel-like Factor 5 (KLF5) Is Critical for Conferring Uterine Receptivity to Implantation.” *Proceedings of the National Academy of Sciences of the United States of America* 109 (4): 1145–50. https://doi.org/10.1073/pnas.1118411109.

Szubert, Sebastian, Dariusz Szpurek, Rafal Moszynski, Michal Nowicki, Andrzej Frankowski, Stefan Sajdak, and Slawomir Michalak. 2014. “Extracellular Matrix Metalloproteinase Inducer (EMMPRIN) Expression Correlates Positively with Active Angiogenesis and Negatively with Basic Fibroblast Growth Factor Expression in Epithelial Ovarian Cancer.” *Journal of Cancer Research and Clinical Oncology* 140 (3): 361–69. https://doi.org/10.1007/s00432-013-1569-z.

Taglauer, Elizabeth S., Kristina M. Adams Waldorf, and Margaret G. Petroff. 2010. “The Hidden Maternal-Fetal Interface: Events Involving the Lymphoid Organs in Maternal-Fetal Tolerance.” *International Journal of Developmental Biology* 54 (2–3): 421–30. https://doi.org/10.1387/ijdb.082800et.

Takamoto, Norio, Bihong Zhao, Sophia Y. Tsai, and Francesco J. DeMayo. 2002. “Identification of Indian Hedgehog as a Progesterone-Responsive Gene in the Murine Uterus.” *Molecular Endocrinology* 16 (10): 2338–48. https://doi.org/10.1210/me.2001-0154.

Tang, J, Y-M Wu, P Zhao, X-M Yang, J-L Jiang, and Z-N Chen. 2008. “Overexpression of HAb18G/CD147 Promotes Invasion and Metastasis via Alpha3beta1 Integrin Mediated FAK-Paxillin and FAK-PI3K-Ca2+ Pathways.” *Cellular and Molecular Life Sciences : CMLS* 65 (18): 2933–42. https://doi.org/10.1007/s00018-008-8315-8.

Tang, wei, sharon Chang, Martin Hemler, and hemler martin. 2004. “Links between CD147 Function, Glycosylation, and Caveolin-1.” *Molecular Biology of the Cell* 15: 4043–50. https://doi.org/10.1091/mbc.E04.

Tang, Wei, and Martin E. Hemler. 2004. “Caveolin-1 Regulates Matrix Metalloproteinases-1 Induction and CD147/EMMPRIN Cell Surface Clustering.” *Journal of Biological Chemistry* 279 (12): 11112–18. https://doi.org/10.1074/jbc.M312947200.

Tang, Yi, Prabakaran Kesavan, Marian T Nakada, and Li Yan. 2004. “Tumor-Stroma Interaction: Positive Feedback Regulation of Extracellular Matrix Metalloproteinase Inducer (EMMPRIN) Expression and Matrix Metalloproteinase-Dependent Generation of Soluble EMMPRIN.” http://mcr.aacrjournals.org/content/2/2/73.full-text.pdf.

Tang, Yi, Marian T Nakada, Prabakaran Kesavan, Francis Mccabe, Hillary Millar, Patricia Rafferty, Peter Bugelski, and Li Yan. 2005. “Extracellular Matrix Metalloproteinase Inducer Stimulates Tumor Angiogenesis by Elevating Vascular Endothelial Cell Growth Factor and Matrix Metalloproteinases.” http://www.raybiotech.com.

Tang, Yi, Marian T Nakada, Patricia Rafferty, Jenny Laraio, Francis L Mccabe, Hillary Millar, Mark Cunningham, Linda A Snyder, Peter Bugelski, and Li Yan. 2006. "Regulation of Vascular Endothelial Growth Factor Expression by EMMPRIN via the PI3K-Akt Signaling Pathway." https://doi.org/10.1158/1541-7786.MCR-06-0042.

Tranguch, S., T. Daikoku, Y. Guo, H. Wang, and S. K. Dey. 2005. "Molecular Complexity in Establishing Uterine Receptivity and Implantation." *Cellular and Molecular Life Sciences* 62 (17): 1964–73. https://doi.org/10.1007/s00018-005-5230-0.

Tsou, Ann Ping, Chu Wen Yang, Chi Ying F. Huang, Ricky Chang Tze Yu, Yuan Chii G. Lee, Cha Wei Chang, Bo Rue Chen, et al. 2003. "Identification of a Novel Cell Cycle Regulated Gene, HURP, Overexpressed in Human Hepatocellular Carcinoma." *Oncogene* 22 (2): 298–307. https://doi.org/10.1038/sj.onc.1206129.

Turgut, A., N. Y. Goruk, S. Y. Tunc, E. Agaçayak, U. Alabalik, A. Yalinkaya, and T. Gül. 2014. "Expression of Extracellular Matrix Metalloproteinase Inducer (EMMPRIN) in the Endometrium of Patients with Repeated Implantation Failure after in Vitro Fertilization." *European Review for Medical and Pharmacological Sciences* 18 (2): 275–80.

VanWijk, Marja J., Kees Boer, Esther T. Van Der Meulen, Otto P. Bleker, Jos A.E. Spaan, and Ed VanBavel. 2002. "Resistance Artery Smooth Muscle Function in Pregnancy and Preeclampsia." *American Journal of Obstetrics and Gynecology* 186 (1): 148–54. https://doi.org/10.1067/mob.2002.119184.

VanWijk, Marja J., Eimantas Svedas, Kees Boer, Rienk Nieuwland, Ed VanBavel, and Karolina R. Kublickiene. 2002. "Isolated Microparticles, but Not Whole Plasma, from Women with Preeclampsia Impair Endothelium-Dependent Relaxation in Isolated Myometrial Arteries from Healthy Pregnant Women." *American Journal of Obstetrics and Gynecology* 187 (6): 1686–93. https://doi.org/10.1067/mob.2002.127905.

Vries, Wilhelmine N. de, Alexei V. Evsikov, Bryce E. Haac, Karen S. Fancher, Andrea E. Holbrook, Rolf Kemler, Davor Solter, and Barbara B. Knowles. 2004. "Maternal β-Catenin and E-Cadherin in Mouse Development." *Development* 131 (18): 4435–45. https://doi.org/10.1242/dev.01316.

Wakayama, Tomohiko, Kyoko Nagata, Kazumasa Ohashi, Kensaku Mizuno, Ichiro Tanii, Kazuya Yoshinaga, Tadasuke Oh-oka, and Kiyotaka Toshimori. 2000. "The Expression and Cellular Localization of the Sperm Flagellar Progein Mc31/Ce9 in the Rat Testis: Possible Post Transcriptional Regulation during Rat Spermiogenesis." *Archives of Histological Cytology* 63 (1): 33–41.

Walker, Michael P., Richard P. DiAugustine, Ernest Zeringue, Maureen K. Bunger, Martina Schmitt, Trevor K. Archer, and R. Gregg Richards. 2010. "An IGF1/Insulin Receptor Substrate-1 Pathway Stimulates a Mitotic Kinase (Cdk1) in the Uterine Epithelium during the Proliferative Response to Estradiol." *Journal of Endocrinology* 207 (2): 225–35. https://doi.org/10.1677/JOE-10-0102.

Wang, Bo, Jian Zhong Sheng, Rong Huan He, Yu Li Qian, Fan Jin, and He Feng Huang. 2008. "High Expression of L-Selectin Ligand in Secretory Endometrium Is Associated with Better

Endometrial Receptivity and Facilitates Embryo Implantation in Human Being." *American Journal of Reproductive Immunology* 60 (2): 127–34. https://doi.org/10.1111/j.1600-0897.2008.00604.x.

Wang, Chaoqun, Kin Lam Fok, Zhiming Cai, Hao Chen, and Hsiao Chang Chan. 2016. "CD147 Regulates Extrinsic Apoptosis in Spermatocytes by Modulating NFκB Signaling Pathways." *Oncotarget* 8 (2): 3132–43. https://doi.org/10.18632/oncotarget.13624.

Wang, Chaoqun, Kin Lam Fok, Zhiming Cai, Hao Chen, Hsiao Chang Chan, Chaoqun Wang, Kin Lam Fok, Zhiming Cai, Hao Chen, and Hsiao Chang Chan. 2017. "CD147 Regulates Extrinsic Apoptosis in Spermatocytes by Modulating NFkappaB Signaling Pathways." *Oncotarget* 8 (2): 3132–43. https://doi.org/10.18632/oncotarget.13624.

Wang, Chaoqun, Aihong Jin, Wenqing Huang, Lai Ling Tsang, Zhiming Cai, Xiaping Zhou, Hao Chen, and Hsiao Chang Chan. 2015. "Up-Regulation of Bcl-2 by CD147 through ERK Activation Results in Abnormal Cell Survival in Human Endometriosis." *Journal of Clinical Endocrinology and Metabolism* 100 (7): E955–63. https://doi.org/10.1210/jc.2015-1431.

Wang, Haibin, and Sudhansu K. Dey. 2006. "Roadmap to Embryo Implantation: Clues from Mouse Models." *Nature Reviews Genetics* 7 (3): 185–99. https://doi.org/10.1038/nrg1808.

Wang, Haibin, Shuang Zhang, Haiyan Lin, Shuangbo Kong, Shumin Wang, Hongmei Wang, and D. Randall Armant. 2013. "Physiological and Molecular Determinants of Embryo Implantation." *Molecular Aspects of Medicine* 34 (5): 939–80. https://doi.org/10.1016/j.mam.2012.12.011.

Wang, Weidong, Thomas Van De Water, and Thomas Lufkin. 1998. "Inner Ear and Maternal Reproductive Defects in Mice Lacking the Hmx3 Homeobox Gene." *Development* 125 (4): 621–34.

Wang, Xiaohong, Hiromichi Matsumoto, Xuemei Zhao, Sanjoy Das, and Bibhash Paria. 2004. "Embryonic Signals Direct the Formation of Tight Junctional Permeability Barrier in the Decidualizing Stroma during Embryo Implantation." *Journal of Cell Science* 117 (1): 53–62. https://doi.org/10.1242/jcs.00826.

Wang, Yong-qing, Shu-fang Mi, Jun Li, Yan-ling Wang, and Tao Shang. 2006. "[Differential Expression of Extracellular Matrix Metalloproteinase Inducer in Normal Placenta and Preeclampsia Placenta]." *Zhonghua Fu Chan Ke Za Zhi* 41 (7): 436–39. http://www.ncbi.nlm.nih.gov/pubmed/17083804.

Wang, Yuan, Lin Yuan, Xiang-Min Yang, Ding Wei, Bin Wang, Xiu-Xuan Sun, Fei Feng, et al. 2015. "A Chimeric Antibody Targeting CD147 Inhibits Hepatocellular Carcinoma Cell Motility via FAK-PI3K-Akt-Girdin Signaling Pathway." *Clin Exp Metastasis* 32: 39–53. https://doi.org/10.1007/s10585-014-9689-7.

Wassarman, Paul M. 1999. "Mammalian Fertilization: Molecular Aspects of Gamete Adhesion, Exocytosis, and Fusion." *Cell*. Cell Press. https://doi.org/10.1016/S0092-8674(00)80558-9.

Weidle, Ulrich H., Werner Scheuer, Daniela Eggle, Stefan Klostermann, and Hannes Stockinger.

2010. “Cancer-Related Issues of CD147.” *Cancer Genomics and Proteomics* 7 (3): 157–69.

Weiwei, Yu, Liu Jinhui, Xiong Xiaoliang, Ai Yousheng, and Wang Huamin. 2009. “Expression of MMP9 and CD147 in Invasive Squamous Cell Carcinoma of the Uterine Cervix and Their Implication.” *Pathology Research and Practice* 205 (10): 709–15. https://doi.org/10.1016/j.prp.2009.05.010.

Welsh, Alerick O., and Allen C. Enders. 1987. “Trophoblast-decidual Cell Interactions and Establishment of Maternal Blood Circulation in the Parietal Yolk Sac Placenta of the Rat.” *The Anatomical Record* 217 (2): 203–19. https://doi.org/10.1002/ar.1092170213.

Wesseling, Jelle, Sylvia W. Van Der Valk, and John Hilkens. 1996. “A Mechanism for Inhibition of E-Cadherin-Mediated Cell-Cell Adhesion by the Membrane-Associated Mucin Episialin/MUC1.” *Molecular Biology of the Cell* 7 (4): 565–77. https://doi.org/10.1091/mbc.7.4.565.

Wetendorf, Margeaux, and Francesco J. DeMayo. 2012. “The Progesterone Receptor Regulates Implantation, Decidualization, and Glandular Development via a Complex Paracrine Signaling Network.” *Molecular and Cellular Endocrinology* 357 (1–2): 108–18. https://doi.org/10.1016/j.mce.2011.10.028.

Winuthayanon, W., S. C. Hewitt, G. D. Orvis, R. R. Behringer, and K. S. Korach. 2010. “Uterine Epithelial Estrogen Receptor Is Dispensable for Proliferation but Essential for Complete Biological and Biochemical Responses.” *Proceedings of the National Academy of Sciences* 107 (45): 19272–77. https://doi.org/10.1073/pnas.1013226107.

Woodhead, V E, T J Stonehouse, M H Binks, K Speidel, D A Fox, A Gaya, D Hardie, et al. 2000. “Novel Molecular Mechanisms of Dendritic Cell-Induced T Cell Activation.” *International Immunology* 12 (7): 1051–61. http://www.ncbi.nlm.nih.gov/pubmed/10882417.

Wu, Xiaodong, and Marthe J. Howard. 2002. “Transcripts Encoding Hand Genes Are Differentially Expressed and Regulated by BMP4 and GDNF in Developing Avian Gut.” *Gene Expression* 10 (5–6): 279–93. https://doi.org/10.3727/000000002783992361.

Xiao, L. J., H. L. Diao, X. H. Ma, N. Z. Ding, K. Kadomatsu, T. Muramatsu, and Z. M. Yang. 2002. “Basigin Expression and Hormonal Regulation in the Rat Uterus during the Peri-Implantation Period.” *Reproduction* 124 (2): 219–25. https://doi.org/10.1002/mrd.10128.

Xie, H. 2007. “Maternal Heparin-Binding-EGF Deficiency Limits Pregnancy Success in Mice.” *Proc. Natl. Acad. Sci. USA* 104: 18315–20.

Xin, Xiaoyan, Xianqin Zeng, Huajian Gu, Min Li, Huaming Tan, Zhishan Jin, Teng Hua, Rui Shi, and Hongbo Wang. 2016. “CD147 / EMMPRIN Overexpression and Prognosis in Cancer : A Systematic Review And.” *Scientific Reports*, no. 113: 1–12. https://doi.org/10.1038/srep32804.

Xiong, Lijuan, Carl Edwards, and Lijun Zhou. 2014. “The Biological Function and Clinical Utilization of CD147 in Human Diseases: A Review of the Current Scientific Literature.” *International Journal of Molecular Sciences* 15 (10): 17411–41.

https://doi.org/10.3390/ijms151017411.

Xu, Daosong, and Martin E. Hemler. 2005. “Metabolic Activation-Related CD147-CD98 Complex.” *Molecular & Cellular Proteomics* 4 (8): 1061–71. https://doi.org/10.1074/mcp.M400207-MCP200.

Xu, Qin, Noriyuki Ohara, Jin Liu, Mariko Amano, Regine Sitruk-Ware, Shigeki Yoshida, and Takeshi Maruo. 2008. “Progesterone Receptor Modulator CDB-2914 Induces Extracellular Matrix Metalloproteinase Inducer in Cultured Human Uterine Leiomyoma Cells.” *Molecular Human Reproduction* 14 (3): 181–91. https://doi.org/10.1093/molehr/gan004.

Yamada, Aureo T., Juares R. Bianco, Eliana M.O. Lippe, Karina Y. Degaki, A.F. Dalmorin, Andrew K. Edwards, Patricia D.A. Lima, and Valdemar A. Paffaro. 2014. *Unique Features of Endometrial Dynamics During Pregnancy*. *The Guide to Investigation of Mouse Pregnancy*. Elsevier. https://doi.org/10.1016/B978-0-12-394445-0.00013-8.

Yang, Zeng-Ming -M, Su-Ping -P Le, Dong-Bao -B Chen, Juan Cota, Valentina Siero, Kiyoshi Yasukawa, and Michael J.K. Harper. 1995. “Leukemia Inhibitory Factor, LIF Receptor, and Gp130 in the Mouse Uterus during Early Pregnancy.” *Molecular Reproduction and Development* 42 (4): 407–14. https://doi.org/10.1002/mrd.1080420406.

Ying, Ying, and Guang-Quan Zhao. 2000. “Detection of Multiple Bone Morphogenetic Protein Messenger Ribonucleic Acids and Their Signal Transducer, Smad1, During Mouse Decidualization1.” *Biology of Reproduction* 63 (6): 1781–86. https://doi.org/10.1095/biolreprod63.6.1781.

Yoshinaga, Koji. 2012. “Two Concepts on the Immunological Aspect of Blastocyst Implantation.” *Journal of Reproduction and Development*. https://doi.org/10.1262/jrd.2011-027.

Yurchenko, V., S. Constant, E. Eisenmesser, and M. Bukrinsky. 2010. “Cyclophilin-CD147 Interactions: A New Target for Anti-Inflammatory Therapeutics.” *Clinical and Experimental Immunology* 160 (3): 305–17. https://doi.org/10.1111/j.1365-2249.2010.04115.x.

Yurchenko, Vyacheslav, Matthew O’connor, Wei Wei Dai, Huiming Guo, Bryan Toole, Barbara Sherry, and Michael Bukrinsky. 2001. “CD147 Is a Signaling Receptor for Cyclophilin B.” https://doi.org/10.1006/bbrc.2001.5847.

Yurchenko, Vyacheslav, Gabriele Zybarth, Matthew O’connor, Wei Wei Dai, Giovanni Franchin, Tang Hao, Huiming Guo, et al. 2002. “Active Site Residues of Cyclophilin A Are Crucial for Its Signaling Activity via CD147*.” https://doi.org/10.1074/jbc.M201593200.

Zamani, Nader, and Chester W. Brown. 2011. “Emerging Roles for the Transforming Growth Factor-β Superfamily in Regulating Adiposity and Energy Expenditure.” *Endocrine Reviews*. The Endocrine Society. https://doi.org/10.1210/er.2010-0018.

Zhao, Shu-Hua, Yu Wang, Li Wen, Zhen-Bo Zhai, Zhen-Hua Ai, Nian-Ling Yao, Li Wang, et al. 2013. “Basigin-2 Is the Predominant Basigin Isoform That Promotes Tumor Cell Migration and Invasion and Correlates with Poor Prognosis in Epithelial Ovarian Cancer.” *Journal of Translational Medicine* 11: 92. https://doi.org/10.1186/1479-5876-11-92.

Zheng, H-C, H Takahashi, Y Murai, Z-G Cui, K Nomoto, S Miwa, K Tsuneyama, and Y Takano. 2006. “Upregulated EMMPRIN/CD147 Might Contribute to Growth and Angiogenesis of Gastric Carcinoma: A Good Marker for Local Invasion and Prognosis.” *British Journal of Cancer* 95: 1371–78. https://doi.org/10.1038/sj.bjc.6603425.

Zheng, Xiao-Ying, Gui-An Chen, and Hai-Yan Wang. 2004. “Expression of Cystic Fibrosis Transmembrane Conductance Regulator in Human Endometrium.” *Human Reproduction (Oxford, England)* 19 (12): 2933–41. https://doi.org/10.1093/humrep/deh507.

Zhou, S., H. Zhou, P. J. Walian, and B. K. Jap. 2005. “CD147 Is a Regulatory Subunit of the -Secretase Complex in Alzheimer’s Disease Amyloid -Peptide Production.” *Proceedings of the National Academy of Sciences* 102 (21): 7499–7504. https://doi.org/10.1073/pnas.0502768102.

Zhu, Liyin, and Jeffrey W. Pollard. 2007. “Estradiol-17β Regulates Mouse Uterine Epithelial Cell Proliferation through Insulin-like Growth Factor 1 Signaling.” *Proceedings of the National Academy of Sciences of the United States of America* 104 (40): 15847–51. https://doi.org/10.1073/pnas.0705749104.

CHAPTER THREE

Basigin Conditional Knockout Mouse Model and Fertility Phenotypes

Abstract

Basigin (BSG) is a transmembrane glycoprotein expressed in many cell types and is involved in cell proliferation, induction of MMPs, stimulation of angiogenesis, and tissue remodeling. BSG has been shown to be important in male and female reproduction and global knockout of *Bsg* leads to infertility. Studies of the role of BSG in the uterus have been complicated because most *Bsg* null mutants are embryonic lethal. I hypothesized that uterine expression of BSG is required for normal fertility in mice. To investigate this hypothesis, we generated a conditional knockout (cKO) mouse model to ablate uterine BSG expression using the PR-Cre and LoxP method. The aims of this study were to 1) validate the *Bsg* cKO mouse model and 2) to investigate the fertility phenotype of the cKO females. Knockout of BSG was confirmed by qRT-PCR and histology. Results from a six-month fertility study showed that cKO females had significantly reduced fertility compared to controls. The average litter size and litter frequency in the cKO females were significantly lower than the controls. The litter size of the cKO decreased more severely as parity increased compared to controls. Ovarian functions including ovulation and progesterone production were assessed in the cKO mice and were not different from controls. Ovarian histology appeared similar between the cKO and the controls, as they both possessed follicles of different stages and corpora lutea. Both genotypes responded to ovarian superstimulation by ovulating the same number of oocytes. The cKO mice produced comparable numbers of embryos and had similar progesterone levels as the controls on day 4 of pregnancy. Data from pregnancy day 6-15 showed there were fewer implantation sites and abnormal embryo spacing in the uteri of the cKO

females. In addition to impaired implantation and reduced litter size and frequency, I also observed an increased incidence of dystocia and neonatal death in the cKO females. Overall, the cKO females have a higher rate of implantation failure and pregnancy abnormalities compared to controls. These results support that loss of BSG expression in the uterus causes subfertility in female mice.

Introduction

Infertility has become a common health concern in humans and affects about 10-15% of couples worldwide (Ramathal et al. 2010). Studies have shown that only 50-60% of pregnancies advance beyond 20 weeks of gestation, while the rest are lost in early stages (Norwitz, Schust, and Fisher 2001). Among all the early pregnancy losses, implantation failure is the major cause. With the advancement of assisted reproductive technologies, such as *in vitro* fertilization, many couples with fertility issues are able to have children. However, the success rate of assisted reproductive technologies remains low due to implantation failure (Wang et al. 2013; Sharkey and Smith 2003). This suggests that implantation is a significant hurdle for human pregnancy, and it is critical to understand the mechanisms regulating implantation in order to improve fertility rates.

Implantation is the process in mammals where the hatched blastocyst attaches to the maternal endometrium, invades into the stromal cells and establishes the placenta (Cha, Sun, and Dey 2012). This complicated event is tightly regulated by steroid hormones estrogen and progesterone. It requires synchronized development of the embryo and the uterus. During this process, there is constantly a reciprocal and intricate communication between the embryo and the maternal endometrium. In addition, many genes and molecules have been identified to play key roles in regulating implantation and pregnancy. These genes include cytokines, adhesion

molecules, homeobox transcription factors, developmental genes, and cell cycle regulators etc. (Cha, Sun, and Dey 2012; Hantak, Bagchi, and Bagchi 2014).

BSG is a transmembrane glycoprotein that belongs to the immunoglobulin superfamily (Xin et al. 2016). It is expressed in many cell and tissue types and is involved in different physiological functions (Li and Nowak 2019). BSG is also expressed in the reproductive organs of humans and mice and is essential for successful fertility in both males and females (Braundmeier et al. 2012; Chen et al. 2007; Bi et al. 2013). In female mice, BSG is expressed in the embryo, ovary and the uterus. On day 1 of pregnancy, it is expressed in the luminal and glandular epithelium, and on day 4 of pregnancy, it is expressed in the stromal cells. Following implantation, BSG is expressed in the secondary decidual zone and eventually in the undifferentiated stromal cells (Chen et al. 2007; Chen, Belton, and Nowak 2009). Igakura and colleagues first showed that BSG expression both in the embryo and the mother is crucial for successful pregnancy (Tadahiko Igakura et al. 1998). Limited global knockout studies have shown that female mice lacking BSG are profoundly infertile, likely due to failed fertilization and implantation (Tadahiko Igakura et al. 1998; Kuno et al. 1998). However, global knockout of *Bsg* is highly embryonic lethal, making it difficult to study the role of BSG in reproduction since so few pups are born. In fact, only about 4-5% of *Bsg* global knockout mice are born and half of them die prematurely. Among the mice that survive to adulthood, they are also more susceptible to develop pneumonia and neurological disorders (Naruhashi et al. 1997; Tadahiko Igakura et al. 1996; Muramatsu and Miyauchi 2003). Thus, in order to bypass the embryonic lethality caused by global deletion of *Bsg*, we generated a tissue specific *Bsg* knockout mouse model using the progesterone receptor (PR)-Cre and loxP system to study the function of BSG in female reproduction. Therefore, the goals of this study were twofold: 1) to generate and validate the *Bsg* cKO mouse model and 2) to investigate the

fertility phenotype in these *Bsg* cKO mice. Here I demonstrate that the cKO animal model is successful as BSG expression is deleted in the PR positive cells such as in the uterus and oviduct, but it is still present in the PR negative cells. In addition, cKO of *Bsg* in the uterus leads to subfertility in mice.

Material and Methods

Animals

C57/Bl6 mice were housed at the University of Illinois, Urbana-Champaign, at the Institute for Genomic Biology Animal Facility in polysulfone cages. Food (Harlan Teklad 8604) and filtered water were provided for the mice *ad libitum*. The room was maintained at a temperature of 22 ± 1 °C and on a 12-hour light-dark cycle. All experimental procedures including animal care, surgery, euthanasia and tissue collection were approved by the Institutional Animal Care and Use Committee at the University of Illinois, Urbana–Champaign.

Genotyping

Mice were weaned and sexed at 21 days of age. Upon weaning, mice were ear-tagged and tail-clipped. The tail tips were used to extract DNA and genotyped. Briefly, DNA of each tail tip was extracted with extraction solution (Sigma E7526) at 55 °C for 3 minutes, with addition of neutralization buffer (Sigma N3910). Then 2 µl of DNA solution were added to 10 µl of Red Extract-N-Amp PCR Ready Mix buffer (Sigma R4775) and primer sets for a total volume of 20 µl PCR mix for each sample. The DNA was amplified by PCR using a thermal cycler for 30 cycles. After PCR, DNA was loaded on a 1% agarose gel containing 1 µl of ethidium bromide and run by electrophoresis at 120V for 60 minutes. A LSM4000 Image Quant system was used to visualize the DNA and determine the genotypes of the mice.

Fertility Study

A 6-month fertility study was carried out to determine whether the cKO females experienced subfertility or infertility. To do this, eight female mice at 2-months of age for each genotype were housed individually with one wild type male mouse of proven fertility continuously for six months. During this time, mice were checked daily for pregnancy and parturition. Fertility outcomes including the number of litters born per female, the number of pups born per litter, the pup weight and pup sex were recorded and analyzed. These mice were used only for observation of litter size and frequency.

Tissue Collection and Hormone Level Analysis

Another set of animals for tissue collection at different days of pregnancy were used. Mice of each genotype were placed with wild type males at two months of age. The day of vaginal plug was designated as day 1 of pregnancy. Four to eight mice per genotype were euthanized by CO_2 to collect uterine tissue on pregnancy days 1, 4, 5, 6, 9, 12, and 15. Uteri were weighed and photographed. One uterine horn was snap-frozen in liquid nitrogen and stored at -80°C for later RNA extraction. The other uterine horn was fixed in 10 mL of 10% buffered formalin for 24 hours, transferred into 70% ethanol and processed for histology. The uterine tissues were processed with a VipTek tissue processor, embedded in paraffin blocks, and then sectioned into 5 µm thick sections using a microtome. The slides were dried for at least 24 hours before processed for further analysis. Serum samples were collected for hormone measurement on day 4 of pregnancy. Briefly, blood was drawn immediately after euthanasia from the posterior vena cava. The blood samples were cooled on ice for 30 minutes, then 15 minutes at RT to clot. The samples were centrifuged at 1000 x g for 10 minutes to remove the clot, and the supernatant liquid component (serum) was collected and frozen at -20 °C. The serum was subjected to an Enzyme-linked immunosorbent

assay (ELISA) using a commercially available progesterone ELISA kit (DRG EIA1561) for progesterone levels. The kit has a sensitivity of 0.0045 ng/ml and detects progesterone ranges from 0-40 ng/ml.

RNA isolation and quantitative reverse transcription-PCR (qRT-PCR)

Total RNA was extracted from uterine tissues of mice on day 4 of pregnancy using the Qiagen RNeasy Mini kit (Qiagen #74104) according to the manufacturer's instructions. The concentration of mRNA was determined by a nanodrop and the quality of the mRNA was assessed using the Bioanalyzer at the Functional Genomics Center at the University of Illinois, Urbana-Champaign (https://biotech.illinois.edu/functionalgenomics). One microgram of total RNA was reverse transcribed using the First Strand cDNA Synthesis Kit from Roche (#4379012001) following the manufacturer's instructions. After cDNA was synthesized, qRT-PCR was performed to assess the mRNA level of *Bsg* in the uteri of the mice of both genotypes in triplicates using Power Sybr Green Master Mix (Life Tech A25742). Briefly, 5 µl of a 1:7 diluted cDNA sample was mixed with 10 µl of master mix (7.5 µl of Sybr Green Mix, 0.6 µl primer set and 1.9 µl of water) for a total volume of 15 µl per well in a MicroAmp optical 384-well reaction plate. Three technical replicates were performed for each sample. qPCR amplification and quantitation were performed using a Quant Studio (Applied Biosytem) from the Functional Genomics Center. The reaction was run for 40 cycles (95 °C for 15 sec, 60 °C for 1 minute). The comparative CT method (ΔΔCT) was used for quantification of gene expression. Relative fold changes in gene expression for *Bsg* were normalized to Peptidylprolyl isomerase A (*Ppia)* and Ribosomal protein, large, P0 (*Rplp0)* endogenous housekeeping genes. The primer sequences of these genes are listed in **Table 3.1**

Immunohistochemistry

To assess the protein abundance of BSG in the uteri, oviduct and kidney, immunohistochemistry (IHC) was performed on samples collected on day 4 of pregnancy. Briefly, uterine, oviduct and kidney sections were deparaffinized using three xylenes, rehydrated through a series of decreasing concentration of ethanol, and then subjected to heat-induced antigen retrieval with DAKO Target Retrieval Solution at 1:10 dilution (10X pH9) (Dako Denmark A/S, Denmark, Part Number: S236784-2, Code: S2367) at 100 ◦C for 30 minutes and allowed to cool to room temperature (RT). This was followed by inactivation of endogenous peroxidase activity with 0.3% H_2O_2/methanol for 15 minutes in the dark. The samples were then rinsed with phosphate buffered saline containing tween-20 (PBST) and incubated in blocking solution consisting of 5% horse serum (Vectastain ABC kit, Vector Laboratories, Inc. Burlingame, CA) diluted in 1%BSA/PBST at RT for 60 minutes. Tissue sections were incubated with a primary anti-BSG antibody (R&D system AF772) at 1:200 dilution overnight at 4 ◦C. The negative control sections were incubated in a non-specific IgG of the same species as the primary antibodies to confirm specificity of the primary antibody. On the following day, slides were rinsed with PBST prior to incubation with anti-rabbit biotinylated secondary antibody (Vectastain ABC kit, Vector Laboratories, Inc. Burlingame, CA) at 1:100 dilution in PBST for 60 minutes at RT. Slides were then rinsed and incubated in ABC solution (PBS: A: B=50:1:1) (Vectastain ABC kit, Vector Laboratories, Inc. Burlingame, CA) for 30 minutes at RT. For visualization of the immunoreactivity, all slides were subjected to chromogen 3’3-diaminobenzidine (DAB) (Vector Laboratories, Inc. Burlingame, CA) for 30 seconds. Slides were rinsed in tap water for 10 minutes to stop the DAB reaction. Thereafter, the slides were counterstained with hematoxylin (1 g/L) for one minute followed by dehydration

in xylenes and cover-slipping. After drying for 24 hours, the slides were cleaned and loaded into a Hamamatsu Nanozoomer 2.0 HT for scanning.

Immunofluorescence Staining

To assess the protein abundance and localization of BSG in the uteri in an alternative method, immunofluorescence (IF) staining for BSG was performed on samples on day4 of pregnancy. Briefly, uterine slides were deparaffinized using three xylenes, rehydrated through a series of decreasing concentrations of ethanol, and then subjected to heat-induced antigen retrieval with DAKO Target Retrieval Solution at 1:10 dilution (10X pH9) (Dako Denmark A/S, Denmark, Part Number: S236784-2, Code: S2367) at 100 ◦C for 30 minutes and allowed to cool to RT. The slides were then incubated in blocking solution consisting of 5% horse serum (Vectastain ABC kit, Vector Laboratories, Inc. Burlingame, CA) diluted in 1%BSA/PBST at RT for 60 minutes. The tissue sections were incubated with a primary anti-BSG antibody (R&D systems, AF772) at 1:200 dilution overnight at 4 ◦C. The negative control sections were incubated in a non-specific IgG of the same species as the primary antibodies to confirm specificity of the primary antibody. On the following day, slides were rinsed with PBST prior to incubation with anti-goat Alexa488 conjugated secondary antibody (Jackson Immuno Research # 805-545-180) at 1:200 dilution for 1 hour at RT. After incubation, slides were rinsed with PBS and covered with a DAPI containing mounting medium (Vector Laboratories, H-1200). To visualize the immunoreactivity, all slides were imaged using a Zeiss LSM 710 confocal microscope at the Institute for Genomic Biology at the University of Illinois, Urbana-Champaign.

Superovulation

To assess ovarian response to hormonal stimuli and ovulation of the cKO mice, a superovulation experiment was performed. Nine mice of each genotype were injected *ip* with 6 IU

of pregnant mare serum gonadotropin (PMSG, Prospec HOR-272) at 3 pm on day on. The mice were rested for 2 days before receiving 6 IU of human chorionic gonadotropin (HCG, Millipore #230734) 46 hours later at 1 pm on day 3. After superovulation, the mice were euthanized the next day (day 4) at 10 am to collect the oviducts. After transferring to the lab, the oviducts were gently pierced at the ampulla region to release a cloud of oocytes in a complex with cumulus cells. The oocytes were first incubated in 500 µl of PBS with 20 µl of hyaluronidase (Sigma H4272) for 20 minutes to remove the excess cumulus cells. The oocytes were then transferred to a new petri dish with a drop of PBS and then imaged by a light microscope to count the number.

Embryo Flushing

To assess the number of embryos reaching the uterine horn at the time of implantation, embryos were flushed on day 4 of pregnancy from both cKO and control mice. To do this, 7 female mice of each genotype were individually housed with one wild type male of known fertility. Mating behavior was checked daily and the presence of a vaginal plug was designated as day 1 of pregnancy. On day 4 of pregnancy, mice were euthanized, and the uterine horns were collected. After transferring the uteri back to the lab, a 1 ml syringe with 30-gauge needle was used to flush the embryos. Briefly, one end of each uterine horn was held by a pair of forceps over a petri dish, the needle was inserted into the opening of the uterine horn to forcefully inject 1 ml of PBS. The PBS flushed the uterine horn was collected in a petri dish. This flushing was repeated 3 times to ensure flushing of all embryos. The number of embryos was determined using a light microscope and photographic images were taken to evaluate the development stages of the embryos.

Statistical Analysis

All data were analyzed utilizing GraphPad Prism software 8 (GraphPad Prism, San Diego, CA). Data are presented as means ± standard error of the means (SEM). For normally distributed

data, unpaired t tests were used to compare the control group and the experimental group. For non-normally distributed data, Mann-Whitney tests were used. A statistical significance was assigned at $p \leq 0.05$. A trending difference was assigned when p value was between 0.05 and 0.1.

Results

Generation of the *Bsg* cKO mice

To generate the *Bsg* cKO mice, we made a *Bsg* floxed C57/BL6 mouse where two LoxP sites were inserted into the genome, flanking exon 1 of the *Bsg* gene. We then crossed this mouse line with another C57/BL6 line containing a Cre recombinase inserted into the genome under the PR promotor region in exon 1. This cross results in a new transgenic mouse where in the PR positive cells, the expressing Cre recombinase deleted exon 1 of the *Bsg* gene. As **Figure 3.1** B shows, *Bsg* F/F and PR +/+ female mice were crossed with *Bsg* F/F and PR cre/+ male mice, to generate *Bsg* F/F and PR cre/+ (conditional *Bsg* knockout) and *Bsg* F/F and PR +/+ (littermate control) female offspring. Genotypes were determined by PCR and DNA gel electrophoresis, where the presence of one band alone at 283 bp indicates a control mouse, while two bands at 283 and 594 bp indicate a cKO mouse (**Figure 3.2**).

Confirmation of loss of BSG expression in the uterus of *Bsg* cKO mice

Knockout of *Bsg* in the uterus was confirmed by qRT-PCR and histology. **Figure 3.3** shows that the mRNA level of *Bsg* in whole uteri collected in the cKO on day 4 of pregnancy was downregulated by 75%, which was significantly lower than the controls. **Figure 3.4** shows the IHC results for BSG protein in the kidney, oviducts and uteri in mice of both genotypes on day 1, 4 and 6 of pregnancy. On day 1 of pregnancy, BSG was expressed mainly in the luminal epithelial cells and glandular epithelial cells in the control uterus (**B**). In the cKO, BSG expression

disappeared in the luminal and glandular epithelial cells (**C**). On day 4 of pregnancy, BSG was expressed abundantly in the stromal cells in the control uterus (**E**). In the cKO, BSG expression was only detected in some scattered endothelial cells and immune cells (**F**). On day 6 of pregnancy, BSG was heavily expressed in the embryo and the secondary decidual zone and undifferentiated stromal cells in the control uterus (**H**). In the cKO, BSG expression level was much reduced, mainly in endothelial cells and immune cells in the stroma (**I**). The non-specific IgG slides of the uteri in the control mice on day 1, 4 and 6 showed no immunostaining of BSG (**A, D and H**). BSG was also expressed in the ampulla of the oviduct in the control mouse (**K**), but not in the cKO mouse (**L**). The kidney is known to express high levels of BSG and served as a positive control. The kidney of the cKO female showed extensive BSG expression (**J**), suggesting that the targeted knockout in PR positive cells was specific. Immunofluorescence staining for BSG in uteri on day 4 of pregnancy also confirmed cell membrane localization of BSG in the stromal cells of the controls, but not in the cKO mice (**Figure 3.5**).

Deletion of *Bsg* in uterine cells reduces fertility of female mice.

A six-month fertility study was carried out to determine the fertility outcomes of the cKO female mice, and the results are summarized in **Table 3.2**. During the six-month period, the eight control females produced 40 litters total, which was 5 litters per female on average. However, the eight cKO females produced 27 litters total, which was an average of 3.38 litters per female. The litter frequency of the cKO females was significantly smaller than the controls (**Figure 3.6 B**). cKO females produced 123 pups total, which was 4.56 per litter, and this was significantly smaller than the 309 total pups and 7.73 pups per litter produced by the controls (**Figure 3.6 A**). Although the cKO mice had fewer pups, the number of dead pups at parturition was much higher than the controls at a 27:7 ratio. Two of the cKO females died due to dystocia and had to be replaced. In

addition to the smaller litter frequency and litter size, the fertility decreased much more severely in the cKO females compared to the controls over time. The controls still produced six pups per litter at their fifth parity, while the cKO females produced almost no pups at the fifth parity (**Figure 3.6 C**). This suggests that BSG may play a role in reproductive aging. There was no difference in the pups' weight at birth between the cKO females and the control females (**Figure 3.6 D**). The sex ratio of the pups was also not different.

***Bsg* cKO females have normal ovarian morphology.**

Ovaries are the sources of oocytes and the sites of steroid hormone production, which are critical for reproduction (Jamnongjit and Hammes 2006). Ovaries on day 4 of pregnancy were collected and stained by hematoxylin and eosin to assess the morphological differences between the cKO females and the controls (**Figure 3.7**). The ovarian morphology appeared similar between the two genotypes. The cKO ovary had similar number of follicles at different developmental stages as the controls. There were also corpora lutea present in the ovaries of the cKO mice.

Progesterone levels are normal in the *Bsg* cKO females.

Progesterone is key for maintenance of all events of normal pregnancy (Terakawa et al. 2012). In order to assess progesterone levels, serum was collected on day 4 of pregnancy and subjected to progesterone ELISA. The cKO females had 19.12 ng/ml progesterone, which was not different from the 19.35 ng/ml levels measured in the controls (**Figure 3.8**). Thus, the subfertility of the cKO females was not due to differences in progesterone levels.

Response to ovarian superstimulation is not altered in the *Bsg* cKO females.

To test ovarian function, including ovulation and response to hormones, a superovulation experiment was performed. After stimulating with PMSG and HCG, the cKO females ovulated 16.44 oocytes, which was comparable to the 20.44 oocytes produced by the controls (**Figure 3.9**

A). The superovulated oocytes were collected and imaged under a light microscope. The morphology and size of the oocytes were similar between the cKO and the control mice (**Figure 3.9 B** and **C**).

Embryo number and developmental stage are normal in the *Bsg* cKO females.

Uteri of both genotypes were harvested on the morning of gestational day 4 and the embryos were flushed and collected. We retrieved an average of 6.29 embryos per mouse from the seven cKO females, which was similar to the 7.86 embryos retrieved from each of the seven control mice (**Figure 3.10 A**). After collection, embryos were imaged under a light microscope to evaluate developmental stages. Most of the embryos were at the mature blastocyst stage, or morula stage, regardless of the genotypes of the mother (**Figure 3.10 B** and **C**). The cKO females had an average of 0.71 unfertilized or degenerative eggs, which was similar to the 0.43 unfertilized or degenerative eggs observed in the controls.

***Bsg* cKO females experience uterine defects at multiple time points of gestation.**

After identifying the cause of subfertility to uterine defects, the timing of the defects was assessed. For this purpose, uteri from animals with both genotypes were collected on different days of pregnancy. Examples of uteri on days 6, 9, 12 and 15 of gestation for both cKO and control mice are shown in **Figure 3.11**. For each time point checked, the cKO females had some uteri with implantation failure. In cKO mice with implantation, some had fewer implantation sites, abnormal spacing or crowded implantation sites. On days 12 and 15, there were signs of embryo resorption and growth restriction in the cKO females. There were also signs of hemorrhage at implantation sites in the cKO mice. This indicates that pregnancy complications occurred at multiple time points throughout the gestational period and led to a subfertility phenotype in the cKO females.

***Bsg* cKO females have higher incidence of implantation failure and abnormal pregnancy.**

After carefully checking the pregnancy status of mice at every time point of pregnancy, mice were divided into three groups based on observation of the uteri: 1. No implantation; 2. Abnormal pregnancy and 3. Normal pregnancy. Only 15.4% of the controls had no implantation and 7.7% had abnormal pregnancies, while the majority of controls had normal pregnancies (76.9%). On the other hand, 25% of the cKO females had no implantation, and 39.3% had abnormal pregnancies. Only 35.7% of the cKO females had normal pregnancies, which was much lower than the controls (**Figure 3.12**).

Discussion

BSG is a highly glycosylated, type-1 transmembrane protein in the immunoglobulin superfamily and plays a role in numerous physiological functions (Hahn, Kaushik, and Yong 2015; Fossum, Mallett, and Neil Barclay 1991). Global deletion of *Bsg* is highly embryonic lethal and only 4% of global knockout pups are born. Of the few that are born, half of them are small, weak, and susceptible to develop interstitial pneumonia and die prematurely. The ones that survive to adulthood also exhibit neurological and cognitive disorders such as decreased sensitivity to irritating odors and lights, hypersensitivity to electric foot shock and deficits in learning and memory (T Igakura et al. 1998; Tadahiko Igakura et al. 1996; Hori et al. 2000; Ochrietor and Linser 2004; Naruhashi et al. 1997; Fadool and Linser 1993). Thus, the global *Bsg* knockout mouse model is not amenable to studying the role of BSG in reproduction.

To bypass this high embryonic lethality of mice lacking *Bsg*, we utilized the PR-Cre and LoxP system to generate a PR positive cell specific *Bsg* knockout animal model. We produced a *Bsg* floxed mouse where the two LoxP sites flank exon 1 of the *Bsg* gene. This mouse model was

crossed with a PR-Cre knock-in mouse line where a Cre recombinase is inserted in to exon 1 of the PR sequence as described by Soyal and colleagues (Soyal et al. 2005). The breeding scheme to generate the PR-Cre *Bsg* cKO mice is illustrated in **Figure 2.1**. The qRT-PCR results showed that the *Bsg* mRNA level was significantly downregulated in the uteri of the cKO mice. The immunostaining results showed that the BSG protein expression was also deleted in the uterine luminal epithelial and stromal cells, as well as the ampulla of the oviduct in the cKO mice. Kidney is known to express BSG (Fukuoka et al. 2012) and is negative for PR. Because BSG was still heavily expressed in the kidney, these data suggest that the knockout of *Bsg* was successful and limited to PR positive cells.

Following validation of the knockout mouse model, I hypothesized that loss of BSG expression in the uterus would lead to infertility or subfertility in female mice. The six-month fertility study results showed that the cKO females produced markedly smaller litter numbers and litter size compared to the controls, indicating reduced fertility in cKO mice. In addition, there was a much higher incidence of neonatal death of the cKO mice. An interesting observation was that as the parity increased, the fertility of the cKO mice decreased more severely compared to the controls. Normally, the fertility of animals gradually decreases as they age, however, this age-associated fertility decrease in the cKO mice was accelerated compared to the controls, suggesting a possible role of BSG in reproductive aging. Overall, these results demonstrated that loss of BSG in the uterus caused subfertility in female mice, instead of complete infertility.

After demonstrating the subfertility phenotype caused by loss of BSG in the uterine cells, it was important to determine where the problems were occurring. Ovaries are critical for reproductive functions as they are the sources of the oocytes and the sites of steroid hormone production (Jamnongjit and Hammes 2006). However, there were no morphological differences in

the ovarian structures between the two genotypes: both contained follicles at each developmental stages and corpora lutea. There was no difference in the number of superovulated oocytes produced by the cKO mice compared to the controls, suggesting that the ovaries in the cKO mice responded normally to hormonal stimulations. Progesterone is referred to as the "pregnancy hormone" as it is essential for maintenance of pregnancy in most mammals studied (Dey et al. 2004). Progesterone levels are usually at high levels on day 4 of pregnancy in mice, causes a cessation of the luminal epithelial cell proliferation and promotes the stromal cell proliferation. The uterus also enters the pre-receptive stage for the incoming blastocyst at this time (Tranguch et al. 2005). The ELISA results showed that the progesterone levels on day 4 of pregnancy in the cKO mice were not different compared to the controls. These results suggested that the ovarian functions including ovulation and progesterone production were comparable between the groups, and thus were not the cause of the subfertility in the cKO mice. The fertilized zygote undergoes several rounds of cell division to develop into a blastocyst, which will hatch from the zona pellucida before implantation can occur (Rossant 2016). A similar number of embryos were retrieved from the uteri of both genotypes on day 4 of pregnancy. In both genotypes, most of the embryos were fertilized and at the blastocyst stage as they possessed a blastocoel, indicating that the embryonic development was not affected in the cKO mice. Collectively, these results suggested that the decreased fertility observed in the cKO mice was not likely due to an impairment of the hypothalamic-pituitary-ovarian axis. Based on these findings, I determined that the uterine defects were the cause of the subfertility in the cKO mice.

To confirm the hypothesis and determine the time of gestation when the problems occurred, I collected the uteri of mice in both genotypes at different gestation times. Results showed that only 15.4% and 7.7% of the controls had no implantation or abnormal pregnancy respectively, and

76.9% had normal pregnancy. However, in the cKO mice, only 35.7% had normal pregnancy. A quarter of the cKO mice did not implant and 39.3% of them had problematic pregnancy. These findings suggest that loss of BSG results in complications throughout pregnancy at multiple time points. Over the course of pregnancy, BSG may be involved in regulating processes including implantation, decidualization and placentation. In addition, parturition could likely be affected by the loss of BSG because two cKO mice died due to dystocia and there were more dead pups at birth in the cKO mice in the fertility study. These results provide evidence on the possible negative effects of loss of BSG in implantation and decidualization and direct me to investigate these processes in the future studies. It has been accepted that during the dynamic process of pregnancy, any major aberration will terminate pregnancy at the time of insult or perpetuate negative effects throughout pregnancy (Cha, Sun, and Dey 2012). Recent studies have proposed the concept of the "ripple effect of implantation", which means the quality of implantation determines the quality of the ongoing pregnancy. If the gestation starts with a poor-quality implantation, it is likely to have other defects in later course of the pregnancy (Wang et al. 2013). Therefore, it is not surprising that if loss of BSG in the uterus causes implantation defects, it will likely lead to other complications later on during pregnancy.

The PR-Cre and LoxP system provides a valuable tool for targeted gene deletion in the uterus of mice. Many genes have been conditionally knocked out to study their functions in reproduction using this method. For example, Indian Hedgehog (IHH) cKO mice are infertile due to failed uterine receptivity and impaired artificial decidualization response (ADR) (Lee et al. 2007). Similarly, loss of the transcription factor Chicken Ovalbumin Upstream-Promoter Transcription Factor II (COUP-TFII) also caused failed embryo attachment, defective decidual response in nature or by stimuli, and results in complete infertility of the mice (Kurihara et al.

2007). In Bone Morphogenetic Protein 2 (BMP2) cKO mice, the ovarian functions are normal, and the embryos are able to attach to the luminal epithelium, but decidualization failed specifically at stromal cell proliferation and differentiation steps. This leads to complete infertility of the mice (Lee et al. 2007). Interestingly, the *Bmp7* cKO mice are subfertile, instead of infertile, due to impaired uterine receptivity, decidualization and placentation (Monsivais et al. 2017). Loss of the transcription factors Activin-Like Kinases (ALK) 2 and 3 both cause infertility in mice, but the mechanisms are different. *Alk2* cKO mice experience delayed implantation and compromised decidualization, while *Alk3* cKO mice failed implantation due defects in the luminal epithelial cell functions (Clementi et al. 2013; Monsivais et al. 2016). In addition to complete infertility, loss of some genes in the uterus results in subfertility of the mice. For instance, loss of the gap junction protein Connexin 43 (CX43) does not alter ovarian functions or implantation, but compromises decidualization, decreases angiogenesis and impairs intrauterine embryo growth (Laws et al. 2008). Forkhead Box Protein A2 (FOXA2) cKO mice have underdeveloped uterine glands, which disrupts implantation and causes subfertility (Jeong et al. 2010). The subfertility phenotype caused by loss of BSG is very similar to the findings in several gene knockout studies, such as the *Bmp7* and *Cx43* cKO mice.

In summary, the results validated the *Bsg* cKO mouse model and demonstrated a subfertility phenotype of the mice due to the loss of BSG in the uterus. I found that BSG was successfully deleted in the PR positive cells in the reproductive tract of the mice such as in the uterus and oviduct but remained expression in the PR negative cells such as in the kidney. Loss of *Bsg* in the uteri was also confirmed by qRT-PCR. The fertility study results showed that the cKO mice had significantly smaller litter size and litter frequency compared to controls. The cKO mice had accelerated reduction in fertility than the controls. The superovulation and progesterone

ELISA experiments showed that the ovarian functions including ovulation and steroidogenesis were not affected by the loss of BSG. Embryo flushing experiments showed that fertilization and early embryo development were similar between the two genotypes. The loss of BSG in the uterus led to defects throughout the pregnancy and caused subfertility in mice. Future studies will focus on the role of BSG in implantation and decidualization *in vivo*.

Tables and Figures

Table 3.1 Primer sequences used for quantitative-PCR

Genes	NCBI Gene Reference	Left Primer Sequence	Right Primer Sequence
Rplp0	NM_007475.5	actggtctaggacccgagaag	ctcccaccttgtctccagtc
Ppia	NM_008907.1	ggaccaaacacaaacggttc	catgccttctttcaccttcc
Bsg	NM_009768.2	acagcagtggcgttgaca	ggtcatctgcgtccactatgt

Table 3.2 Summary of the six-month fertility study

Genotype	No. of animals	No. of Litters born	No. litters per animal	No. of pups born	No. of pups per litter	No. of dead pups	Pup weight
Bsg$^{f/f}$	8	40	**5.0 ± 0.38**	309	**7.73 ± 0.35**	7	1.41 ± 0.01
Bsg$^{d/d}$	8	27	**3.38 ± 0.46***	123	**4.56 ± 0.52***	27	1.38 ± 0.02

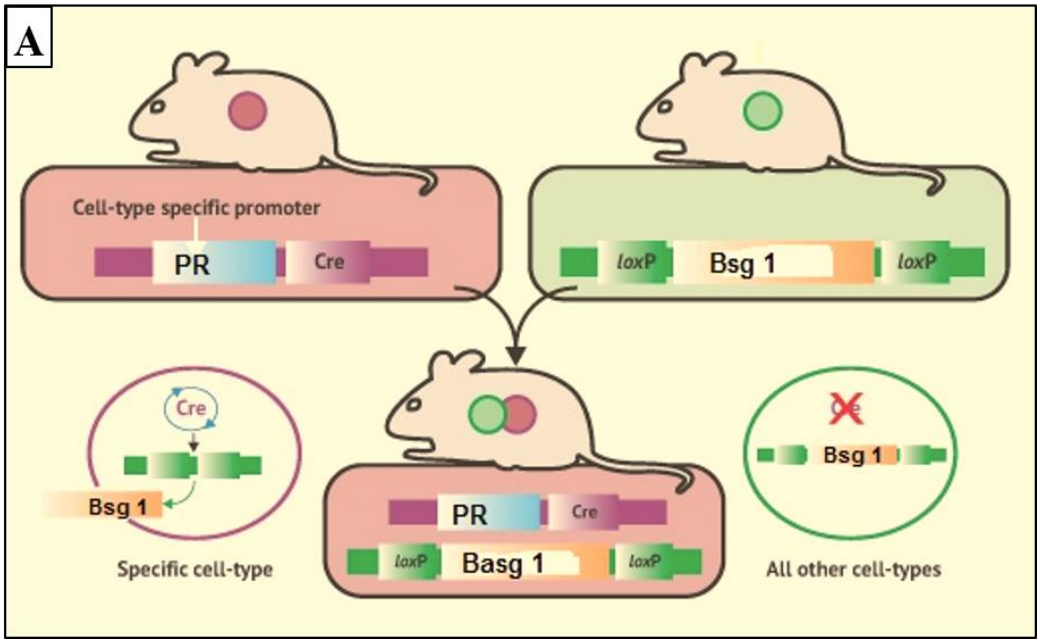

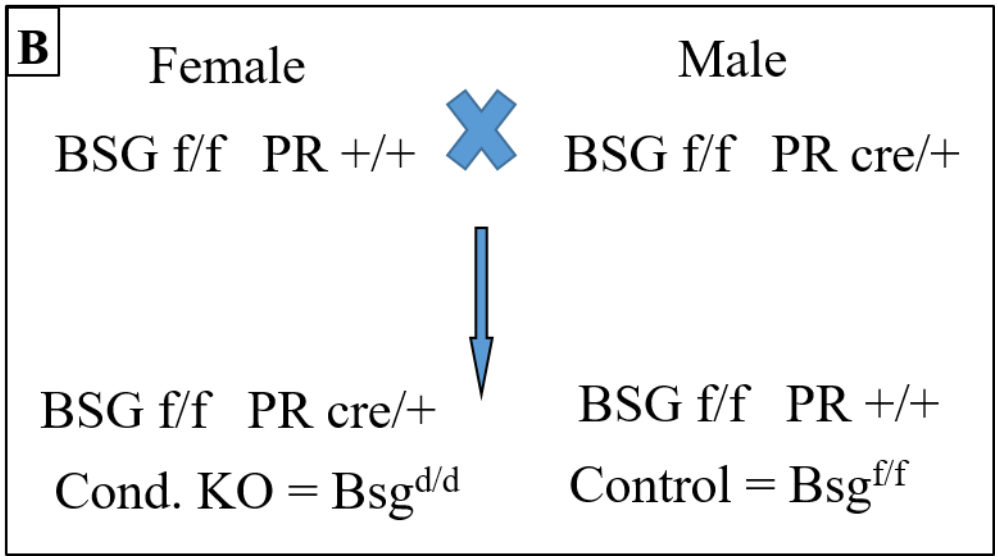

Figure 3.1 Breeding Schemes. A: a diagram illustrating how the basigin cKOs were generated. PR: progesterone receptor. B: a scheme of breeding pairs showing the genotypes of F0 parents to produce the basigin cKO and controls.

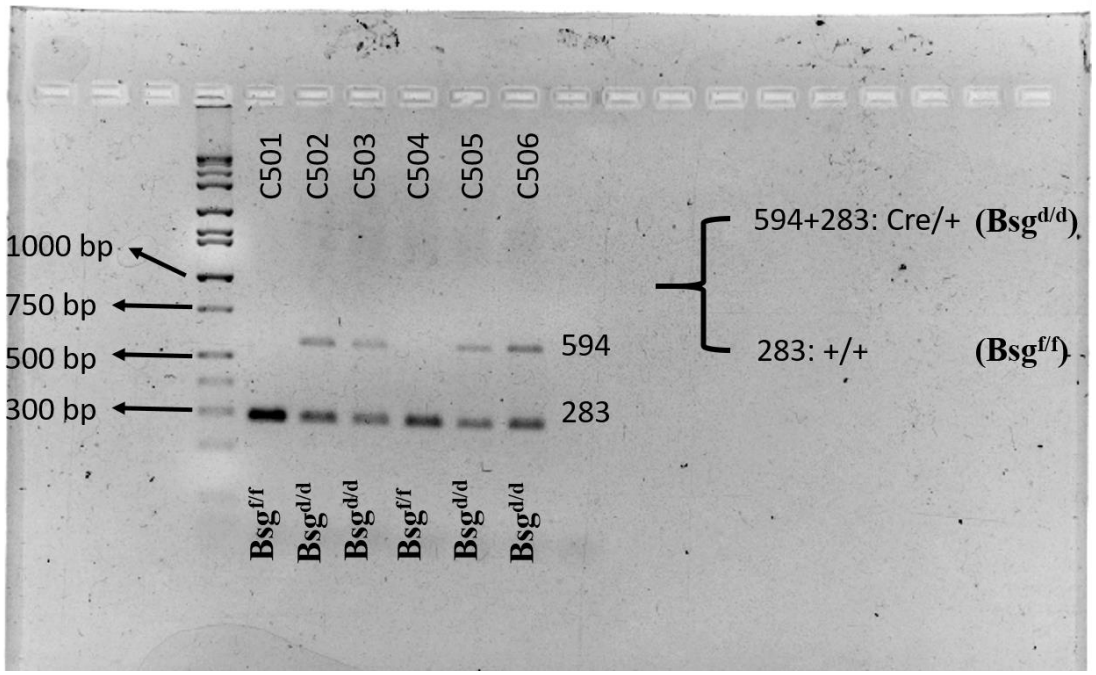

Figure 3.2 DNA Gel Electrophoresis Result. An example DNA gel image showing how to determine the genotype of the mice. Left lane: DNA standard ladder. C501-C506: 6 mice examined in this experiment.

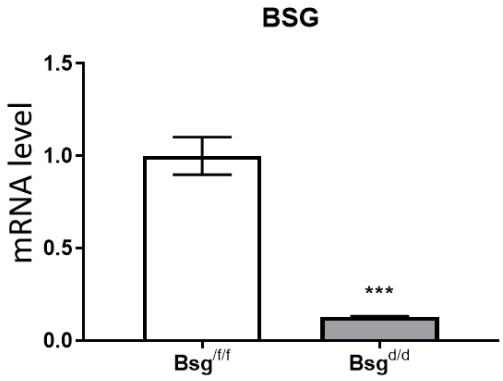

Figure 3.3 mRNA Level of *Bsg*. mRNA levels of *Bsg* in the uteri of both genotypes on day 4 of pregnancy. N=4 each. P≤0.001

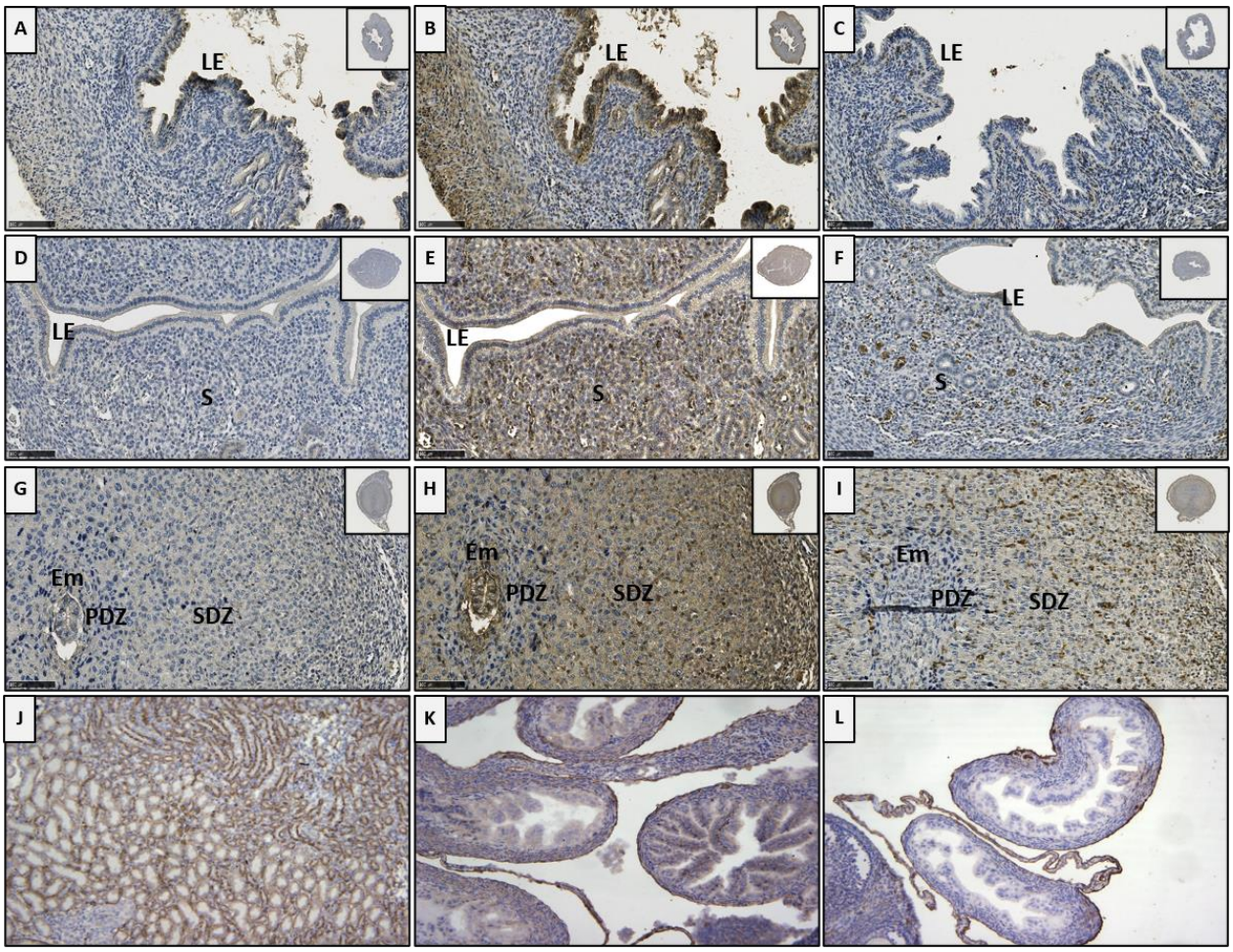

Figure 3.4 Validation of Bsg knockout in the mouse. Negative control slides of the uteri of a control mouse on day 1, 4 and 6 of pregnancy (A, D and G). Bsg expression in the uteri on day 1, 4 and 6 of pregnancy in control mice (B, E and H) and the cKO mice (C, F, and I). Bsg expression in a kidney cross section of a cKO mouse (J). Bsg expression in the oviducts of a control mouse (K) and a cKO mouse (L). Em:embryo. LE: luminal epithelium. S: stroma. PDZ: primary decidual zone. SDZ: secondary decidual zone.

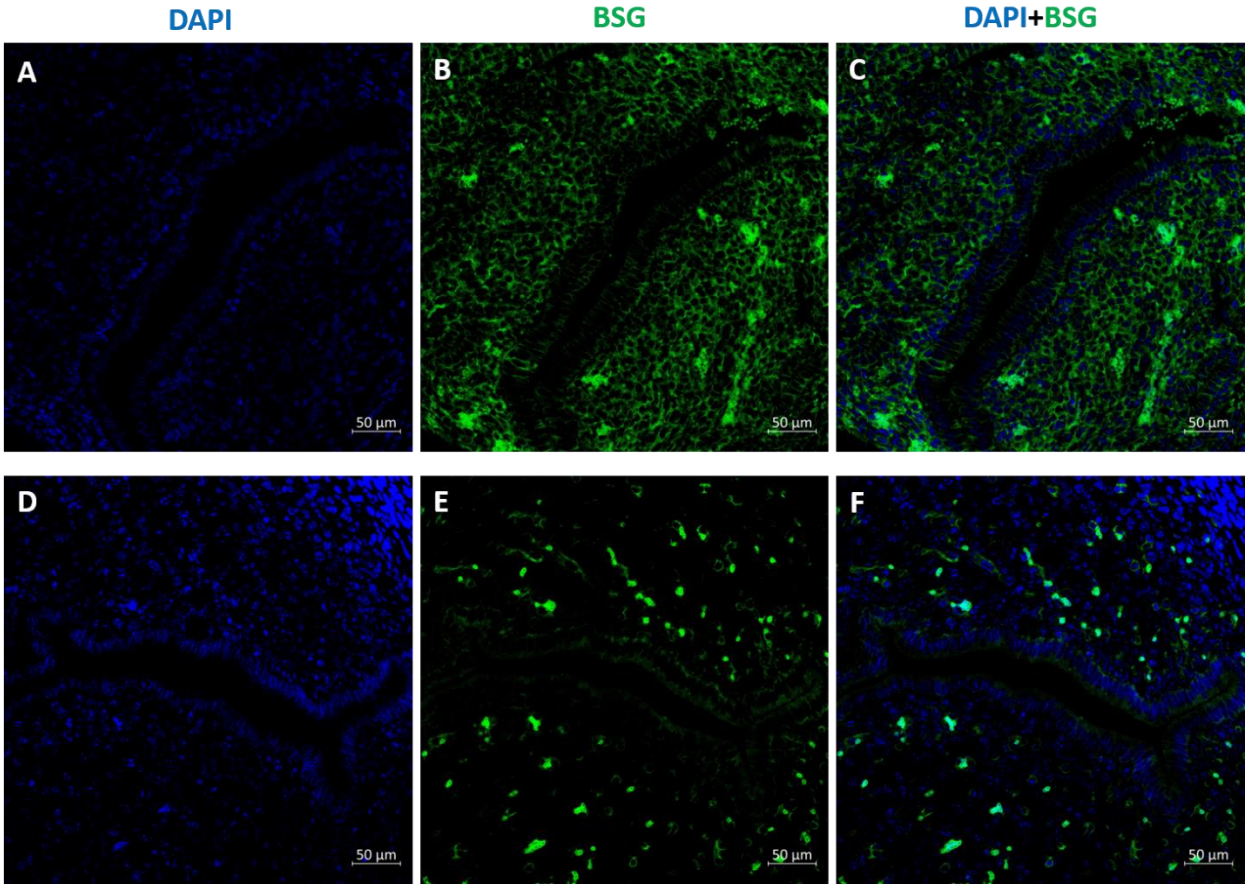

Figure 3.5 Validation of Bsg knockout in the mouse uterus by immunofluorescence. Expression of *Bsg* in a control mouse (top lane) and a cKO mouse (bottom lane) on day 4 of pregnancy. A, D: DAPI; B, E: Basigin; C, F: merged. Blue: DAPI. Green: Basigin.

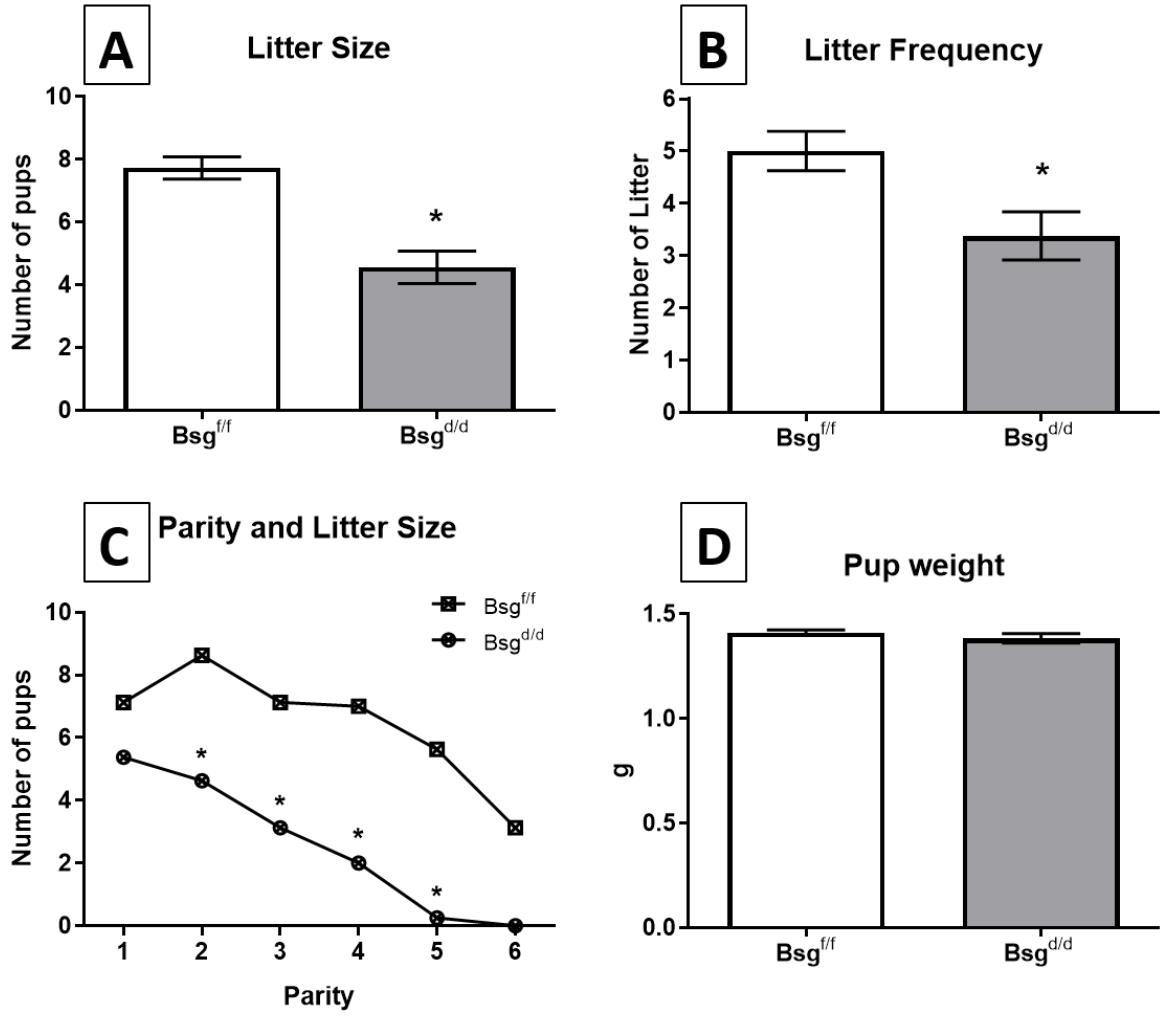

Figure 3.6 Fertility Study Results. A: average litter size of control and cKO mice. B: Average litter frequency of the control and cKO mice. C: Litter size of each parity of the control and cKO mice over six-month. D: average pup weight at birth of the control and cKO mice.

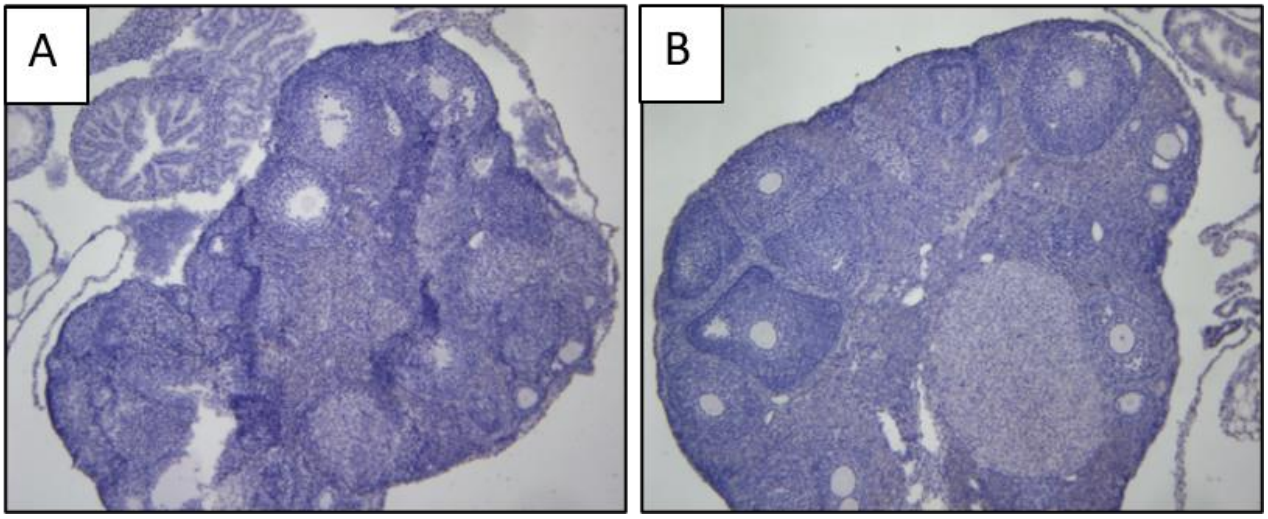

Figure 3.7 Ovarian structure. Hematoxylin stain of the ovary of a control mouse (A) and a cKO mouse (B) on day 4 of pregnancy.

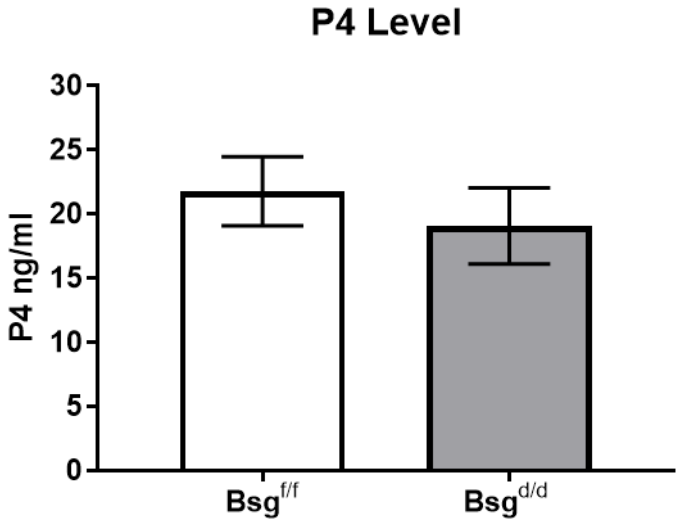

Figure 3.8 Progesterone levels. Serum progesterone level of the control and cKO mice on day 4 of pregnancy. N=8 for each genotype.

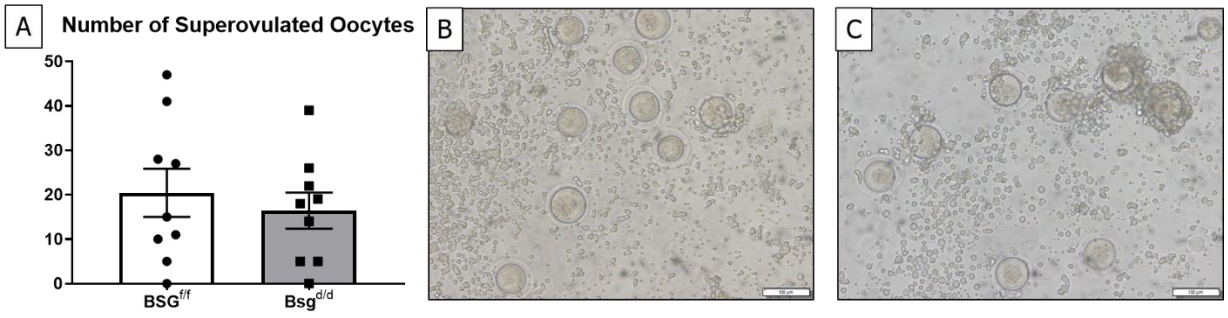

Figure 3.9 Superovulation results. A: average number of superovulated oocytes from the control and cKO mice. Images of oocytes superovulated from the control (B) and the cKO (C) mice. N=9 for each genotype.

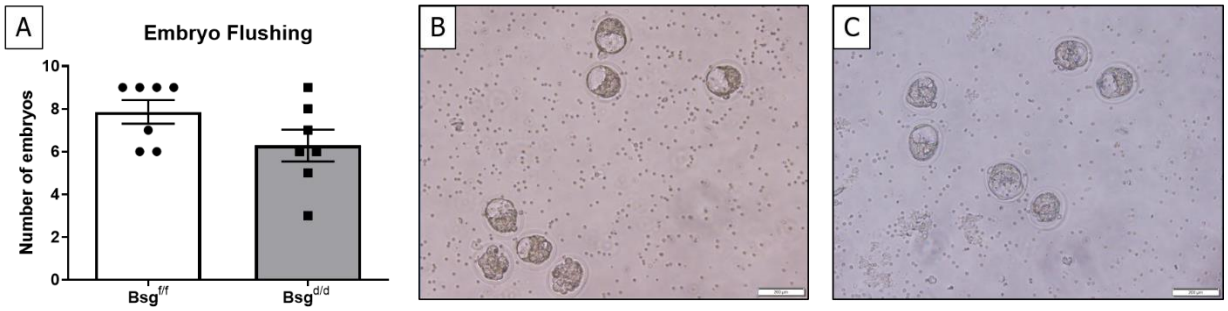

Figure 3.10 Embryo flushing results. A: average number of embryos retrieved from flushing of the control and cKO mice on day 4 of pregnancy. Images of embryos from the control (B) and the cKO (C) mice on day 4 of pregnancy. N=7 for each genotype.

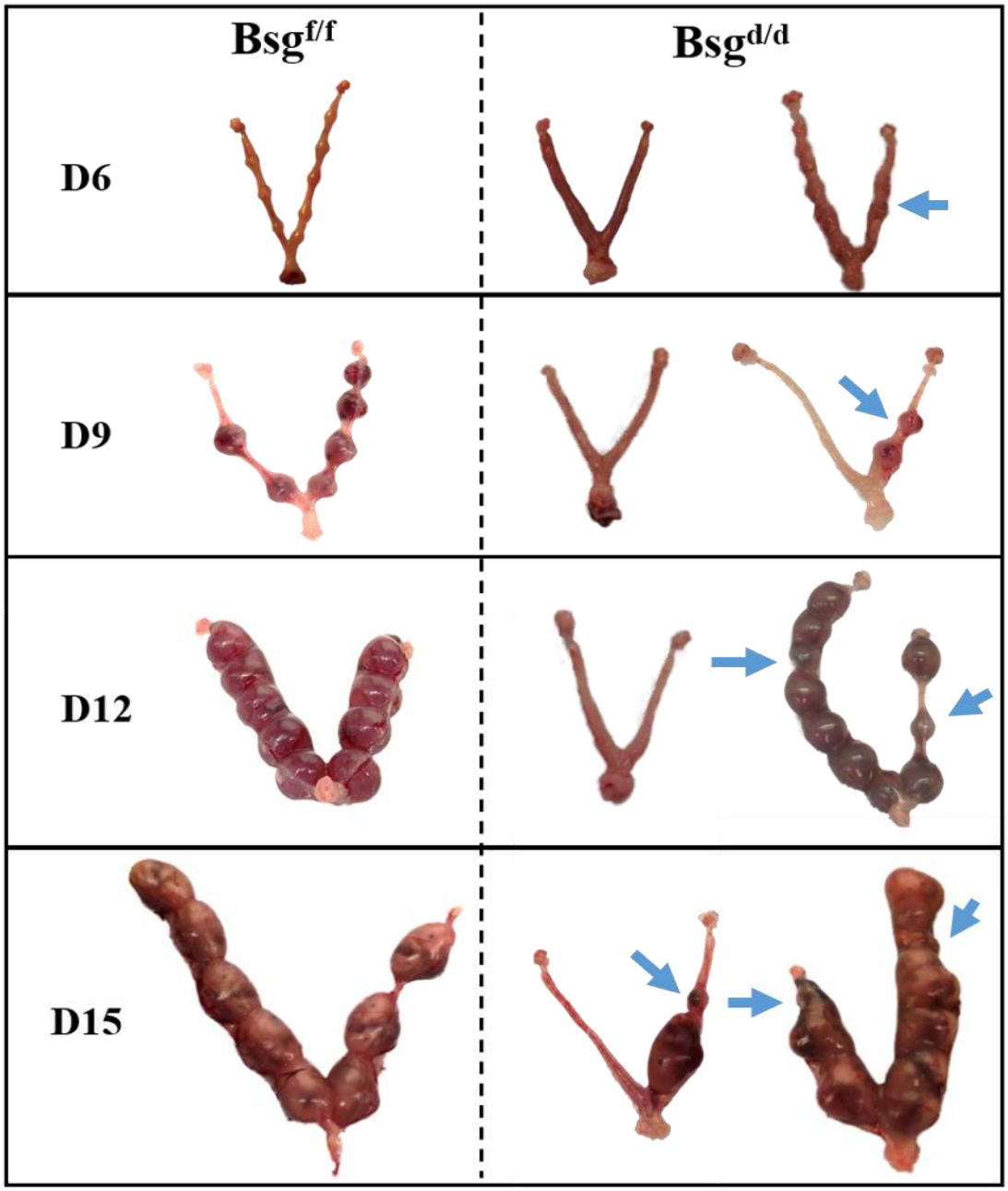

Figure 3.11 Pregnancy status at different gestational times in both genotypes. Left: cKO mice. Right: control mice. Each lane (from top to bottom): day 6, day 9, day 12 and day 15 of pregnancy. Arrows indicate embryo growth, restriction resorption and hemorrhage.

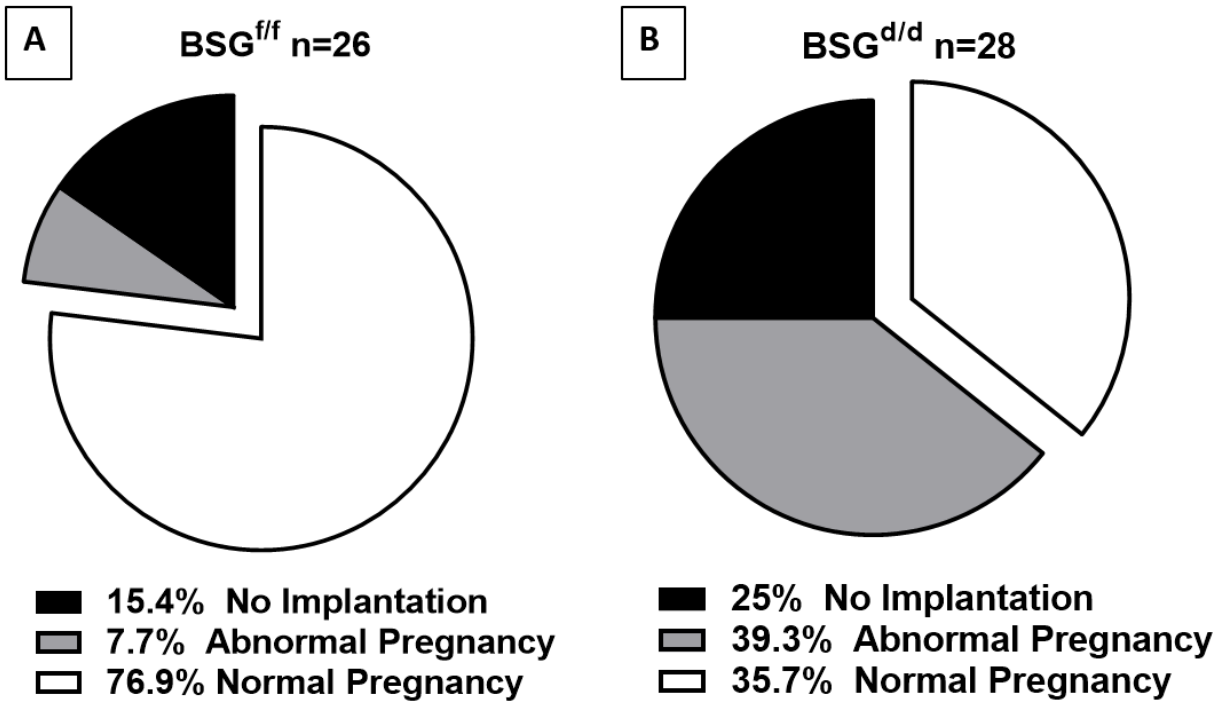

Figure 3.12 Post-implantation Pregnancy Success Rate. Pie chart of post-implantation pregnancy success rate of the control mice (A) and cKO mice (B). Black: no implantation. Grey: Abnormal pregnancy. White: normal pregnancy.

References

Bi, Jiajia, Yanfen Li, Fengyun Sun, Anja Saalbach, Claudia Klein, David J. Miller, Rex Hess, and Romana A. Nowak. 2013. "Basigin Null Mutant Male Mice Are Sterile and Exhibit Impaired Interactions between Germ Cells and Sertoli Cells." *Developmental Biology* 380 (2): 145–56. https://doi.org/10.1016/j.ydbio.2013.05.023.

Braundmeier, A. G., C. A. Dayger, P. Mehrotra, R. J. Belton, and R. A. Nowak. 2012. "EMMPRIN Is Secreted by Human Uterine Epithelial Cells in Microvesicles and Stimulates Metalloproteinase Production by Human Uterine Fibroblast Cells." *Reproductive Sciences* 19 (12): 1292–1301. https://doi.org/10.1177/1933719112450332.

Cha, Jeeyeon, Xiaofei Sun, and Sudhansu K. Dey. 2012. "Mechanisms of Implantation: Strategies for Successful Pregnancy." *Nature Medicine*. Nature Publishing Group. https://doi.org/10.1038/nm.3012.

Chen, Li, Robert J. Belton, and Romana a. Nowak. 2009. "Basigin-Mediated Gene Expression Changes in Mouse Uterine Stromal Cells during Implantation." *Endocrinology* 150 (2): 966–76. https://doi.org/10.1210/en.2008-0571.

Chen, Li, Masaaki Nakai, Robert J. Belton, and Romana A. Nowak. 2007. "Expression of Extracellular Matrix Metalloproteinase Inducer and Matrix Metalloproteinases during Mouse Embryonic Development." *Reproduction (Cambridge, England)* 133 (2): 405–14. https://doi.org/10.1530/rep.1.01020.

Clementi, C, S K Tripurani, M J Large, M A Edson, and C J Creighton. 2013. "Activin-Like Kinase 2 Functions in Peri-Implantation Uterine Signaling in Mice and Humans." *PLoS Genet* 9 (11): 1003863. https://doi.org/10.1371/journal.pgen.1003863.

Dey, S. K., H. Lim, Sanjoy K. Das, Jeff Reese, B. C. Paria, Takiko Daikoku, and Haibin Wang. 2004. "Molecular Cues to Implantation." *Endocrine Reviews* 25 (3): 341–73. https://doi.org/10.1210/er.2003-0020.

Fadool, James M., and Paul J. Linser. 1993. "5A11 Antigen Is a Cell Recognition Molecule Which Is Involved in Neuronal-glial Interactions in Avian Neural Retina." *Developmental Dynamics* 196 (4): 252–62. https://doi.org/10.1002/aja.1001960406.

Fossum, Sigbjorn, Susan Mallett, and A. Neil Barclay. 1991. "The MRC OX-47 Antigen Is a Member of the Immunoglobulin Superfamily with an Unusual Transmembrane Sequence." *European Journal of Immunology* 21 (3): 671–79. https://doi.org/10.1002/eji.1830210320.

Fukuoka, Miyoko, Makoto Hamasaki, Kaori Koga, Hiroyuki Hayashi, Mikiko Aoki, Tatsuhiko Kawarabayashi, Shingo Miyamoto, and Kazuki Nabeshima. 2012. "Expression Patterns of Emmprin and Monocarboxylate Transporter-1 in Ovarian Epithelial Tumors." *Virchows Archiv* 461 (4): 457–66. https://doi.org/10.1007/s00428-012-1302-3.

Hahn, J. N., D. K. Kaushik, and V. W. Yong. 2015. "The Role of EMMPRIN in T Cell Biology and Immunological Diseases." *Journal of Leukocyte Biology* 98 (1): 33–48. https://doi.org/10.1189/jlb.3RU0215-045R.

Hantak, Alison, Indrani Bagchi, and Milan Bagchi. 2014. “Role of Uterine Stromal-Epithelial Crosstalk in Embryo Implantation.” *International Journal of Developmental Biology* 58 (0): 139–46. https://doi.org/10.1126/science.1249098.Sleep.

Hori, K., N. Katayama, S. Kachi, M. Kondo, K. Kadomatsu, J. Usukura, T. Muramatsu, S. Mori, and Y. Miyake. 2000. “Retinal Dysfunction in Basigin Deficiency.” *Investigative Ophthalmology and Visual Science* 41 (10): 3128–33.

Igakura, T, K Kadomatsu, T Kaname, H Muramatsu, Q W Fan, T Miyauchi, Y Toyama, et al. 1998. “A Null Mutation in Basigin, an Immunoglobulin Superfamily Member, Indicates Its Important Roles in Peri-Implantation Development and Spermatogenesis.” *Developmental Biology* 194 (2): 152–65. https://doi.org/10.1006/dbio.1997.8819.

Igakura, Tadahiko, Kenji Kadomatsu, Tadashi Kaname, Hisako Muramatsu, Qi Wen Fan, Teruo Miyauchi, Yoshiro Toyama, et al. 1998. “A Null Mutation in Basigin, an Immunoglobulin Superfamily Member, Indicates Its Important Roles in Peri-Implantation Development and Spermatogenesis.” *Developmental Biology* 194 (2): 152–65. https://doi.org/10.1006/dbio.1997.8819.

Igakura, Tadahiko, Kenji Kadomatsu, Osamu Taguchi, Hisako Muramatsu, Tadashi Kaname, Teruo Miyauchi, Ken Ichi Yamamura, Kimiyoshi Arimura, and Takashi Muramatsu. 1996. “Roles of Basigin, a Member of the Immunoglobulin Superfamily, in Behavior as to an Irritating Odor, Lymphocyte Response, and Blood-Brain Barrier.” *Biochemical and Biophysical Research Communications* 224 (1): 33–36. https://doi.org/10.1006/bbrc.1996.0980.

Jamnongjit, Michelle, and Stephen R. Hammes. 2006. “Ovarian Steroids: The Good, the Bad, and the Signals That Raise Them.” *Cell Cycle*. Taylor and Francis Inc. https://doi.org/10.4161/cc.5.11.2803.

Jeong, Jae-Wook, Inseok Kwak, Kevin Y. Lee, Tae Hoon Kim, Michael J. Large, Colin L. Stewart, Klaus H. Kaestner, John P. Lydon, and Francesco J. DeMayo. 2010. “Foxa2 Is Essential for Mouse Endometrial Gland Development and Fertility.” *Biology of Reproduction* 83 (3): 396–403. https://doi.org/10.1095/biolreprod.109.083154.

Kuno, Naohiko, Kenji Kadomatsu, Qi Wen Fan, Masako Hagihara, Takao Senda, Shigehiko Mizutani, and Takashi Muramatsu. 1998. “Female Sterility in Mice Lacking the Basigin Gene, Which Encodes a Transmembrane Glycoprotein Belonging to the Immunoglobulin Superfamily.” *FEBS Letters* 425 (2): 191–94. https://doi.org/10.1016/S0014-5793(98)00213-0.

Kurihara, Isao, Dong Kee Lee, Fabrice G. Petit, Jaewook Jeong, Kevin Lee, John P. Lydon, Francesco J. DeMayo, Ming Jer Tsai, and Sophia Y. Tsai. 2007. “COUP-TFII Mediates Progesterone Regulation of Uterine Implantation by Controlling ER Activity.” *PLoS Genetics* 3 (6): 1053–64. https://doi.org/10.1371/journal.pgen.0030102.

Laws, Mary J., Robert N. Taylor, Neil Sidell, Francesco J. DeMayo, John P. Lydon, David E. Gutstein, Milan K. Bagchi, and Indrani C. Bagchi. 2008. “Gap Junction Communication between Uterine Stromal Cells Plays a Critical Role in Pregnancy-Associated Neovascularization and Embryo Survival.” *Development* 135 (15): 2659–68.

https://doi.org/10.1242/dev.019810.

Lee, K. Y., J.-W. Jeong, J. Wang, L. Ma, J. F. Martin, S. Y. Tsai, J. P. Lydon, and F. J. DeMayo. 2007. “Bmp2 Is Critical for the Murine Uterine Decidual Response.” *Molecular and Cellular Biology* 27 (15): 5468–78. https://doi.org/10.1128/mcb.00342-07.

Li, Kailiang, and Romana A Nowak. 2019. “The Role of Basigin in Reproduction.” *Reproduction (Cambridge, England)*, September. https://doi.org/10.1530/REP-19-0268.

Monsivais, Diana, Caterina Clementi, Jia Peng, Paul T Fullerton, Renata Prunskaite-Hyyryï ainen, Seppo J Vainio, and Martin M Matzuk. 2017. “BMP7 Induces Uterine Receptivity and Blastocyst Attachment.” *Endocrinology* 158 (4): 979–92. https://doi.org/10.1210/en.2016-1629.

Monsivais, Diana, Caterina Clementi, Jia Peng, Mary M. Titus, James P. Barrish, Chad J. Creighton, John P. Lydon, Francesco J. DeMayo, and Martin M. Matzuk. 2016. “Uterine ALK3 Is Essential during the Window of Implantation.” *Proceedings of the National Academy of Sciences* 113 (3): E387–95. https://doi.org/10.1073/pnas.1523758113.

Muramatsu, Takashi, and T. Miyauchi. 2003. “Basigin (CD147): A Multifunctional Transmembrane Protien Involved in Reproduction, Neural Function, Inflammation and Tumor Invasion.” *Histology and Histopathology* 18 (3): 981–87.

Naruhashi, Kazumasa, Kenji Kadomatsu, Tadahiko Igakura, Qi Wen Fan, Naohiko Kuno, Hisako Muramatsu, Teruo Miyauchi, et al. 1997. “Abnormalities of Sensory and Memory Functions in Mice Lacking Bsg Gene.” *Biochemical and Biophysical Research Communications* 236 (3): 733–37. https://doi.org/10.1006/bbrc.1997.6993.

Norwitz, Errol, Danny Schust, and Susan Fisher. 2001. “Implantation and the Survival of Early Pregnancy.” *The New England Journal of Medicine* 345 (19): 1400–1408.

Ochrietor, Judith D., and Paul J. Linser. 2004. “5A11/Basigin Gene Products Are Necessary for Proper Maturation and Function of the Retina.” *Developmental Neuroscience* 26 (5–6): 380–87. https://doi.org/10.1159/000082280.

Ramathal, Cyril, Indrani Bagchi, Robert Taylor, and Milan Bagchi. 2010. “ENDOMETRIAL DECIDUALIZATION: OF MICE AND MEN.” *Semin Reprod Med* 28 (1): 17–26. https://doi.org/10.1055/s-0029-1242989.ENDOMETRIAL.

Rossant, Janet. 2016. “Making the Mouse Blastocyst: Past, Present, and Future.” In *Current Topics in Developmental Biology*, 117:275–88. Academic Press Inc. https://doi.org/10.1016/bs.ctdb.2015.11.015.

Sharkey, Andrew M., and Stephen K. Smith. 2003. “The Endometrium as a Cause of Implantation Failure.” *Best Practice and Research: Clinical Obstetrics and Gynaecology* 17 (2): 289–307. https://doi.org/10.1016/S1521-6934(02)00130-X.

Soyal, Selma M., Atish Mukherjee, Kevin Y.S. Lee, Jie Li, Huaiguang Li, Francesco J. DeMayo, and John P. Lydon. 2005. “Cre-Mediated Recombination in Cell Lineages That Express the Progesterone Receptor.” *Genesis* 41 (2): 58–66. https://doi.org/10.1002/gene.20098.

Terakawa, Jumpei, Takaho Watanabe, Rutsuko Obara, Makoto Sugiyama, Naoko Inoue,

Yasushige Ohmori, Yoshinao Z. Hosaka, and Eiichi Hondo. 2012. “The Complete Control of Murine Pregnancy from Embryo Implantation to Parturition.” *Reproduction* 143 (3): 411–15. https://doi.org/10.1530/REP-11-0288.

Tranguch, S., T. Daikoku, Y. Guo, H. Wang, and S. K. Dey. 2005. “Molecular Complexity in Establishing Uterine Receptivity and Implantation.” *Cellular and Molecular Life Sciences* 62 (17): 1964–73. https://doi.org/10.1007/s00018-005-5230-0.

Wang, Haibin, Shuang Zhang, Haiyan Lin, Shuangbo Kong, Shumin Wang, Hongmei Wang, and D. Randall Armant. 2013. “Physiological and Molecular Determinants of Embryo Implantation.” *Molecular Aspects of Medicine* 34 (5): 939–80. https://doi.org/10.1016/j.mam.2012.12.011.

Xin, Xiaoyan, Xianqin Zeng, Huajian Gu, Min Li, Huaming Tan, Zhishan Jin, Teng Hua, Rui Shi, and Hongbo Wang. 2016. “CD147 / EMMPRIN Overexpression and Prognosis in Cancer : A Systematic Review And.” *Scientific Reports*, no. 113: 1–12. https://doi.org/10.1038/srep32804.

CHAPTER FOUR

Basigin Expression in the Uterus is Required for Proper Implantation and Decidualization *in vivo*

Abstract

Basigin (BSG) is a transmembrane glycoprotein involved in cell proliferation, angiogenesis and tissue remodeling and is essential for male and female reproduction. Due to high embryonic lethality of global knockout of BSG, a PR-Cre mediated uterine tissue-specific *Bsg* knockout model was generated to study the role of uterine BSG in reproduction. A fertility study showed that the conditional knockout (cKO) females had significantly reduced fertility, and complications occurred throughout the course of pregnancy. I hypothesized that BSG is required for normal implantation and proper decidualization of uterine stromal cells in mice. To test the hypothesis, uteri of day 5 pregnancy mice were collected to assess implantation sites. Based on epithelial markers, the luminal epithelium of the cKO mice did not undergo apoptosis and the embryos were not able to penetrate the stromal layers. Jones' silver stain results revealed that the integrity of the basement membrane of the cKO mice was not disrupted. To investigate decidualization, an artificially induced decidualization response (ADR) experiment was performed. Ovariectomized mice of each genotype were given 100 ng estradiol/day for three days, rested for two days, then given 10 ng estradiol and 1 mg progesterone/day for three days. One uterine horn was injected with 15 µl corn oil as a stimulus while the other horn was an un-injected internal control. Mice were supplied with 1 mg progesterone/day for four days before tissue collection and analysis. The injected uterine horn weight increased 2.2-fold in cKO mice compared to the un-injected horn, which was significantly lower than the 9-fold increase observed in control mice. Histology analysis determined that the uterine cross-sections of the decidua were much smaller in the knockout mice.

qRT-PCR analysis demonstrated significantly lower expression of the decidualization genes *Bmp2* and *Cebpβ* in the cKO decidual tissue. Immunohistochemistry showed significantly lower expression of the decidualization markers CEBPβ and HAND2 in the decidua of cKO mice. Immunofluorescent results on uteri of day 5 pregnant mice showed lower expression levels of CEBPβ and HAND2. Protein localization and abundance of the lactate transporter MCT1 were altered in the cKO mice compared to the controls. The angiogenic marker CD31 was reduced in cKO mice on day 6 of pregnancy, indicating impaired angiogenesis. These results support the conclusion that uterine expression of BSG is required for normal implantation and decidualization in female mice.

Introduction

Embryo implantation is the process where the mature blastocyst attaches to the maternal endometrium forming the placenta (Ye 2020). It is a mandatory step for reproduction in mammalian species and requires synchronized development of the embryo and the uterus, as well as highly organized communication between the two (Cha, Sun, and Dey 2012). In humans, natural conception per cycle is only 30%; about 75% of pregnancy losses are thought to be results of implantation failure (Norwitz, Schust, and Fisher 2001). Because of the ethical issues and the many conserved mechanisms between mice and humans, mice have been widely used as animal models for investigating the embryo implantation process (Aplin and Ruane 2017). In mice, implantation occurs at day 4.5. The luminal epithelium is the first maternal cell layer that an embryo comes into contact with, and serves as the transient gateway for embryo implantation and subsequent embryo development (Ye 2020). After attachment is completed, the embryo must penetrate through the luminal epithelium and the basement membrane for a pregnancy to be

successful. The luminal epithelial cells at the implantation site undergo specific changes such as controlled disassembly of adhesive complexes and apoptosis to assist the invasion of the embryo (Parr, Tung, and Parr 1987). When this is completed, the embryo needs to break through the basement membrane. The basement membrane is a specialized extracellular scaffold composed of type IV collagen, laminin, perlecan, peroxidasin and nidogen (Blankenship and Given 1995; Fisher et al. 1985; Jones-Paris et al. 2017). It is a contiguous layer prior to implantation and becomes disrupted at the site of implantation. Once the removal of the luminal epithelium and the basement membrane has occurred, the trophoblast and the stromal cells come into close contact with each other and further development of the pregnancy continues.

After implantation occurs, the stromal cells surrounding the embryo undergo further proliferation and differentiation into large, round, sometimes multinucleated decidual cells. This physiological change is known as decidualization and it is a process in rodents and humans during early pregnancy (Cha, Dey, and Lim 2014). It is well accepted that proper decidualization is essential for successful implantation and normal pregnancy (Singh, Chaudhry, and Asselin 2011). The reason is that decidualization has numerous functions, for example providing the implanted embryo with growth factors and cytokines, controlling the implantation window and selection of embryos, establishing the local immune microenvironment at the fetal-maternal interface, maintaining tissue homeostasis during trophoblast invasion, protecting the embryo from inflammation and reactive oxygen species, and supporting the angiogenesis processes to nourish the growing embryo as well as promoting formation of the placenta (Ramathal et al. 2010; Wetendorf and DeMayo 2012; Monsivais et al. 2017; Bhurke, Bagchi, and Bagchi 2016). This critical morphological and functional transformation is dependent upon the action of the steroid hormone progesterone, epithelial cell secreted factors, cell cycle regulators and transcription

factors and immune cells (Conneely, Mulac-Jericevic, and Lydon 2003; Wetendorf and DeMayo 2012; Das 2009; Croy et al. 2012). Many genes and signaling pathways have been identified to play a role in decidualization. For example, progesterone promotes Bone morphogenetic protein 2 (BMP2), stimulates its downstream target Wingless-related integration site 4 (WNT4) to regulate decidualization. Loss of either BMP2 or WNT4 leads to failed decidualization and infertility (Lee et al. 2007; Franco et al. n.d.). In addition, BMP2 also regulates the cell cycle transcription factor CCAAT enhancer-binding protein beta (CEBPβ), which acts via the Signal transducer and activator of transcription 3 (STAT3) pathway to modulate decidualization. Mice with conditional deletion of CEBP and STAT3 in the uterus also show decidualization defects (Cheng et al. 2001; W. Wang et al. 2012). Development of genetically engineered mouse models has provided a wealth of information about the signaling pathways in implantation and decidualization; however, the role of BSG involved in implantation and decidualization remains unclear.

BSG is a highly glycosylated transmembrane protein and is expressed ubiquitously in humans and mice (K. Li and Nowak 2019). Studies by our laboratory and others have shown that BSG is expressed in the reproductive tissues of both female and male mice, and is important for successful pregnancy and spermatogenesis (Braundmeier et al. 2012; Chen et al. 2007; Bi et al. 2013). BSG was first identified to play a role in reproduction by Igakura and colleagues, who demonstrated that both embryonic and maternal expression of BSG is required for normal pregnancy in a *Bsg* null mutant mouse model (Tadahiko Igakura et al. 1998; Kuno et al. 1998). However, global deletion of *Bsg* results in high embryo death and limits our understanding of the role of BSG in reproduction. Thus we generated a PR-Cre and lox cKO mouse model to study the role of BSG *in vivo*. The results in the previous chapter validated this animal model and demonstrated reduced fertility in the cKO mice. I also targeted the pregnancy complication to

uterine defects at a variety of times. It is important to improve our knowledge of how BSG is involved in regulating early pregnancy; therefore, I investigated the implantation and decidualization processes in this chapter. The goals of this study were: 1) to investigate the luminal epithelial cell and basement membrane integrity at the implantation site, 2) to evaluate the status of the decidualization process by ADR or natural pregnancy and 3) to investigate post-implantation defects such as lactate transporter localization and angiogenesis in the cKO mice *in vivo*. Here, I demonstrate that loss of uterine expression of BSG leads to failures in the breakdown of the luminal epithelium and basement membrane at the implantation sites, a compromised decidualization response, and reduction in lactate transporter abundance and angiogenesis leading to decreased fertility in mice.

Material and Methods

Animals

C57/Bl6 mice were housed at the University of Illinois at Urbana-Champaign, the Institute for Genomic Biology Animal Facility in polysulfone cages. Food (Harlan Teklad 8604) and filtered water were provided for the mice *ad libitum*. The room was maintained at a temperature of 22 ± 1 °C and on a 12 hour light-dark cycle. All experimental procedures including animal care, surgery, euthanasia and tissue collection were approved by the Institutional Animal Care and Use Committee at the University of Illinois at Urbana–Champaign.

Tissue Collection and Histological Processing

Female mice of each genotype were bred with wild type males at two months of age. The day of a vaginal plug was designated as day 1 of pregnancy. On pregnancy day 4, day 5 morning, day 5 evening and day 6, mice were euthanized by CO_2 to collect uterine tissue. Uterine tissues

were weighed and photographed. One uterine horn was snap-frozen in liquid nitrogen and stored at -80°C for later RNA extraction. The other uterine horn was fixed in 10 mL of 10% buffered formalin for 24 hours, transferred into 70% ethanol and processed for histology. The uterine tissues were processed in a VipTek tissue processor, embedded with paraffin into 5 mm thick blocks and then sectioned into 5 µm thick sections using a microtome. The slides were dried for at least 24 hours before being processed for further analysis.

RNA isolation and quantitative reverse transcription-PCR (qRT-PCR)

Total RNA was extracted from uterine tissues from mice on day 4 and day 5 of pregnancy or from ADR decidual tissue using the Qiagen RNeasy Mini kit (Qiagen #74104) according to the manufacturer's instructions. The concentration of mRNA was determined by a nanodrop and the quality of the mRNA was assessed using the Bioanalyzer at the Functional Genomics Center at the University of Illinois, Urbana-Champaign (https://biotech.illinois.edu/functionalgenomics). One microgram of total RNA was reverse transcribed using the First Strand cDNA Synthesis Kit from Roche (#4379012001) following the manufacturer's instructions. After cDNA was synthesized, qRT-PCR was performed to assess the mRNA level of decidualization and other gene markers in the uteri and decidua of the mice using Power Sybr Green Master Mix (Life Tech A25742). Briefly, 5 µl of a 1:7 diluted cDNA sample were mixed with 10 µl of master mix (7.5 µl of Sybr Green Mix, 0.6 µl primer sets and 1.9 µl of water) for a total volume of 15 µl per well in a MicroAmp optical 384-well reaction plate. Three technical replicates were performed for each sample. qRT-PCR amplification and quantitation were performed using a Quant Studio (Applied Biosytem) from the Functional Genomics Center. The reaction was run for 40 cycles (95 °C for 15 seconds, 60 °C for 1 minute). The comparative CT method (ΔΔCT) was used for quantification of gene expression. Relative fold changes in gene expression for all tested genes were normalized

to Peptidylprolyl isomerase A(*Ppia)* and Ribosomal protein, large, P0 (*Rplp0)* endogenous housekeeping genes. Genes analyzed include *Bsg*, *Cebpβ*, *Bmp2*, Heart and neural crest derivatives-expressed protein 2 (*Hand2*), *Wnt4*, Alkaline phosphatase (*Alph*) and Epiregulin encoding gene (*Ereg*). The primer sequences of these genes are listed in **Table 4.1**

Immunohistochemistry

To assess the abundance of BSG, Monocarboxylate transporter 1 (MCT1), Cluster of differentiation 98 (CD98), Cluster of differentiation 31 (CD31), cytokeratin (CK), HAND2 and CEBPβ, immunohistochemistry (IHC) was performed on samples collected on day 4, day 5 or day 6 of pregnancy. Briefly, slides of uterine horns were deparaffinized using three xylenes and rehydrated though a series of decreasing concentrations of ethanol, then subjected to heat-induced antigen retrieval with DAKO Target Retrieval Solution at 1:10 dilution (10X pH9) (Dako Denmark A/S, Denmark, Part Number: S236784-2, Code: S2367) at 100 ◦C for 30 minutes and allowed to cool to room temperature (RT). This was followed by inactivation of endogenous peroxidase activity with 0.3% H_2O_2/methanol for 15 minutes in the dark. The samples were then rinsed with phosphate buffered saline with Tween-20 (PBST) and incubated in blocking solution consisting of 5% horse serum (Vectastain ABC kit, Vector Laboratories, Inc. Burlingame, CA) diluted in 1%BSA/PBST at RT for 60 minutes. The tissue sections were incubated with a primary antibody at specific concentrations overnight at 4 ◦C. The primary antibodies used were: BSG (R&D system AF772) at 1:200 dilution, MCT1 (LSBio c335287) at 1:100 dilution, CD98 (Santa Cruz Sc9160) at 1:200 dilution, CEBPβ (Santa Cruz sc-150) at 1:100 dilution, pan cytokeratin (Sigma c2562) at 1:200 dilution and CD31 (Abcam, ab28364) at 1:50 dilution. The negative control sections were incubated in a non-specific IgG of the same species as the primary antibodies to confirm specificity of the primary antibodies. On the following day, slides were rinsed with PBST prior to incubation

with anti-rabbit, anti-goat or anti-mouse biotinylated secondary antibody (Vectastain ABC kit, Vector Laboratories, Inc. Burlingame, CA) at 1:200 dilution in PBST for 60 minutes at RT. Slides were then rinsed and incubated in ABC solution (PBS: A: B=50:1:1) (Vectastain ABC kit, Vector Laboratories, Inc. Burlingame, CA) for 30 minutes at RT. For visualization of the immunoreactivity, all slides were subjected to chromogen 3'3-diaminobenzidine (DAB) (Vector Laboratories, Inc. Burlingame, CA) for 30 seconds. Slides were rinsed in tap water for 10 minutes to stop the DAB reaction. Thereafter, the slides were counterstained with hematoxylin for one minute followed by dehydration and cover-slipping. After drying for 24 hours, the slides were cleaned and loaded into a Hamamatsu Nanozoomer 2.0 HT for scanning.

Immunofluorescence Staining

To assess the abundance and localization of BSG, cytokeratin, E-cadherin, HAND2, CEBPβ, MCT1 and CD31 in the uteri at the time of implantation and later stages, immunofluorescence (IF) staining was performed on samples on day4, day 5 and day 6 of pregnancy. Briefly, uterine slides were deparaffinized using three xylenes and rehydrated through a series of decreasing concentration of ethanol, and then subjected to heat-induced antigen retrieval with DAKO Target Retrieval Solution at 1:10 dilution (10X pH9) (Dako Denmark A/S, Denmark, Part Number: S236784-2, Code: S2367) at 100 ◦C for 30 minutes and allowed to cool to RT. The slides were then incubated in blocking solution consisting of 5% horse serum (Vectastain ABC kit, Vector Laboratories, Inc. Burlingame, CA) diluted in 1%BSA/PBST at RT for 60 minutes. The tissue sections were incubated with a primary antibody at specific concentrations overnight at 4 ◦C. The primary antibodies used were: BSG (R&D system AF772) at 1:200 dilution, MCT1 (LSBio c335287) at 1:100 dilution, E-cadherin (R&D system af748) at 1:100 dilution, pan cytokeratin (Sigma c2562) at 1:200 dilution and CD31 (Abcam, ab28364) at 1:50 dilution. The

negative control sections were incubated in a non-specific IgG of the same species as the primary antibodies to confirm specificity of the primary antibodies. On the following day, slides were rinsed with PBST prior to incubation with either an anti-goat Alexa488 conjugated secondary antibody (Jackson Immuno Research # 805-545-180), an anti-rabbit Cy3 conjugated secondary antibody (Jackson Immuno Research # 711-165-152) or an anti-mouse Cy5 conjugated secondary antibody (Jackson Immuno Research # 715175151) at 1:200 dilution for 1 hour at RT. After incubation, slides were rinsed with PBS and covered with a DAPI containing mounting medium (Vector Laboratories, H-1200). To detect the immunoreactivity, all slides were imaged using a Zeiss LSM 710 confocal microscope at the Institute for Genomic Biology at the University of Illinois, Urbana-Champaign.

Jones' Silver Stain

To assess the uterine basement membrane integrity of the cKO females at the time and site of implantation, Jones' silver stain was performed. Briefly, slides of uterine horns on day 5 were deparaffinized using three xylenes and rehydrated through a series of decreasing concentrations of ethanol, and then oxidized in 0.5% periodic acid solution for 11 minutes. After rinsing thoroughly in distilled, deionized water, slides were placed in freshly made methenamine silver solution (3% methenamine and 5% silver nitrate) at 70 ◦C for 60 minutes. The slides were checked every 20 minutes for precipitate formation. Once a medium brown color stain appeared, slides were rinsed in distilled deionized water at 70 ◦C. The slides were then placed in 0.2% gold chloride solution for 1 minute, rinsed in distilled water and treated with sodium thiosulfate for 1 min. The slides were then rinsed in running tap water for 10 minutes before counterstaining. Fast green (Fisher) was used for 1 minute as a counterstain. The slides were then dehydrated and covered. After drying

for 24 hours, the slides were cleaned and loaded into a Hamamatsu Nanozoomer 2.0 HT for scanning.

Artificial Decidualization Response

To evaluate the decidualization response of the cKO females, an ADR experiment was conducted as illustrated in **Figure 4.1**. Ten female mice of each genotype were ovariectomized and rested for two weeks to eliminate innate circulating steroid hormones. To precisely control the level of hormones in the animals, estradiol and progesterone were injected into the animals subcutaneously daily for two weeks. First, 100 ng of estradiol was injected for 3 days, then the mice were rested for two days before daily injection of 10 ng estradiol and 1 mg progesterone were administered for another 3 days. On the third day of estradiol and progesterone injection, the mice were anesthetized with 8.7 mg/ml ketamine and 1.5 mg.ml xylazine (provided by the Division of Animal Resources at the University of Illinois, Urbana-Champaign). A small incision was made on the abdominal side to expose the right uterine horn. Then 15 µl of corn oil (Sigma c8267) were injected into the uterine horn from the basal part to serve as a stimulus for decidualization. The other uterine horn was not injected as an internal control. The wound was sutured, and the mice were allowed to recover. Following the oil injection, the mice were injected with 1 mg progesterone every day for another 3 days before tissue collection. One control mouse was lost during the surgery, but all the remaining mice were subjected to euthanasia and tissue collection. After euthanizing the mice, the uterine horns were weighed separately and photographed. The injected uterine horn was cut in half. One half was snap frozen in liquid nitrogen for further RNA isolation and qRT-PCR analysis. The other half was fixed in 10% buffered formalin for 24 hours, then transferred to 70% ethanol and processed for histological analysis. To measure the size of the cross section of the decidua tissue, H&E stained slides were loaded into a Hamamatsu Nanozoomer

2.0 HT for scanning. The area, perimeter and diameter of the cross sections were measured and recorded for each animal.

Statistical Analysis

All data were analyzed utilizing GraphPad Prism software 8 (GraphPad Prism, San Diego, CA). Data are presented as means ± standard error of the means (SEM). For normally distributed data, unpaired t tests were used to compare the control group and the experimental group. For non-normally distributed data, Mann-Whitney tests were used. A statistical significance was assigned at $p \leq 0.05$. A trending difference was assigned when the p value was between 0.05 and 0.1.

Results

Luminal epithelial cell integrity is not affected at implantation in the cKO females.

In order to determine if implantation was impaired in the cKO mice, uterine samples of females of both genotypes were collected on day 5 of pregnancy. The uteri slides were stained with a pan-cytokeratin antibody by IHC and IF. The IHC results (**Figure 4.2**) showed that in the control animals (top panel), at the embryo implantation site, there was no cytokeratin, indicating a disruption of the epithelial layer. However, the embryo in the cKO females (bottom panel) was surrounded by a continuous layer of epithelial cells as highlighted by the positive brown color of cytokeratin, indicating the embryo was not able to break the epithelium and invade into the stromal layers. In the IF results (**Figure 4.3**), the embryos were marked with green for BSG as they express BSG, and the epithelium was marked with red for cytokeratin. In the controls (top panel), at the site far away from the embryo, there was continuous expression of cytokeratin, highlighting the luminal epithelium, but at the site of implantation, the expression of cytokeratin was disrupted.

However, in the cKO (bottom panel), the embryo was clearly restrained in the pocket of epithelial layer.

Immunofluorescence staining of E-cadherin was performed to evaluate the function of the luminal epithelium at the implantation site on the evening of day 5 of pregnancy (**Figure 4.4**). There was no E-cadherin at the site of implantation in the control mice (top panel), indicating a complete breakdown and apoptosis of the luminal epithelial cells. This suggests the embryo was able to penetrate the luminal epithelial barrier and successfully invade into the stromal layer. However, in the cKO (bottom panel), the embryo was still surrounded by an intact layer of epithelium with intense E-cadherin. The integrity of the epithelium was preserved, indicating failed luminal epithelial breakdown and embryo invasion in the cKO mice. This was assessed on the evening of day 5, when the embryo should have completed attachment and invasion as the control mice showed (Ye 2020). Thus, it suggests that the embryo surrounded by the intact luminal epithelium in cKO was not due to delayed implantation, but due to failed implantation.

Basement membrane is not disrupted at implantation site in the cKO females.

The penetration and breakdown of the uterine luminal epithelial basement is required for successful implantation (Blankenship and Given 1995). To assess the basement membrane status of the cKO females, Jones' silver stain was performed (**Figure 4.5**) on implantation sites collected on day 5 evening of pregnancy. In the controls, the black stain lining the luminal epithelium was found away from the embryo, but there was no positive stain at the site of embryo attachment, suggesting a breakdown of the basement membrane. In the cKO, the black color positive stain was still present at the basal side of the luminal epithelium around the embryo, suggesting an unaltered basement membrane.

cKO females have an impaired artificial decidualization response.

Proper decidualization is critical for normal pregnancy (Ramathal et al. 2010). An ADR experiment was carried out in both genotypes as **Figure 4.1** showed. Uteri were photographed at collection and images are shown in **Figure 4.6**. The results revealed that in the controls, most of the animals displayed a robust response to the stimuli (top panel). However, in the cKO mice, there was a very modest response or no response at all in most of the animals (bottom panel).

Each uterine horn was weighed and the ratio of injected horn to uninjected horn weight was calculated (**Figure 4.7 A**). In the controls, on average, the injected uterine horn had a 9.13-fold increase in weight in response to the stimuli. However, in the cKO mice, there was only a modest 2.2-fold increase in the weight of the injected uterine horn, indicating an impaired decidual response. The body weight of each mouse was also measured (**Figure 4.7 B**). The cKO mice weighed 22.73 g on average, which was not different compared to the controls at 23.67 g. This suggests that the differences in the uterine weights between the genotypes of mice was due to different responses to the experimental stimuli, rather than body weight differences.

ADR-induced decidua size is much smaller in the cKO females.

To quantify the size of the decidua, cross sections of the decidual tissue were captured and measured using the Nanozoomer (**Figure 4.8**). The size was measured as the area, perimeter and diameter of the cross section. The area of the controls was 7.2 mm^2, which was significantly higher than the area of the cKO at 3.86 mm^2. The perimeter of the controls was 10.74 mm, which was much higher than the 7.38 mm of the cKO. The diameter of the controls was also significantly higher than the cKO, at 3.17 mm to 2.19 mm. These results confirmed that the decidua was much smaller in the cKO mice compared to the controls.

Expression of decidualization markers is downregulated in the cKO females.

I evaluated the expression levels of several genes known to regulate decidualization by qRT-PCR and the results are shown in **Figure 4.9**. *Bsg* gene expression levels in the cKO were downregulated by 86% of the levels in the controls as expected. *Cebpβ* expression in the cKO was significantly downregulated by 75% of the levels in the controls and *Bmp2* expression in the cKO mice was also significantly downregulated by 88% of the levels in the controls. The expression levels of *Hand2* and *Wnt4* tended to be lower in the cKO, both at 50% of the levels in the controls, but not statistically different. *Alph* and *Ereg* expression levels were not significantly altered. These results confirm that specific decidualization marker genes were downregulated in the cKO, leading to the incomplete decidualization response.

CEBPβ protein abundance is reduced in the cKO females.

To determine whether the protein expression level was consistent with gene expression level for some of the decidualization genes, I chose CEBPβ and HAND2 for immunohistochemical analysis. Results shown in **Figure 4.10** confirm there was abundant CEBPβ protein expression in the decidual tissue in the control mice (**A**), but there was very little CEBPβ expression in the cKO mice (**B**). This confirmed that the CEBPβ protein abundance level was much reduced in the cKO compared to the controls. Similar results were observed in the uteri of mice on the evening of day 5 pregnancy using IF staining. In **Figure 4.12**, uterine sections were double stained with BSG and CEBPβ. The results in the control animals (top panel) showed abundant CEBPβ expression (orange color) present in the primary decidual zone surrounding the embryo. In the cKO females, however, the area of CEBPβ positive cells was much smaller (bottom panel). Similarly, in **Figure 4.13**, uterine of day 5 pregnant mice were double stained with E-cadherin (green) and CEBPβ (orange). These results showed that the controls lost E-cadherin expression at the implantation site but had

a broad region of stromal cells expressing CEBPβ (top panel). In the cKO (bottom panel), the embryo was restrained within a circle of intact, E-cadherin positive luminal epithelium, and the expression of CEBPβ was limited to a smaller region of stromal cells close to the embryo.

HAND2 protein abundance is reduced in the cKO females.

HAND2 protein abundance was also evaluated in the decidual tissue in both the controls and the knockouts using IHC. **Figure 4.11** showed in the decidual tissue of the controls, HAND2 was abundant in the stromal cells over a wide area. However, in the cKO mice, HAND2 was greatly reduced compared to the controls. Similar results were confirmed in the uteri of day 5 pregnant mice using IF staining. In **Figure 4.14**, uterine sections of both genotypes were double stained with E-cadherin and HAND2. The top panel illustrated that the controls lost E-cadherin at the site of embryo implantation but maintained E-cadherin in the luminal epithelium away from the embryo implantation site. HAND2 protein was found in the subepithelial stromal cells surrounding the embryo. In the cKO showed in the bottom panel, the luminal epithelium still maintained E-cadherin. As a result, the embryo was not able to penetrate through the luminal epithelium. There was some HAND2 in the subepithelial stromal cells, but compared to the controls, the area of HAND2 positive cells was much smaller. Taken together, these data support that HAND2 abundance was reduced in the cKO females.

CD98 protein localization is not altered in the cKO females.

CD98 interacts with BSG and is found in the apical surface of endometrial epithelium during implantation and is important for adhesion and metabolism (Guo et al. 2015; Domínguez et al. 2010). To examine the localization pattern of CD98, IHC for CD98 was performed on samples from day 1 and day 4 of pregnancy. There was no difference in the localization of CD98 on day 1 of pregnancy (top panel) in the controls compared to the cKO, as CD98 was normal in

the luminal epithelium. Similarly, CD98 was found the stromal layers on day 4 of pregnancy in both the cKO and control uteri (**Figure 4.15**). This indicates the localization of CD98 was not affected by loss of BSG in the cKO females.

MCT1 protein localization is altered in uterus of the cKO females.

MCTs are important for lactate transport and metabolic homeostasis, and MCT1 and MCT4 are shuttled to the membrane by their chaperone protein BSG (Halestrap 2012; Woodhead et al. 2000; Gallagher et al. 2007). To assess the abundance and localization of MCT1 in the cKO females, I performed IHC and IF on uterine sections at day 4 and day 6 of pregnancy. IHC results in **Figure 4.16** revealed that, on day 4 of pregnancy, the controls (**A**) showed MCT1 on the basal side of the luminal epithelium, but this localization was not present in the cKO mice (**B**). On day 6 of pregnancy, MCT was found in the embryo and in the cell membrane of the stromal cells in the deep stromal layer in the controls (**C**). However, in the cKO females, BSG was only found in the embryo, not in the cell membrane of the deep stromal cells (**D**).

Immunofluorescence staining showed similar results in **Figure 4.17.** In the controls, BSG was abundant in the deep undifferentiated stromal cells and MCT1 was localized in the same region (**B and C**). In contrast, BSG was found only in some immune cells and endothelial cells in a scattered pattern within the stroma of the cKO females on day 6 of pregnancy (**F**). MCT1 was very weak at a low magnification (**G**), and there was no co-localization of the two proteins (**H**). At a higher magnification focused at the deep stromal layer in **Figure 4.18**, BSG was abundant in the cell membrane (**B**) in the uteri of the controls. MCT1 was also found in the cell membrane (**C**) and these two co-localized in the merged image (**D**). However, in the cKO females, there was no such co-localization of BSG and MCT1 in the same area. These results confirm that the localization and abundance of MCT1 were altered in the uteri of the cKO females.

CD31 protein abundance is reduced in the cKO females.

To evaluate the status of angiogenesis in the cKO mice, I performed IHC for the angiogenic marker CD31 on uterine sections on day 6 of pregnancy. **Figure 4.19** shows that, CD31 was abundant in the embryo and also in the endothelial cells among deep stromal cells in the controls (**B**). The abundance of CD31 was much lower in the cKO mice (**E**). A higher magnification of the deep stromal layer in **Figure 4.20** showed clearly that abundance of CD31 (red) was much higher in the control (**B**) compared to the cKO female (**E**). To quantify the abundance of CD31, images of five fields were randomly selected and measured for their signal intensity. The results showed that the signal intensity in sections from the controls was 34.92, which was significantly higher than the value of 20.3 in the cKO females (**Figure 4.21**). These results revealed a markedly decreased abundance of CD31 in the uteri of the cKO mice, suggesting reduced angiogenesis at the implantation sites in these animals.

Discussion

BSG is a transmembrane glycoprotein expressed in many tissue and cell types, including the reproductive organs in both humans and mice (Fossum, Mallett, and Neil Barclay 1991; Chen et al. 2007). Studies have shown that *Bsg* null mice were infertile likely due to failed fertilization or implantation (Kuno et al. 1998; T Igakura et al. 1998). Implantation is a dynamic event that involves a series of physical and physiological interactions between the implanting blastocyst and the receptive uterus (H. Wang and Dey 2006). At the time of implantation, the luminal epithelial cells at the implantation site undergo apoptosis and the basement membrane is breached for further invasion of the embryo (Pampfer and Donnay 1999). Cytokeratin assembles into a flexible dynamic network of intermediate filaments and determine the cell shape of epithelial cells (Fuchs

and Weber 1994). During peri-implantation period, cytokeratin is downregulated in the endometrium of mice, rabbits and cows (Gou et al. 2019; Olson et al. 2002; Haeger et al. 2015). The results showed that the luminal epithelial cells at the site of implantation still expressed cytokeratin in many cKO mice on the evening of day 5 pregnancy. E-cadherin, a $Ca2^{+}$-dependent transmembrane protein that forms adhesion junctions, is expressed in the luminal epithelium (Wesseling, Van Der Valk, and Hilkens 1996). During implantation, expression of E-cadherin is downregulated due to cell remodeling to assist blastocyst attachment and invasion in mice, rats and rabbits. (Paria et al. 1999; Q. Li et al. 2002; Gou et al. 2019). Paria and colleague reported that E-cadherin is expressed in the luminal epithelium prior to implantation, but it is lost during implantation and transiently appears in the stromal cells in mice (Paria et al. 1999). Nallasamy and colleague showed that persistent expression of E-cadherin results in implantation failure (Nallasamy et al. 2012). The results showed that in the cKO uteri, E-cadherin was expressed throughout the uterine luminal epithelium at the time of implantation. Similarly, the activin-like kinase (ALK)-3 cKO mice also expressed E-Cadherin in the luminal epithelium at this time and had implantation failure and infertility (Monsivais et al. 2016).

During early pregnancy in rodents and humans, the endometrial stromal cells respond to the invasion of the embryo by undergoing proliferation followed by differentiation; this morphological and functional transformation is known as decidualization. (Peng et al. 2008). It is widely accepted that a fully developed decidua is a prerequisite for successful implantation, and abnormal decidualization can result in implantation failure, miscarriages, preeclampsia and intrauterine growth restrictions (Ramathal et al. 2010; Kong, Aronow, and Handwerger 2006; Singh, Chaudhry, and Asselin 2011). The ADR results showed that most of the cKO females either did not have a decidual response or had a modest decidual response, whereas the control females

had a robust response. The qRT-PCR results showed that *Bmp2* and *Cebpβ* in the cKO decidual tissue have been significantly downregulated compared to the controls. BMP ligands and receptors are expressed in the uterus of pregnant mice, and play key roles in regulating implantation (Clementi et al. 2013). BMP2 is most studied and loss of BMP2 in the uterus caused infertility of mice due to failures in embryo attachment and decidualization. BMP2 acts through its receptor ALK2 to regulate decidualization; Alk2 null mice failed to undergo uterine decidualization (Monsivais et al. 2016; Clementi et al. 2013). Microarray analysis revealed that CEBPβ is downstream of ALK2 and CEBPβ expression is suppressed in ALK2 cKO mice. CEBPβ is a transcription factor involved in cell cycle under regulation of steroid hormones, and is expressed in the endometrial stromal cells in mice, baboons and humans and (W. Wang et al. 2010; Kannan et al. 2010; Bhurke, Bagchi, and Bagchi 2016; Clementi et al. 2013). In mice, its expression is rapidly induced at the time of blastocyst attachment, and further increased during decidualization in the proliferating and decidualized stromal cells surrounding the blastocyst. Studies have shown that CEBPβ is a key regulator of decidualization as CEBPβ-lacking uteri failed to undergo decidualization and lacked a response to artificial decidualization stimulation similar to these results in this chapter (Bagchi et al. 2006; Mantena et al. 2006). It is also reported that CEBPβ acts through its direct downstream target STAT3 to regulate decidual response in human and mice (Cheng et al. 2001; W. Wang et al. 2012). Interestingly, BSG is reported to promote STAT3 activity in cancer cells (L. Li et al. 2013). Together with the downregulation of *Bmp2*, it suggests that loss of BSG in the uterus leads to defective decidualization, likely through BMP-ALK2-CEBPβ-STAT3 pathway. HAND2 is a transcription factor that is expressed in the uterine stromal cells in mice (Q. Li et al. 2011). Studies have shown that HAND2 mRNA and protein levels increase in mouse uterine stromal cells during decidualization and this upregulation is not embryo

dependent (DV Huyen 2011). Reduction of HAND2 expression in these cells using RNA knock down approaches leads to reduced decidualization in both mouse and human *in vitro* (DV Huyen 2011). These results showed that both mRNA and protein abundance of HAND2 were downregulated in the decidual tissue from the ADR experiment and the uteri on day 5 of pregnancy in the cKO mice compared to the controls. These results indicate that loss of BSG in the uterus leads to compromised decidualization through regulating Hand2 expression.

MCTs are short-chain fatty acids transporters for lactate, pyruvate and ketone bodies and play important role in metabolic homeostasis in many tissue types including the uterus (Halestrap 2012). BSG is a chaperone protein for MCT1 and MCT4 and is responsible for shuttling these MCTs to the membrane (Woodhead et al. 2000; Amit-Cohen, Rahat, and Rahat 2013; Gallagher et al. 2007). MCT1 and BSG co-localize and form a heterodimer through its transmembrane domain and is critical for cells with a high glycolytic rate under hypoxic conditions. The increase in glycolytic flux are also seen in physiological processes with rapidly proliferating cells such as in embryo implantation (Bougatef et al. 2009; Chen, Belton, and Nowak 2009). The IHC and IF results showed that MCT1 abundance and localization were altered in the cKO mice compared to the controls on day 4 and day 6 of pregnancy. Studies have shown that BSG regulates MCTs abundance and localization, for instance, in the retina of *Bsg* null mice, MCT1 and MCT4 were lost (Philp et al. 2003). Silencing of *Bsg* in human malignant melanoma cells abrogated the expression of MCT1 and downregulated glycolysis (Su, Chen, and Kanekura 2009). Similarly, in lung fibroblast cells, knocking down of *Bsg* suppressed MCT1 and MCT4 expression and reduced glycolysis and lactate export of the cells (Le Floch et al. 2011). Therefore, lactate transport in the cKO mice needs to be investigated.

Angiogenesis during decidualization is crucial for pregnancy establishment and maintenance (H. Wang et al. 2013). The differentiating stromal cells form an avascular primary decidual zone on day 5 surrounding the embryos, then form a well vascularized secondary decidual zone by day 8 (X. Wang et al. 2004). BSG is important in promoting angiogenesis as study shows BSG overexpression promotes tumor angiogenesis and growth by inducing vascular endothelial growth factors (VEGFs) and matrix metalloproteinases (MMPs) expression in both human and mouse (Tang et al. 2005). These results showed that there was a significantly reduction in angiogenic marker CD31 in the cKO mice on day 6 of pregnancy. This is very similar to the study on the role of gap junction protein connexin 43 (Cx43) in female reproduction. The Cx43 cKO mice are subfertile due to failed decidualization by natural mating and ADR. Loss of Cx43 also caused strikingly impairment in angiogenesis with reduction in the abundance of CD31 and VEGF (Laws et al. 2008). These results indicate loss of BSG leads to a reduced angiogenesis in these animals. Future studies on the expression of VEGFs in the cKO mice need to be investigated to further support these findings.

The data results in this chapter clearly demonstrated that loss of uterine BSG results in impaired implantation, decidualization and angiogenesis, and eventually causes subfertility in mice. The results on the gross morphology of uteri at different gestational days in Chapter 3 showed 25% cKO mice did not have implantation and about 40% had abnormal pregnancy. In this study, I found six out of nine cKO mice had implantation failure and 70% cKO had no response or very modest response in the ADR experiment. This reveals that only a subset of the animals was negatively affected by lacking BSG in the uteri during pregnancy. There are potentially several explanations for their unaffected or partially affected fertility of the cKO mice. First, PR is not expressed in all uterine compartment and cell types. Studies have shown that PR is expressed in

the luminal and glandular epithelial cells, stromal cells and myometrium of the cycling mice, with only PRB in the luminal epithelium, and both PRA and PRB in the stroma and myometrium (Binder et al. 2014; Mote et al. 2006). In ovariectomized mice, PR expression is intense in the luminal and glandular epithelium, but only approximately 16% and 29% of the myometrial and stromal cells express PR respectively. When, treated with estradiol, luminal epithelial expression of PR is much downregulated, whereas glandular epithelial expression is the same. Stromal and myometrial expression of PR increases to about 60% and 80%. When treated with both estradiol and progesterone, PR expression in the epithelium is much downregulated, and stromal and myometrial expression remains high at 60% and 70% (Tibbetts et al. 1998). It's worth noted that not all stromal cells express PR. In the report of Soyal et al on characterization of the PR-Cre and Lox mouse model, it is clear that some stromal cells did not possess the Cre activity (Soyal et al. 2005; Ismail et al. 2002). Although it is a powerful tool for genetical modification *in vivo*, it does not guarantee 100% effectiveness of deletion. Indeed, the qRT-PCR results of *Bsg* mRNA level on day 4 and day 5 pregnant mouse uteri and endothelial stromal cells (discussed in Chapter 5) showed that about 20%-25% of the cKO samples still expressed comparable levels of *Bsg* to the controls, indicating that not all of the animals or cells have lost BSG in the uteri. The second explanation is that the PR negative cells in the uterus still express BSG and this is enough to maintain some fertility for the cKO animals. For example, the uterus contain many immune cells and blood vessels, which are PR negative (Ismail et al. 2002). However, BSG is expressed in these cell populations (Jennifer Nancy Hahn, Kaushik, and Yong 2015; Xin et al. 2016). The IHC and IF results on the uteri samples showed that BSG was still expressed in the immune cells and endothelial cells as they show intense immunoreactivity in the cKO. These PR negative, BSG positive cells could exert BSG function through paracrine activity. In addition, studies have shown

that BSG is detected in the microvesicles and can be released through microvesicle shedding (J. N. Hahn, Kaushik, and Yong 2015; Nabeshima et al. 2006; Sidhu et al. 2004; Emilova 2012). This way, when the luminal epithelial and stromal cells lost BSG expression, other BSG positive cells close to the embryo, including the immune cells and endothelial cells, are able to release BSG through microvesicles. Thus it is important to investigate whether the microvesicles shed by these cells in the cKO mice contain BSG in the future. The third possible explanation is the compensatory mechanism of BSG related molecules. Compensation is a common phenomenon in complex living organism to maintain biological homeostasis when something goes wrong. For instance, in the uterus of mice, COX2 is critical for implantation, but loss of COX2 leads to compensatory upregulation of COX1, which rescues the female infertility (H. Wang et al. 2004). Similarly, embigin, the founding member of the Ig superfamily, is expressed in the uterus and acts as an ancillary protein when BSG is absent (Nakai, Chen, and Nowak 2006). MCT1 and MCT4 have highest affinity for binding BSG, but when BSG is absent, they can also bind to embigin. Furthermore, embigin is required for shuttling MCT2 to the cell surface. MCT2, in turn, can compensate for the loss of MCT1 function (Nakai, Chen, and Nowak 2006; Doherty and Cleveland 2013). Whether the abundance of the other MCTs are altered in the cKO mice should be further investigated. Therefore, the effectiveness of the PR knockout, paracrine activity or microvesicle shedding by BSG positive cells, as well as compensatory effort by embigin together could explain the subfertility caused by loss of uterine BSG using this PR-Cre mouse model.

In summary, the results in current studies show that the uteri lacking BSG expression failed implantation and decidualization in mice. I found that luminal epithelial integrity was not affected in the cKO mice at the time of implantation as cytokeratin and E-cadherin were still expressed at the implantation site. The basement membrane was also intact in the cKO mice, when it was

supposed to be disrupted as in the controls. As a result, embryos in many of the cKO mice were not able to attach or break the barrier of luminal epithelium. The ADR experiment showed that the cKO mice had a compromised decidualization as they responded less to the artificial stimulus and formed smaller decidua. qRT-PCR results on decidualization markers showed that *Bmp2* and *Cebpβ* were markedly downregulated in the cKO. IHC and IF results showed that protein levels of CEBPβ and HAND2 were downregulated in the cKO mice compared to the controls. The localization and abundance of MCT1 were abnormal in the cKO mice, suggesting a possible altered lactate transport. This will be investigated in the next chapter. CD31 abundance was significantly reduced in the cKO mice, indicating a suppressed angiogenesis in these animals compared to the controls. Collectively, these findings suggest that loss of BSG in the uterus led to failed implantation, impaired decidualization, altered MCT localization and decreased angiogenesis *in vivo*. Future studies will focus on the role of BSG in decidualization and lactate transport *in vitro*.

Tables and Figures

Table 4.1 Primer sequences used for quantitative RT-PCR

Genes	NCBI Gene Reference	Left Primer Sequence	Right Primer Sequence
Rplp0	NM_007475.5	actggtctaggacccgagaag	ctcccaccttgtctccagtc
Ppia	NM_008907.1	ggaccaaacacaaacggttc	catgccttctttcaccttcc
Bsg	NM_009768.2	acagcagtggcgttgaca	ggtcatctgcgtccactatgt
Cebpβ	NM_001287739.1	aagatgcgcaacctggag	cagggtgctgagctctcg
Bmp2	NM_007553.3	agatctgtaccgcaggcact	gttcctccacggcttcttc
Hand2	NM_010402.4	tgagcagcaacgacaagaaa	tgctctcctcttcttcactgc
Wnt4	NM_009523.2	actggactccctccctgtct	tgcccttgtcactgcaaa
Alph	NM_007431.3	cggatcctgaccaaaaacc	tcatgatgtccgtggtcaat
Ereg	NM_007950.2	ttgacgctgctttgtctagg	ggatcacggttgtgctgat

Table 4.2 ADR Weight Measurements

	Body Weight	**Uninj Ut Weight**	**Inj Ut Weight**	**Total Ut Weight**	**Inj Ut/Uninj Ut Ratio**	**Ut/ BW Ratio**	**Inj Ut/BW Ratio**
$BSG^{f/f}$ (n=9)	23.667	0.026	**0.118**	**0.144**	**9.131**	0.006	0.005
$BSG^{d/d}$(n=10)	22.730	0.022	**0.047***	**0.069***	**2.195***	0.003	0.002

Table 4.3 ADR Decidua Size

Decidua Size	**Area**	**Perimeter**	**Diameter**
$BSG^{f/f}$ (n=4)	7.20	10.74	3.17
$BSG^{d/d}$(n=4)	3.86*	7.38*	2.19*

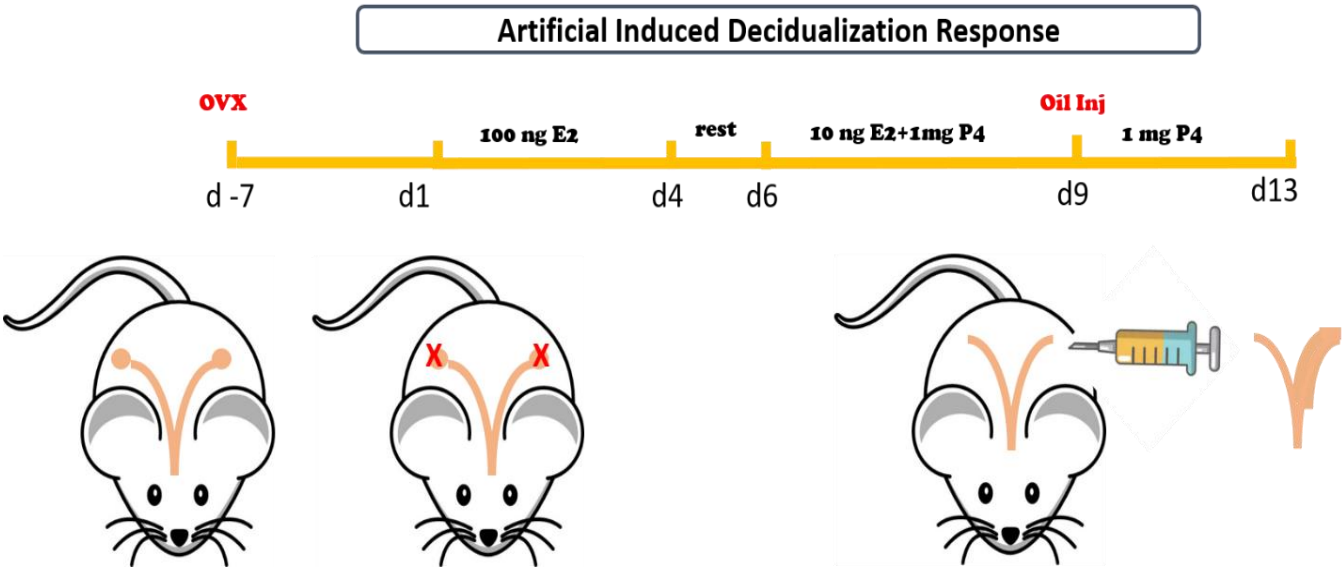

Figure 4.1 ADR experiment design and timeline. Mice were ovariectomized and rested for 7 days. Then 100 ng of E2 was given to each mouse subcutaneously for 3 days, rest for 2 days, then 10 ng of E2 and 1 mg of P4 were given to each mouse for 3 days. On day 9, 20 µl of corn oil was injected into the left uterine horn. 1 mg of P4 was given for 4 more days before the mice were euthanized and collected for tissues.

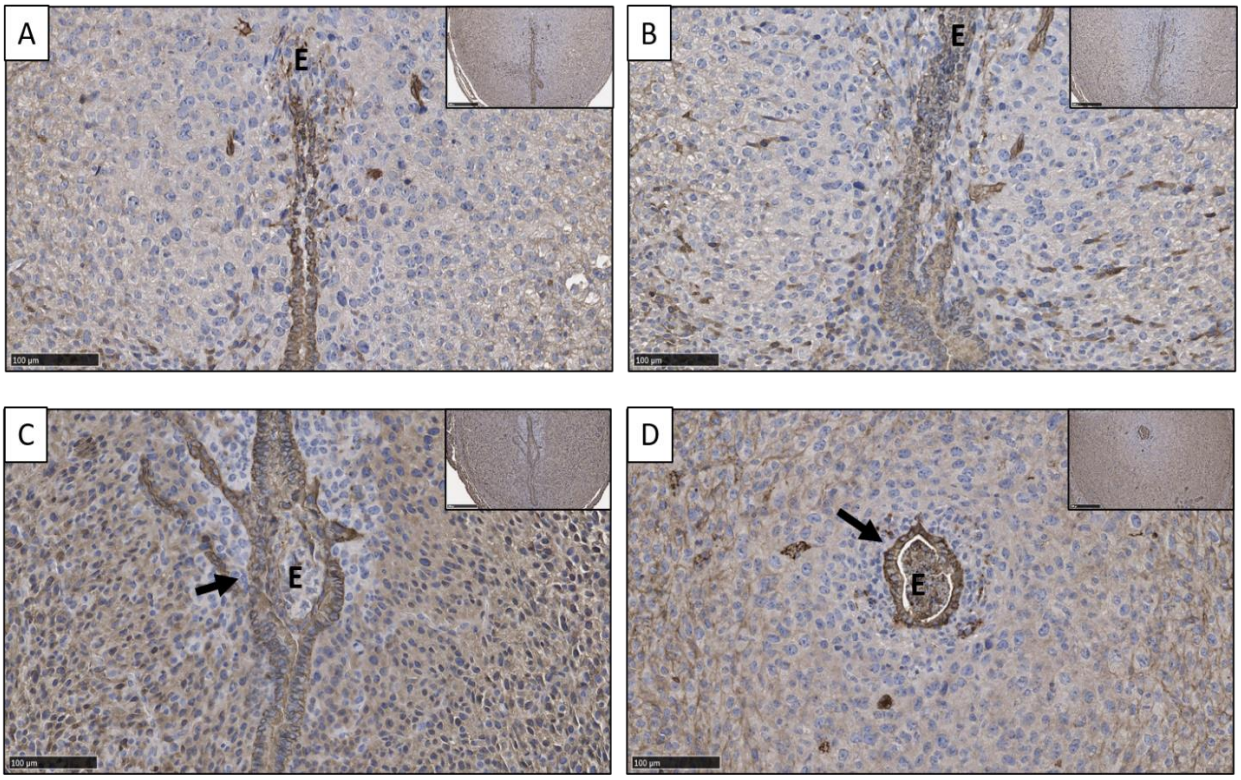

Figure 4.2 Luminal epithelial cell integrity at implantation. IHC for cytokeratin on implantation sites of control females (A and B) and cKO females (C and D) on day 5 evening of pregnancy. Arrows indicate intact luminal epithelium at the site of implantation. E: embryo.

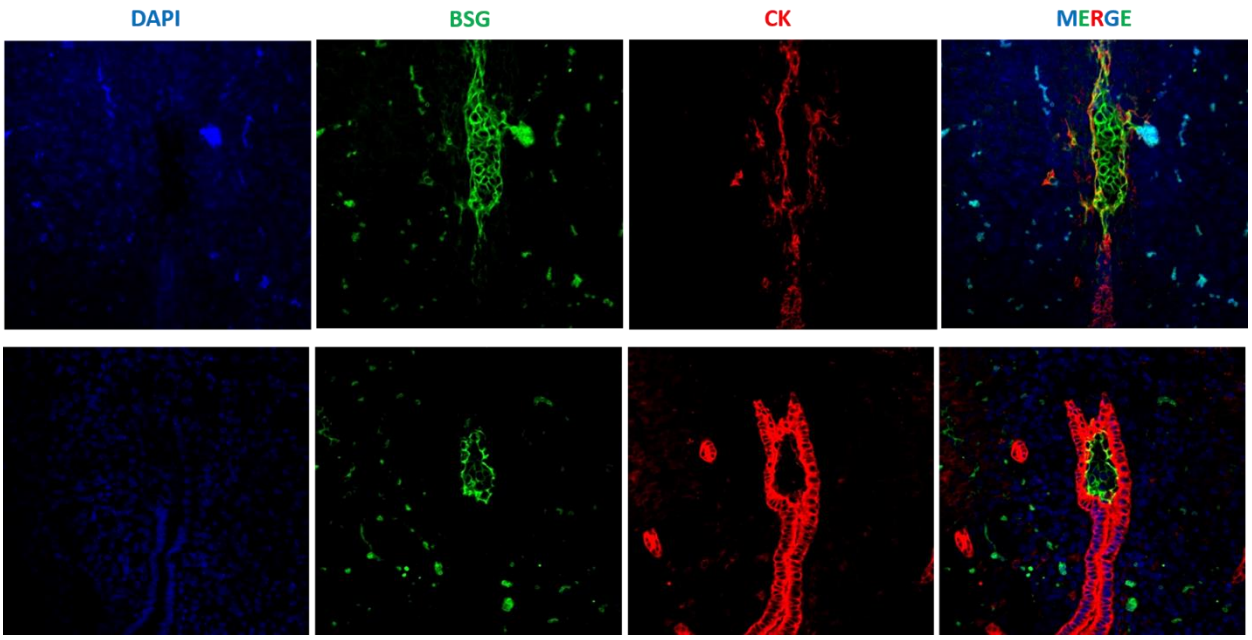

Figure 4.3 Luminal epithelial cell integrity at implantation. Immunofluorescent stain against bsg (green), cytokeratin (red) on implantation sites of control females (top lane) and cKO females (bottom lane) on day 5 evening of pregnancy. Blue: DAPI; Green: BSG; Red: cytokeratin.

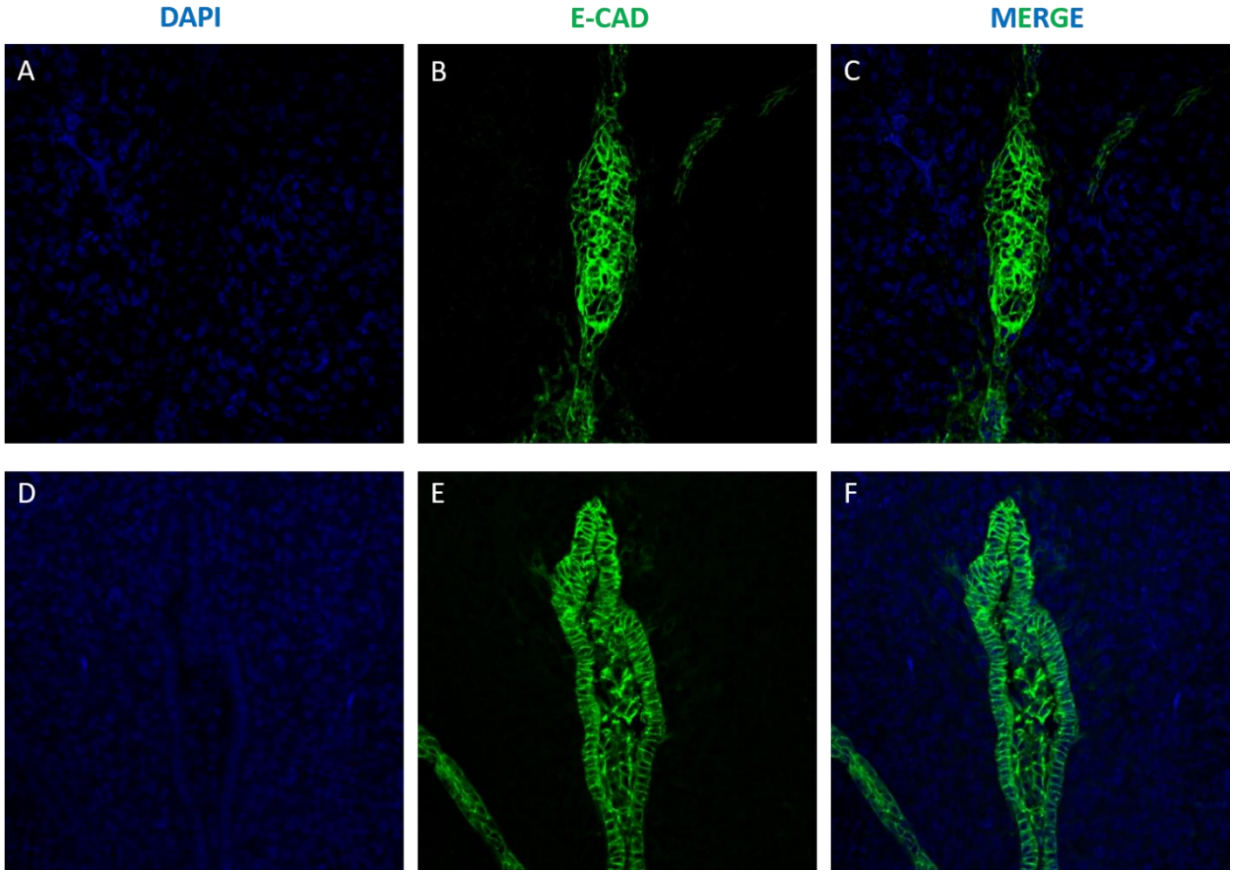

Figure 4.4 Luminal epithelial cell integrity at implantation. Immunofluorescent stain against e-cadherin (green) on implantation sites of control females (top lane) and cKO females (bottom lane) on day 5 evening of pregnancy. Blue: DAPI; Green: E-cad.

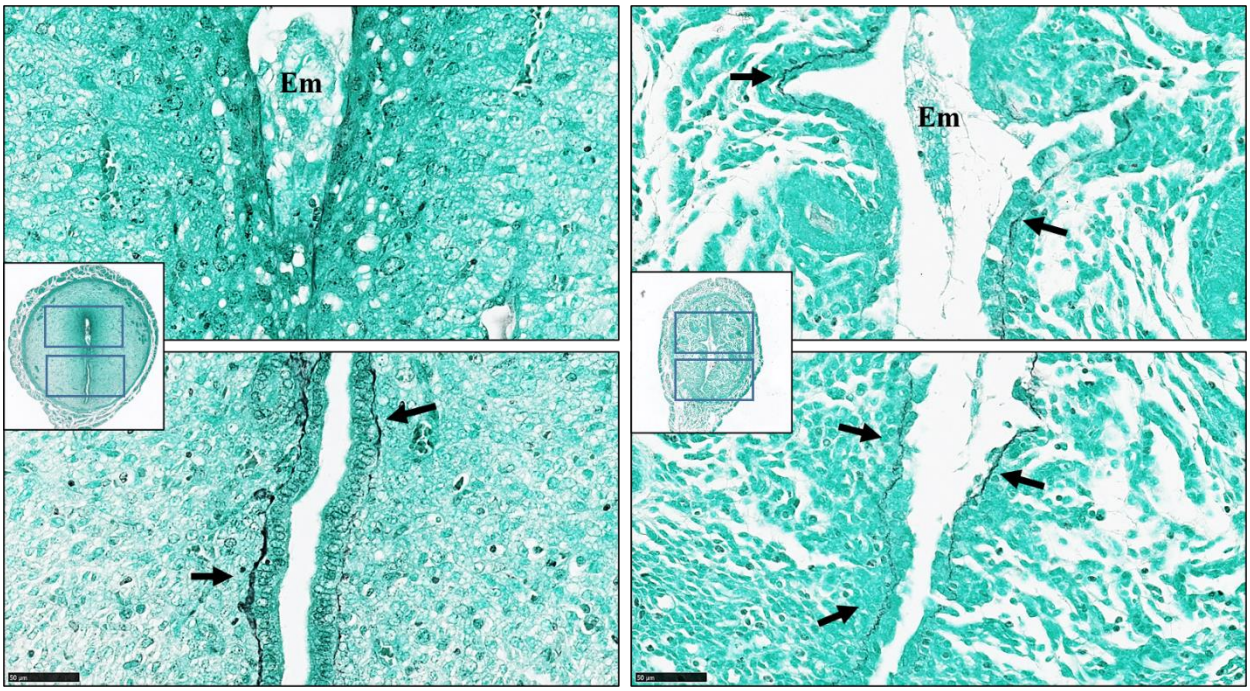

Figure 4.5 Basement membrane integrity at implantation. Jones' silver stain of uterine cross-sections at the implantation site on day 5 evening of a control (A) and a cKO (B) mouse. Black line is the positive stain for basement membrane. Arrows indicate the intact basement membrane. E: embryo.

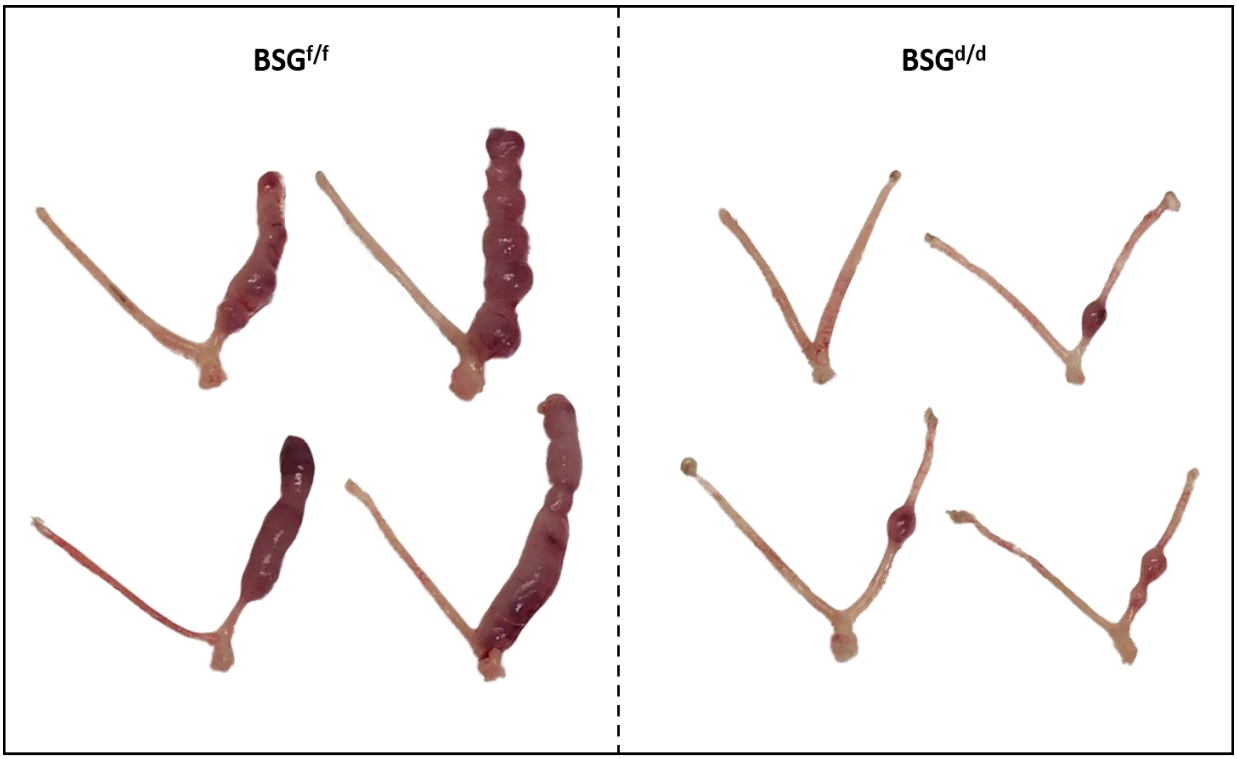

Figure 4.6 Artificial decidualization response images. Photos of uteri undergone ADR experiment of control females (top lane) and of cKO females (bottom lane).

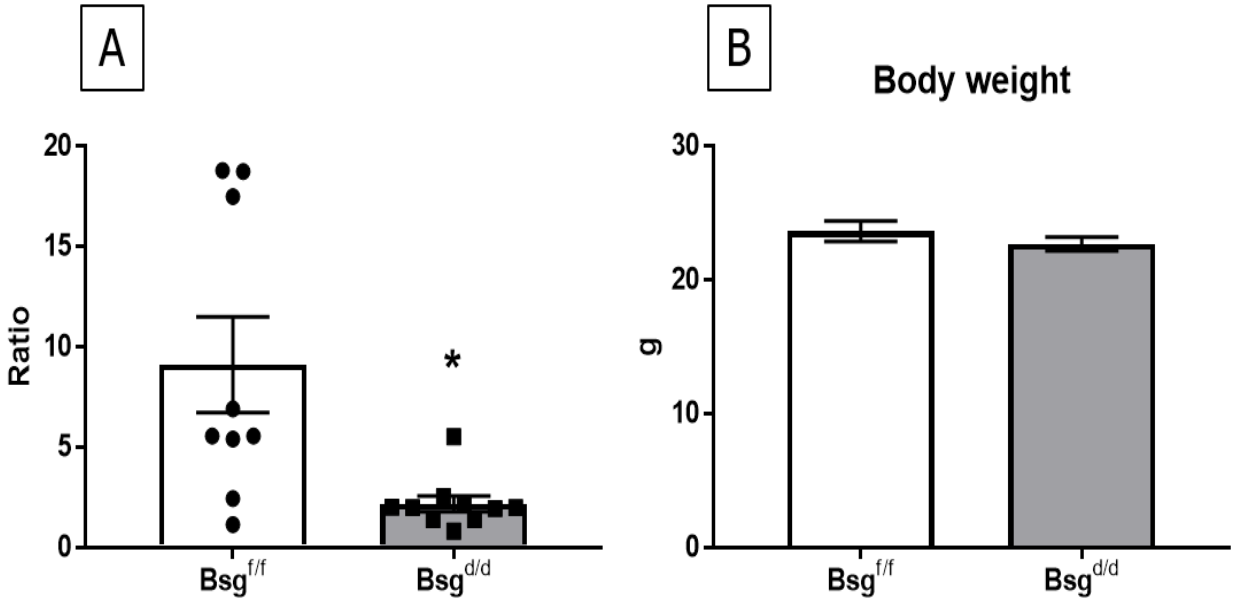

Figure 4.7 Artificial decidualization response results. A: Injected to uninjected uterine weight ratio of the mice undergone ADR. B: body weight of mice undergone ADR.

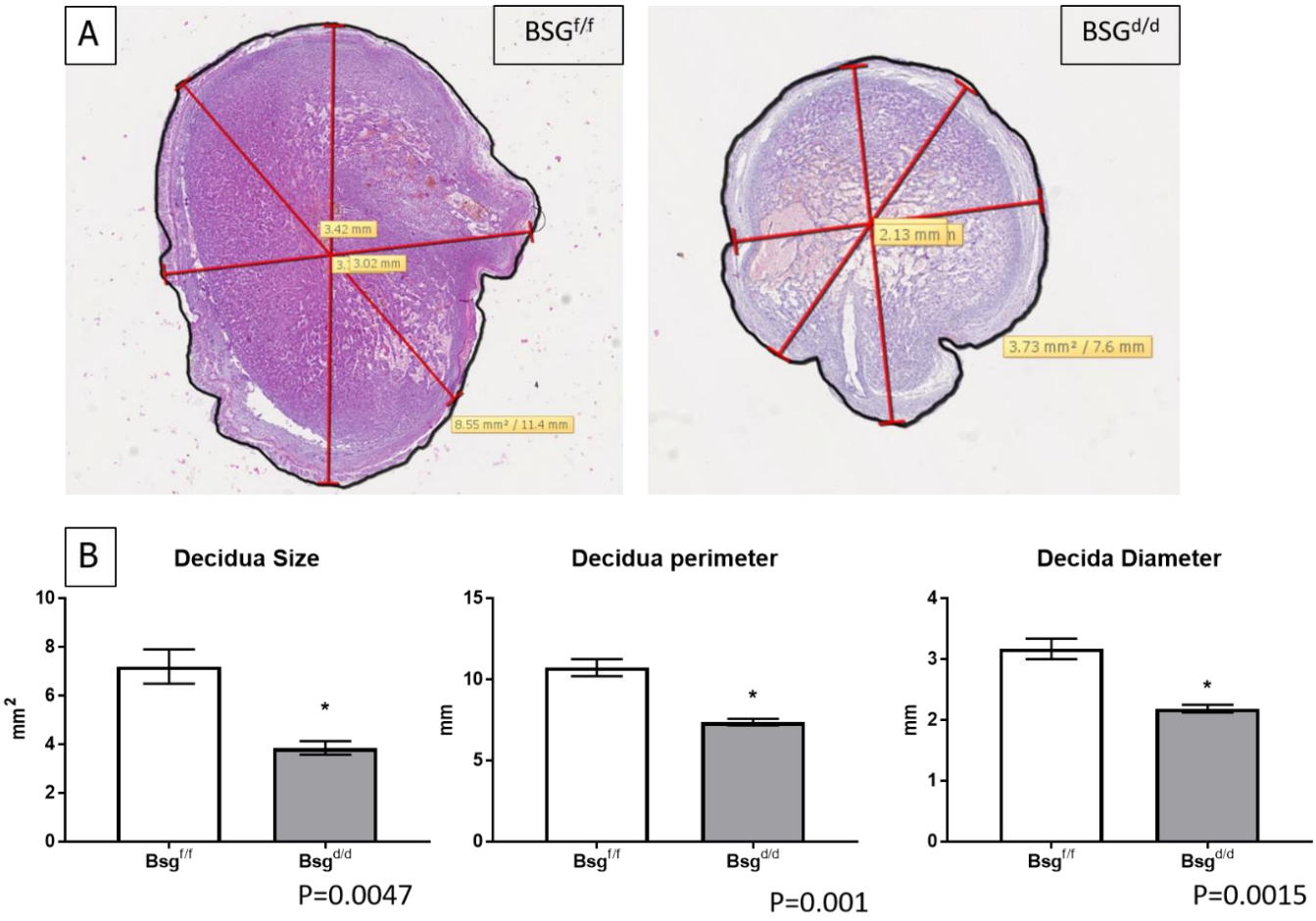

Figure 4.8 ADR cross section size. A: H&E stain on cross sections of decidua from a control female (left) and cKO female (right). B: quantitation of decidua size measured by area (left), perimeter (middle) and diameter (right).

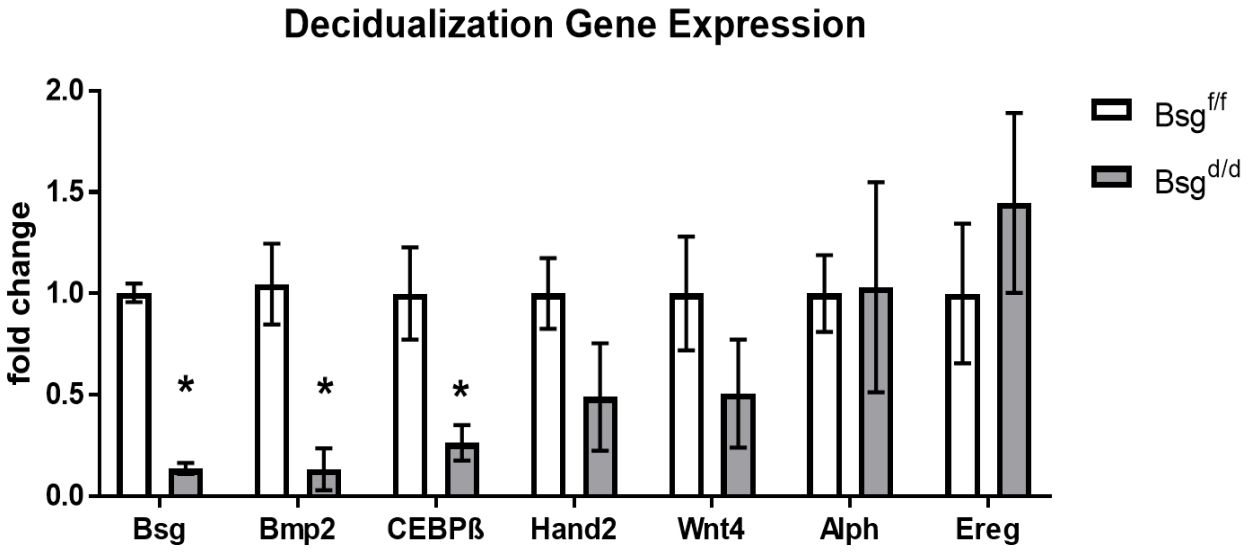

Figure 4.9 Decidualization gene expression results on RNA extracted from decidua of both genotypes. *Bsg*, *Bmp2*, and *Cebpβ* were significantly downregulated in the cKO decidual tissues compared to the controls ($p<0.05$). *Hand2* and *Wnt4* expression levels were lower in the cKO decidual tissue, but not statistically significant. *Alp* and *Ereg* expression levels were not different.

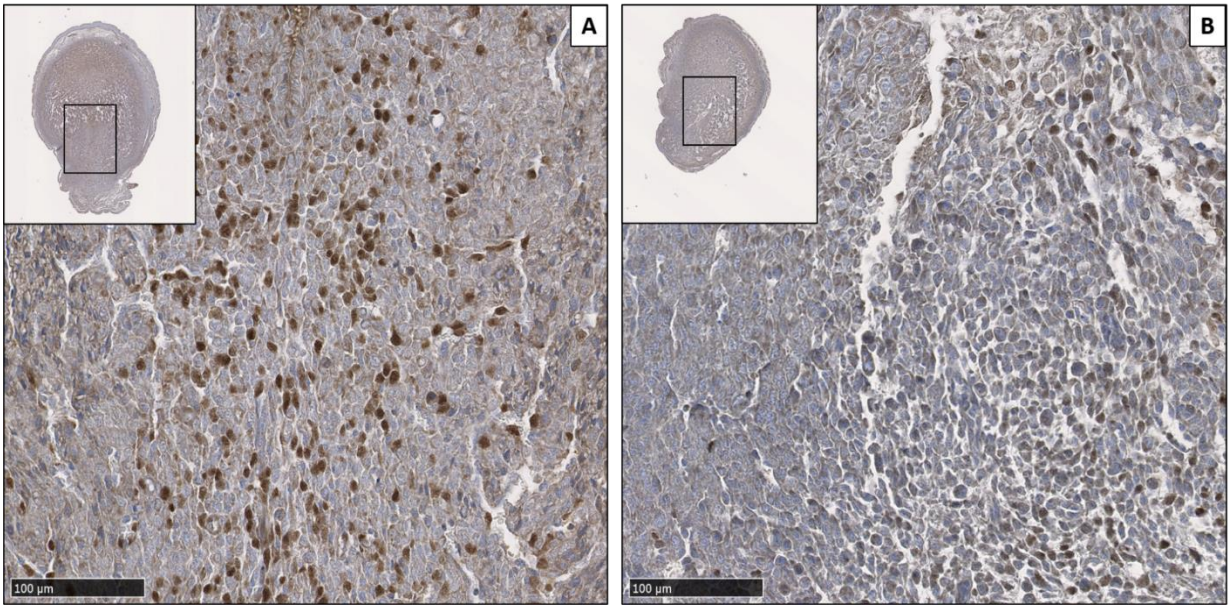

Figure 4.10 Cebpβ localization. IHC for decidualization marker CEBPβ in the decidua from a control (A) and a cKO (B) female.

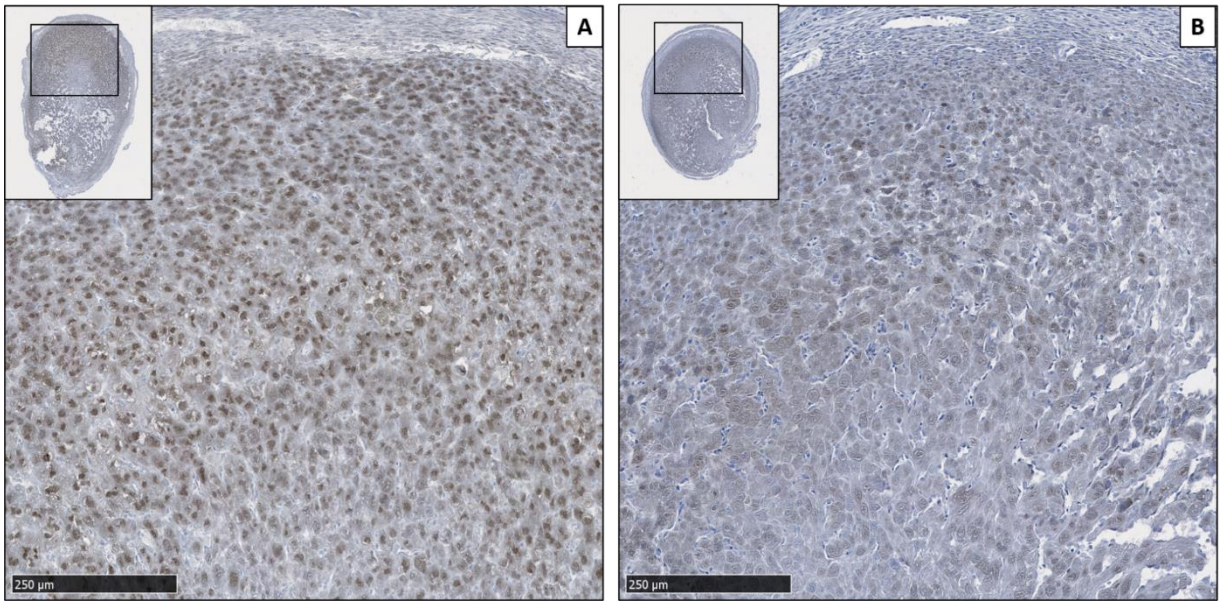

Figure 4.11 HAND2 localization. IHC for decidualization marker HAND2 in the decidua from a control (A) and a cKO (B) female.

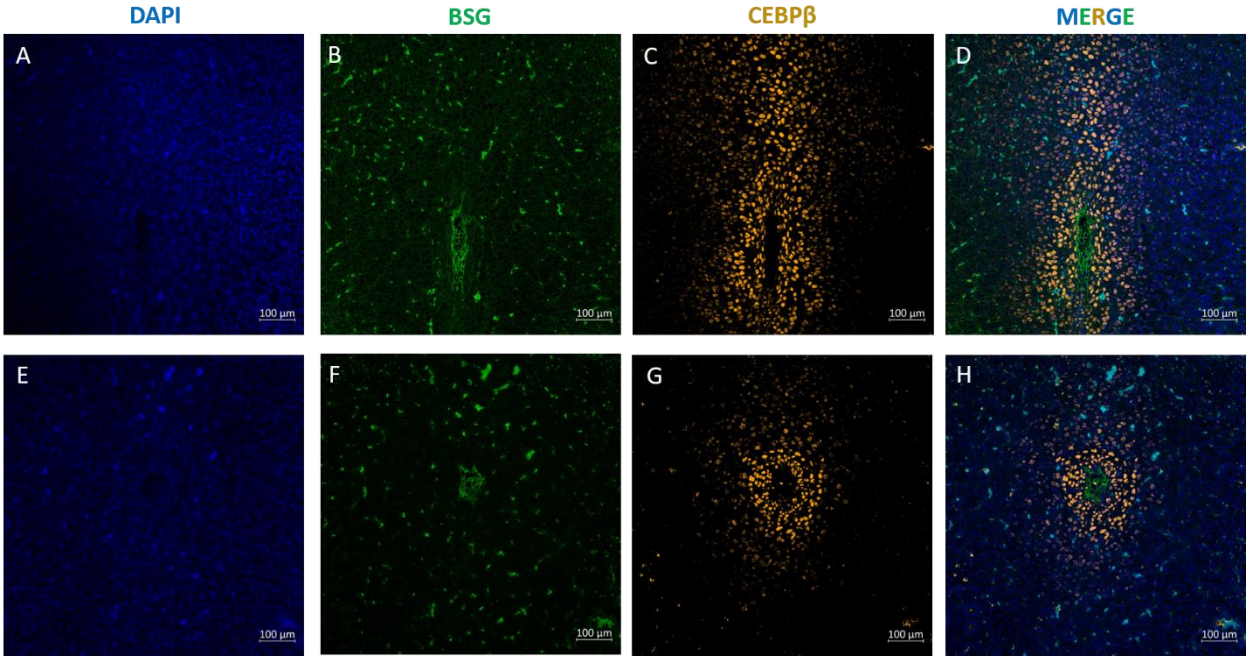

Figure 4.12 CEBPβ and BSG localization in the uteri of day 5 pregnant mice. IF stain for BSG (green) and CEBPβ (orange) on uterine sections of cKO mice (A-D) and control mice (E-H) on day 5 of pregnancy. Images were taken at 10X magnification.

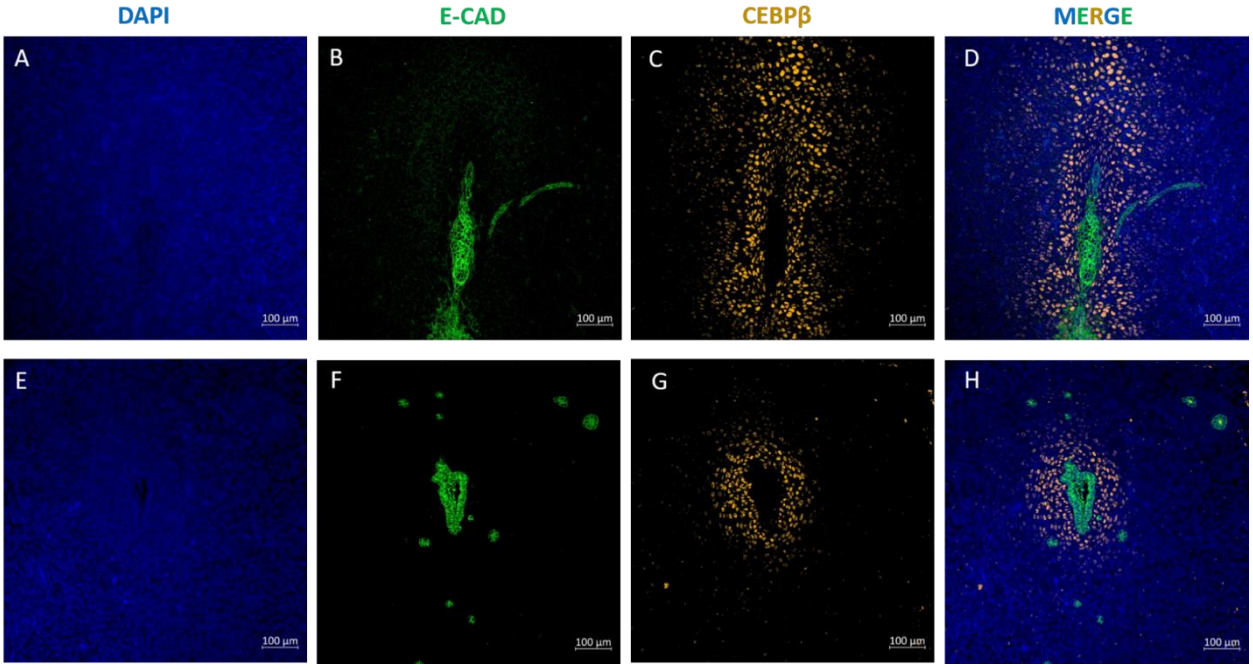

Figure 4.13 CEBPβ and E-CAD in the uteri of day 5 pregnant mice. IF stain for BSG (green) and E-CAD (orange) on uterine sections of cKO mice (A-D) and control mice (E-H) on day 5 of pregnancy. Images were taken at 10X magnification.

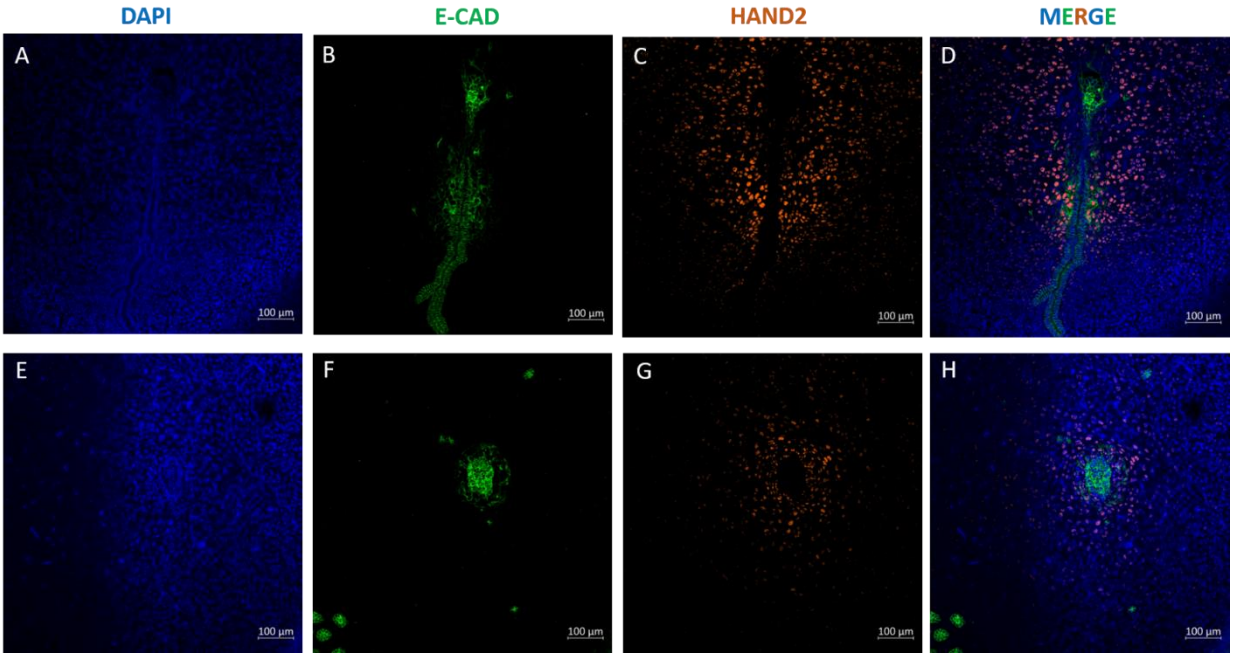

Figure 4.14 HAND2 and E-CAD in the uteri of day 5 pregnant mice. IF stain for E-CAD (green) and HAND2 (orange) on uterine sections of cKO mice (A-D) and control mice (E-H) on day 5 of pregnancy. Images were taken at 10X magnification.

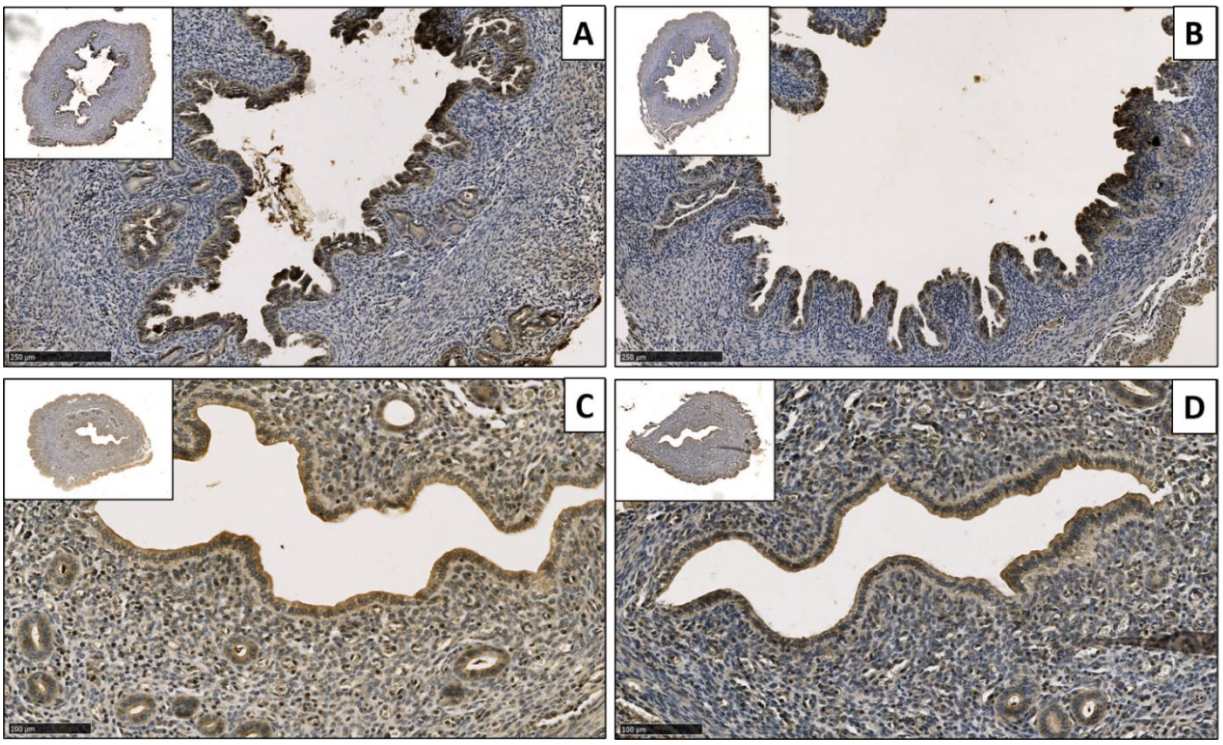

Figure 4.15 CD98 localization. IHC for CD98 on uterine cross sections of control mice (A, C) and cKO mice (B, D) on day 1 (top lane) and day 4 (bottom) lane of pregnancy.

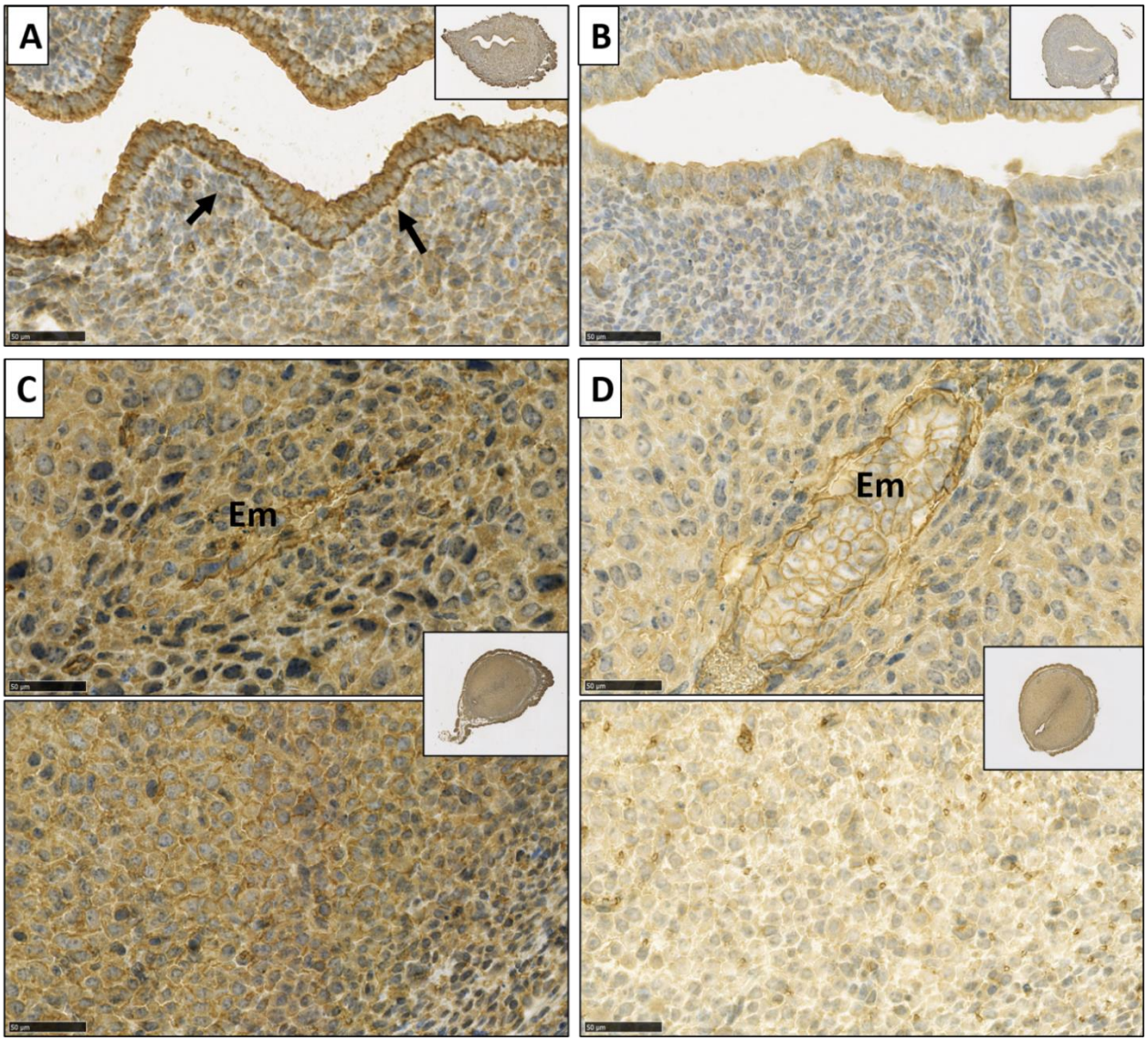

Figure 4.16 MCT localization. IHC for MCT1 on uterine sections of control mice (A, C) and cKO mice (B, D) on day 4 (top lane) and day 6 (bottom lanes) of pregnancy.

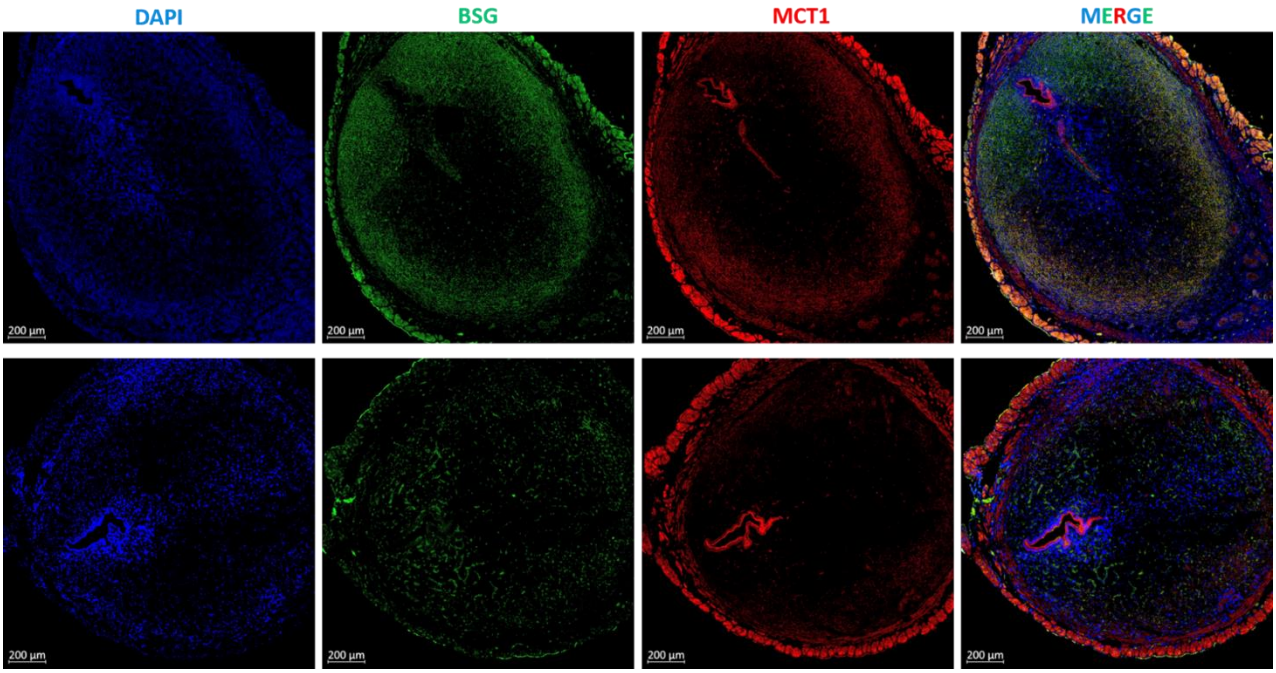

Figure 4.17 MCT1 localization at low magnification. IF stain for MCT1 (red) and BSG (green) on uterine sections of cKO mice (A-D) and control mice (E-H) on day 6 of pregnancy. Images were taken at 5X magnification.

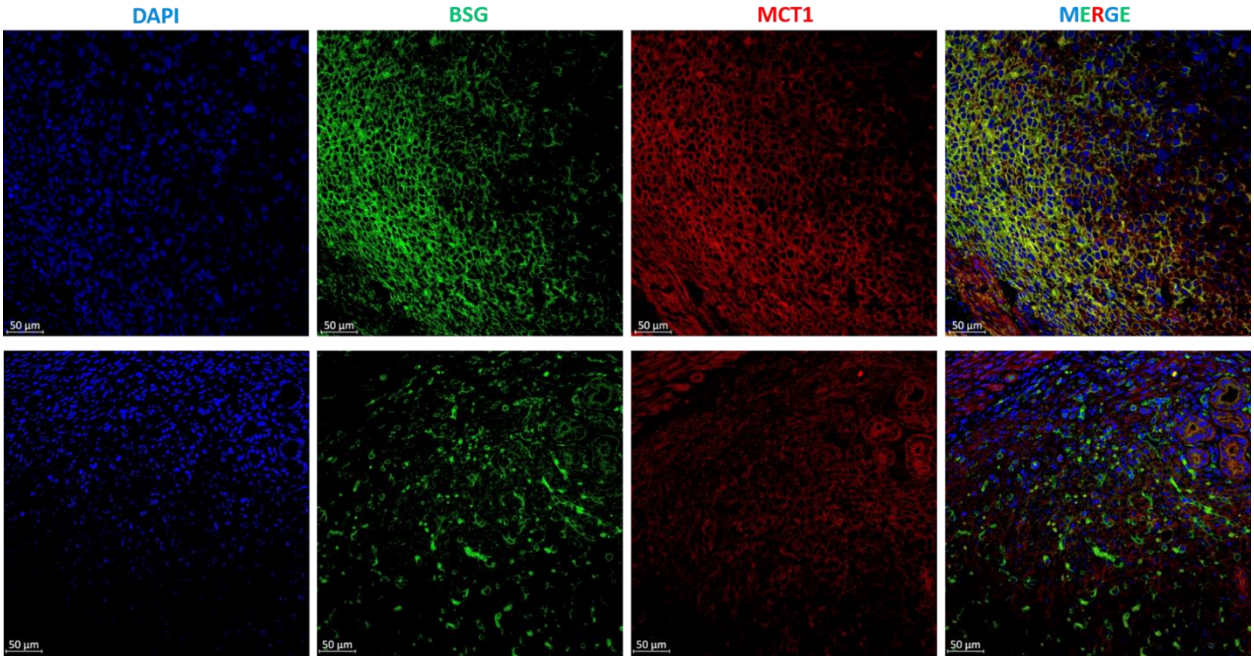

Figure 4.18 MCT1 localization at high magnification. IF stain for MCT1 (red) and BSG (green) on uterine sections of cKO mice (A-D) and control mice (E-H) on day 6 of pregnancy. Images were taken at 20X magnification.

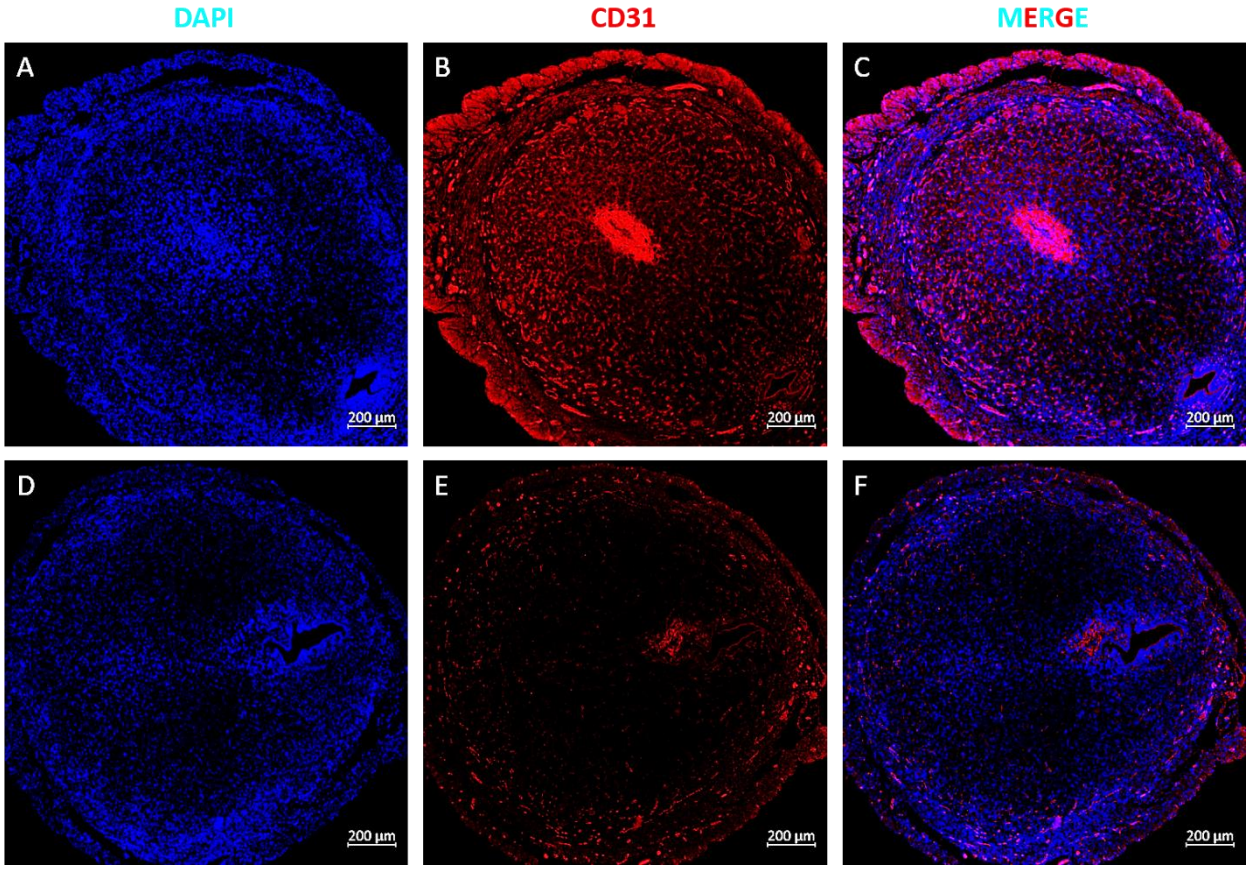

Figure 4.19 CD31 localization at low magnification. IF stain for CD31 (red) on uterine sections of cKO mice (A-C) and control mice (D-F) on day 6 of pregnancy. Images were taken at 5X magnification.

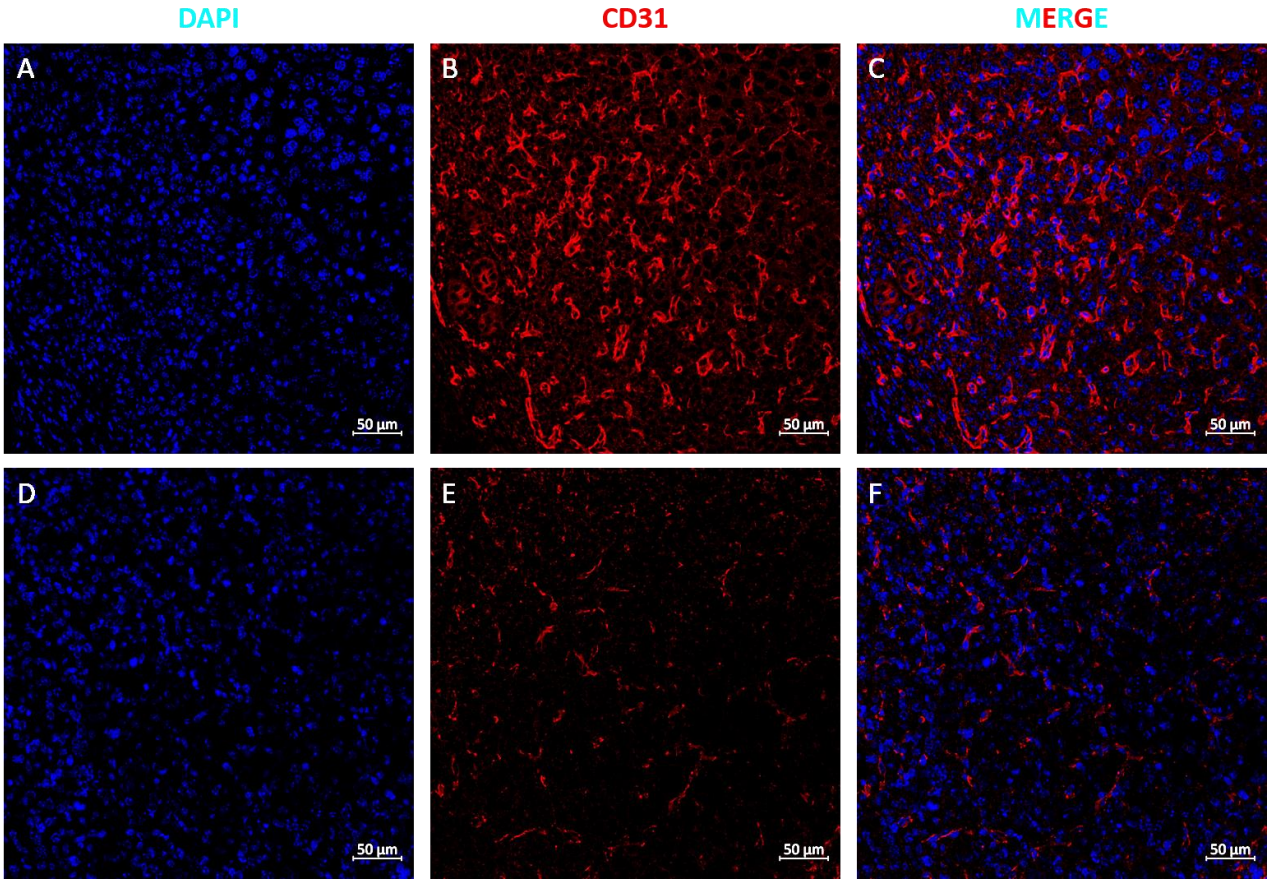

Figure 4.20 CD31 localization at high magnification. IF stain for CD31 (red) on uterine sections of cKO mice (A-C) and control mice (D-F) on day 6 of pregnancy. Images were taken at 20X magnification.

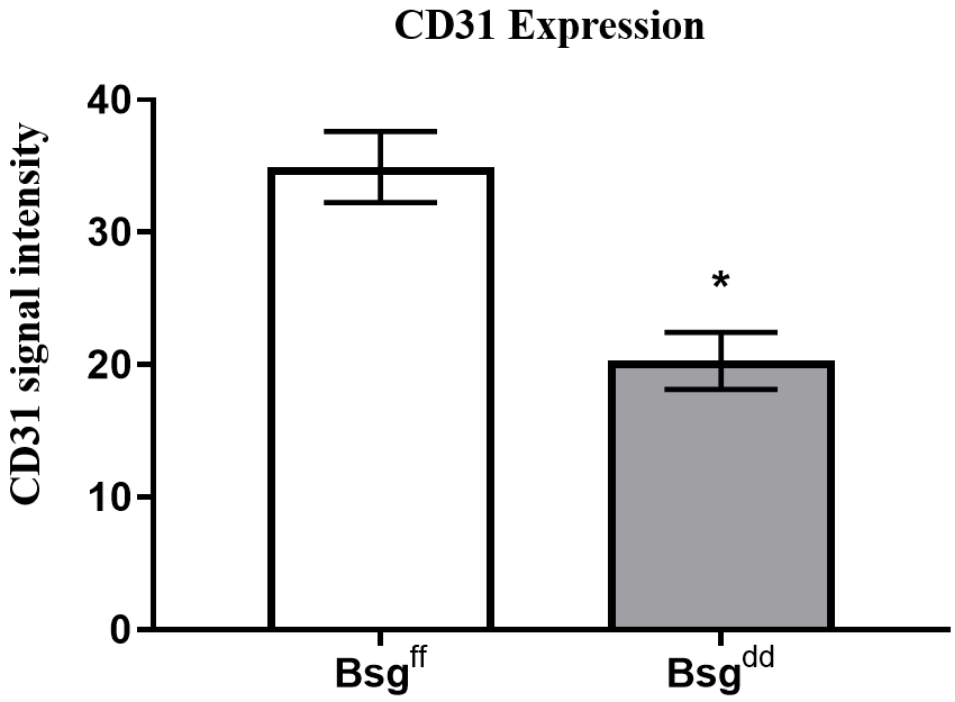

Figure 4.21 Quantification of CD31 abundance. Quantification of CD31 signal intensity in the uterine sections of control and cKO mice on day 6 of pregnancy.

References

Amit-Cohen, Bat-Chen, Michal A. Maya M. Rahat, and Michal A. Maya M. Rahat. 2013. "Tumor Cell-Macrophage Interactions Increase Angiogenesis through Secretion of EMMPRIN." *Frontiers in Physiology* 4: 178. https://doi.org/10.3389/fphys.2013.00178.

Aplin, John D., and Peter T. Ruane. 2017. "Embryo-Epithelium Interactions during Implantation at a Glance." *Journal of Cell Science* 130 (1): 15–22. https://doi.org/10.1242/jcs.175943.

Bagchi, Milan K., Srinivasa R. Mantena, Athilakshmi Kannan, and Indrani C. Bagchi. 2006. "Control of Uterine Cell Proliferation and Differentiation by C/EBPβ: Functional Implications for Establishment of Early Pregnancy." *Cell Cycle*. Taylor and Francis Inc. https://doi.org/10.4161/cc.5.9.2712.

Bhurke, Arpita S., Indrani C. Bagchi, and Milan K. Bagchi. 2016. "Progesterone-Regulated Endometrial Factors Controlling Implantation." *American Journal of Reproductive Immunology* 75 (3): 237–45. https://doi.org/10.1111/aji.12473.

Bi, Jiajia, Yanfen Li, Fengyun Sun, Anja Saalbach, Claudia Klein, David J. Miller, Rex Hess, and Romana A. Nowak. 2013. "Basigin Null Mutant Male Mice Are Sterile and Exhibit Impaired Interactions between Germ Cells and Sertoli Cells." *Developmental Biology* 380 (2): 145–56. https://doi.org/10.1016/j.ydbio.2013.05.023.

Binder, April K., Wipawee Winuthayanon, Sylvia C. Hewitt, John F. Couse, and Kenneth S. Korach. 2014. *Steroid Receptors in the Uterus and Ovary*. *Knobil and Neill's Physiology of Reproduction: Two-Volume Set*. Fourth Edi. Vol. 1. Elsevier. https://doi.org/10.1016/B978-0-12-397175-3.00025-9.

Blankenship, Thomas N., and Randall L. Given. 1995. "Loss of Laminin and Type IV Collagen in Uterine Luminal Epithelial Basement Membranes during Blastocyst Lmplantation in the Mouse." *The Anatomical Record* 243 (1): 27–36. https://doi.org/10.1002/ar.1092430105.

Bougatef, F., C. Quemener, S. Kellouche, B. Naimi, M.-P. Podgorniak, G. Millot, E. E. Gabison, et al. 2009. "EMMPRIN Promotes Angiogenesis through Hypoxia-Inducible Factor-2 - Mediated Regulation of Soluble VEGF Isoforms and Their Receptor VEGFR-2." *Blood* 114 (27): 5547–56. https://doi.org/10.1182/blood-2009-04-217380.

Braundmeier, A. G., C. A. Dayger, P. Mehrotra, R. J. Belton, and R. A. Nowak. 2012. "EMMPRIN Is Secreted by Human Uterine Epithelial Cells in Microvesicles and Stimulates Metalloproteinase Production by Human Uterine Fibroblast Cells." *Reproductive Sciences* 19 (12): 1292–1301. https://doi.org/10.1177/1933719112450332.

Cha, Jeeyeon, Sudhansu K. Dey, and Hyunjung Lim. 2014. *Embryo Implantation*. *Knobil and Neill's Physiology of Reproduction: Two-Volume Set*. Fourth Edi. Vol. 2. Elsevier. https://doi.org/10.1016/B978-0-12-397175-3.00038-7.

Cha, Jeeyeon, Xiaofei Sun, and Sudhansu K. Dey. 2012. "Mechanisms of Implantation: Strategies for Successful Pregnancy." *Nature Medicine*. Nature Publishing Group. https://doi.org/10.1038/nm.3012.

Chen, Li, Robert J. Belton, and Romana a. Nowak. 2009. “Basigin-Mediated Gene Expression Changes in Mouse Uterine Stromal Cells during Implantation.” *Endocrinology* 150 (2): 966–76. https://doi.org/10.1210/en.2008-0571.

Chen, Li, Masaaki Nakai, Robert J. Belton, and Romana A. Nowak. 2007. “Expression of Extracellular Matrix Metalloproteinase Inducer and Matrix Metalloproteinases during Mouse Embryonic Development.” *Reproduction (Cambridge, England)* 133 (2): 405–14. https://doi.org/10.1530/rep.1.01020.

Cheng, Jr Gang, Jim Ray Chen, Lidia Hernandez, W. Greg Alvord, and Colin L. Stewart. 2001. “Dual Control of LIF Expression and LIF Receptor Function Regulate Stat3 Activation at the Onset of Uterine Receptivity and Embryo Implantation.” *Proceedings of the National Academy of Sciences of the United States of America* 98 (15): 8680–85. https://doi.org/10.1073/pnas.151180898.

Clementi, C, S K Tripurani, M J Large, M A Edson, and C J Creighton. 2013. “Activin-Like Kinase 2 Functions in Peri-Implantation Uterine Signaling in Mice and Humans.” *PLoS Genet* 9 (11): 1003863. https://doi.org/10.1371/journal.pgen.1003863.

Conneely, Orla M., Biserka Mulac-Jericevic, and John P. Lydon. 2003. “Progesterone-Dependent Regulation of Female Reproductive Activity by Two Distinct Progesterone Receptor Isoforms.” *Steroids* 68 (10–13): 771–78. https://doi.org/10.1016/S0039-128X(03)00126-0.

Croy, B. Anne, Zhilin Chen, Alexander P. Hofmann, Edith M. Lord, Abigail L. Sedlacek, and Scott A. Gerber. 2012. “Imaging of Vascular Development in Early Mouse Decidua and Its Association with Leukocytes and Trophoblasts1.” *Biology of Reproduction* 87 (5): 1–11. https://doi.org/10.1095/biolreprod.112.102830.

Das, Sanjoy K. 2009. “Cell Cycle Regulatory Control for Uterine Stromal Cell Decidualization in Implantation.” *Reproduction* 137 (6): 889–99. https://doi.org/10.1530/REP-08-0539.

Doherty, Jr, and Jl Cleveland. 2013. “Targeting Lactate Metabolism for Cancer Therapeutics.” *The Journal of Clinical Investigation* 123 (9): 3685–92. https://doi.org/10.1172/JCI69741.transcription.

Domínguez, Francisco, Carlos Simón, Alicia Quiñonero, Miguel Ángel Ramírez, Elena Gonzá lez-Muñoz, Hans Burghardt, Ana Cervero, et al. 2010. “Human Endometrial CD98 Is Essential for Blastocyst Adhesion.” *PLoS ONE* 5 (10). https://doi.org/10.1371/journal.pone.0013380.

DV Huyen, BM Bany. 2011. “Evidence for a Conserved Function of Heart and Neural Crest Derivatives Expressed Transcript 2 in Mouse and Human Decidualization.” *Reproduction* 142: 353–68.

Emilova, Viktoriya. 2012. “BASIGIN in TROPHOBLAST CELLS VIA MICROVESICLE SHEDDING Viktoriya Thesis.”

Fisher, Susan J., Mark S. Leitch, Marsha S. Kantor, Carol B. Basbaum, and Randall H. Kramer. 1985. “Degradation of Extracellular Matrix by the Trophoblastic Cells of First-trimester Human Placentas.” *Journal of Cellular Biochemistry* 27 (1): 31–41. https://doi.org/10.1002/jcb.240270105.

Floch, Renaud Le, Johanna Chiche, Ibtissam Marchiq, Tanesha Naiken, Tanesha Naïken, Karine

Ilc, Karine Ilk, et al. 2011. “CD147 Subunit of Lactate/H+ Symporters MCT1 and Hypoxia-Inducible MCT4 Is Critical for Energetics and Growth of Glycolytic Tumors.” *Proceedings of the National Academy of Sciences of the United States of America* 108 (40): 16663–68. https://doi.org/10.1073/pnas.1106123108.

Fossum, Sigbj⊘Rn, Susan Mallett, and A. Neil Barclay. 1991. “The MRC OX-47 Antigen Is a Member of the Immunoglobulin Superfamily with an Unusual Transmembrane Sequence.” *European Journal of Immunology* 21 (3): 671–79. https://doi.org/10.1002/eji.1830210320.

Franco, Heather L, Daisy Dai, Kevin Y Lee, Cory A Rubel, Dennis Roop, Derek Boerboom, Jae-Wook Jeong, et al. n.d. “WNT4 Is a Key Regulator of Normal Postnatal Uterine Development and Progesterone Signaling during Embryo Implantation and Decidualization in the Mouse.” *The FASEB Journal • Research Communication*. Accessed April 20, 2020. https://doi.org/10.1096/fj.10-175349.

Fuchs, E, and K Weber. 1994. “Intermediate Filaments: Structure, Dynamics, Function and Disease.” *Annual Review of Biochemistry* 63 (1): 345–82. https://doi.org/10.1146/annurev.bi.63.070194.002021.

Gallagher, Shannon M., John J. Castorino, Dian Wang, and Nancy J. Philp. 2007. “Monocarboxylate Transporter 4 Regulates Maturation and Trafficking of CD147 to the Plasma Membrane in the Metastatic Breast Cancer Cell Line MDA-MB-231.” *Cancer Research* 67 (9): 4182–89. https://doi.org/10.1158/0008-5472.CAN-06-3184.

Gou, Jinhai, Tingwenyi Hu, Lin Li, Luqi Xue, Xia Zhao, Tao Yi, and Zhengyu Li. 2019. “Role of Epithelial-Mesenchymal Transition Regulated by Twist Basic Helix-Loop-Helix Transcription Factor 2 (Twist2) in Embryo Implantation in Mice.” *Reproduction, Fertility and Development* 31 (5): 932–40. https://doi.org/10.1071/RD18314.

Guo, Na, Kui Zhang, Minghua Lv, Jinlin Miao, Zhinan Chen, and Ping Zhu. 2015. “CD147 and CD98 Complex-Mediated Homotypic Aggregation Attenuates the CypA-Induced Chemotactic Effect on Jurkat T Cells.” *Molecular Immunology* 63 (2): 253–63. https://doi.org/10.1016/j.molimm.2014.07.005.

Haeger, J. D., N. Hambruch, V. Dantzer, M. Hoelker, K. Schellander, K. Klisch, and C. Pfarrer. 2015. “Changes in Endometrial Ezrin and Cytokeratin 18 Expression during Bovine Implantation and in Caruncular Endometrial Spheroids in Vitro.” *Placenta* 36 (8): 821–31. https://doi.org/10.1016/j.placenta.2015.06.001.

Hahn, J. N., D. K. Kaushik, and V. W. Yong. 2015. “The Role of EMMPRIN in T Cell Biology and Immunological Diseases.” *Journal of Leukocyte Biology* 98 (1): 33–48. https://doi.org/10.1189/jlb.3RU0215-045R.

Hahn, Jennifer Nancy, Deepak Kumar Kaushik, and V. Wee Yong. 2015. “The Role of EMMPRIN in T Cell Biology and Immunological Diseases.” *Journal of Leukocyte Biology* 98 (1): 33–48. https://doi.org/10.1189/jlb.3RU0215-045R.

Halestrap, Andrew P. 2012. “The Monocarboxylate Transporter Family-Structure and Functional Characterization.” *IUBMB Life* 64 (1): 1–9. https://doi.org/10.1002/iub.573.

Igakura, T, K Kadomatsu, T Kaname, H Muramatsu, Q W Fan, T Miyauchi, Y Toyama, et al.

1998. “A Null Mutation in Basigin, an Immunoglobulin Superfamily Member, Indicates Its Important Roles in Peri-Implantation Development and Spermatogenesis.” *Developmental Biology* 194 (2): 152–65. https://doi.org/10.1006/dbio.1997.8819.

Igakura, Tadahiko, Kenji Kadomatsu, Tadashi Kaname, Hisako Muramatsu, Qi Wen Fan, Teruo Miyauchi, Yoshiro Toyama, et al. 1998. “A Null Mutation in Basigin, an Immunoglobulin Superfamily Member, Indicates Its Important Roles in Peri-Implantation Development and Spermatogenesis.” *Developmental Biology* 194 (2): 152–65. https://doi.org/10.1006/dbio.1997.8819.

Ismail, Preeti M., Jie Li, Francesco J. DeMayo, Bert W. O’Malley, and John P. Lydon. 2002. “A Novel LacZ Reporter Mouse Reveals Complex Regulation of the Progesterone Receptor Promoter during Mammary Gland Development.” *Molecular Endocrinology* 16 (11): 2475–89. https://doi.org/10.1210/me.2002-0169.

Jones-Paris, Celestial R., Sayan Paria, Taloa Berg, Juan Saus, Gautam Bhave, Bibhash C. Paria, and Billy G. Hudson. 2017. “Embryo Implantation Triggers Dynamic Spatiotemporal Expression of the Basement Membrane Toolkit during Uterine Reprogramming.” *Matrix Biology* 57–58 (January): 347–65. https://doi.org/10.1016/j.matbio.2016.09.005.

Kannan, Athilakshmi, Asgerally T. Fazleabas, Indrani C. Bagchi, and Milan K. Bagchi. 2010. “The Transcription Factor C/EBPβ Is a Marker of Uterine Receptivity and Expressed at the Implantation Site in the Primate.” *Reproductive Sciences* 17 (5): 434–43. https://doi.org/10.1177/1933719110361384.

Kong, Sue, Bruce J Aronow, and Stuart Handwerger. 2006. “Gene Expression Microarray Data Analysis of Decidual and Placental Cell Differentiation.” In *Methods in Molecular Medicine*, 121:425–38.

Kuno, Naohiko, Kenji Kadomatsu, Qi Wen Fan, Masako Hagihara, Takao Senda, Shigehiko Mizutani, and Takashi Muramatsu. 1998. “Female Sterility in Mice Lacking the Basigin Gene, Which Encodes a Transmembrane Glycoprotein Belonging to the Immunoglobulin Superfamily.” *FEBS Letters* 425 (2): 191–94. https://doi.org/10.1016/S0014-5793(98)00213-0.

Laws, Mary J., Robert N. Taylor, Neil Sidell, Francesco J. DeMayo, John P. Lydon, David E. Gutstein, Milan K. Bagchi, and Indrani C. Bagchi. 2008. “Gap Junction Communication between Uterine Stromal Cells Plays a Critical Role in Pregnancy-Associated Neovascularization and Embryo Survival.” *Development* 135 (15): 2659–68. https://doi.org/10.1242/dev.019810.

Lee, K. Y., J.-W. Jeong, J. Wang, L. Ma, J. F. Martin, S. Y. Tsai, J. P. Lydon, and F. J. DeMayo. 2007. “Bmp2 Is Critical for the Murine Uterine Decidual Response.” *Molecular and Cellular Biology* 27 (15): 5468–78. https://doi.org/10.1128/mcb.00342-07.

Li, Kailiang, and Romana A Nowak. 2019. “The Role of Basigin in Reproduction.” *Reproduction (Cambridge, England)*, September. https://doi.org/10.1530/REP-19-0268.

Li, Ling, Wenhua Tang, Xiaoqing Wu, David Karnak, Xiaojie Meng, Rachel Thompson, Xinbao Hao, et al. 2013. “HAb18G/CD147 Promotes PSTAT3-Mediated Pancreatic Cancer Development via CD44s.” *Clinical Cancer Research* 19 (24): 6703–15.

https://doi.org/10.1158/1078-0432.CCR-13-0621.

Li, Quanxi, Athilakshmi Kannan, Francesco J. DeMayo, John P. Lydon, Paul S. Cooke, Hiroyuki Yamagishi, Deepak Srivastava, Milan K. Bagchi, and Indrani C. Bagchi. 2011. "The Antiproliferative Action of Progesterone in Uterine Epithelium Is Mediated by Hand2." *Science* 331 (6019): 912–16. https://doi.org/10.1126/science.1197454.

Li, Quanxi, Jun Wang, D. Randall Armant, Milan K. Bagchi, and Indrani C. Bagchi. 2002. "Calcitonin Down-Regulates E-Cadherin Expression in Rodent Uterine Epithelium during Implantation." *Journal of Biological Chemistry* 277 (48): 46447–55. https://doi.org/10.1074/jbc.M203555200.

Mantena, Srinivasa Raju, Athilakshmi Kannan, Yong-Pil Cheon, Quanxi Li, Peter F Johnson, Indrani C Bagchi, and Milan K Bagchi. 2006. "CEBP Is a Critical Mediator of Steroid Hormone-Regulated Cell Proliferation and Differentiation in the Uterine Epithelium and Stroma." Vol. 103. www.pnas.orgcgidoi10.1073pnas.0507261103.

Monsivais, Diana, Caterina Clementi, Jia Peng, Paul T Fullerton, Renata Prunskaite-Hyyryï ainen, Seppo J Vainio, and Martin M Matzuk. 2017. "BMP7 Induces Uterine Receptivity and Blastocyst Attachment." *Endocrinology* 158 (4): 979–92. https://doi.org/10.1210/en.2016-1629.

Monsivais, Diana, Caterina Clementi, Jia Peng, Mary M. Titus, James P. Barrish, Chad J. Creighton, John P. Lydon, Francesco J. DeMayo, and Martin M. Matzuk. 2016. "Uterine ALK3 Is Essential during the Window of Implantation." *Proceedings of the National Academy of Sciences* 113 (3): E387–95. https://doi.org/10.1073/pnas.1523758113.

Mote, Patricia A., Rebecca L. Arnett-Mansfield, Natalie Gava, Anna DeFazio, Biserka Mulac-Jericevic, Orla M. Conneely, and Christine L. Clarke. 2006. "Overlapping and Distinct Expression of Progesterone Receptors A and B in Mouse Uterus and Mammary Gland during the Estrous Cycle." *Endocrinology* 147 (12): 5503–12. https://doi.org/10.1210/en.2006-0040.

Nabeshima, Kazuki, Hiroshi Iwasaki, Kaori Koga, Hironobu Hojo, Junji Suzumiya, and Masahiro Kikuchi. 2006. "Emmprin (Basigin/CD147): Matrix Metalloproteinase Modulator and Multifunctional Cell Recognition Molecule That Plays a Critical Role in Cancer Progression." *Pathology International* 56 (7): 359–67. https://doi.org/10.1111/j.1440-1827.2006.01972.x.

Nakai, Masaaki, Li Chen, and Romana A. Nowak. 2006. "Tissue Distribution of Basigin and Monocarboxylate Transporter 1 in the Adult Male Mouse: A Study Using the Wild-Type and Basigin Gene Knockout Mice." *Anatomical Record - Part A Discoveries in Molecular, Cellular, and Evolutionary Biology* 288 (5): 527–35. https://doi.org/10.1002/ar.a.20320.

Nallasamy, Shanmugasundaram, Quanxi Li, Milan K. Bagchi, and Indrani C. Bagchi. 2012. "Msx Homeobox Genes Critically Regulate Embryo Implantation by Controlling Paracrine Signaling between Uterine Stroma and Epithelium." *PLoS Genetics* 8 (2): e1002500. https://doi.org/10.1371/journal.pgen.1002500.

Norwitz, Errol, Danny Schust, and Susan Fisher. 2001. "Implantation and the Survival of Early Pregnancy." *The New England Journal of Medicine* 345 (19): 1400–1408.

Olson, Gary E, Virginia P Winfrey, Gareth L Blaeuer, John R Palisano, and Subir K Nagdas. 2002. "Stage-Specific Expression of the Intermediate Filament Protein Cytokeratin 13 in Luminal Epithelial Cells of Secretory Phase Human Endometrium and Peri-Implantation Stage Rabbit Endometrium 1." *BIOLOGY OF REPRODUCTION*. Vol. 66. http://www.biolreprod.org.

Pampfer, Serge, and Isabelle Donnay. 1999. "Apoptosis at the Time of Embryo Implantation in Mouse and Rat." *Cell Death and Differentiation* 6 (6): 533–45. https://doi.org/10.1038/sj.cdd.4400516.

Paria, Bibhash C., Xuemei Zhao, Sanjoy K. Das, Sudhansu K. Dey, and Koji Yoshinaga. 1999. "Zonula Occludens-1 and E-Cadherin Are Coordinately Expressed in the Mouse Uterus with the Initiation of Implantation and Decidualization." *Developmental Biology* 208 (2): 488–501. https://doi.org/10.1006/dbio.1999.9206.

Parr, Earl L., H. N. Tung, and Margaret B. Parr. 1987. "Apoptosis as the Mode of Uterine Epithelial Cell Death during Embryo Implantation in Mice and Rats1." *Biology of Reproduction* 36 (1): 211–25. https://doi.org/10.1095/biolreprod36.1.211.

Peng, Sha, Jing Li, Chenglin Miao, Liwei Jia, Zeng Hu, Ping Zhao, Juxue Li, Ying Zhang, Qi Chen, and Enkui Duan. 2008. "Dickkopf-1 Secreted by Decidual Cells Promotes Trophoblast Cell Invasion during Murine Placentation." *Reproduction* 135 (3): 367–75. https://doi.org/10.1530/REP-07-0191.

Philp, Nancy J., Judith D. Ochrietor, Carla Rudoy, Takashi Muramatsu, and Paul J. Linser. 2003. "Loss of MCT1, MCT3, and MCT4 Expression in the Retinal Pigment Epithelium and Neural Retina of the 5A11/Basigin-Null Mouse." *Investigative Opthalmology & Visual Science* 44 (3): 1305. https://doi.org/10.1167/iovs.02-0552.

Ramathal, Cyril, Indrani Bagchi, Robert Taylor, and Milan Bagchi. 2010. "ENDOMETRIAL DECIDUALIZATION: OF MICE AND MEN." *Semin Reprod Med* 28 (1): 17–26. https://doi.org/10.1055/s-0029-1242989.ENDOMETRIAL.

Sidhu, Sukhvinder S, Aklilu T Mengistab, Andrew N Tauscher, Jennifer LaVail, and Carol Basbaum. 2004. "The Microvesicle as a Vehicle for EMMPRIN in Tumor–Stromal Interactions." *Oncogene* 23 (4): 956–63. https://doi.org/10.1038/sj.onc.1207070.

Singh, Mohan, Parvesh Chaudhry, and Eric Asselin. 2011. "Bridging Endometrial Receptivity and Implantation: Network of Hormones, Cytokines, and Growth Factors." *Journal of Endocrinology* 210 (1): 5–14. https://doi.org/10.1530/JOE-10-0461.

Soyal, Selma M., Atish Mukherjee, Kevin Y.S. Lee, Jie Li, Huaiguang Li, Francesco J. DeMayo, and John P. Lydon. 2005. "Cre-Mediated Recombination in Cell Lineages That Express the Progesterone Receptor." *Genesis* 41 (2): 58–66. https://doi.org/10.1002/gene.20098.

Su, Juan, Xiang Chen, and Takuro Kanekura. 2009. "A CD147-Targeting SiRNA Inhibits the Proliferation, Invasiveness, and VEGF Production of Human Malignant Melanoma Cells by down-Regulating Glycolysis." *Cancer Letters* 273 (1): 140–47. https://doi.org/10.1016/j.canlet.2008.07.034.

Tang, Yi, Marian T Nakada, Prabakaran Kesavan, Francis Mccabe, Hillary Millar, Patricia Rafferty, Peter Bugelski, and Li Yan. 2005. "Extracellular Matrix Metalloproteinase Inducer

Stimulates Tumor Angiogenesis by Elevating Vascular Endothelial Cell Growth Factor and Matrix Metalloproteinases." http://www.raybiotech.com.

Tibbetts, Todd A, Marisela Mendoza-Meneses, Bert W O'malley, and Orla M Conneely. 1998. "Mutual and Intercompartmental Regulation of Estrogen Receptor and Progesterone Receptor Expression in the Mouse Uterus 1." *BIOLOGY OF REPRODUCTION*. Vol. 59. https://academic.oup.com/biolreprod/article-abstract/59/5/1143/2740899.

Wang, Haibin, and Sudhansu K. Dey. 2006. "Roadmap to Embryo Implantation: Clues from Mouse Models." *Nature Reviews Genetics* 7 (3): 185–99. https://doi.org/10.1038/nrg1808.

Wang, Haibin, Wen Ge Ma, Lovella Tejada, Hao Zhang, Jason D. Morrow, Sanjoy K. Das, and Sudhansu K. Dey. 2004. "Rescue of Female Infertility from the Loss of Cyclooxygenase-2 by Compensatory Up-Regulation of Cyclooxygenase-1 Is a Function of Genetic Makeup." *Journal of Biological Chemistry* 279 (11): 10649–58. https://doi.org/10.1074/jbc.M312203200.

Wang, Haibin, Shuang Zhang, Haiyan Lin, Shuangbo Kong, Shumin Wang, Hongmei Wang, and D. Randall Armant. 2013. "Physiological and Molecular Determinants of Embryo Implantation." *Molecular Aspects of Medicine* 34 (5): 939–80. https://doi.org/10.1016/j.mam.2012.12.011.

Wang, Wei, Quanxi Li, Indrani C Bagchi, and Milan K Bagchi. 2010. "The CCAAT/Enhancer Binding Protein Is a Critical Regulator of Steroid-Induced Mitotic Expansion of Uterine Stromal Cells during Decidualization." *Endocrinology* 151 (8): 3929–40. https://doi.org/10.1210/en.2009-1437.

Wang, Wei, Robert N. Taylor, Indrani C. Bagchi, and Milan K. Bagchi. 2012. "Regulation of Human Endometrial Stromal Proliferation and Differentiation by C/EBPβ Involves Cyclin E-Cdk2 and STAT3." *Molecular Endocrinology* 26 (12): 2016–30. https://doi.org/10.1210/me.2012-1169.

Wang, Xiaohong, Hiromichi Matsumoto, Xuemei Zhao, Sanjoy Das, and Bibhash Paria. 2004. "Embryonic Signals Direct the Formation of Tight Junctional Permeability Barrier in the Decidualizing Stroma during Embryo Implantation." *Journal of Cell Science* 117 (1): 53–62. https://doi.org/10.1242/jcs.00826.

Wesseling, Jelle, Sylvia W. Van Der Valk, and John Hilkens. 1996. "A Mechanism for Inhibition of E-Cadherin-Mediated Cell-Cell Adhesion by the Membrane-Associated Mucin Episialin/MUC1." *Molecular Biology of the Cell* 7 (4): 565–77. https://doi.org/10.1091/mbc.7.4.565.

Wetendorf, Margeaux, and Francesco J. DeMayo. 2012. "The Progesterone Receptor Regulates Implantation, Decidualization, and Glandular Development via a Complex Paracrine Signaling Network." *Molecular and Cellular Endocrinology* 357 (1–2): 108–18. https://doi.org/10.1016/j.mce.2011.10.028.

Woodhead, V E, T J Stonehouse, M H Binks, K Speidel, D A Fox, A Gaya, D Hardie, et al. 2000. "Novel Molecular Mechanisms of Dendritic Cell-Induced T Cell Activation." *International Immunology* 12 (7): 1051–61. http://www.ncbi.nlm.nih.gov/pubmed/10882417.

Xin, Xiaoyan, Xianqin Zeng, Huajian Gu, Min Li, Huaming Tan, Zhishan Jin, Teng Hua, Rui Shi, and Hongbo Wang. 2016. “CD147 / EMMPRIN Overexpression and Prognosis in Cancer : A Systematic Review And.” *Scientific Reports*, no. 113: 1–12. https://doi.org/10.1038/srep32804.

Ye, Xiaoqin. 2020. “Uterine Luminal Epithelium as the Transient Gateway for Embryo Implantation.” *Trends in Endocrinology & Metabolism* 31 (2): 165–80. https://doi.org/10.1016/j.tem.2019.11.008.

CHAPTER FIVE

Loss of Basigin in the Mouse Endometrial Stromal Cells Leads to Impaired Decidualization and Lactate Transport *in vitro*

Abstract

Basigin (BSG) is a member of the Ig superfamily and plays a role in cell proliferation, induction of MMPs for tissue remodeling and promoting angiogenesis. BSG is expressed in many tissues including the male and female reproductive tracts and is important for fertility. The previous studies showed that conditional knockout (cKO) of BSG in the uterus led to subfertility in mice due to impaired implantation, compromised decidualization, and altered abundance of the lactate transporters *in vivo*. Here I hypothesized that BSG is required for proper decidualization and normal lactate transport in the endometrial stromal cells cultured *in vitro*. To test this hypothesis, we used a primary cell culture system to isolate and culture mouse endometrial stromal cells (MESC). The aims of this study were 1) to investigate *in vitro* decidualization and 2) to investigate lactate transport in the cKO MESC. The results showed that proliferation of the cKO MESCs was not different compared to the controls at 24 hour and 48 hours of culture, indicating that the loss of BSG does not affect cell proliferation in the MESCs. Decidualization was suppressed in the cKO MESCs as expression of the decidualization markers *Prl8a2, Cebpβ, Bmp2* and *Hand2* were downregulated at some point during the four-day cell culture period. Protein levels of CEBPβ were not affected in the cKO MESCs. MMP9 immunofluorescent staining revealed there was no difference in the localization and abundance of MMP9 in the MESCs of the two genotypes. The concentrations of lactate secreted by the stromal cells were significantly reduced in the cell culture medium of the cKO MESCs compared to the controls on day 2 and day 4 of culture. MESCs were

also cultured under hypoxic conditions to investigate decidualization and lactate concentrations. These results showed that gene expression levels of decidualization markers were similar in the cKO MESCs compared to the controls under hypoxic condition. In agreement with the results from normoxia, lactate concentrations in the medium were significantly lower in the cKO MESCs compared to the controls when cultured under hypoxia. Collectively, these results suggest that the loss of BSG suppressed *in vitro* decidualization and reduced the concentration of lactate secreted by the MESCs.

Introduction

Pregnancy is a complex process that consists of discrete events such as implantation, decidualization, placentation and parturition (Cha, Sun, and Dey 2012). Implantation is the process where the blastocyst makes the first physical and physiological interaction with the maternal endometrium, and this event requires synchronization between the embryo and the receptive endometrium (H. Wang et al. 2013). After implantation, the uterine endometrium undergoes a unique transformation in mice and humans, known as decidualization, where the fibroblast-like endometrial stromal cells proliferate and terminally differentiate into large, round polyploid decidual cells (W. Wang et al. 2012; Kong, Aronow, and Handwerger 2006). This process is delicately controlled by steroid hormones, epithelial cell secreted factors, cell cycle regulators and immune cells (Conneely, Mulac-Jericevic, and Lydon 2003; Wetendorf and DeMayo 2012; Das 2009; Croy et al. 2012). Normal decidualization is a prerequisite for successful pregnancy because it is involved in many important functions, including regulating trophoblast growth and invasiveness, providing nutrition to the developing blastocyst, establishing maternal-fetal immune-microenvironment, synthesizing hormones and promoting angiogenesis prior to the

formation of a functional placenta (Peng et al. 2008; X. Wang et al. 2004; Welsh and Enders 1987; Bombail et al. 2010).

During implantation and decidualization, the maternal microenvironment is under a hypoxic condition as the concentration of oxygen within the lumen of the uterus has been reported to be in the range of 1.5% to 5% depending on the species (Fischer and Bavister 1993). With limited levels of oxygen available, the embryos increase glucose consumption. This low oxygen environment and upregulation of glucose consumption are associated with high levels of lactate formation (Gardner 2015). Studies have shown that in the implanting embryo, 90% of the consumed glucose is converted to lactate (Clough and Whittingham 1983). The metabolism of the endometrial stromal cells at the time of implantation and decidualization is not clear, but it is reported that glucose metabolism is also important for decidualization of the endometrial stromal cells in humans and mice (Tsai et al. 2014). Lactate transport is facilitated by the monocarboxylate transporters (MCT). There are four MCTs in mice and their transmembrane localization requires the chaperone proteins BSG and embigin (Le Floch et al. 2011; Nagai et al. 2010; Kirk et al. 2000).

BSG, also known as CD147 and EMMPRIN in humans; OX-47, MC31 and CE9 in rats; and HT7 in chickens, is a highly glycosylated protein with two immunoglobulin-like domains (K. Li and Nowak 2019). BSG plays multiple roles in both physiological and pathological processes including tumorigenesis, inflammation, tissue remodeling and neurological functions (Grass and Bryan 2016; Tang et al. 2005; Guindolet and Gabison Eric 2019; Weidle et al. 2010). BSG is also expressed in the reproductive tissues and is important for male and female reproduction (Chen et al. 2010; Bi et al. 2013). The previous chapters demonstrated, using a PR-Cre cKO model, that the loss of BSG led to subfertility in female mice. This is due to defective implantation and decidualization *in vivo*. The goals of this study were: 1) to investigate whether *in vitro*

decidualization is compromised in the MESCs of cKO mice and 2) to determine whether the lactate concentrations secreted into the culture medium by the MESCs from the cKO mice were different compared to the controls under normal oxygen levels and hypoxic conditions. Here I demonstrate that lack of BSG in the MESCs of the cKO mice led to compromised decidualization, as well as a reduction in the amount of lactate transported out of the cells into the medium under normal and hypoxic conditions.

Material and Methods

Animals

C57/Bl6 mice were housed at the University of Illinois, Urbana-Champaign, at the Institute for Genomic Biology Animal Facility in polysulfone cages. Food (Harlan Teklad 8604) and filtered water were provided for the mice *ad libitum*. The room was maintained at a temperature of 22 ± 1 °C and on a 12 hour light-dark cycle. All experimental procedures including animal care, surgery, euthanasia and tissue collection were approved by the Institutional Animal Care and Use Committee at the University of Illinois, Urbana–Champaign.

Animal mating

To collect mouse endometrial stromal cells (MESC), two-month-old female mice of each genotype were mated naturally with one wild type male of proven fertility. One female and one male were housed together. The presence of a vaginal plug indicated successful mating behavior and the morning of the plug detection was designated as day 1 of pregnancy.

Isolation of MESCs

Female mice were euthanized on day 4 of pregnancy, and the uteri were collected and transferred back to the laboratory in cold HBSS supplemented with 1% penicillin-streptomycin

(Fisher). The uterine horns were cut open longitudinally to expose the uterine lumen and placed in a Petri dish with fresh HBSS. The digestion mix pancreatin solution was made by dissolving 0.25 g pancreatin (Sigma) in 10 ml 0.25% trypsin (Fisher) and then warmed in a 37 °C water bath for at least 1 hour prior to tissue isolation. The uteri were transferred into the pancreatin digestion mix and incubated horizontally for 60 minutes at 4 °C on an orbital shaker, then horizontally for 45 minutes at room temperature (RT) without shaking and finally horizontally for 15 minutes at 37 °C without shaking. After this two-hour incubation, the supernatant solution was poured away, and the uteri were transferred into a Petri dish containing cold medium containing 10% serum to inactivate trypsin activity for 5 minutes. The uteri were transferred to a 15 ml tube containing 3 ml of cold HBSS and vortexed for 10 seconds to release the epithelial sheets, then rinsed in a clean Petri dish with 3 ml HBSS. This vortexing and rinsing step was repeated two more times to remove the epithelial cells. The uteri were then transferred to digestion solution I and incubated for 30 minutes at RT. For each animal, digestion solution I was made consisting of 30 mg dispase II (Sigma), 125 mg pancreatin (Sigma), 1% penicillin-streptomycin (Fisher) in 5 ml HBSS. Following 30 minutes of incubation, the same volume of stop solution (consisting of 10% FBS and 1% penicillin-streptomycin in HBSS) was added to the digestion solution. The supernatant was discarded, and the uterine tissues were washed twice in HBSS before transferring into digestion solution II to incubate for 45 minutes at 37 °C. Digestion solution II was made by diluting 2.5 mg collagenase IA (Sigma) and 1% penicillin-streptomycin in 5 ml HBSS for each uterine sample. After completion of this incubation, the same volume of stop solution was added and the tube was vortexed for 10 seconds. The stromal cells were collected by passing the solution through a 40 µm nylon mesh filter (Fisher) into a new 50 ml tube. The cell-containing suspension was then centrifuged at 450 g for 6 minutes. The supernatant was discarded, and the cells were resuspended

with 10 ml of HBSS. After another centrifugation at 450 g for 6 minutes, the supernatant was aspirated, and the cells were resuspended and plated in DMEM/F12 medium. The DMEM/F12 medium contained 10% FBS, 10 nM estradiol, 1 μM progesterone and 1% penicillin-streptomycin.

Mouse endometrial stromal cell culture

Following isolation of the MESCs, cell culture studies were performed under either normal or hypoxic conditions. For the normoxic conditions (20% O_2), the cells from each animal (minimum five animals per genotype) were plated into two 75 cm^2 culture flasks. The cells were incubated for 3-5 days, and the medium was changed every two days. For flask 1, on day 2, serum free medium was added to the flask. On day 3, the cells were trypsinized and collected for RNA extraction. Ten ml of the serum free medium were collected and stored in -80 ◦C for future analysis. For flask 2, regular medium was changed on day 2, then the serum free medium was added on day 4. On day 5, cells were trypsinized and collected for future RNA extraction. Ten ml of the serum free medium were collected and stored at -80 ◦C for further analysis. For hypoxic conditions (1% O_2), the cells were plated in two 75 cm^2 culture flasks and incubated in a regular incubator overnight before transferring to a Biospherix hypoxia incubator for 3-5 days. For flask 1, on day 3, the medium was collected for lactate assay and the cells were trypsinized and collected for RNA extraction. For flask 2, the medium was changed on day 3. On day 5, the medium was collected for lactate assay and the cells were trypsinized and collected for RNA extraction.

MESCS proliferation assay

MESCs of both genotypes were seeded at a density of 10^5 cell/dish in 35 mm Petri dishes and were cultured in DMEM/F12 medium for 48 hours. At 24 hours and 48 hours, the cells were photographed, then trypsinized and harvested. The numbers of cells were counted using a Hemocytometer. Four dishes of cells were counted at each time point for each genotype.

RNA isolation and quantitative reverse transcription-PCR (qRT-PCR)

Total RNA was extracted from the MESCs on day 0 (cells collected immediately after isolation on day 4 of pregnancy), 2, and 4 from normoxia incubation and on day 3 from hypoxia incubation using the Qiagen RNeasy Mini kit (Qiagen #74104) according to the manufacturer's instructions. The concentration of the mRNA was determined by Nanodrop and the quality of the mRNA was assessed using the Bioanalyzer at the Functional Genomics Center at the University of Illinois, Urbana-Champaign (https://biotech.illinois.edu/functionalgenomics). One microgram of total RNA was reverse transcribed using the First Strand cDNA Synthesis Kit from Roche (#4379012001) following the manufacturer's instructions. After the cDNA was synthesized, qRT-PCR was performed to assess the mRNA levels of the decidualization markers in the stromal cells of the mice using the Power Sybr Green Master Mix (Life Tech #A25742). Briefly, 5 µl of a 1:7 diluted cDNA sample were mixed with 10 µl of master mix (7.5 µl of Sybr Green Mix, 0.6 µl of primer set and 1.9 µl of water) for a total volume of 15 µl per well in a MicroAmp optical 384-well reaction plate. Three technical replicates were performed for each sample. qRT-PCR amplification and quantitation were performed using a Quant Studio (Applied Biosytem) from the Functional Genomics Center. The reaction was run for 40 cycles (95 °C for 15 seconds, 60 °C for 1 minute). The comparative CT method (ΔΔCT) was used for quantification of gene expression. Relative fold changes in gene expression for all tested genes were normalized to Peptidylprolyl isomerase A (*Ppia)* and Ribosomal protein, large, P0 (*Rplp0)* endogenous housekeeping genes. Genes analyzed include *Bsg*, Decidual prolactin-related protein family 8, subfamily a, member 2 (*Prl8a2*), CCAAT enhancer-binding protein beta (*Cebpβ*), Bone morphogenetic protein 2 (*Bmp2*), Heart and neural crest derivatives-expressed protein 2 (*Hand2*) and Wingless-related integration site 4 (*Wnt4*). The primer sequences of these genes are listed in **Table 5.1**

Immunofluorescence Staining

To assess the protein abundance and localization of BSG, CEBPβ and MMP-9 in the MESCs, immunofluorescence (IF) staining was performed on cells incubated for two or four days after collection on day 4 of pregnancy. Briefly, the MESCs were plated in six-well plates with coverslips coated with poly L-lysine (Sigma Aldrich) and incubated for two days. Then the MESCs were fixed with freshly made 4% paraformaldehyde (Fisher) for 30 minutes at RT (RT). After washing cells with PBS three times, 1 ml of 0.5% Triton 100 (Sigma) was added to each well to permeabilize the cells for 15 minutes at RT. The cells were washed with PBS before blocking with 5% horse serum (Vectastain ABC kit, Vector Laboratories, Inc. Burlingame, CA) diluted in 1%BSA/PBST at RT for 60 minutes. The cells were incubated with primary antibodies at specific concentrations overnight at 4 ◦C. The primary antibodies used were: BSG (R&D System AF772) at 1:200 dilution, CEBPβ (Santa Cruz sc-150) at 1:100 dilution and MMP-9 (Abcam Ab38898) at 1:100 dilution. The negative control cells were incubated with a non-specific IgG of the same species as the primary antibodies to confirm specificity of the primary antibodies. On the following day, the cells were rinsed with PBST prior to incubation with either an anti-goat Alexa488 conjugated secondary antibody (Jackson Immuno Research # 805-545-180), or an anti-rabbit Cy3 conjugated secondary antibody (Jackson Immuno Research # 711-165-152) at 1:200 dilution for 1 hour at RT. After incubation, the cells were rinsed with PBS and covered with a DAPI containing mounting medium (Vector Laboratories, H-1200). To visualize the immunoreactivity, all slides were imaged using a Zeiss LSM 710 confocal microscope at the Institute for Genomic Biology at the University of Illinois, Urbana-Champaign.

Lactate Assay

To determine the amount of lactate secreted by the cells under both normoxic and hypoxic conditions, a colorimetric assay was performed using a Lactate Assay kit (Millipore Sigma #MAK064) according to manufacturer's instructions. Medium from cultured cells collected at each time point and stored in -80 ◦C was thawed on ice. The lactate standard was made by adding 0, 2, 4, 6, 8 and 10 µl of the standard solution to each well of a 96-well plate to generate 0, 2, 3, 4, 8 and 10 nM/well standards. 10 µl of cell culture medium were added to each well and the assay was run in duplicate. For each well, 50 µl of the master reaction mix (46 µl of lactate assay buffer, 2 µl of lactate enzyme mix and 2 µl of lactate probe) were added to each well along with 40 µl of the assay buffer and the 10 µl samples for a total volume of 100 µl. The plate was incubated for 30 minutes at RT, then read at the 670 nm wavelength for absorbance in a plate reader. A standard curve was generated with the standard samples and the best fit line was calculated. The lactate concentrations were calculated by plotting the readings into the standard curve.

Statistical Analysis

All data were analyzed utilizing GraphPad Prism software 8 (GraphPad Prism, San Diego, CA). Data are presented as means ± standard error of the means (SEM). For normally distributed data, unpaired t tests were used to compare the control group to the experimental group. For non-normally distributed data, Mann-Whitney tests were used. Statistical significance was assigned at $p \leq 0.05$. Trending difference was assigned when the p value was between 0.05 and 0.1.

Results

Cell proliferation is not different in the cKO MESCs compared to the controls.

The MESCs were isolated from uteri of both control and *Bsg* cKO mice to set up the primary cell cultures. The numbers of cells were counted at 24 hours and 48 hours to quantify cell

proliferation (**Figure 5.1** A). After 24 hours, there were 1.52 x 10^5 cells on average in the control MESCs and 1.55 x 10^5 cells in the cKO MESCs. After 48 hours, there were 5.64 x 10^5 cells in the control MESCs on average and 4.68 x 10^5 cells in the cKO MESCs. There were no significant differences between the two genotypes at either time point. Microscopic images of the cells taken at 48 hours (**Figure 5.1 B and C**) showed that both the cell populations appeared healthy and similar in cell morphology. These data suggest that the loss of BSG did not affect cell proliferation in the MESCs.

Expression of decidualization genes is altered in the MESCs of cKO cultured *in vitro*.

The mRNA expression levels of *Bsg* and of specific decidualization markers (*Prl8a2, Cebpβ, Bmp2, Hand2 and Wnt4*) were analyzed in MESCs on day 0, 2 and 4 of culture (**Figure 5.2**). The results showed that *Bsg* mRNA in the cKO MESCS was markedly lower compared to the controls at every time point as expected. *Prl8a2* was not detected in MESCs on day 0 for either genotype and increased dramatically from day 2 to day 4 by 7-fold. However, in the cKO MESCs, *Prl8a2* mRNA remained at the same low level at days 2 and 4 of culture and was downregulated by over 80% compared to the controls. The level of *Cebpβ* mRNA in the controls also increased over time. The *Cebpβ* level in the cKO MESCs was downregulated by approximately 60% on day 0, then increased to a comparable level on day 2, then showed lower expression by about 50% on day 4 compared to the controls. The levels of *Bmp2*, *Hand2* and *Wnt4* in the control MESCs all decreased slowly overtime, but levels of expression in the cKO MESCs were different. The level of *Bmp2* mRNA in the cKO cells on day 0 was significantly downregulated by 80% as compared to the controls. Later on, there was a slight upregulation on day 2 and then a slight downregulation on day 4 in the cKO cells, which was not significantly different from the controls. Expression of *Hand2* in the cKO cells continued to decline over time. On day 2, *Hand2* was decreased by 25%,

and on day 4, the level was significantly downregulated to half of the levels seen in controls. Surprisingly, the *Wnt4* level in the cKO MESCs was comparable to the controls on day 0, but significantly increased by two-fold on day 2 and then decreased again to levels similar to the controls on day 4.

CEBPβ protein localization is similar in the cKO and control MESCs.

The protein localization of CEBPβ in the MESCs of the cKO mice and control mice was evaluated by performing IF double staining for BSG and CEBPβ after 2 days in culture (**Figure 5.3**). These results showed that BSG in the cKO cells was successfully downregulated, with only a few cells expressing BSG, compared to the control cells, where most cells expressed abundant BSG (**B and F**). However, the CEBPβ localization appeared to be the same in the cKO MESCs as compared to the controls, since most of the cell showed positive immunoreactivity for CEBPβ in the cells of both genotypes (**C and G**). There was no difference in the protein localization of CEBPβ in the cKO cells compared to the controls in this short time experiment.

MESCs of the cKO mice secreted lower levels of lactate into the medium.

The previous studies showed that MCT1 abundance and localization were altered in the uterine cells of cKO mice *in vivo*, and MCT1 is important for transporting lactate out of these cells. In order to determine the amount of lactate secreted out of the cell by the MESCs of the cKO mice, I carried out lactate assays. The lactate assay results (**Figure 5.4**) showed that on both day 2 and day 4 of culture, the cKO MESCs secreted less lactate into the medium compared to the control MESCs. On day 2, the medium of cKO MESCs contained 97.74 ng/µl lactate, which was markedly lower than the concentration of lactate at 106.2 ng/µl in the medium from control MESCs. Similarly, on day 4, there was, on average, 32.66 ng/µl lactate in the medium from cKO MESCs, significantly lower than the 76 ng/µl concentration in the medium from control MESCs. These

data suggest that the loss of BSG in the cells inhibited the ability of cells to transport lactate out of the cell into the cell culture medium.

MMP9 protein abundance and localization are not different in the cKO MESCs compared to the controls.

Secretion of MMPs and VEGFs are increased in early pregnancy and are important for tissue remodeling and angiogenesis (Sharkey and Smith 2003). To examine MMP9 protein levels in the MESCs, I performed an IF staining for MMP9 in cultured cells of both genotypes (**Figure 5.5**). The results showed that there did not appear to be any difference in the abundance or localization of MMP9 in the cKO MESCs compared to the controls. There was no apparent difference in the two groups of cells at either the lower or higher magnification (**A and B**). The higher magnification did show some accumulated localization of MMP9 on the edges of the cells of both genotypes (**C and D**). These results suggest that the MMP9 was not altered in the MESCs of the cKO mice.

Decidualization marker expression levels were similar in the cKO and control MESCs under hypoxic conditions.

Implantation occurs in a hypoxic environment in humans and mice and this low oxygen favors embryo survival (Shahbazi et al. 2016). To better mimic the cell response *in vivo*, I cultured the MESCs of both genotypes under hypoxic conditions to evaluate the decidualization response. The results in **Figure 5.6** show that the expression of decidualization markers was not altered in the cKO MESCs compared to the controls, although the *Bsg* level was much lower in the cKO MESCs. Expression of all the genes analyzed, *Prl8a2*, *Bmp2*, *Wnt4* and *Cebpβ* was not statistically different in the cKO MESCs compared to the controls.

MESCs of the cKO mice secrete lower level of lactate under hypoxic conditions.

I also measured the lactate concentrations in the medium of the MESCs of both genotypes under hypoxic conditions using the lactate assay. Similar to the results for the cells under normoxic conditions, the cKO MESCs secreted much less lactate into the medium compared to the controls when cultured for 48 hours under hypoxic conditions at day 3 of culture (**Figure 5.7**). The medium from cKO MESCs contained 23.62 ng/µl lactate, which was significantly lower than the concentration in the control medium at 46.67 ng/µl. These results support the hypothesis that the loss of BSG in the cells inhibits the ability to transport lactate into the culture medium under hypoxic conditions.

Discussion

The immunoglobulin superfamily member BSG is expressed in diverse tissues and play important roles in lymphocyte migration, tissue remodeling, stimulation of angiogenesis, lactate transport and energy metabolism (K. Li and Nowak 2019). The expression of BSG in the uterus during early pregnancy has been characterized and null mutant mice are profoundly infertile (Chen et al. 2007; Chen, Belton, and Nowak 2009; Igakura et al. 1998). To overcome the high embryonic lethality of global deletion of *Bsg*, our laboratory generated and validated a PR-Cre *Bsg* cKO model. The previous results showed that loss of BSG caused impaired implantation and decidualization *in vivo*, eventually lead to a reduction of fertility in mice. In this study, I examined the role of BSG in decidualization and lactate transport *in vitro* using a primary MESC culture system.

Decidualization of the endometrium is a crucial step for the uterus to become receptive for embryos and further events in pregnancy. During decidualization, the endometrial stromal cells

undergo extensive proliferation first, then terminal differentiation to become the decidualized stromal cells (Zhu et al. 2014). Bagchi et al have reported that insufficient proliferation of the stromal cells leads to failed differentiation in mice (Bagchi et al. 2006). Studies have shown that BSG promotes cell proliferation in tumor cells in humans (Sidhu et al. 2010; Knutti, Kuepper, and Friedrich 2015; Hasaneen et al. 2016). These results showed that the number of cells at 24 hours or 48 hours of incubation were not different between the two genotypes. This agrees with the KI67 results of the uteri of mice on day 4 pregnancy *in vivo,* that there was no difference in the number of proliferating stromal cells in the cKO mice compared to the controls. Interestingly, this is contrary to the findings in human endometrial stromal cells (HESC), where knocking down of *Bsg* by siRNA inhibits stromal cell proliferation after 72 hours (Bi 2013). However, this result is consistent with the results from MESCs of *Bsg* null mice study, which showed BSG does not affect stromal cell proliferation *in vitro* (Chen 2006). This indicates that BSG might play different roles in stromal cell proliferation in the humans than in the mice, or culturing for 48 hours was not long enough to see the effects.

A set of decidualization marker genes was analyzed for mRNA levels in the MESCs on day 0, 2 and 4 of culture to determine their changes over time. These results showed that in the control MESCs, *Prl8a2* and *Cebpβ* were upregulated over time, but *Bmp2, Hand2* and *Wnt4* were downregulated over time. For the cKO MESCs, *Prl8a2*, *Cebpβ, Bmp2* and *Hand2* were all downregulated compared to the controls at some point. This is consistent with the results on decidualization marker expression levels *in vivo,* where *Bmp2, Cebpβ* and *Hand2* were downregulated in the decidua of cKO females. Similarly, in HESC, siRNA knocking down of *Bsg* leads to impaired decidualization with downregulated mRNA levels of decidual markers *Igfbp1* and *Prolactin* (Bi 2013). In the HESC study microarray results, knocking down of *Bsg* leads to

downregulation of *Wnt* family members, indicating involvement of BSG in *Wnt4*/β-catenin pathway (Bi 2013). In these results, however, *Wnt4* mRNA level was upregulated and then downregulated to the same level as the controls. This indicates that it is different than in the humans, BSG may regulate decidualization in mice through mechanisms other than the BSG-*Wnt4*/β-catenin pathway. Studies have shown that BMP2 acts through its downstream target activin-like kinases 2 (ALK2) and CEBPβ, then via CEBPβ's downstream target signal transducer and activator of transcription 3 (STAT3) to regulate decidualization (Monsivais et al. 2016; Clementi et al. 2013; Kannan et al. 2010; Cheng et al. 2001). BSG has also been shown to promote the STAT3 activity in the pancreatic cancer cells (L. Li et al. 2013). Therefore, it is possible that BSG is involved in a BMP-ALK2-CEBPβ-STAT3 pathway to regulate decidualization in mice. Further studies are needed to explore the direct relationships between BSG and ALK2 and STAT3 in the endometrial stromal cells.

MMPs are a family of proteolytic enzymes, including collagenases (MMP1, 8, 13), stromelysins (MMP3, 7, 10) and gelatinases (MMP2, 9) (Davidson et al. 2003). Studies have shown that MMP2 and MMP9 are produced by the endometrial stromal cells and the decidual cells, and their main function is to degrade and reorganize the extracellular matrix during decidualization (Gellersen et al. 2010; Guo et al. 2011). Studies on BSG also reported that it mediates the expression and activity of MMP1, 2, 3 and 9 (Sun and Hemler 2001; Weidle et al. 2010; Xiong, Edwards, and Zhou 2014; Nabeshima et al. 2006; Braundmeier et al. 2006; Chen, Belton, and Nowak 2009). In this study, MMP9 protein abundance and localization were not different in the MESCS of the cKO or the control mice. Chen reported a rapid and marked decrease in mRNA levels of *MMP3* and *MMP9* during *in vitro* decidualization, which could be upregulated once treated with recombinant BSG protein (Chen, Belton, and Nowak 2009). *MMP2*, *MMP3* and

MMP9 mRNA levels were not different in the BSG null mice decidual tissues (Chen 2006). These results showed that MMP9, at least at the protein abundance level, was not reduced in the MESC cells lacking BSG. This may be because that other factors, such as interleukin-1 (IL-1) and Transforming growth factor beta (TNFβ), also regulate MMP9 productions (Anumba et al. 2010) and promote expression of MMPs in compensation to loss of BSG. Since MMPs are secreted proteins, it would be important to examine the amount of MMPs secreted into the culture medium by the stromal cells by immunoblotting and ELISA in the future.

Under hypoxic conditions at the time of implantation, cells produce a large amount of lactate (Gardner 2015). MCTs are important in lactate transport and maintaining the metabolic homeostasis in a variety of cell types (Halestrap 2012). BSG is a chaperone protein for MCT1 and MCT4, and is responsible for translocating them to the cell membrane (Marchiq et al. 2015). In the previous chapter, I demonstrated that the loss of BSG altered the abundance and localization of MCT1 *in vivo*. The lactate assay results under normoxic conditions showed the medium of the cKO MESCs contained significantly lower concentration of lactate compared to the controls at both time points. Unfortunately, I was only able to collect the cells and the culture medium on day 3 of incubation under hypoxic conditions (48 hours under hypoxia) due to contaminations and equipment problems. These results showed that although the level of *Bsg* was markedly lower in the cKO MESCs compared to the controls, expression of other decidualization marker was not different. This could indicate that either none of the two MESCs decidualized, or the cKO MESCs were able to decidualize to the same extend as the control MESCs under hypoxic conditions. Regardless, this experiment should be repeated with longer periods of incubation to characterize the change of decidualization marker gene expression over time. The lactate results showed that the cKO MESCs secreted significantly lower concentration of lactate into the medium compared

to the control MESCs under hypoxic conditions, which is consistent with the lactate assay results under normal oxygen level. This indicates that the loss of BSG in the MESCs decreases the concentration of lactate transported by the cells into the medium. The concentrations of lactate secreted by both MESCs were lower in the hypoxic conditions compared to the normoxic conditions. This might be because that the total number of cells under hypoxic conditions were lower than the normoxic conditions for both genotypes. The number of cells in the hypoxic conditions were not quantified because a large portion of cells did not detach from the culture flasks even hours after trypsin treatment, preventing an accurate quantification. In the future, the number of cells under hypoxic conditions need to be quantified using alternative methods.

In summary, the results in this study showed that loss of BSG in the MESCs, without altering cell proliferation, suppressed decidualization and reduced lactate secretion into the medium *in vitro*. I discovered that most decidualization marker genes analyzed, including *Prl8a2*, *Cebpβ*, *BMP2* and *Hand2,* were downregulated at a point during *in vitro* decidualization. The MMP9 protein abundance was not different in the cKO MESCs compared to the controls. The lactate assay results showed that the lactate concentrations secreted into the medium of the cKO MESCs were markedly lower than the controls on day 2 and day 4 of culture under nomoxic conditions. Under hypoxic conditions, the decidualization marker expression levels were similar in the cKO MESCs compared to the controls, but lactate concentrations secreted into the medium was significantly lower in the cKO MESCs. These findings suggest that the loss of BSG in the MESCs leads to suppression of *in vitro* decidualization and reduction in lactate secretion.

Table and Figures

Table 5.1 Primer sequences used for quantitative RT-PCR

Genes	NCBI Gene Reference	Left Primer Sequence	Right Primer Sequence
Rplp0	NM_007475.5	actggtctaggacccgagaag	ctcccaccttgtctccagtc
Ppia	NM_008907.1	ggaccaaacacaaacggttc	catgccttctttcaccttcc
Bsg	NM_009768.2	acagcagtggcgttgaca	ggtcatctgcgtccactatgt
Prl8a2	NM_010088.2	gctggacaatttgaaacacttg	tgggtttgtgacattagagtgg
Cebpβ	NM_001287739.1	aagatgcgcaacctggag	cagggtgctgagctctcg
Bmp2	NM_007553.3	agatctgtaccgcaggcact	gttcctccacggcttcttc
Hand2	NM_010402.4	tgagcagcaacgacaagaaa	tgctctcctcttcttcactgc
Wnt4	NM_009523.2	actggactccctccctgtct	tgcccttgtcactgcaaa

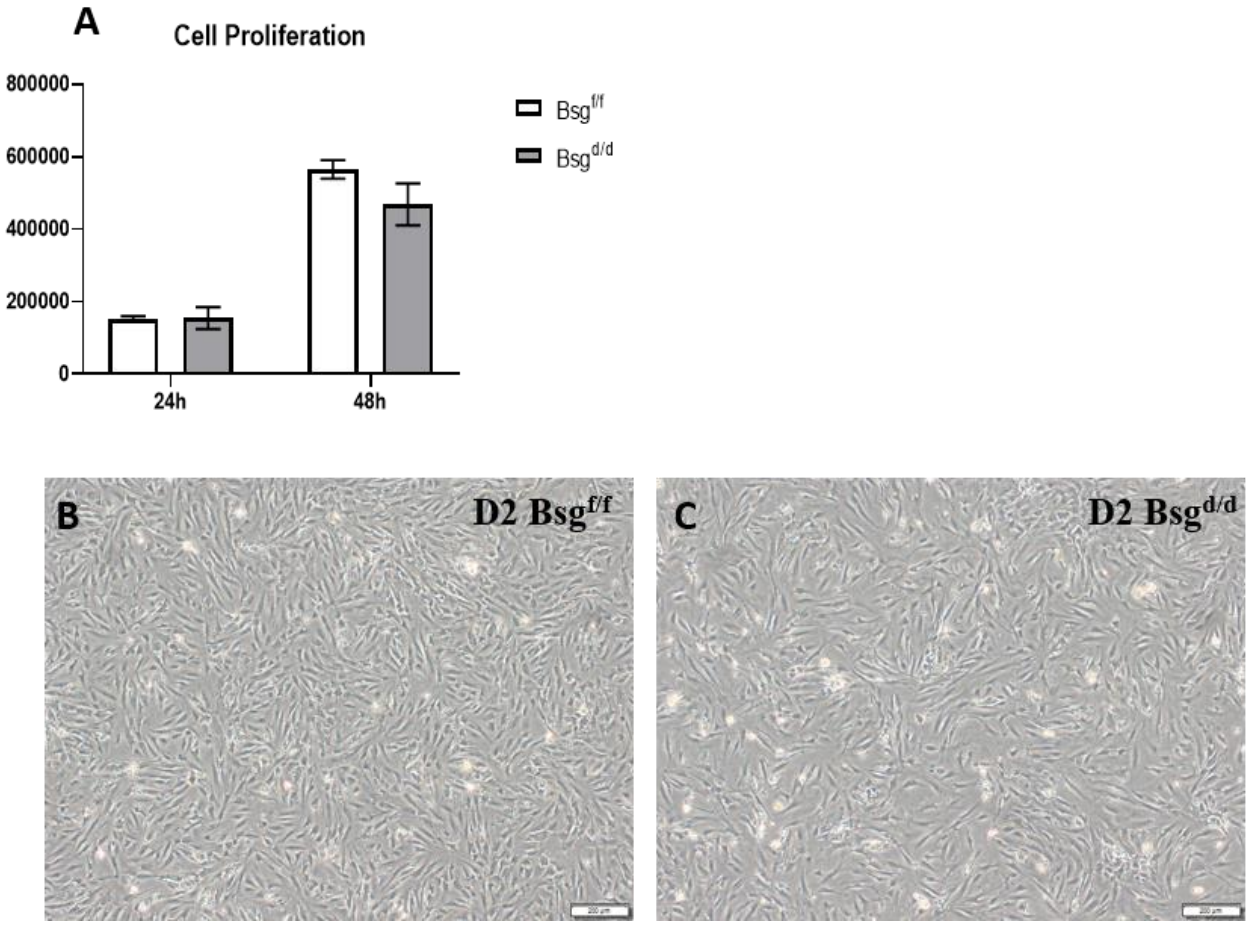

Figure 5.1 MESCs proliferation. A: number of MESCs at 24 hours and 48 hours of incubation. B and C: representative images of MESC of a control mouse (left) and a cKO mouse (right) on day 2 of culture. N=4 for each genotype.

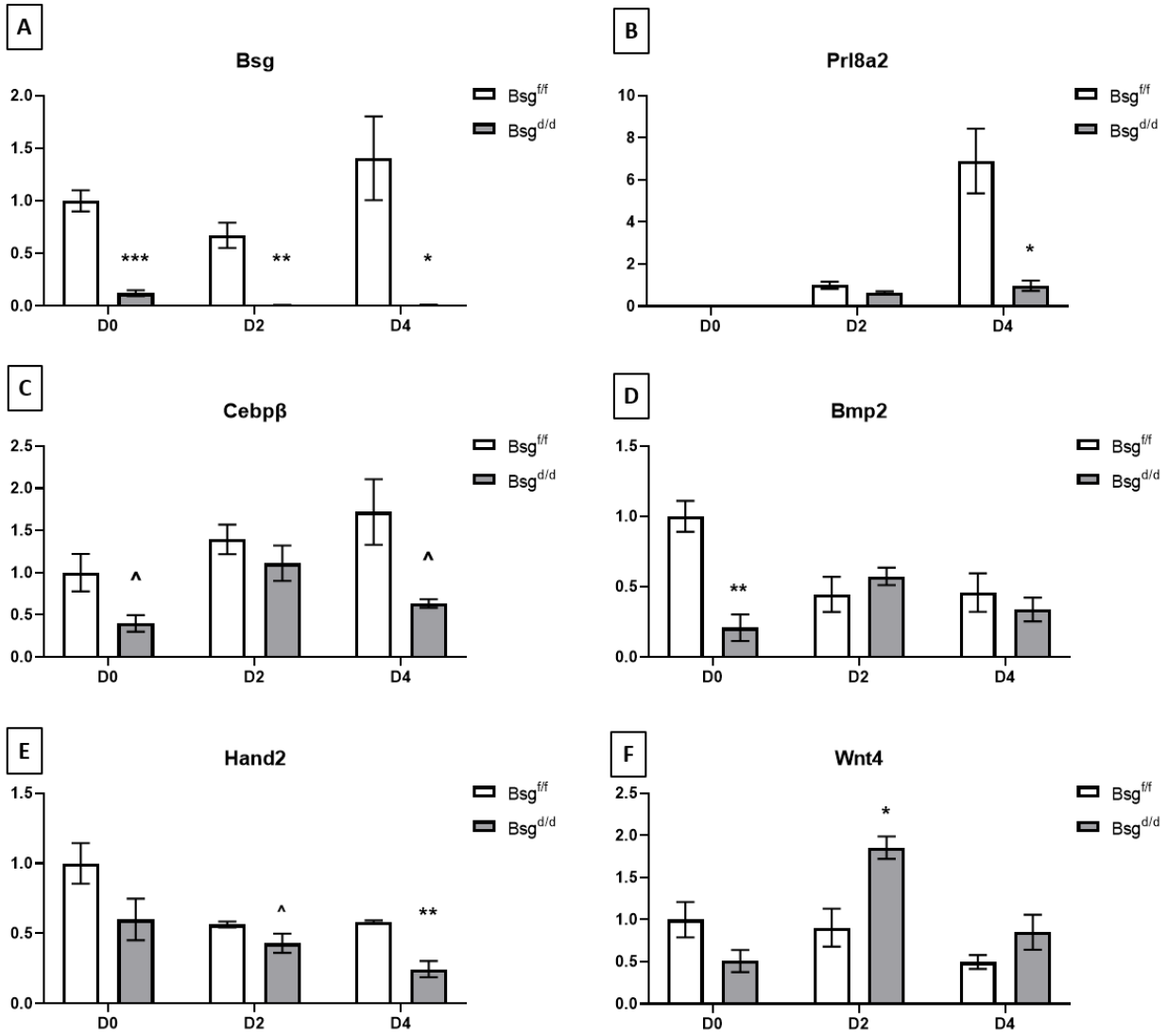

Figure 5.2 Decidualization marker expression levels in the MESCs from D0-D4. qRT-PCR gene expression levels of *Bsg* (A), *Prl8a2* (B), *Cebpβ* (C), *Bmp2* (D), *Hand2* (E) and *Wnt4* (F) in the MESCs from the control mice (white bars) and the cKO mice (grey bars) from cell culture day 0 to day 4. N=4 for each genotype.

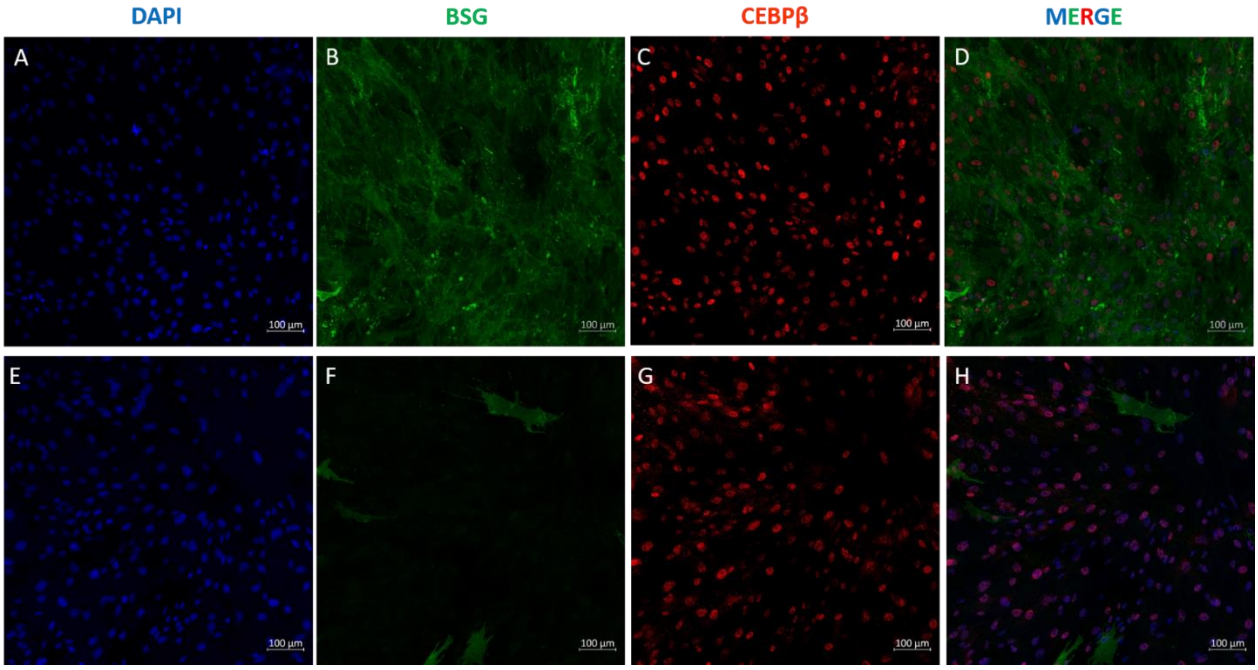

Figure 5.3 CEBPβ localization in MESCs. Localization of BSG (green) and CEBPβ in MESCs of a control mouse (top panel) and a cKO mouse (bottom panel).

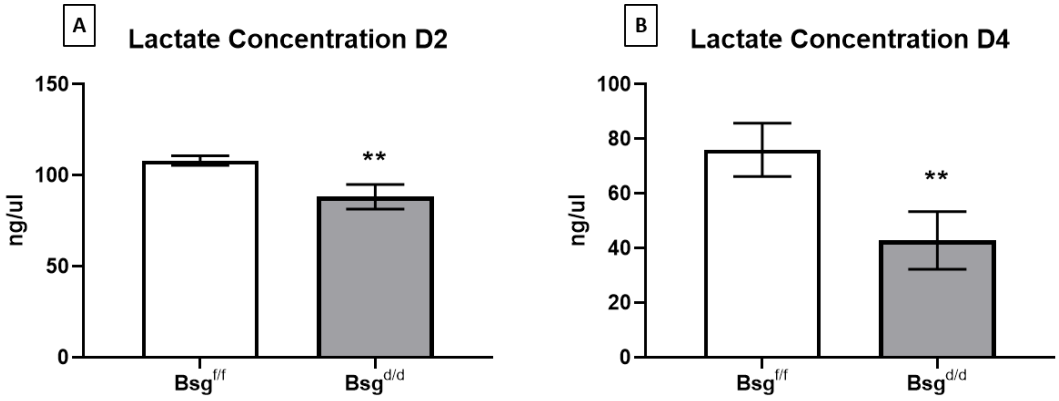

Figure 5.4 MESCs lactate production on day 2 and day 4. Lactate concentrations in the medium of the MESCs from the control mice (white) and the cKO mice (grey) on day 2 (A) and day 4 (B) of culture under normal oxygen level. N=4 for each genotype.

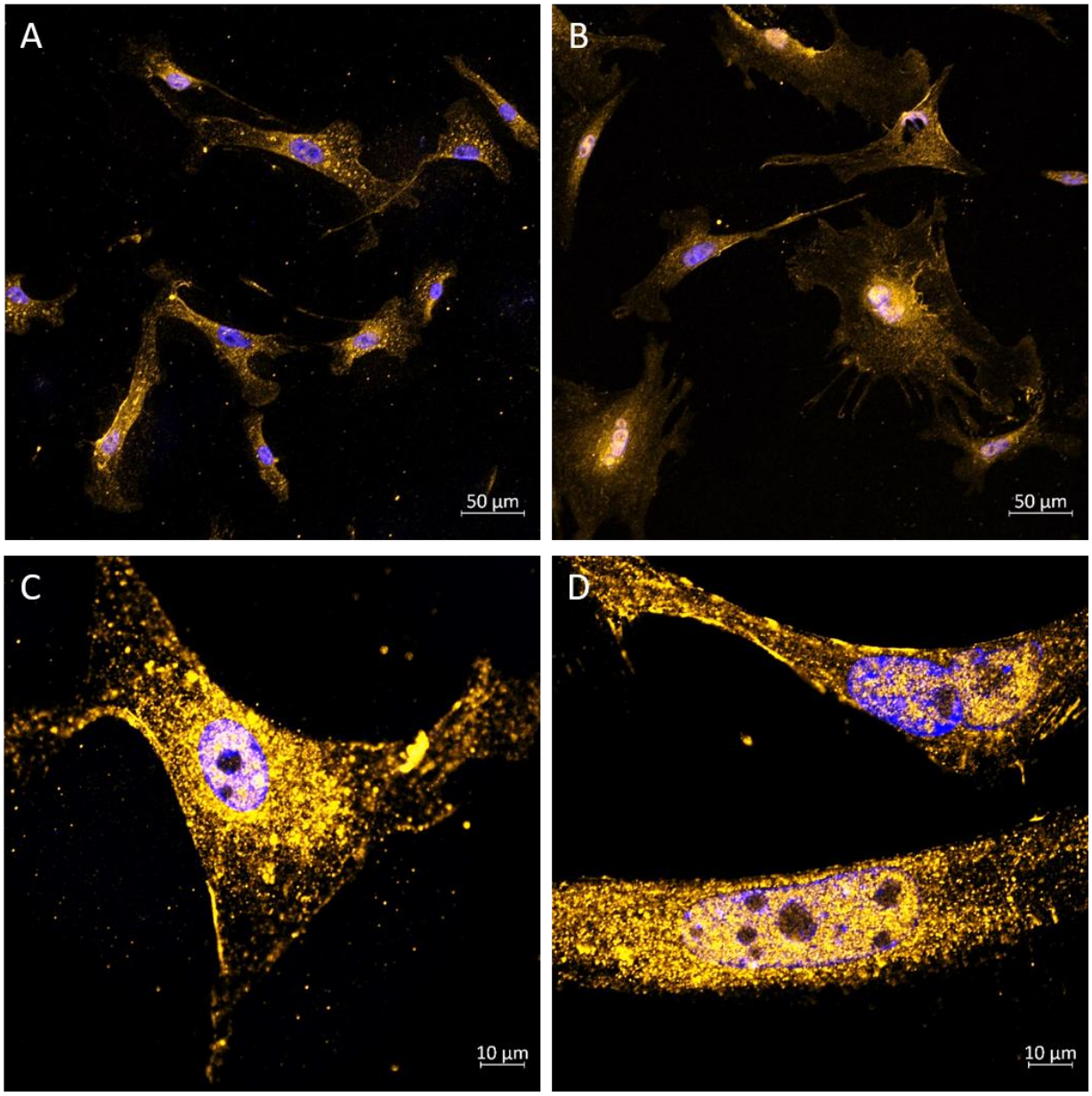

Figure 5.5 MMP9 protein localization in the MESCs. MMP9 protein abundance in the MESCs. MMP9 (orange) abundance in the MESCs of a control mouse (A and C) and a cKO mouse (B and D) at low and high magnification, respectively.

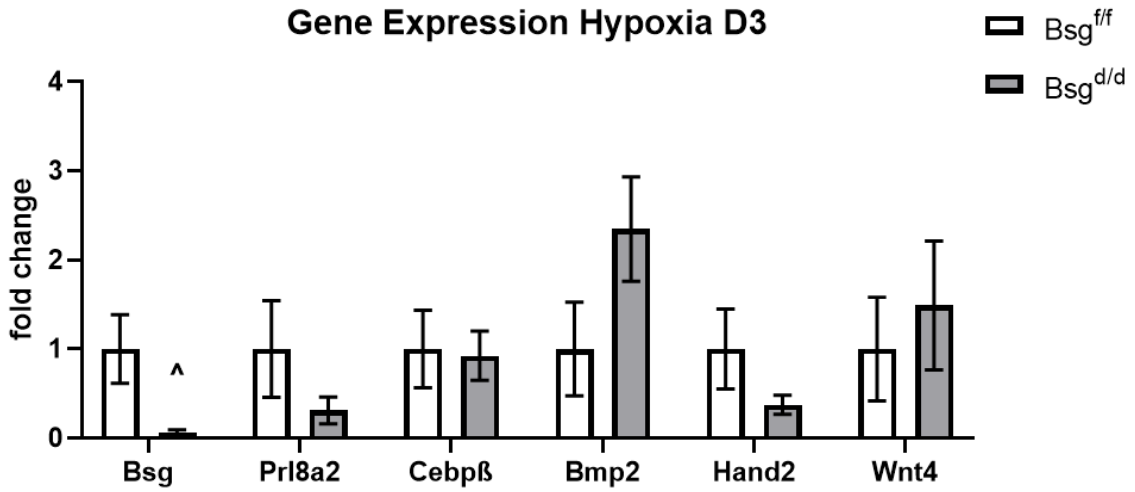

Figure 5.6 Decidualization marker expression levels under hypoxic condition in the MESCs. qRT-PCR gene expression levels of *Bsg*, *Prl8a2*, *Cebpβ*, *Bmp2*, *Wn4* and *Hand2* in the MESCs from the control mice (white) and the cKO mice (grey) on day 3 of culture under hypoxic condition. N=4 for each genotype.

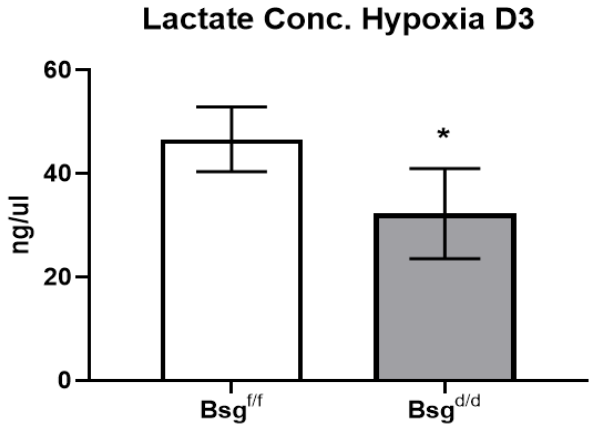

Figure 5.7 Lactate production under hypoxic condition. The lactate concentrations produced by the MESCs from the control mice (white bar) and the cKO mice (grey bar) on day 3 under hypoxic conditions. N=4 for each genotype.

References

Anumba, Dilly OC, Saad El Gelany, Sarah L Elliott, and Tin C Li. 2010. "Circulating Levels of Matrix Proteases and Their Inhibitors in Pregnant Women with and without a History of Recurrent Pregnancy Loss." *Reproductive Biology and Endocrinology* 8 (1): 62. https://doi.org/10.1186/1477-7827-8-62.

Bagchi, Milan K., Srinivasa R. Mantena, Athilakshmi Kannan, and Indrani C. Bagchi. 2006. "Control of Uterine Cell Proliferation and Differentiation by C/EBPβ: Functional Implications for Establishment of Early Pregnancy." *Cell Cycle*. Taylor and Francis Inc. https://doi.org/10.4161/cc.5.9.2712.

Bi, Jiajia. 2013. "EXPRESSION AND FUNCTION OF BASIGIN DURING EARLY PREGNANCY AND SPERMATOGENESIS."

Bi, Jiajia, Yanfen Li, Fengyun Sun, Anja Saalbach, Claudia Klein, David J. Miller, Rex Hess, and Romana A. Nowak. 2013. "Basigin Null Mutant Male Mice Are Sterile and Exhibit Impaired Interactions between Germ Cells and Sertoli Cells." *Developmental Biology* 380 (2): 145–56. https://doi.org/10.1016/j.ydbio.2013.05.023.

Bombail, Vincent, Douglas A. Gibson, Frances Collins, Sheila MacPherson, Hilary O.D. Critchley, and Philippa T.K. Saunders. 2010. "A Role for the Orphan Nuclear Receptor Estrogen-Related Receptor α in Endometrial Stromal Cell Decidualization and Expression of Genes Implicated in Energy Metabolism." *Journal of Clinical Endocrinology and Metabolism* 95 (10). https://doi.org/10.1210/jc.2010-0154.

Braundmeier, A. G., A. T. Fazleabas, B. A. Lessey, H. Guo, B. P. Toole, and R. A. Nowak. 2006. "Extracellular Matrix Metalloproteinase Inducer Regulates Metalloproteinases in Human Uterine Endometrium." *Journal of Clinical Endocrinology and Metabolism* 91 (6): 2358–65. https://doi.org/10.1210/jc.2005-0601.

Cha, Jeeyeon, Xiaofei Sun, and Sudhansu K. Dey. 2012. "Mechanisms of Implantation: Strategies for Successful Pregnancy." *Nature Medicine*. Nature Publishing Group. https://doi.org/10.1038/nm.3012.

Chen, Li. 2006. "Expression and Function of Basigin during Implantation in the Mouse." university of illinois.

Chen, Li, Robert J. Belton, and Romana a. Nowak. 2009. "Basigin-Mediated Gene Expression Changes in Mouse Uterine Stromal Cells during Implantation." *Endocrinology* 150 (2): 966–76. https://doi.org/10.1210/en.2008-0571.

Chen, Li, Jiajia Bi, Masaaki Nakai, David Bunick, John F. Couse, Kenneth S. Korach, and Romana Nowak. 2010. "Expression of Basigin in Reproductive Tissues of Oestrogen Receptor Alpha or Beta Null Mice." *Reproduction* 139 (6): 1507–1066. https://doi.org/10.1007/s10741-014-9462-7.Natural.

Chen, Li, Masaaki Nakai, Robert J. Belton, and Romana A. Nowak. 2007. "Expression of Extracellular Matrix Metalloproteinase Inducer and Matrix Metalloproteinases during Mouse

Embryonic Development." *Reproduction (Cambridge, England)* 133 (2): 405–14. https://doi.org/10.1530/rep.1.01020.

Cheng, Jr Gang, Jim Ray Chen, Lidia Hernandez, W. Greg Alvord, and Colin L. Stewart. 2001. "Dual Control of LIF Expression and LIF Receptor Function Regulate Stat3 Activation at the Onset of Uterine Receptivity and Embryo Implantation." *Proceedings of the National Academy of Sciences of the United States of America* 98 (15): 8680–85. https://doi.org/10.1073/pnas.151180898.

Clementi, C, S K Tripurani, M J Large, M A Edson, and C J Creighton. 2013. "Activin-Like Kinase 2 Functions in Peri-Implantation Uterine Signaling in Mice and Humans." *PLoS Genet* 9 (11): 1003863. https://doi.org/10.1371/journal.pgen.1003863.

Clough, J. R., and D. G. Whittingham. 1983. "Metabolism of [14C]Glucose by Postimplantation Mouse Embryos in Vitro." *Journal of Embryology and Experimental Morphology* Vol. 74: 133–42.

Conneely, Orla M., Biserka Mulac-Jericevic, and John P. Lydon. 2003. "Progesterone-Dependent Regulation of Female Reproductive Activity by Two Distinct Progesterone Receptor Isoforms." *Steroids* 68 (10–13): 771–78. https://doi.org/10.1016/S0039-128X(03)00126-0.

Croy, B. Anne, Zhilin Chen, Alexander P. Hofmann, Edith M. Lord, Abigail L. Sedlacek, and Scott A. Gerber. 2012. "Imaging of Vascular Development in Early Mouse Decidua and Its Association with Leukocytes and Trophoblasts1." *Biology of Reproduction* 87 (5): 1–11. https://doi.org/10.1095/biolreprod.112.102830.

Das, Sanjoy K. 2009. "Cell Cycle Regulatory Control for Uterine Stromal Cell Decidualization in Implantation." *Reproduction* 137 (6): 889–99. https://doi.org/10.1530/REP-08-0539.

Davidson, Ben, Vered Givant-Horwitz, Philip Lazarovici, Björn Risberg, Jahn M. Nesland, Claes G. Trope, Erik Schaefer, and Reuven Reich. 2003. "Matrix Metalloproteinases (MMP), EMMPRIN (Extracellular Matrix Metalloproteinase Inducer) and Mitogen-Activated Protein Kinases (MAPK): Co-Expression in Metastatic Serous Ovarian Carcinoma." *Clinical and Experimental Metastasis* 20 (7): 621–31. https://doi.org/10.1023/A:1027347932543.

Fischer, B., and B. D. Bavister. 1993. "Oxygen Tension in the Oviduct and Uterus of Rhesus Monkeys, Hamsters and Rabbits." *Journal of Reproduction and Fertility* 99 (2): 673–79. https://doi.org/10.1530/jrf.0.0990673.

Floch, R. Le, J. Chiche, I. Marchiq, T. Naiken, K. Ilc, C. M. Murray, S. E. Critchlow, et al. 2011. "CD147 Subunit of Lactate/H+ Symporters MCT1 and Hypoxia-Inducible MCT4 Is Critical for Energetics and Growth of Glycolytic Tumors." *Proceedings of the National Academy of Sciences* 108 (40): 16663–68. https://doi.org/10.1073/pnas.1106123108.

Gardner, David K. 2015. "Lactate Production by the Mammalian Blastocyst: Manipulating the Microenvironment for Uterine Implantation and Invasion?" *BioEssays* 37 (4): 364–71. https://doi.org/10.1002/bies.201400155.

Gellersen, B, K Reimann, A Samalecos, S Aupers, and A.-M Bamberger. 2010. "Invasiveness of Human Endometrial Stromal Cells Is Promoted by Decidualization and by Trophoblast-Derived Signals." *Human Reproduction* 25 (4): 862–73.

https://doi.org/10.1093/humrep/dep468.

Grass, G Daniel, and P Bryan. 2016. “How , with Whom and When : An Overview of CD147-Mediated Regulatory Networks Influencing Matrix Metalloproteinase Activity.” *Biosci. Rep.*, 1–16. https://doi.org/10.1042/BSR20150256.

Guindolet, Damien, and Gabison Eric. 2019. “Role of CD147 (EMMPRIN/Basigin) in Tissue Remodeling.” *The Anatomical Record*. https://onlinelibrary.wiley.com/doi/pdf/10.1002/ar.24089.

Guo, Yong, Bin He, Xiangbo Xu, and Jiedong Wang. 2011. “Comprehensive Analysis of Leukocytes, Vascularization and Matrix Metalloproteinases in Human Menstrual Xenograft Model.” Edited by Haibin Wang. *PLoS ONE* 6 (2): e16840. https://doi.org/10.1371/journal.pone.0016840.

Halestrap, Andrew P. 2012. “The Monocarboxylate Transporter Family-Structure and Functional Characterization.” *IUBMB Life* 64 (1): 1–9. https://doi.org/10.1002/iub.573.

Hasaneen, Nadia A., Jian Cao, Ashleigh Pulkoski-Gross, Stanley Zucker, and Hussein D. Foda. 2016. “Extracellular Matrix Metalloproteinase Inducer (EMMPRIN) Promotes Lung Fibroblast Proliferation, Survival and Differentiation to Myofibroblasts.” *Respiratory Research* 17 (1): 17. https://doi.org/10.1186/s12931-016-0334-7.

Igakura, Tadahiko, Kenji Kadomatsu, Tadashi Kaname, Hisako Muramatsu, Qi Wen Fan, Teruo Miyauchi, Yoshiro Toyama, et al. 1998. “A Null Mutation in Basigin, an Immunoglobulin Superfamily Member, Indicates Its Important Roles in Peri-Implantation Development and Spermatogenesis.” *Developmental Biology* 194 (2): 152–65. https://doi.org/10.1006/dbio.1997.8819.

Kannan, Athilakshmi, Asgerally T. Fazleabas, Indrani C. Bagchi, and Milan K. Bagchi. 2010. “The Transcription Factor C/EBPβ Is a Marker of Uterine Receptivity and Expressed at the Implantation Site in the Primate.” *Reproductive Sciences* 17 (5): 434–43. https://doi.org/10.1177/1933719110361384.

Kirk, P, M C Wilson, C Heddle, M H Brown, a N Barclay, and a P Halestrap. 2000. “CD147 Is Tightly Associated with Lactate Transporters MCT1 and MCT4 and Facilitates Their Cell Surface Expression.” *The EMBO Journal* 19 (15): 3896–3904. https://doi.org/10.1093/emboj/19.15.3896.

Knutti, Nadine, Michael Kuepper, and Karlheinz Friedrich. 2015. “Soluble Extracellular Matrix Metalloproteinase Inducer (EMMPRIN, EMN) Regulates Cancer-Related Cellular Functions by Homotypic Interactions with Surface CD147.” *FEBS Journal* 282 (21): 4187–4200. https://doi.org/10.1111/febs.13414.

Kong, Sue, Bruce J Aronow, and Stuart Handwerger. 2006. “Gene Expression Microarray Data Analysis of Decidual and Placental Cell Differentiation.” In *Methods in Molecular Medicine*, 121:425–38.

Li, Kailiang, and Romana A Nowak. 2019. “The Role of Basigin in Reproduction.” *Reproduction (Cambridge, England)*, September. https://doi.org/10.1530/REP-19-0268.

Li, Ling, Wenhua Tang, Xiaoqing Wu, David Karnak, Xiaojie Meng, Rachel Thompson, Xinbao

Hao, et al. 2013. “HAb18G/CD147 Promotes PSTAT3-Mediated Pancreatic Cancer Development via CD44s.” *Clinical Cancer Research* 19 (24): 6703–15. https://doi.org/10.1158/1078-0432.CCR-13-0621.

Marchiq, Ibtissam, Jean Albrengues, Sara Granja, Cédric Gaggioli, and Marie-pierre Simon. 2015. “Knock out of the BASIGIN / CD147 Chaperone of Lactate / H + Symporters Disproves Its pro-Tumour Action via Extracellular Matrix Metalloproteases (MMPs) Induction.” *Oncotarget* 2015 (28): 1–14. https://doi.org/10.18632/oncotarget.4323.

Monsivais, Diana, Caterina Clementi, Jia Peng, Mary M. Titus, James P. Barrish, Chad J. Creighton, John P. Lydon, Francesco J. DeMayo, and Martin M. Matzuk. 2016. “Uterine ALK3 Is Essential during the Window of Implantation.” *Proceedings of the National Academy of Sciences* 113 (3): E387–95. https://doi.org/10.1073/pnas.1523758113.

Nabeshima, Kazuki, Hiroshi Iwasaki, Kaori Koga, Hironobu Hojo, Junji Suzumiya, and Masahiro Kikuchi. 2006. “Emmprin (Basigin/CD147): Matrix Metalloproteinase Modulator and Multifunctional Cell Recognition Molecule That Plays a Critical Role in Cancer Progression.” *Pathology International* 56 (7): 359–67. https://doi.org/10.1111/j.1440-1827.2006.01972.x.

Nagai, A., K. Takebe, J. Nio-Kobayashi, H. Takahashi-Iwanaga, and T. Iwanaga. 2010. “Cellular Expression of the Monocarboxylate Transporter (MCT) Family in the Placenta of Mice.” *Placenta* 31 (2): 126–33. https://doi.org/10.1016/j.placenta.2009.11.013.

Peng, Sha, Jing Li, Chenglin Miao, Liwei Jia, Zeng Hu, Ping Zhao, Juxue Li, Ying Zhang, Qi Chen, and Enkui Duan. 2008. “Dickkopf-1 Secreted by Decidual Cells Promotes Trophoblast Cell Invasion during Murine Placentation.” *Reproduction* 135 (3): 367–75. https://doi.org/10.1530/REP-07-0191.

Shahbazi, Marta N., Agnieszka Jedrusik, Sanna Vuoristo, Gaelle Recher, Anna Hupalowska, Virginia Bolton, Norah M.E. Fogarty, et al. 2016. “Self-Organization of the Human Embryo in the Absence of Maternal Tissues.” *Nature Cell Biology* 18 (6): 700–708. https://doi.org/10.1038/ncb3347.

Sharkey, Andrew M., and Stephen K. Smith. 2003. “The Endometrium as a Cause of Implantation Failure.” *Best Practice and Research: Clinical Obstetrics and Gynaecology* 17 (2): 289–307. https://doi.org/10.1016/S1521-6934(02)00130-X.

Sidhu, S S, R Nawroth, M Retz, H Lemjabbar-Alaoui, V Dasari, and C Basbaum. 2010. “EMMPRIN Regulates the Canonical Wnt/Beta-Catenin Signaling Pathway, a Potential Role in Accelerating Lung Tumorigenesis.” *Oncogene* 29 (29): 4145–56. https://doi.org/10.1038/onc.2010.166.

Sun, Jianxin, and Martin E Hemler. 2001. “Regulation of MMP-1 and MMP-2 Production through CD147 / Extracellular Matrix Metalloproteinase Inducer Interactions Regulation of MMP-1 and MMP-2 Production through CD147 / Extracellular Matrix.” *Cancer Research* 61: 2276–81.

Tang, Yi, Marian T Nakada, Prabakaran Kesavan, Francis Mccabe, Hillary Millar, Patricia Rafferty, Peter Bugelski, and Li Yan. 2005. “Extracellular Matrix Metalloproteinase Inducer Stimulates Tumor Angiogenesis by Elevating Vascular Endothelial Cell Growth Factor and

Matrix Metalloproteinases." http://www.raybiotech.com.

Tsai, Jui-He, Maggie M-Y Chi, Maureen B Schulte, and Kelle H Moley. 2014. "The Fatty Acid Beta-Oxidation Pathway Is Important for Decidualization of Endometrial Stromal Cells in Both Humans and Mice 1." *BIOLOGY OF REPRODUCTION* 90 (2): 1–12. https://doi.org/10.1095/biolreprod.113.113217.

Wang, Haibin, Shuang Zhang, Haiyan Lin, Shuangbo Kong, Shumin Wang, Hongmei Wang, and D. Randall Armant. 2013. "Physiological and Molecular Determinants of Embryo Implantation." *Molecular Aspects of Medicine* 34 (5): 939–80. https://doi.org/10.1016/j.mam.2012.12.011.

Wang, Wei, Robert N. Taylor, Indrani C. Bagchi, and Milan K. Bagchi. 2012. "Regulation of Human Endometrial Stromal Proliferation and Differentiation by C/EBPβ Involves Cyclin E-Cdk2 and STAT3." *Molecular Endocrinology* 26 (12): 2016–30. https://doi.org/10.1210/me.2012-1169.

Wang, Xiaohong, Hiromichi Matsumoto, Xuemei Zhao, Sanjoy Das, and Bibhash Paria. 2004. "Embryonic Signals Direct the Formation of Tight Junctional Permeability Barrier in the Decidualizing Stroma during Embryo Implantation." *Journal of Cell Science* 117 (1): 53–62. https://doi.org/10.1242/jcs.00826.

Weidle, Ulrich H., Werner Scheuer, Daniela Eggle, Stefan Klostermann, and Hannes Stockinger. 2010. "Cancer-Related Issues of CD147." *Cancer Genomics and Proteomics* 7 (3): 157–69.

Welsh, Alerick O., and Allen C. Enders. 1987. "Trophoblast-decidual Cell Interactions and Establishment of Maternal Blood Circulation in the Parietal Yolk Sac Placenta of the Rat." *The Anatomical Record* 217 (2): 203–19. https://doi.org/10.1002/ar.1092170213.

Wetendorf, Margeaux, and Francesco J. DeMayo. 2012. "The Progesterone Receptor Regulates Implantation, Decidualization, and Glandular Development via a Complex Paracrine Signaling Network." *Molecular and Cellular Endocrinology* 357 (1–2): 108–18. https://doi.org/10.1016/j.mce.2011.10.028.

Xiong, Lijuan, Carl Edwards, and Lijun Zhou. 2014. "The Biological Function and Clinical Utilization of CD147 in Human Diseases: A Review of the Current Scientific Literature." *International Journal of Molecular Sciences* 15 (10): 17411–41. https://doi.org/10.3390/ijms151017411.

Zhu, Ha, Cong Cong Hou, Ling Feng Luo, Yan Jun Hu, and Wan Xi Yang. 2014. "Endometrial Stromal Cells and Decidualized Stromal Cells: Origins, Transformation and Functions." *Gene*. Elsevier. https://doi.org/10.1016/j.gene.2014.08.047.

CHAPTER SIX

Summary and Future Directions

Summary

The overall goal of this doctoral dissertation work was to investigate the role of uterine basigin (BSG) in early reproduction in female mice. Implantation is the process where the blastocyst attaches to the maternal endometrium. It is a complex event delicately orchestrated by steroid hormones, cytokines, adhesion molecules, developmental transcription factors and cell cycle regulators. Proper implantation is a prerequisite for successful pregnancy and a poor-quality implantation causes adverse ripple effects in the later course of pregnancy. BSG is a cell membrane glycoprotein expressed in many tissues, including the reproductive organs, and is important for fertility in both males and females. However, studies on BSG have been complicated due to the high embryonic lethality in the *Bsg* global knockout mouse model. Therefore, in this dissertation, we generated a tissue specific *Bsg* knockout mouse model to study the role of BSG in female reproduction in mice. Using this improved animal model, I was able to investigate the hypotheses and aims. This doctoral dissertation work provided insights into the role of BSG in early pregnancy in mice to further advance our understanding of the mechanisms of implantation. Collectively, these studies show that loss of uterine BSG leads to subfertility and BSG is required for normal implantation and decidualization in mice.

In Chapter Three, I generated and validated the *Bsg* cKO mouse model. I was able to generate the cKO mouse model by using the progesterone receptor (PR)-Cre and lox method to delete *Bsg* in the PR positive cells. I crossed the BSG FF and PR Cre +/- male mice with the BSG FF and PR +/+ female mice to produce pups. The genotype of the pups was determined by PCR.

The BSG FF and PR Cre +/- mice are the cKO mice and the BSG FF and PR +/+ mice are the littermate controls. The successful ablation of BSG in the reproductive tissues was confirmed by quantitative real time PCR (qRT-PCR) and histology. The qRT-PCR results showed that the mRNA level of *Bsg* in the uteri of the cKO mice was significantly decreased compared to the controls. The histology results also confirmed that BSG was no longer in the PR positive cells in the uteri and oviduct of the cKO mice. In addition, the cKO mice still expressed BSG in the kidney, indicating the knockout was indeed PR positive cell specific.

I also undertook investigation of the fertility phenotype of the cKO mice in Chapter Three. I hypothesized that loss of BSG in the uterus would lead to infertility or subfertility in the mice. The six-month breeding study results showed that the cKO females had significantly reduced fertility compared to the controls. The cKO mice had much smaller litter size and litter frequency. There were more dead pups at parturition and higher incidence of dystocia in the cKO females. The fertility of the cKO mice decreased more severely as they aged compared to the controls. There was no difference in the weight or sex ratio of the pups between the two genotypes.

After demonstrating the subfertility caused by knocking out uterine BSG, I wanted to determine when and where the problems were occurring in the cKO mice. In Chapter Three, I eliminated the possibility of ovarian failures and identified uterine defects as the cause of subfertility in the cKO mice. Histology of the ovarian morphology revealed similar structures between the two genotypes. The superovulation results showed there was no difference in the number of oocytes ovulated by the females of both genotypes. They also produced the same levels of progesterone on day 4 of pregnancy. Therefore, the cKO mice had normal ovulation and steroidogenesis. The uterine horns of both genotypes were flushed to collect embryos on day 4 of pregnancy, and the results showed no difference in the number of embryos retrieved from the

control or cKO mice. Most of the embryos were fertilized and at the blastocyst stage, indicating fertilization and early embryo development were not affected in the cKO females. These results together suggested that the subfertility originated from a uterine defect. To determine the timing of the problems, I euthanized mice at different times of gestation from day 4 to day 15 and discovered pregnancy defects throughout gestation in the uteri of the cKO mice. Some females had no implantations; some had abnormal implantation such as fewer implantation sites, crowded implantation sites or smaller implantation chambers. At later stages of pregnancy, at days 12 and 15, the cKO females showed increased embryo resorption, intrauterine growth restriction and hemorrhage in the uteri on day 12 and day15 of pregnancy. The pregnancy status results showed that many more of the cKO females had implantation failure or abnormal pregnancy compared to the controls.

In Chapter Four, I examined the luminal epithelial cell integrity in the cKO females *in vivo* after identifying the uterus as the origin of the fertility problem. I hypothesized that BSG is required for normal implantation in mice. The immunohistochemistry (IHC) and immunofluorescence (IF) results showed that in many of the cKO mice, the embryos were not able to breach the luminal epithelium in the uteri on day 5 of pregnancy. There was still strong abundance of E-cadherin at the site of implantation in the cKO uteri, compared to the loss of E-cadherin in the control uteri. Similar results were observed in cytokeratin abundance in the luminal epithelial cells. These suggest that the embryos in the cKO females were restricted in the uterine lumen, and not able to penetrate through the luminal epithelium. Subsequently, I investigated the integrity of the basement membrane in the cKO mice using Jones' silver stain. The results showed that, in some of the cKO mice, the basement membrane was still intact, indicating the embryos in

the cKO mice were not able to penetrate the basement membrane and invade into the endometrial stromal cells. These results showed about 70% of mice examined had implantation failures.

In Chapter Four, I also investigated the role of BSG in decidualization *in vivo* and formulated the hypothesis that BSG is necessary for proper decidualization in mice. To test my hypothesis, I conducted an artificially induced decidualization response (ADR) experiment by ovariectomizing the mice, supplementing them with hormones and then stimulating the decidual response by injection of corn oil into one of the uterine horns. The results showed that while the controls had a robust decidual response, the cKO mice only had a modest response or no response to the stimuli. The total uterine weight was also significantly lower in the cKO females. There was no difference in the body weight between the two genotypes, indicating the decreased uterine weight and injected uterine weight in the cKO mice were due to an impaired decidual response. Histology analysis showed that the cross-sections of the decidua were much smaller in the cKO mice. qRT-PCR results on the expression levels of several decidualization marker genes showed that *Cebpβ* and *Bmp2* were significantly downregulated in the cKO mice compared to the controls. IHC results also showed that CEBPβ and HAND2 protein levels were markedly lower in the cKO mice compared to the controls. This indicates that BSG is possibly involved in the Bmp2-Alk2-Cebpβ-Stat3 pathway to regulate decidualization in mice.

In addition, I investigated additional post-implantation defects in angiogenesis and lactate transport in the cKO females. To achieve this, I examined the localization of a few proteins that are known to interact with BSG and play a role in metabolism and angiogenesis. CD98 is found on the apical side of the luminal epithelium at the time of implantation, and it interacts with BSG to form amino acid transporters to function in energy metabolism. The IHC results for CD98 on the uteri of day 1 and day 4 of pregnancy showed no difference in the protein abundance and

localization of CD98 in the cKO mice compared to the controls. BSG is a chaperon protein for MCT1/4 and is required for shuttling these MCTs to the cell membrane, where they function as lactate transporters. MCT1 protein was decreased in the cKO mouse uteri on day 4 and 6 of pregnancy compared to the controls, possibly leading to a difference in lactate transport in the cKO mice. To investigate the effect of loss of BSG on angiogenesis, I immunostained uterine cross-sections of day 6 pregnant mice for the angiogenic marker CD31. The results showed greatly reduced CD31 abundance in the endothelial cells in the secondary decidual zone and the undifferentiated stromal layer in the cKO mice compared the controls. Quantification of the CD31 signal intensity confirmed significantly lower CD31 levels in the cKO, indicating loss of uterine BSG leads to reduced angiogenesis in mice.

In Chapter Five, I examined the role of BSG in decidualization using an *in vitro* system. I hypothesized that BSG is required for normal decidualization *in vitro*. To test my hypothesis, I isolated the endometrial stromal cells (MESCs) from mice of both genotypes and set up a primary cell culture system. Decidualization involves extensive proliferation and then terminal differentiation. I first determined whether BSG played a role in cell proliferation in these MESCs by culturing the cells for 48 hours. The cell numbers were the same between the cKO MESCs and control MESCs at 24 and 48 hours of culture, indicating BSG does not affect cell proliferation over this time period *in vitro*. The mRNA was extracted from cultured cells to determine the expression levels of several decidualization markers over a four-day cell culture period. The qRT-PCR results showed that *Bsg* level was significantly lower in the cKO MESCs, as expected. In the controls, *Prl8a2* and *Cebpβ* levels increased over time, while *Bmp2* and *Hand2* levels decreased over the four days. In the cKO MESCs, the levels of *Prl8a2*, *Cebpβ*, *Bmp2* and *Hand2* were all significantly downregulated at some point compared to the controls. These results agree with the

in vivo decidualization results. MMP9 protein abundance and localization did not appear to be affected in the cKO MESCs. These findings indicate that the loss of BSG in the MESCs leads to suppression in decidualization *in vitro*.

I also investigated whether BSG plays a role in regulating lactate transport *in vitro* in Chapter Five and hypothesized that loss of BSG would lead to altered lactate secretion by the MESCs. To investigate my hypothesis, I cultured the MESCs of both genotypes for four days and collected the cell medium to measure the lactate concentrations in the medium. The results showed that on both day 2 and day 4, the lactate concentrations in the medium of the cKO MESCs were markedly lower compared to the controls. In addition, I also incubated the cells under the hypoxic conditions for three days to mimic the low oxygen environment in the uterus during implantation. The results showed that the expression levels of the decidualization markers did not differ in either genotype, but the lactate concentrations in the medium of cKO MESCs were significantly lower than the control MESCs. These findings suggest that BSG is required for normal lactate secretion in the MESCs.

Based on the studies demonstrated in this dissertation, I propose a model for the potential roles of BSG in early pregnancy in mice in **Figure 6.1**. BSG is involved in normal events during implantation such as the luminal epithelium breakdown and basement membrane degradation. BSG regulates *Bmp2* and *Cebpβ* and may act through the Bmp2-Alk2-Cebpβ-Stat3 pathway to promote decidualization in mice. BSG also controls *Hand2* expression in regulating decidualization. In addition, BSG appears to regulate angiogenesis at the implantation sites and MCT1 for lactate transport post-implantation. The loss of BSG dysregulates the early events of implantation and decidualization, causing adverse ripple effects that leads to increased incidence

of complications in later stages of pregnancy, such as hemorrhage, embryo resorption and dystocia, and eventually results in subfertility in mice.

Future Directions

Despite the findings presented in this dissertation; many additional questions need to be investigated to better elucidate the comprehensive role of BSG in regulating implantation and pregnancy. I would propose a few questions for future directions. First, additional novel genes and signaling pathways need to be examined for understanding the functions of BSG in implantation and decidualization. For example, the gene expression levels of *Alk2* and *Stat3* should be evaluated to confirm that BSG indeed act through this pathway to regulate decidualization. Further, it is important to determine whether BSG regulates early differentiation or late phase of decidualization. The ADR and *in vitro* MESC decidualization experiments could be repeated with longer experimental period and more collection time points. More marker genes of either early or late decidualization should be examined. The mechanisms underlying the problems with the breaching of the luminal epithelium in the cKO mice at the time of implantation remains unclear. Whether BSG is involved in facilitating apoptosis in these luminal epithelial cells needs to be studied. The degradation of the basement membrane is mediated by MMPs, which can be induced by BSG. Although I did not observe any differences in the abundance of MMP9 in the cKO mice, it is important to better quantify the abundance of MMP9 and other MMPs, such as MMP2 and MMP3. Immunoblotting and ELISA are recommended because MMPs are secreted proteins. Second, BSG has been found in microvesicles and exosomes and can transmit signals through microvesicle shedding. Thus, it would be important to collect the serum free medium of MESCs and isolate the extracellular vesicles. Determining whether the microvesicles from stromal or

epithelial cells of cKO mice contain BSG by immunoblotting would provide useful information. Third, it is worth repeating the hypoxic cell culture experiments with more time points and replicates because it is helpful to better understand the impact of hypoxic conditions on decidualization and lactate production. Fourth, BSG is found in the placental trophoblast cells and the endothelial cells in humans and mice. Lower abundance of BSG in the placenta is associated with preeclampsia in humans and the underlying mechanisms remain unknown. Thus, further investigations on the role of BSG in placenta development and later stages of pregnancy would be valuable.

There are limitations using this PR-Cre model to study the role of BSG in the uterus. First, PR-Cre did not show very high efficiency of recombination. Secondly PR-Cre deletes *Bsg* in the epithelium, stroma and myometrium of the uterus, thus making it difficult to determine the cell type-specific function of *Bsg*. Other Cre mouse lines may be useful to distinguish the function of *Bsg* in a specific cell type. For example, Wnt7a-Cre deletes gens in the epithelial cells and Amhr2-Cre deletes genes in the mesenchymal cells. However, like the PR-Cre mouse, these genes are expressed in other tissues, and the recombination occurs prior to sexual maturity of the animals, which could affect the development of the uterus. Lactoferrin (Ltf)-iCre mouse only deletes genes in the uterine luminal epithelium of adult mice, thus could be used to study the luminal epithelial-specific function of BSG in the adult mice. More animal models with cell type (e.g. stromal cells) specific deletions need to be developed to study the role of BSG in a specific uterine compartment.

In conclusion, my doctoral dissertation work shows that loss of BSG in the reproductive tract leads to subfertility in mice. The subfertility is due to uterine defects throughout the courses of pregnancy. Specifically, deletion of BSG in the uterine cells results in impaired implantation and decidualization *in vitro* and *in vivo*, as well as reduction in angiogenesis and lactate transport.

These findings provide important new information on the role of BSG in early pregnancy and contributes to our knowledge on the mechanisms of implantation. Understanding the role of BSG in female reproduction helps to explain the implantation and decidualization associated reproductive disorders in women and improve fertility.

Figure

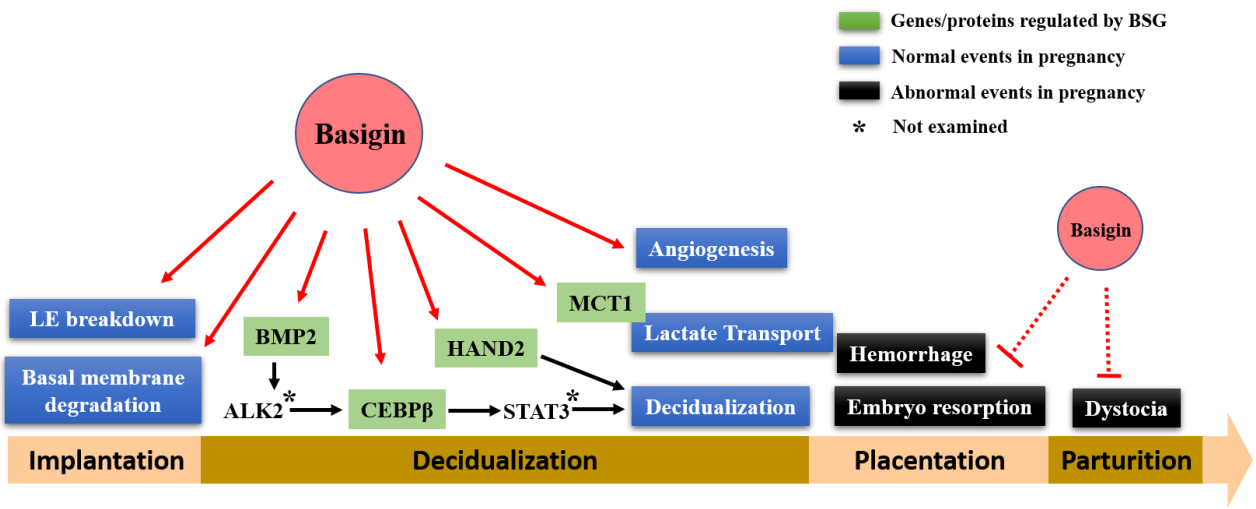

Figure 6.1 A schematic diagram highlighting the role of BSG in pregnancy in mice. BSG is required for the luminal epithelium breakdown and the basement membrane degradation during implantation. BSG regulates Bmp2, Cebpβ and Hand2 to stimulate decidualization. BSG regulate CD31 and MCT1 for angiogenesis and lactate transport. Loss of BSG impairs implantation and decidualization, possibly placentation and parturition too, and results in subfertility in mice.

Appendix

Acronyms and Abbreviations

Adm	adrenomedullin
ADR	Artificially-induced decidualization response
ALK2	Activin-like kinases 2
ALPH	Alkaline phosphatase
AM	Antimesometrial
BCL2	B cell lymphoma 2
Bl	Blastocyst
Bmp	Bone morphogenetic protein
BSA	Bovine serum albumin
BSG	Basigin
BTEB1	basic transcription element-binding protein 1
CEBPβ	CCAAT enhancer-binding protein beta
CD31	Cluster of differentiation 31
CD98	Cluster of differentiation 98
CD147	Cluster of differentiation 147
CFTR	Cystic fibrosis transmembrane conductance regulator
COUP TFII	Chicken ovalbumin upstream promoter transcription factor 2
COX	Cycloocygenase
Cre	Cyclization recombinase
Cyp-A	Cyclophilin A
Cyp-B	Cyclophilin B
DAB	3,3'-Diaminobenzidine
DEDD	Death effector domain-containing protein
DMEM/F12	Dulbecco's modified eagle medium/nutrient mixture F-12
DNA	Deoxyribonucleic acid
E2	Estradiol
EC	Extracellular
ECM	Extracellular matix
ELISA	Enzyme linked immunosorbent assay
Em	Embryo
EMMPRIN	Extracellular matrix metalloproteinase inducer
ENaC	Epithelial Na^+ channel
ER	Estrogen receptor
Ereg	Epiregulin encoding gene
ERK	Extracellular signal-regulated kinases
EV	Extracellular vesicle
FAK	Focal adhesion kinase
Fkbp52	FK506 binding protein 4
Foxa2	Forkhead box protein A2
FSH	Follicle stimulating hormone

Gal	Galectins
GE	Glandular epithelium
Gp130	Glycoprotein 130
GSK3β	Glycogen synthase kinase 3 beta
Hand2	Heart and neural crest derivatives-expressed protein 2
HBSS	Hank's balanced salt solution
HCG	Human chorionic gonadotropin
H&E	Hematoxylin and eosin
HESC	Human endometrial stromal cells
Hoxa	Homeobox A gene
Hurp	Hepatoma upregulated protein
HUVEC	Human umbilical vein endothelial cell
IFN-β	Interferon beta
Ig	Immunoglobulin
IF	Immunofluorescent
IGF1	Insulin-like growth factor 1
IHC	Immunohistochemistry
Ihh	Indian hedgehog
IL	Interleukin
IVF	*in vitro* fertilization
JAK	Janus Kinase
KLF5	Kruppel-like factor 5
KO	Knockout
KS	Kaposi's sarcoma
LAT1	Large neutral amino acid transporter 1
LE	Luminal epithelium
LH	Leutinizing hormone
LIF	Leukemia inhibitory factor
LoxP	locus of cross-over of P1
M	mesometrial
MAPK	Mitogen-activated protein kinases
MCF7	Michigan Cancer Foundation-7
MCT1	Monocarboxylate transporter 1
MESC	Mouse endometrial stromal cells
MMP	Matrix metalloproteinase
mRNA	messenger RNA
MSH	Muscle segment homeobox gene
Msx	Msh homeobox gene
NCAM	Neural cell adhesion molecule
NFκB	Nuclear factor kappa-light-chain-enhancer of activated B cells
P4	Progesterone
PBS	Phosphate buffered saline
PBST	Phosphate buffered saline with tween-20
PC6	Proprotein convertase 6
PCR	Polymerase chain reaction
PDL1	Programmed death ligand 1

PDZ	Primary decidual zone
PI3K	Phosphoinositide 3 kinases
PMSG	Pregnant mare serum gonadotropin
PPIA	peptidylprolyl isomerase A
PR	Progesterone receptor
Prl8a2	Decidual prolactin-related protein family 8, subfamily a, member 2
PTCH1	Protein patched homolog 1
Ptgs2	Postaglandin-endoperoxide synthase 2
qPCR	Quantitative polymerase chain reaction
RGD	Arginine-glycine-aspartic acid
RNA	Ribonucleic acid
RPLP0	Ribosomal protein, large, P0
RT	Room temperature
S	Stroma
SDZ	Secondary decidual zone
SEM	Standard error of the means
Sgk1	Serum and glucocorticoid-regulated kinase 1
shRNA	Short hairpin RNA
siRNA	Small interfering RNA
STAT3	Signal transducer and activator of transcription 3
TCSF	Tumor cell collagenase-stimulatory factor
TGFβ	Transforming growth factor beta
TNF	Tumor necrosis factor
TRAF2	TNF receptor-associated factor 2
Trp53	Transformation related protein 53
VEGF	Vascular endothelial growth factor
Wnt	Wingless-related integration site

Supplementary Figures

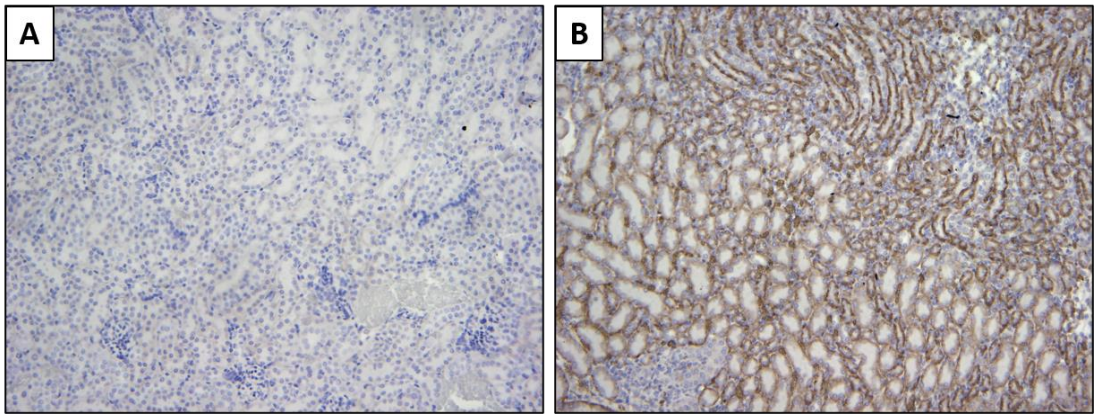

Figure A1. BSG expression in kidney. A cKO kidney cross section stained for nonspecific IgG (A) and BSG (B)

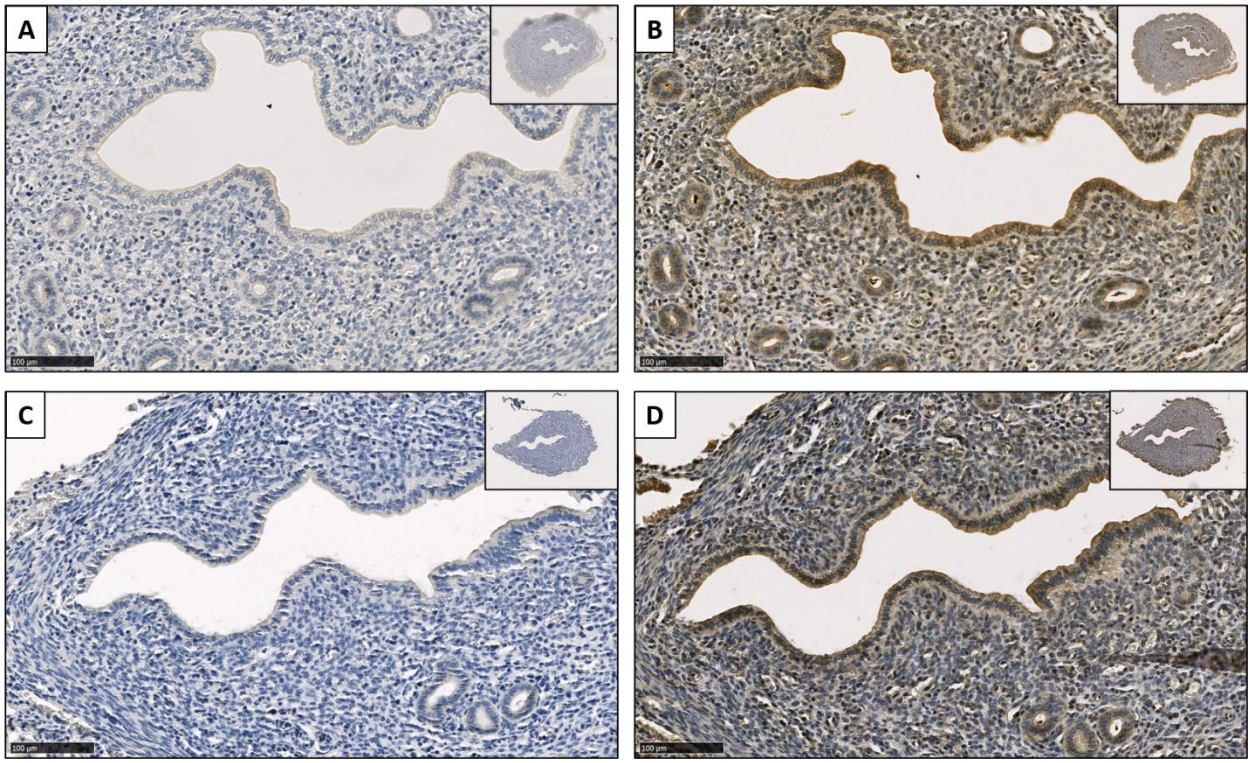

Figure A2. CD98 expression in the uterus on day 4 of pregnancy. Top panel: a control mouse uterus stained for nonspecific IgG (A) and CD98 (B). Bottom panel: a cKO mouse uterus stained for nonspecific IgG (C) and CD98 (D).

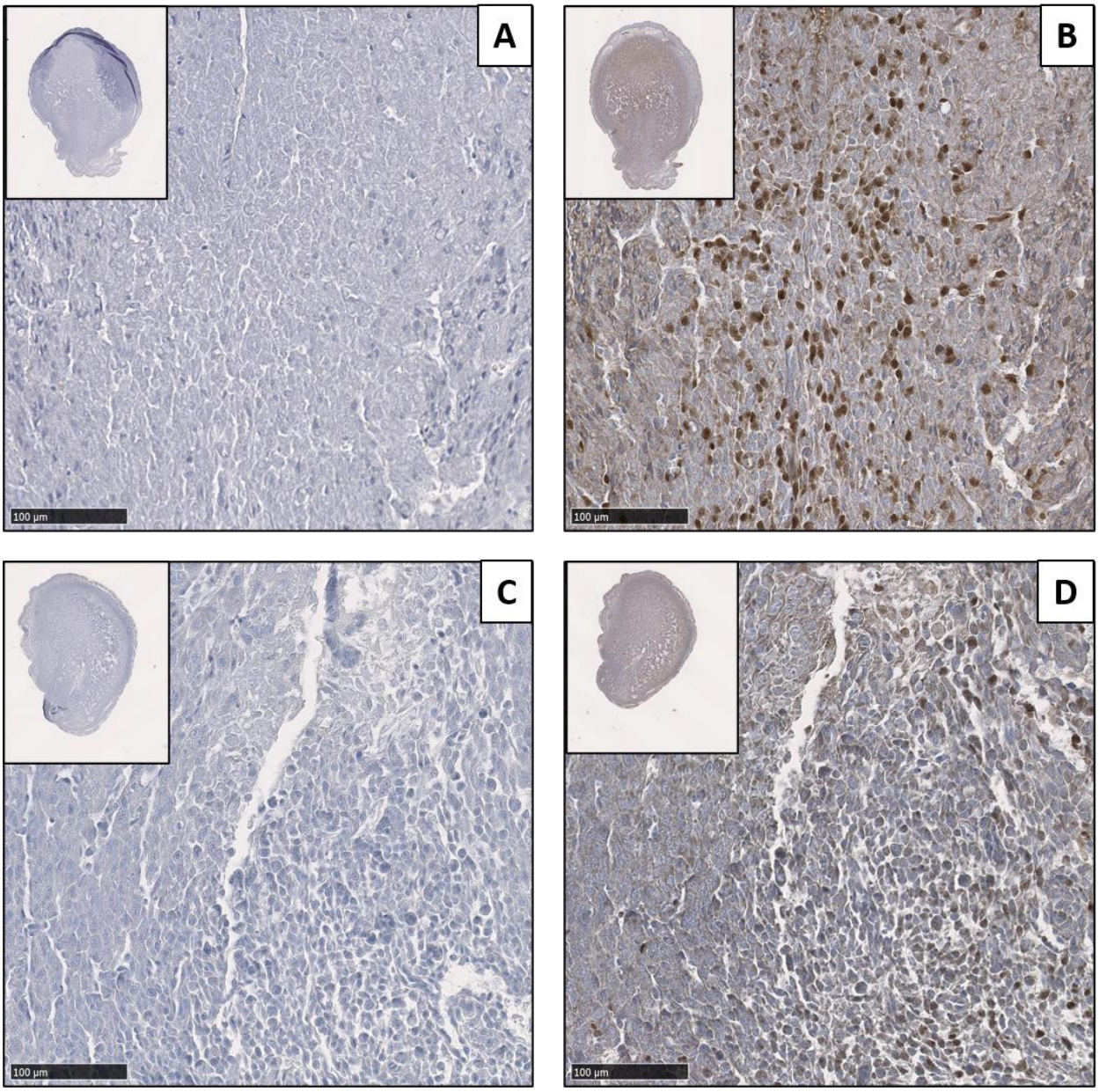

Figure A3. CEBPβ expression in the ADR decidual tissues. Top panel: a control mouse decidual cross section stained for nonspecific IgG (A) and CEBPβ (B). Bottom panel: a cKO mouse decidual cross section stained for nonspecific IgG (C) and CEBPβ (D)

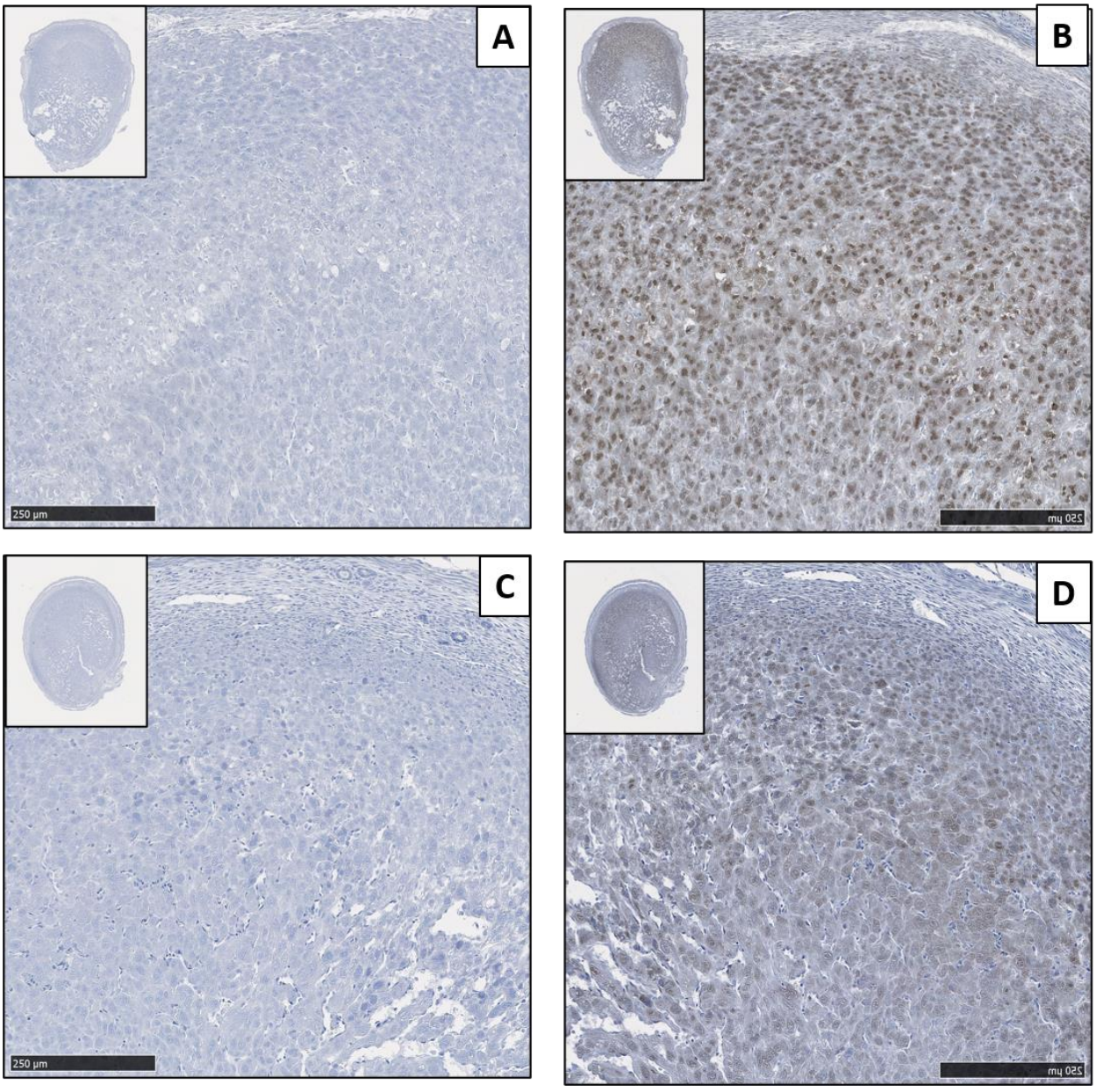

Figure A4. HAND2 expression in the ADR decidual tissues. Top panel: a control mouse decidual cross section stained for nonspecific IgG (A) and HAND2 (B). Bottom panel: a cKO mouse decidual cross section stained for nonspecific IgG (C) and HAND2 (D)

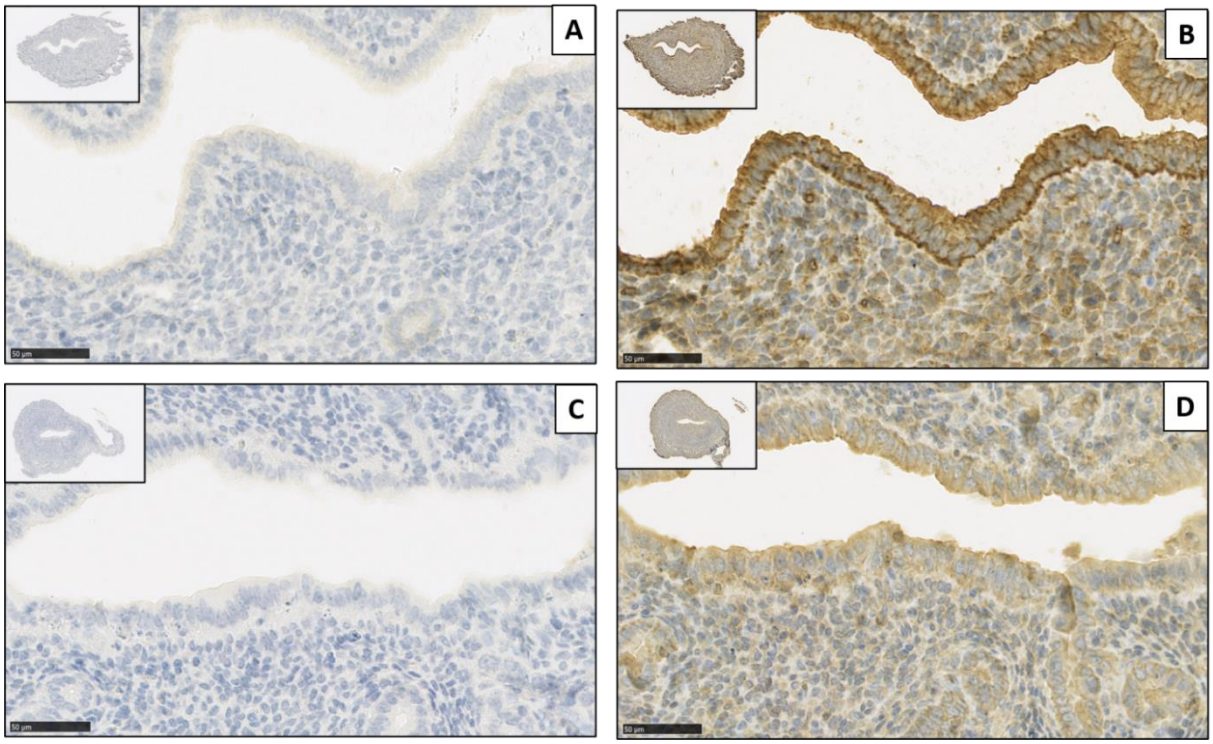

Figure A5. MCT1 expression in the uterus on day 4 of pregnancy. Top panel: a control mouse uterus stained for nonspecific IgG (A) and MCT1 (B). Bottom panel: a cKO mouse uterus stained for nonspecific IgG (C) and MCT1 (D).

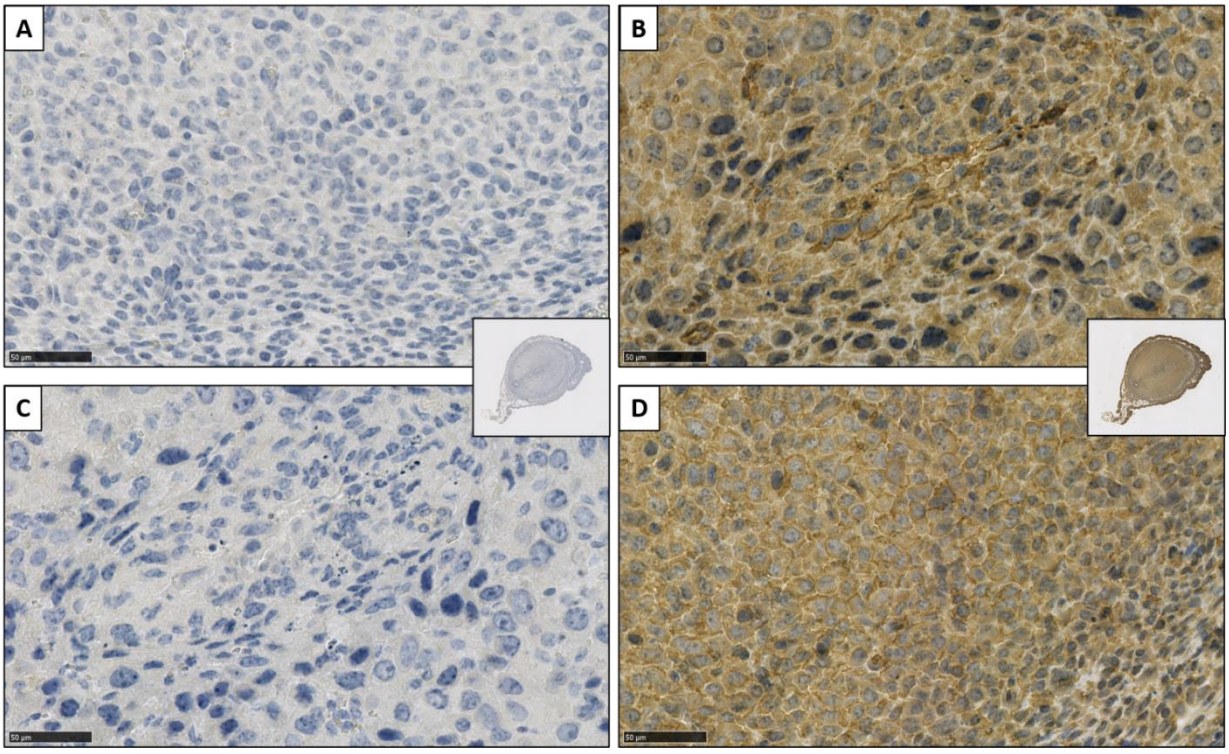

Figure A6. MCT1 expression in the control uterus on day 6 of pregnancy. Top panel: a control mouse uterus stained for nonspecific IgG (A) and MCT1 (B) at the implantation site. Bottom panel: a control mouse uterus stained for nonspecific IgG (C) and MCT1 (D) in the undifferentiated stromal cells.

.

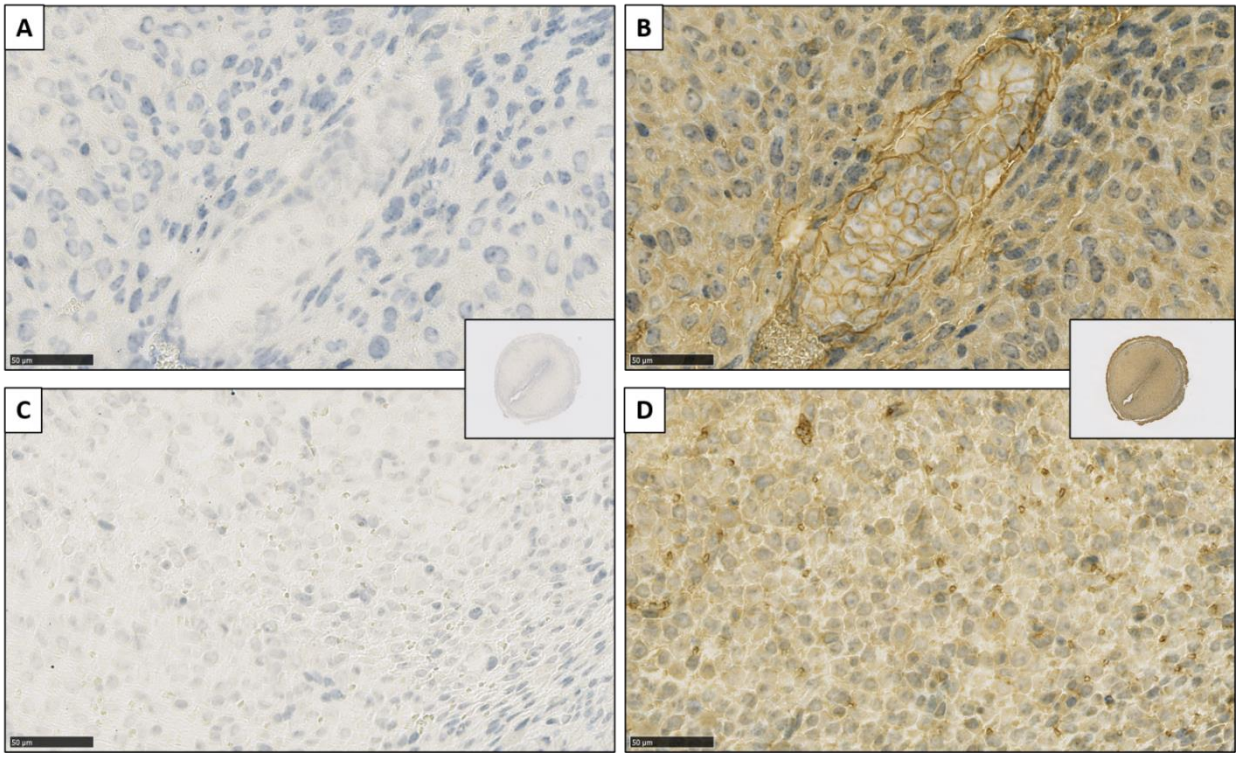

Figure A7. MCT1 expression in the cKO uterus on day 6 of pregnancy. Top panel: a cKO mouse uterus stained for nonspecific IgG (A) and MCT1 (B) at the implantation site. Bottom panel: a cKO mouse uterus stained for nonspecific IgG (C) and MCT1 (D) in the undifferentiated stromal cells.

Antibody List

Name	Supplier	Cat. #	Host	Species reactivity	Application	Other
Alkaline Phosphatase	Abcam	Ab95462	Rabbit	R,H,(M)	**IHC**: 1/400 WB: 1/500-5000	Implantation marker
Basigin/EMMPRIN/CD147	R&D systems	AF772	Goat	M	**IHC**:	
Basigin/EMMPRIN/CD147	R&D systems	AF972	Goat	H	**IHC**:	
Wnt-4 (C-14)	Santa cruz	Sc-5214	Goat	H, (M)	**WB**: 1/1000 IHC: 1/50-500	
GAPDH	Novusbio	NB300-221	Mouse	H, M, R, A, B, CH, Ham,	IHC:1/100 **WB**:1/1000	WB loading control
IkB-α	Cell signaling	9242	Rabbit	H, M, R, MK, B, DG, PG	IHC: 1/50 **WB**: 1/1000	
Active-β-catenin (Anti-ABC)	Millipore	05-665	Mouse	H, M, R	**WB**: 1/500-5000	
KI67	Abcam	Ab 16667	Rabbit	M, R, H,	**IHC**:1/100-200 WB: 1/1000	
Claudin 4	Abcam	Ab53156	Rabbit	H, M, R, Pg	**IHC**:1/250 WB:1/1000	Antigen retrieval pH9
Cytokeratin 19	Abcam	52625	Rabbit	M, H	**IHC1**/400-800 WB:1/5000	
Placental lactogen 1 (c-12)	Santa cruz	376436	Mouse	M, r, h	**Ihc**: 1/50-500 Wb: 1/1000	Trophoblast cell
CD98 (H300)	Santa cruz	Sc-9160	Rabbit	M, H, R	**IHC1**/50-500 WB:1/1000	
MCT-1/SLC16A1	LSBio	Ls-c335287	Rabbit	H, M	**Ihc**: 1/50-200 WB:1/1000	good
MCT-1/SLC16A1	Novusbio	59656H	Rabbit	H, M	Experiment	Not good
C/EBPβ (c-19)	Santa curz	Sc-150	Rabbit	M, R, H	**IHC**: 1/50-500 WB: 1/1000	
CD31/PECAM1	Abcam	Ab28364	Rabbit	M, H, Pg	IHC:1/50 WB:1/500	
VEGF (A-20)	Santa cruz	Sc-152	Rabbit	M, R, H	IHC:1/50-500 WB:1/1000	
LIF (N-18)	Santa cruz	Sc-1336	Goat	M, R H	IHC: 1/50-500 WB:1/1000	
EMMPRIN (C-19)	Santa cruz	Sc-9754	Goat	H	**WB**:1/1000	
EMMPRIN (N-19)	Santa cruz	Sc-9752	Goat	H	**WB**:1/1000	
GPR30 (K-19)-R	Santa cruz	Sc-48524-R	Rabbit	H, M, R	**WB**:1/1000 IHC:1/50-500	
Chromogranin A	Abcam	Ab15160	Rabbit	M, H, Mk	IHC:1/400 WB: 1/100	
Von Willebrand Factor	Dako	A008229-5	Rabbit	M, R, H, Ch	**IHC**:1/400	
Actin muscle (Huc1-1)	ThermoFisher	MA511874	Mouse	H M R	IHC:1/200	
Actin smooth muscle	Thermo Fisher	PA5-16697	Rabbit	H M R Fe	IHC 1/200	
Hand2	ABCAM	Ab200040	Rabbit	M, R, H	IHC	Good one
Hand	Santa cruz	Sc398167	Mouse			NOT GOOD
MMP-9	Abcam	Ab38898	Rabbit	H,M, Rat	IF 1:100 IHC	
Pan cytokeratin	Sigma	C2562	Mouse	H,M,	IHC, IF 1:200	Good
E-cadherin	R&D system	AF748	Goat	H;M	1:200	good

Genes and Primer Sequences

Genes	NCBI Gene Reference	Left Primer Sequence	Right Primer Sequence
Alph	NM_007431.3	cggatcctgaccaaaaacc	tcatgatgtccgtggtcaat
Angpt1	NM_001286062.1	ggaagatggaagcctggat	accagagggattcccaaaac
Angptl1	NM_028333.2	gatggctctgtcaatttcttca	caatgtttccaaacccttttctt
Angpt2	NM_007426.4	ccaccagtggcatctacaca	acccacgtccatgtcacag
Angpt4	NM_009641.2	cgcctggtacggattgtag	tggaacactggcttaggtgtc
Bmp2	NM_007553.3	agatctgtaccgcaggcact	gttcctccacggcttcttc
Bmp5	NM_007555.4	ccgcaataaatccaactctca	tgcaggcttgtttttgttca
Bmp7	NM_007557.3	cgagaccttccagatcacagt	cagcaagaagaggtccgact
Bsg	NM_009768.2	acagcagtggcgttgaca	ggtcatctgcgtccactatgt
Ccnd1	NM_007631.2	catccatgcggaaaatcg	gcgggaagacctcctctt
Cd31	NM_001032378.2	cggtgttcagcgagatcc	actcgacaggatggaaatcac
Cebpβ	NM_001287739.1	aagatgcgcaacctggag	cagggtgctgagctctcg
E-cadherin	NM_009864.3	gctctcatcatcgccacag	gatgggagcgttgtcattg
Ereg	NM_007950.2	ttgacgctgctttgtctagg	ggatcacggttgtgctgat
Esr1	NM_001302532.1	caactgggcaaagagagtgc	ccagacgagaccaatcatca
Esr2	NM_207707.1	gaccctcactggcacgtt	aatcccttccacgcacttc
Hand2	NM_010402.4	tgagcagcaacgacaagaaa	tgctctcctcttcttcactgc
Hoxa10	NM_008263.3	ccttcagaaaacagtaaagcttcg	aagggcagcgtttcttcc
Itgav	NM_008402.3	ggtgtggatcgagctgtctt	caaggccagcatttacagtg
Itgb1	NM_010578.2	caaccacaacagctgcttctaa	tcagccctcttgaattttaatgt
Mct1	NM_009196.4	gaatgctgccctgtcctc	ccacaagcccagtacgtgtat
Mct4	NM_001310705.1	gtcatcactccgtttctctgc	acgtcccaagaatggaggta
Mmp2	NM_008610.3	gtgggacaagaaccagatcac	gcatcatccacggtttcag
Mmp3	NM_010809.2	tgcagctctactttgttctttga	agagatttgcgccaaaagtg
Mmp9	NM_013599.4	cagaggtaacccacgtcagc	gggatccaccttctgagactt
Mmp14	NM_008608.4	gagaacttcgtgttgcctga	ctttgtgggtgaccctgact
Pcna	NM_011045.2	ctagccatgggcgtgaac	gaatactagtgctaaggtgtctgcatt
Pgr	NM_008829.2	tgcacctgatctaatcctaaatga	ggtaaggcacagcgagtagaa
Ppia	NM_008907.1	ggaccaaacacaaacggttc	catgccttctttcaccttcc
Prl8a2	NM_010088.2	gctggacaatttgaaacacttg	tgggtttgtgacattagagtgg
Rplp0	NM_007475.5	actggtctaggacccgagaag	ctcccaccttgtctccagtc
Vegfa	NM_001025250.3	aaaaacgaaagcgcaagaaa	tttctccgctctgaacaagg
Vegfb	NM_011697.3	gctcaacccagacacctgtag	aggaggttcgcctgtgct
Vegfc	NM_009506.2	cagacaagttcattcaattattagacg	catgtcttgttagctgcctga
Vegfd	NM_001308489.1	gcaactttctatgacactgaaacac	tctctctagggctgcattgg
Vimentin	NM_011701.4	ccaacctttttcttccctgaac	ttgagtgggtgtcaaccaga
Wnt4	NM_009523.2	actggactccctccctgtct	tgcccttgtcactgcaaa

Protocols

Hematoxylin & Eosin staining

Once you start staining, do not allow sections to dry throughout the procedure.

	Solution	Time	
Deparaffinization	Xylene I (Dirty)	5 min	Xylene can interact with gloves. Be careful
	Xylene II (Dirty)	5 min	
	Xylene III (Clean)	5 min	
Rehydration	100% EtOH I	1 min	Number of ethanol dilutions can be increased or decreased as needed.
	100% EtOH II	1 min	
	70% EtOH	1 min	
Wash	DI water	1 min	
Nuclear Staining	Hematoxylin	1-2 min	Mayer's Hematoxylin (Sigma)
Wash	Running TAP water	5-15 min	Not DI water. Check the color (Blue to purple)
Cytoplasmic Stain	1% Eosin	1 min	May need to increase or decrease time depending on fixatives, tissue types, etc…
Dehydration	70% EtOH	1 min	No need to wash. The Eosin will stain the ethanol solutions which then need to be discarded in the ethanol+eosin waste so as not to interfere with subsequent experiments.
	80% EtOH	1 min	
	90% EtOH	1 min	
	100% EtOH I	1 min	
	100% EtOH II	1 min	
	100% EtOH III	1 min	
Clearing	Xylene I (Dirty)	1 min	
	Xylene II (Dirty)	1 min	
	Xylene III (Clean)	1 min	Remove each slide from xylene to mount the coverslip. Leave remaining slides in xylene while doing so.
Cover slip	Permount/Clear Mount		Do not dry sections before covering.

Results

Nuclei: Blue

Erythocytes: Red

Cytoplasm, Connective tissue: Pink

Periodic Acid Optimized Schiff's Stain (PAS)
(American MasterTech #KTPASPT)

Deparaffinize:
_____ 5 min Xylene
_____ 5 min Xylene
_____ 10-12 dips in 100% Ethanol
_____ 10-12 dips in 100% Ethanol
_____ 10-12 dips in 100% Ethanol
_____ 10-12 dips in 95% Ethanol
_____ 10-12 dips in 95% Ethanol
_____ 10-12 dips in 70% Ethanol
_____ 1 minute in running tap water
_____ 10-12 dips in DI water
_____ 7 minutes in 0.5% Periodic Acid
_____ 2-3 dips in DI water
_____ 15 minutes in **Optimized Schiff's Solution**
_____ 5 minutes in running tap water
_____ 2 minutes in **Modified Mayer's Hematoxylin**
_____ 3 minutes in running tap water
_____ 2-5 dips in **Light Green Stain**

Dehydration and Cover
_____ 10-12 dips in 70% Ethanol
_____ 10-12 dips in 95% Ethanol
_____ 10-12 dips in 95% Ethanol
_____ 10-12 dips in 100% Ethanol
_____ 10-12 dips in 100% Ethanol
_____ 10-12 dips in 100% Ethanol
_____ 10-12 dips in Xylene
_____ 10-12 dips in Xylene
_____ 10-12 dips in Xylene
_____ Mount cover glass

Jones' silver staining
(for basement membrane)

Deparaffinization and rehydration	Xylene 1: 5 min	
	Xylene 2: 5 min	5 min
	Xylene 3 (clean)	5 min
	100% Ethanol	5 min
	100% Ethanol	5 min
	90% Ethanol	5 min
	80% Ethanol	5 min
	70% Ethanol	5 min
Oxidation	0.5% Periodic acid	11 min
Wash	Distilled deionized water	
Methenamine silver solution	3% methenamine and 5% nitrate, freshly made	60 min at 70 °C
Check every 20 mins	Check for precipitate formation, a medium brown color stain	
Wash	Distilled deionized water	5 min at 70 °C
Gold chloride solution	0.2% gold chloride solution	1 min
Wash	Distilled water treated with sodium thiosulfate	1 min
Wash	Running tap water	10 min
Counter stain	Fast green (Fisher)	1 min
Dehydration and cover	70% Ethanol	1 min
	80% Ethanol	1 min
	90% Ethanol	1 min
	100% Ethanol	1 min
	100% Ethanol	1 min
	Xylene 1	1 min
	Xylene 2	1 min
	Xylene 3 (clean)	1 min

Immunohistochemical staining (IHC)

- For ABC method Keep antibody solutions on ice.
- Do not allow sections to dry once you start staining. Incubation must be performed in a moist chamber.

Day	Procedure	Time
1	Deparaffinization and rehydration	
	Wash in tap water	5 min
	Antigen retrieval in 0.01M citrate buffer or 1X Dako *(make new citrate buffer each time/change Dako weekly)*	Boil for 20 min
	Cool down to room temperature	
	Wash in 1X PBST on shaker	5 min
	Inactivation of endogenous peroxidase in 0.3% H2O2/Methanol *(make new solution each time)*	15 min
	Wash in 1X PBST on shaker	5 min *3
	Encircle section with a PAP pen wihle rinsing in PBST *(make sure draw big circles far from sections to prevent oil blocking)*	
	Blocking of non-specific binding in 5% normal serum and 1% BSA (*never let sections dry out)*	60 min RT
	Incubation in the primary antibody diluted in 1%BSA/PBST	Overnight at 4°C
2	Rinse in PBST on shaker	5 min * 3
	Incubation in biotinylated secondary antibody in 1%BSA/PBST	60 min RT
	Prepare ABC solution in 1%BSA/PBST 30 min before use *(PBS:A:B=50:1:1)*	
	Rinse in PBST on shaker	5 min * 3
	Incubation in ABC solution at RT	30 min
	Rinse in PBST on shaker	5 min * 3
	DAB reaction *(watch under scope for time needed to change color, time varies to different AB)*	~ 30 sec
	Stop DAB reaction in tap water	10 min
	Counterstaining in hematoxylin (*filter hematoxylin*)	2 min
	Wash in tap water *(only tap water, not DI water*)	>10 min
	Dehydration, clearing and cover with permount. *(do not use excess permount)*	

Deparaffinzation and rehydration:	**Dehydration and clearing**
Xylene 1: 5 min	70% Ethanol: 1 min
Xylene 2: 5 min	80% Ethanol: 1 min
Xylene 3 (clean): 5 min	90% Ethanol: 1 min
100% Ethanol: 5 min	100% Ethanol: 1 min
100% Ethanol: 5 min	100% Ethanol: 1 min
90% Ethanol: 5 min	Xylene 1: 1 min
80% Ethanol: 5 min	Xylene 2: 1 min
70% Ethanol: 5 min	Xylene 3 (clean): 1 min

Immunofluorescence staining (IF)

- All procedures are performed at room temperature unless specified
- Keep antibody solutions on ice.
- Do not allow sections to dry once you start staining. Incubation must be performed in a moist chamber.

Day	Procedure	Time
1	Deparaffinization and rehydration	
	Wash in tap water	5 min
	Antigen retrieval in 0.01M citrate buffer or 1X Dako *(make new citrate buffer each time/change Dako weekly)*	Boil for 20 min
	Cool down to room temperature	
	Wash in 1X PBST on shaker	5 min
	Encircle section with a PAP pen wihle rinsing in PBST *(make sure draw big circles far from sections to prevent oil blocking)*	
	Blocking of non-specific binding in 5% normal serum and 1% BSA (*never let sections dry out)*	60 min RT
	Incubation in the primary antibody diluted in 1%BSA/PBST	Overnight at 4°C
2	Rinse in PBST on shaker	5 min * 3
	Incubation in biotinylated secondary antibody in 1%BSA/PBST in dark	60 min RT
	Rinse in PBST on shaker	5 min * 3
	Coverslip with DAPI containing mounting medium	
	Store in 4 °C fridge or image using LSM710 confocal	

Deparaffinzation and rehydration:
Xylene 1: 5 min
Xylene 2: 5 min
Xylene 3 (clean): 5 min
100% Ethanol: 5 min
100% Ethanol: 5 min
90% Ethanol: 5 min
80% Ethanol: 5 min
70% Ethanol: 5 min

Isolation of Mouse Endometrial Stromal Cells (MESC)

(https://www.jove.com/video/55168/isolation-mouse-endometrial-epithelial-stromal-cells-for-vitro - Jove Journal)

Reagents

- digestion mix Pancreatin (may be referred to as MESC digestion mix):

0.25 g pancreatin (Sigma – cat# P3292)
10 ml trypsin 0.25%

Make it in 50 ml conical tube, mix well and let the solution for 1 hour at 37oC in the water bath.

- DIGESTION SOLUTION I – DISPASE

120 mg dispase ---- 4 Jia jia's aliquots or Sigma (cat# D4693-1G Dispase II)
500 mg pancreatin
20 ml HBSS
0.2 ml penstrep (1%)

Make 5 ml of solution per animal. This recipe is for 4 animals = 20 ml.

- STOP SOLUTION (10% FBS in HBSS)

17.8 ml HBSS
0.2 ml pentrep
2 ml FBS

Make the same volume as the Digestion solution I. In this case, 20 ml = 4 animals. Make this solution twice, 2 tubes with 20 ml each.

- DIGESTION SOLUTION II – COLLAGENASE

10 mg Collagenase IA (glass bottle – Sigma cat# 2674)
17.8 ml HBSS
0.2 ml penstrep (1%)

Optional: you can make 500 mL of Hank's Balanced Salt Solution (HBBS) 1x complemented with 100 U/mL penicillin and 100 µg/mL streptomycin (further referred to as HBSS+) and use it to make those solutions.

- ESTRADIOL STOCK 100X (Sigma cat# E8875-1G)

0.00272 g dissolved in 10 ml ethanol 100% - shake vigorously

From this solution make estradiol 1X by diluting 10 µl of the 100X stock into 990 µl ethanol 100%. We used this 1X solution for making the medium. Aliquots made on 12/01/2017 are stored in -20oC.

- PROGESTERONE STOCK 100X (Sigma cat# P8783-1G)

0.0393 g dissolved in 1.25 ml ethanol 100%

From this solution make progesterone 1X by diluting 10 µl of the 100X stock into 990 µl ethanol 100%. We used this 1X solution for making the medium. Aliquots made on 12/01/2017 are stored in -20oC.

- MEDIUM FOR CELLS CULTURE

> For washing steps (200 ml):
178 ml DMEM/F12
20 ml FBS (10%)
2 ml penstrep (1%)

> For seeding and culturing (100 ml):
88.8 ml DMEM/F12
10 ml FBS (10%)
100 µl estradiol 1X (10 nM) ---- check that info!
100 µl progesterone 1X (1 µM) ---- check that info!
1 ml penstrep (1%)

NOTES: You might want to use exosome-depleted FBS in the culture medium. If so, check when to start using this medium during the protocol.
~ It might be interesting to use or not hormones, depending on your goals. These concentrations will likely make the stromal cells decidualize.
~ For more information, check Ramona's lab notebook.

Procedures

1. Isolation of uteri

- In the IGB mouse room, euthanize the animals using an appropriate method such as cervical dislocation or CO2-induced narcosis.
- Spray the carcasses with 70% ethanol in order to generate a sterile environment.
- Grab the uterine horn at the most distal end under the fallopian tube. Dissect the uterine horns from the fallopian tube and remove adipose and connective tissue. Cut out the horn at the distal end above the uterine body and place it in a 15 ml conical tube with 3 mL of HBSS+.
- Repeat this step for the other horn and for the other animals until all uterine horns are collected.
- Back to the laboratory, place the uterine horn in Petri dishes and clean the uterine horn (in HBSS+) further and remove all residual adipose or connective tissue, as well as the cervix.
- Cut the uterine horns open longitudinally to expose the uterine lumen and replace the horn in a new Petri dish with fresh HBSS+.

2. Isolation and Culture of Mouse Endometrial Stromal Cells (MESC):

1. Transfer all uterine horns to the 15 mL tube containing Digestion Mix Pancreatin (pancreatin and trypsin).
2. Incubate horizontally for 60 min at 4 °C on an orbital shaker (50 rpm) – Dr. Bahr's cold room.
3. Incubate horizontally for 45 min at 23 °C (Room Temperature), without shaking.
4. Incubate horizontally for 15 min at 37 °C (water bath), without shaking.
5. NOTE: From now on, further isolation steps are performed in a sterile environment under a laminar flow cabinet.
6. After those 2 h of incubation, carefully pour away the supernatant solution.
7. Transfer the uteri into a Petri dish containing cold medium and incubate for 5 min in order to inactivate trypsin activity.
8. Transfer the uteri to a 15 mL tube containing 3 mL of cold HBSS+ and vortex for 10 s to release the epithelial sheets. (1)
9. Rinse the uteri in a clean Petri dish with 3 mL HBSS+.
10. Transfer the uteri to a new 15 mL tube containing 3 mL of cold HBSS+ and vortex for 10 s to release the epithelial sheets. (2)
11. Rinse the uteri in a new clean Petri dish with 3 mL HBSS+.
12. Transfer the uteri to a new 15 mL tube containing 3 mL of cold HBSS+ and vortex for 10 s to release the epithelial sheets. (3)
13. Rinse the uteri in a clean Petri dish with 3 mL HBSS+.
14. Transfer the uteri tissue to Digestion solution I (containing Dispase and Pancreatin) and incubate that for 30 minutes at room temperature.

15. After the 30 minutes incubation in Digestion Solution I (containing Dispase and Pancreatin) add the Stop Solution in the conical tube and mix well – use the same amount as digestion solution, in this case, 20 ml.
16. Remove and discard the supernatant.
17. Pick the tissue and wash in 5 ml of HBSS+ in a Petri dish, twice.
18. Place tissue in Digestion solution II – Collagenase for 45 minutes at 37oC (water bath).
19. After that, add Stop Solution to the tube and mix by vortexing for 10 seconds – use the same amount as digestion solution, in this case, 20 ml.
20. Collect the stromal cells by passing this solution through a 40 µm nylon mesh strainer into a new 50 ml conical tube. I used 2 tubes and 2 strainers because they clogged.
21. Centrifuge the cell suspension at 450 g for 6 min.
22. Discard supernatant and resuspend the pellet in 10 ml HBSS+.
23. Centrifuge again at 450 g for 6 minutes.
24. Aspirate supernatant, resuspend pellet and plate stromal cells in DMEM/F12 medium at the desired concentration in the desired surface.

RNA Extraction from animal tissue using Qiagen RNeasy Mini Kit

*RNA later stabilized samples *Using QIAshredder homogenizer *Add 10 ul b-Mercaptoethanol (bME) per 1 ml RLT buffer.

1. Excise the tissue sample from the animal or remove it from storage. Remove RNAlater stabilized tissues from the reagent using forceps. Determine the amount of tissue. Do not use more than 30 mg. Note: If the tissues were stored in RNAlater Reagent at –20°C, be sure to remove any crystals that may have formed.

2. Disruption using a mortar and pestle followed by homogenization using **a QIAshredder homogenizer**: Immediately place the weighed (fresh, frozen, or RNAlater stabilized) tissue in liquid nitrogen, and grind thoroughly with a mortar and pestle. Decant tissue powder and liquid nitrogen into an RNase-free, liquid-nitrogen–cooled, 2 ml microcentrifuge tube. Allow the liquid nitrogen to evaporate, but do not allow the tissue to thaw.

3. Add the **600 ul of Buffer RLT (with BME)**. Pipet the lysate directly into a **QIAshredder** spin column placed in a 2 ml collection tube.

4. Centrifuge the lysate for **3 min** at **full speed**. Carefully remove the supernatant by pipetting, and transfer it to a new microcentrifuge tube. Use only this supernatant (lysate) in subsequent steps.

In some preparations, very small amounts of insoluble material will be present after the 3 min centrifugation, making the pellet invisible.

5. Add **600 ul of 70% ethanol** to the cleared lysate, and mix immediately by pipetting. Do not centrifuge. Proceed immediately to step 6. Note: The volume of lysate may be less than 350 µl or 600 µl due to loss during homogenization and centrifugation. Note: Precipitates may be visible after addition of ethanol. This does not affect the procedure.

6. Transfer up to **700 µl of the sample**, including any precipitate that may have formed, to an RNeasy **spin column** placed in a 2 ml collection tube (supplied). Close the lid gently, and centrifuge for **15 s at ≥8000 x g (≥10,000 rpm**). Discard the flow-through. If the sample volume exceeds 700 µl, centrifuge successive aliquots in the same RNeasy spin column. Discard the flow-through after each centrifugation.

7. Add **350 µl Buffer RW1** to the RNeasy spin column. Close the lid gently, and centrifuge for **15 s at ≥8000 x g (≥10,000 rpm**) to wash the spin column membrane. Discard the flow-through.

8. Add **10 µl DNase I stock** solution (in -20) to **70 µl Buffer RDD** (in RNase-Free DNase Set in fridge). Mix by gently inverting the tube, and centrifuge briefly to collect residual liquid from the sides of the tube. Note: DNase I is especially sensitive to physical denaturation. Mixing should only be carried out by gently inverting the tube. Do not vortex.

9. Add the **DNase I incubation mix (80 µl)** directly to the RNeasy spin column membrane, and place on the benchtop (20–30°C) for **15 min**. Note: Be sure to add the DNase I incubation mix directly to the RNeasy spin column membrane. DNase digestion will be incomplete if part of the mix sticks to the walls or the O-ring of the spin column.

10. Add **350 µl Buffer RW1** to the RNeasy spin column. Close the lid gently, and centrifuge for **15 s at ≥8000 x g (≥10,000 rpm).** Discard the flow-through.

11. Add **500 µl Buffer RPE** to the RNeasy spin column. Close the lid gently, and centrifuge for **15 s at ≥8000 x g (≥10,000 rpm)** to wash the spin column membrane. Discard the flow-through.

12. Add **500 µl Buffer RPE** to the RNeasy spin column. Close the lid gently, and centrifuge for **2 min at ≥8000 x g (≥10,000 rpm)** to wash the spin column membrane. The long centrifugation dries the spin column membrane, ensuring that no ethanol is carried over during RNA elution. Residual ethanol may interfere with downstream reactions. Note: After centrifugation, carefully remove the RNeasy spin column from the collection tube so that the column does not contact the flow-through. Otherwise, carryover of ethanol will occur.

13. Place the RNeasy spin column in a new 1.5 ml collection tube (supplied). Add **50 µl RNase-free water** directly to the spin column membrane. Close the lid gently, and centrifuge for **2 min at ≥8000 x g (≥10,000 rpm)** to elute the RNA.

If the expected RNA yield is >30 µg, repeat step 11 using another 30–50 µl RNasefree water, or using the eluate from step 11 (if high RNA concentration is required).
14. Use Nanodrop to determine concentration. Then freeze samples in **-80** freezer.

Protocol for RNA Purification

1.) Add - 0.5 volume Ammonium Acetate 7.5 M (4C) or 0.3 M Sodium Acetate (3M stock)
- 2.5 volume 100% EtOH (-20C)
- 1 mg/ml Glycogen about 10 ul for 500 ul RNA

2.) Place in -80 overnight
3.) Spin 4C for 20-30 min (12,000 x8)
4.) Pour off supernatant
5.) Wash with 1 ml 70% EtOH (-20C)
6.) Pour off and pipette out the residual EtOH
7.) Air dry 10 min (don't invert; cover with Kimwipe, place in hood)
8.) Resuspend with sterile DEPC water 25-50ul
9.) Heat at 55C for 15 min if won't dissolve
10.)Quantify on the Nanodrop

*Better procedure when 260/280 is good and 260/230 is bad; as this will pull down salts as well & purity of the sample too.

HWM DNA Isolation

(Isolate DNA from Myo and Fib tissue)

PROTOCOL – Tissue Lysis

1. Remove tissues from liquid nitrogen tank and allow to sit on ice for 1 hour.
2. Cut off a small chunk of tissue.
3. Measure out a chunk of tissue up to 25mg and put it into a 2mL tube.
4. Add 220 uL buffer ATL.
5. Add 20 uL Proteinase K and vortex for 10 seconds.
6. Incubate overnight (16 hours) on a Thermomixer at 56C, 900 rpm.

PROTOCOL – DNA Isolation

1. Spin the tube down to get the liquid to the bottom of the tube.
2. Transfer 200 uL of liquid to a new 2 mL tube.
3. Add 4 uL RNase A and pulse-vortex for 10 seconds.
4. Incubate at RT for 2 minutes.
5. Add 150 uL buffer ATL and pipette up and down several times.
6. Add 280 uL buffer MB.
7. Vortex Suspension G for 3 minutes.
8. Add 40 uL Suspension G to the sample.
9. Incubate on the Thermomixer at 25C, 1400 rpm for 3 minutes.
10. Place tubes on the magnetic base for 1 minute.
11. Still on the magnet, remove all supernatant.
12. Remove tubes from magnet and add 700 uL buffer MW1.
13. Incubate on the Thermomixer at 25C, 1400 rpm for 2 minutes.
14. Place tubes on the magnetic base for 1 minute.
15. Still on the magnet, remove all supernatant.
16. Remove tubes from magnet and add 700 uL buffer MW1.
17. Incubate on Thermomixer at 25C, 1400 rpm for 2 minutes.
18. Place tubes on the magnetic base for 1 minute.
19. Still on the magnet, remove all supernatant.
20. Remove tubes from magnet and add 700 uL buffer PE.
21. Incubate on Thermomixer at 25C, 1400 rpm for 2 minutes.
22. Place tubes on magnetic base for 1 minute.
23. Still on the magnet, remove all supernatant.
24. Remove tubes from magnet and add 700 uL buffer PE.
25. Incubate on the Thermomixer at 25C, 1400 rpm for 2 minutes.
26. Place tubes on the magnetic base for 1 minute.
27. Still on the magnet, remove all supernatant.
28. Still on the magnet, rinse pellet with 700 uL distilled water.
    a. Rinse against the side of the tube away from the pellet!
29. Incubate at RT for 1 minute.
30. Still on magnet, remove all supernatant.
31. Still on magnet, rinse pellet with 700 uL distilled water.
32. Incubate at RT for 1 minute
33. Still on magnet, remove all supernatant

34. Remove tubes from magnet and add 100 uL buffer AE.
35. Incubate on thermomixer at 25C, 1400 rpm for 3 minutes.
36. Place tubes on the magnetic base for 1 minute.
37. Still on magnetic base, transfer 100 uL supernatant (DNA we want) to a new tube.
38. Transfer 5 ul of sample to a new tube and label for Quibit → put on ice. (ERML356+sample form)
39. Transfer 5 ul of sample to a new tube for agarose gel (1%)
40. Store the remaining sample in -80 C.

Fibroid/Myometrium Cell Culture Protocol

Cell Culture Medium Recipe

DMEM 1X (Corning cellgro REF 10-013-cv)
10% FBS (use 10% for plating cells, after cells attach, switch to 5%)
1% Pen-Strep
1% L-Glutamine

Freezing Medium: 90% FBS + 10% DMSO

Tissue Digestion and Cell Culture Protocol:

(Day 1)

1. Chop up Fibroid/Myometrium into small pieces
2. Transfer tissue pieces into tube containing medium with 10% collagenase II (200 U/ml) (Stock Conc.: 2000U/ml, Working conc.:200 U/ml)
3. Place tube on shaker in incubator at 37 for overnight. (about 16 hours)

(Day 2)

4. Spin down cells at 600-1000 RPM for 5 min at RT.
5. Aspirate supernatant.
6. Re-suspend cells with small amount of medium.
7. Evenly distribute into multiple plates.
8. Incubate at 37°, 5% CO2. Let cells settle for 48 hours before checking or changing medium.
9. Change medium every 48 hours.

Splitting/Freezing cells

(Day 1)

1. Check cell confluency first.
2. Add 3 ml of 0.25% Trypsin EDTA (Corning REF 25-053-ci) to rinse the plate
3. Aspirate the Trypsin and add 3 ml more of 0.25% Trypsin.
4. Incubate at 37°, 5% CO2 for 10 min. Then check every 3 min for cell detachment. (usually takes about 10-15 min)
5. Transfer cells into a tube with 7 ml of medium.
6. Spin down cells at 600 – 1000 RPM for 5 min at RT.
7. Aspirate supernatant.
8. Re-suspend cells with freezing medium. (Freezing medium: 90% FBS+ 10% DMSO)
9. Transfer cells into cryovials and label the vials.
10. Place vials on ice for 30 min.
11. Place vials in -80° freezer for 24 hours.

(Day 2)

12. Place vials in liquid nitrogen tank to store indefinitely.

Mouse Genotyping Protocol

DNA Extraction

- Add 2mL TP (tissue prep) to 8mL E 9(extraction buffer)
- Add 125 microliters E (extraction buffer) to each tube
- Heat for 10 min at 55 degrees C to activate
- Heat for 3 min at 95 degrees C to stop reaction
- Add 100 microliters of N (neutralizing buffer)
- DNA ready 😊

Making PCR mix:

Components vary based on target gene
Take out components and let thaw. Aliquots are located inside -20 in lab.
Multiplication factor found by taking number of samples (n), adding 1, and multiplying the sum by 1.1
TAQ=PCR mix

Cre(_____ + 1) x 1.1 =

TAQ	**10** microliters		TAQ _____ microliters
P1 (PR cre f1)	**0.4** microliters		P1 _____ microliters
P2 (PR cre f2)	**0.4** microliters	x _____	P2 _____ microliters
P3 (PR cre r)	**0.4** microliters		P3 _____ microliters
H_2O	**6.8** microliters		H_2O _____ microliters
= 18 microliters			

Lox(_____ + 1) x 1.1

TAQ	**10** microliters		TAQ _____ microliters
P1 (Lox 1)	**2** microliters		P1 _____ microliters
P2 (Lox 2)	**2** microliters	x _____	P2 _____ microliters
H_2O	**3** microliters		H_2O _____ microliters
= 17 microliters			

DDR
(_____ + 1) x 1.1

TAQ	**10** microliters		TAQ _____ microliters
P1 (DDR neo II)	**2** microliters		P1 _____ microliters
P2 (Nul 5-2)	**2** microliters	x _____	P2 _____ microliters
P3 (Nul 5-6)	**2** microliters		P3 _____ microliters
H_2O	**3** microliters		H_2O _____ microliters
= 17 microliters			

PCR

Ensure tubes are closed.
Use microcentrifuge to spin tubes, only for a few seconds to ensure contents are at bottom of tubes.

Carefully load into Thermal Cycler machine
Go to Nowak Lab, choose protocol (DDR runs separate from other types)
After a run is complete, machine will infinitely keep samples at 4 degreees C until you return.

Preparing for electrophoresis:

Making Running Solution
Use 1% TBE is a solution for the making of the gel and during the electrophoresis

10% x TBE

Weigh and combine in a beaker:

- 108g Tris Base
- 55g Boric Acid
- 9.3 EDTA

Add DI water until you have 1L total solution
Using pH meter, test pH and make adjustments as needed. The solution should have a pH of 8.3. Adding acid may be necessary to decrease the pH.

To make 1% x TBE, add 100 mL TBE to 900 DI water.

Making Gel
Tape the sides of your box before/while making gel. Make sure to cover open sides and allow for extra tape to prevent leakage from the bottom as well as the sides.

Choose recipe from the following: (Fore cre, etc use 1% gel. For DDR use 1.5%. If you are running both, can use 1% gel for DDR as well)

1% agarose gel with ethidium bromide

Place 1 gram agarose in beaker with 100mL 1x TBE
Heat in microwave for about 40 seconds, swirl beaker, then microwave for another 30 seconds.
Let stand to cool until you can touch the bottom of the beaker (not too much, or the solution may start to gel). Now is a perfect time to tape your box's edges.
Add 5 microliters of ethidium bromide to the beaker, swirl to mix. Ready to pour into box.

Pour gel into box. Pop any bubbles or push them away from center. Place your combs into gel right after pouring. Use the thicker teeth for a larger well. To avoid unnecessary waste, most gels you can use 2 combs and therefore run double samples. Make sure to adjust running time as needed.

Wait for gel to solidify before removing combs.

Running electrophoresis
Load your samples into gel carefully, pipetting the full 20 microliters into each well.

Add 5 microliters of DNA standard
Note placement of samples, order matters!

Set a constant voltage 120V. Your amp is calculated by the machine. Select the amount of time to run your samples, 1 hour.

Reading your gel
Photographing:
Make sure the machine isn't in use!
Select a clear glass tray with the "tissue paper" cover. You may have to rinse the tray/cover. Dry off the tray/cover and place it back onto tray.
Carefully peel your gel out of its box and place onto the paper on the tray. You may now place the tray into the machine
Open the Image Quant LAS program
Adjust your focus first, make sure you can also adjust brightness and contrast as needed.
Use position 4 initially, this should give you a shot of the entire gel. Positions 3, 2, and 1 will bring the gel/tray closer to the lens.
For a standard DNA pcr, we want to use fluorescence (which allows us to visualize the ethidium bromide) and trans UV light
Select the exposure type, set this to position. Exposure time should be manually selected. 1/8 or 1/15 seconds should be sufficient.
Once you have captured an image you would like to save, save it in a folder with the date the gel was run and information such as the sample numbers and what genes you are testing for.

Ideally, you get a picture of the whole gel, one of the top half, and then the bottom half.

Visualizing:

Lox	size (bp)	genotype
•	370	F/F
•	370 + 302	F/+
•	302	+/+
Cre		
•	594 + 283	cre/+
•	283	+/+
DDR		
•	240	wt
•	360/240	+/-
BSG (global)		
•	250	Wt
•	1250/250	+/-
•	1250	KO

Primer sets:
BSG global
- B1
- B2

BSG CKO

- Floxed/Loxp
  - Lox 1
  - Lox 2
- PR cre
  - PRcre f1
  - PRcre f2
  - PRcre r

DDR1

- DDR Neo II
- Nul 5-2
- Nulk 5-6

FLP

- FLP1
- FLP2

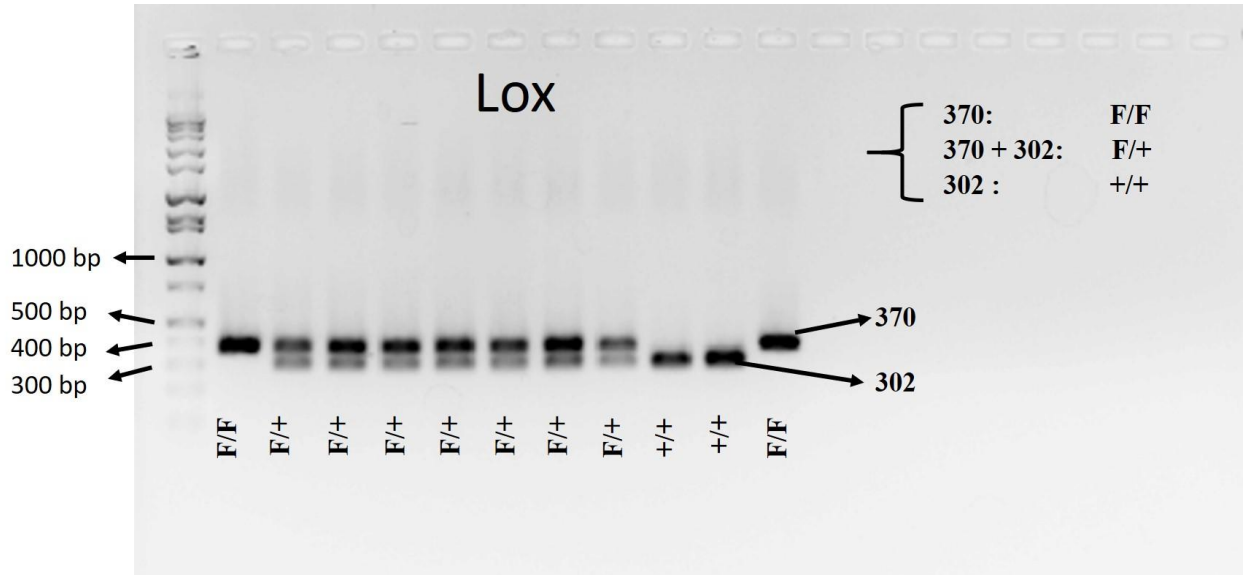

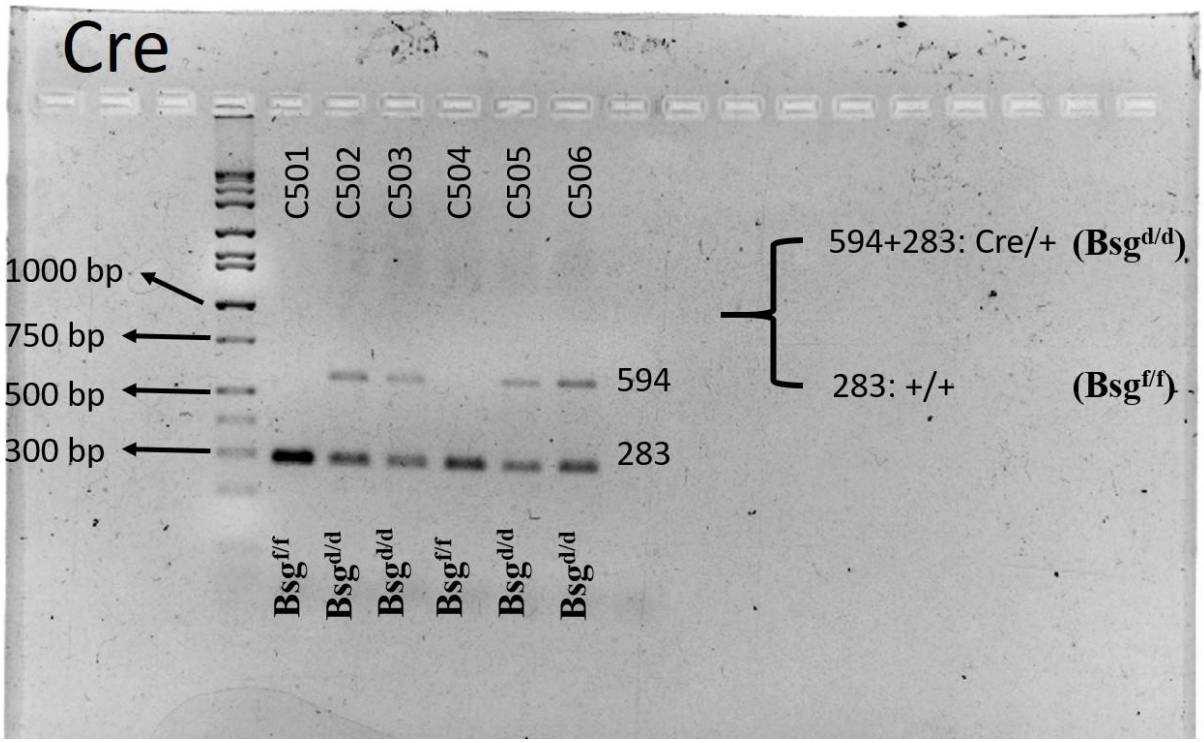
Cre
C501
C502
C503
C504
C505
C506
1000 bp
750 bp
500 bp
300 bp
594
283
594+283: Cre/+ (Bsg^d/d)
283: +/+ (Bsg^f/f)
Bsg^f/f
Bsg^d/d
Bsg^d/d
Bsg^f/f
Bsg^d/d
Bsg^d/d

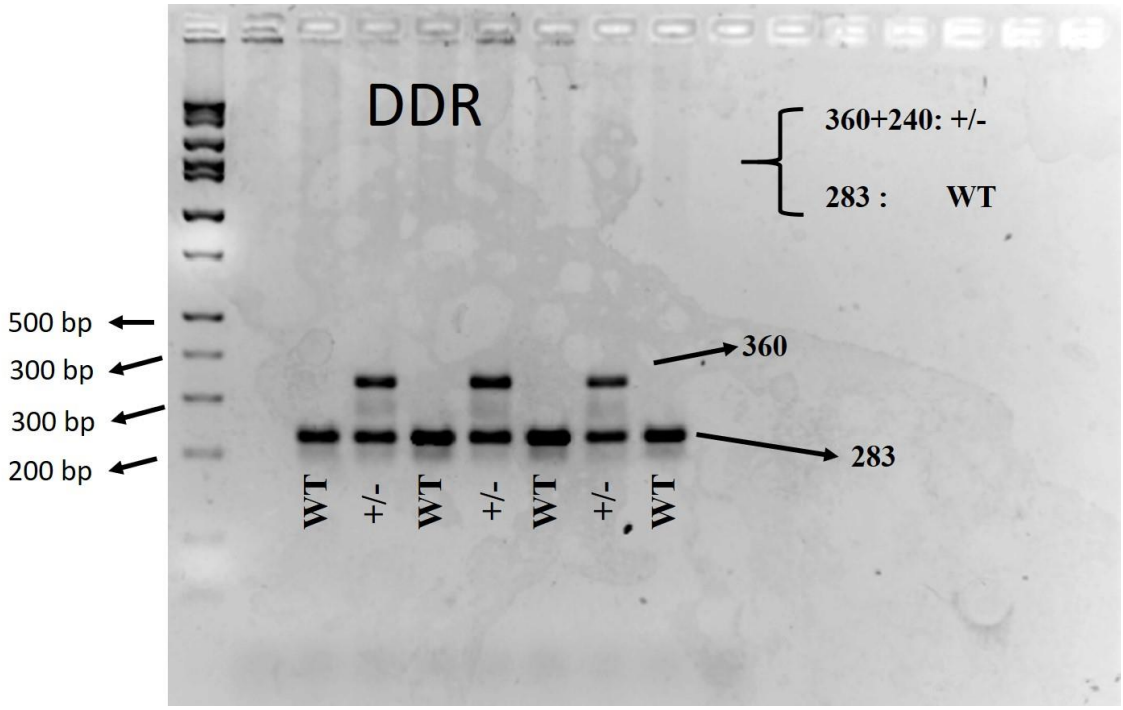
DDR
360+240: +/-
283 : WT
500 bp
300 bp
300 bp
200 bp
360
283
WT
+/-
WT
+/-
WT
+/-
WT

Artificial Decidualization Response (ADR) Timeline and Procedure

s.c. injection of hormones.

!!!	D-10	ovariectomy	D -10
	D-9	Recovery	
	D-8	Recovery	
	D-7	Recovery	
	D-6	Recovery	
	D-5	Recovery	
	D-4	Recovery	
	D-3	Recovery	
	D-2	Recovery	
	D-1	Recovery	
!	D1	100 ng E2 in 0.1 ml corn oil 9am	D1
	D2	100 ng E2 in 0.1 ml corn oil 9am	D2
	D3	100 ng E2 in 0.1 ml corn oil 9am	D3
	D4	Rest	D4
	D5	Rest	D5
!!!	D6	10 ng E2 + 1 mg P4 in 0.1 ml oil 9am	D6 request drugs
	D7	10 ng E2 + 1 mg P4 in 0.1 ml oil 9am	D7
!	D8 Oil injection	10 ng E2 + 1 mg P4 in 0.1 ml oil 9am	D8 Oil injection 15 ul corn oil into right horn 11a-1p. use 30G needle
	D9	1 mg P4 in 0.1 ml oil 9am	D9 24 hr
	D10 r	1 mg P4 in 0.1 ml oil 9am	D10 48 hr
	D11	1 mg P4 in 0.1 ml oil 9am	D11 72 hr
	D12	1 mg P4 in 0.1 ml oil 9am	D12 96hr collect between 11a-1p

Mouse tail vein injection of blue dye

Implantation sites in mice can be detected as early as late at night on day 4 (2200–2300 h) and onward, considering the presence of a copulatory plug as day 1 of pregnancy. This is achieved by intravenous injection of a macromolecular blue dye solution, normally via a tail vein (7).

1. Fill a 1-mL syringe attached to a 27-gauge needle with 1% blue dye solution (Chicago Blue B, Evans blue, or pontamine blue) avoiding any air bubbles inside the syringe.

2. After a mouse is anesthetized, dilate the tail veins by the application of a paper towel soaked in warm water.

3. Locate one of the two lateral veins in the tail (veins are located on both sides of the central artery) and place the mouse on that side.

4. Hold the tail gently between the thumb and forefinger and keep the tail parallel to the body of the mouse (Fig. 5).

5. Align the needle (bevel side up) with the plane of the vein. Insert the needle into the vein and slowly inject the desired amount of dye (0.1 mL/mouse, 0.25 mL/ rat). As a result of increased capillary permeability in the endometrial bed at the sites of implantation, the dye bound with the serum proteins accumulates in the interstitial space at the sites of blastocysts, showing distinct blue bands (Fig. 6). Chicago Blue B dye has been used for many years to identify implantation sites (see Note 4).

6. Animals are sacrificed 3–5 min after dye injection to identify blue bands in the uterus. Identification of uterine implantation sites from day 6 onward does not require blue-dye injection. Visual observation of prominent intermittent swellings in the uterus indicates that blastocyst implantation is in progress.

Lactate Assay Procedure

(Lactate Assay Kit, Millipore Sigma #MAK064)

Lactate Standards for Colorimetric Detection:

- Dilute 10 µL of the 100 nmole/µL Lactate standard with 990 µL of Lactate Assay Buffer to generate a 1 nmole/µL standard solution.
- Add 0, 2, 4, 6, 8, and 10 µL of the 1 nmole/µL Lactate standard into a 96 well plate, generating 0 (blank), 2, 4, 6, 8, and 10 nmole/well standards.
- Add Lactate Assay Buffer to each well to bring the volume to 50 µL.

Sample Preparation:

- Assay requires 50 µL of sample for each reaction (well).
- Serum samples/medium (0.5–10 µL/assay) can be assayed directly by adding in duplicate to 96 well plate.
- Bring samples to final volume of 50 µL/well with Lactate Assay Buffer.
- For unknown samples, it is suggested to test several sample volumes to make sure the readings are within the standard curve range.

Assay Reaction

1. Set up the Master Reaction Mix according to the scheme in Table 1. 50 µL of the Master Reaction Mix is required for each reaction (well).

Reagent	Master Reaction Mix
Lactate Assay Buffer	46 µL
Lactate Enzyme Mix	2 µL
Lactate Probe	2 µL

2. Add 50 µL of the Master Reaction Mix to each of the wells. Mix well using a horizontal shaker or by pipetting, and incubate the reaction for 30 minutes at room temperature. Protect the plate from light during the incubation.
3. For colorometric assays, measure the absorbance at 570 nm (A570). For fluorometric assays, measure fluorescence intensity (λ= 535/ λ = 587 nm).

Concentration of Lactate

$$Sa/Sv = C$$

Sa = Amount of lactate acid in unknown sample (nmole) from standard curve
Sv = Sample volume (µL) added into the wells.
C = Concentration of lactate acid in sample
Lactate molecular weight: 89.07 g/mole

Sample Calculation

- Amount of Lactate (Sa) = 5.07 nmole (e.g.)
- Sample volume (Sv) = 50 µL
- Concentration of lactate in sample:
    - 5.07 nmole/50 µL = 0.101 nmole/µL
    - 0.101 nmole/µL ´ 89.07 ng/nmole= 9.0 ng/µL

Protocol for Western Blotting

1) Switch on the heat block set at 95°C. Thaw samples and 4X LSB on ice. Always check whether the protein needs to be run in a reducing or non-reducing condition. Check the primary antibody product sheet or pertinent references for this information. Accordingly use LSB with or without betamercaptoethanol in it.
2) Prepare samples (3 parts) with 4X LSB (1 part). Load maximum of 20ug of sample in each well for the mini gels. Samples should be loaded in equal quantities (ug of total protein or volume; as needed by specific experimental setup). The total volume of sample+LSB should not exceed 25ul for the 15 well gels and 40ul for the 10 well gels. Always check the gel product sheet specifications for this information.
3) Prepare the Running Buffer: 1 packet per 500 mL of DI H_2O. Running Buffer is BupH Tris-HEPES-SDS Running Buffer (Thermo Scientific Prod #28398) for the gels we use. Always check the type of running buffer needed for the specific type of gel being used). Add the running buffer powder to the DI water in the fume hood, cover and mix on the magnetic stirrer. (The powder contains SDS which should not be inhaled).
4) Need precast gels to be at room temperature prior to use. Type of gel needed is dependent on the molecular weight of the protein being analyzed. Higher molecular weight proteins need a lower percent/concentration of gel and vice versa. Check product sheet and pertinent references for this information. As soon as your gels are ready (at room temperature), take your gels out of their wrap and put them into the gel boxes.
    - **i.** Stack the gels with the shorter plates INWARDS (facing one another) into the gel box inside one of the beige gel holders. Once both gels are in (and facing each other), push them down with one hand while closing the clear doors with other hand.
    - **ii.** Pour your Running buffer into the center between the two gels first. Check for leaks. If there are no leaks, continue to add Running buffer until you reach the outer lip of the gel box. Make sure the gels are covered and continue. (Don't fill too much it will leak from the sides)
5) Place all the tubes with your samples on the 95°C heat block for 5-6 minutes. Check to make sure the samples have mixed thoroughly with the LSB.
6) Make sure the wells in the gel are devoid of air bubbles or the gel preservative buffer by pipetting in small volumes of running buffer into each well before loading your samples.
7) Get a protein ladder aliquot from the -20°C. Each aliquot is 12ul. Load 6-12ul per gel. Position of the ladder in the gel may be decided depending on whether the membrane will be used as a whole (well#1) or cut into sections and incubated under different conditions (any of the central wells).
8) Load 20ul of 1xLSB (with dye) in all of the wells that will remain empty i.e. spaces between your samples according to how you planned your gel. This is done to balance the gel & keep the samples from running crooked down the gel.
9) Once done with the heat block, quickly spin down the samples in the table-top microfuge. Load all of your samples as soon as they are done from the centrifuge. Load your positive control first and then proceed with the samples.
10) Once you have loaded all of your samples on both gels (or on one gel, depends how many samples you have), place the green cover on the top of the gel box making sure that the **red-red and black-black** pins match. Make sure of this as it will affect how the gel runs when plugged into the voltage machine.
11) Use a piece of tape (colored) on the front of the gel box to make sure you know which side is the front (so you can tell the gels apart).
12) Once you have plugged in your gel box (red-red and black-black) you can turn on the power switch on the side. If this is plugged in incorrectly, you'll end up running your samples off the gel… and that's no fun.

13) The gel can be run with different voltage and time parameters. Lower voltage makes the proteins move slowly down the gel and hence needs a longer run time and vice versa. Voltage may be set between 80-120V and run for 45 -95 minutes depending on specific experimental set up. Then start the machine (running man symbol) and check for bubbles. The bubbles need to move up from the bottom of the gel box and the samples need to slowly run downward.
14) While it is running, you want to check the separation of your protein ladder bands. Do not let the samples run off the gel. Stop the machine once the blue sample "line" reaches below the green mark/line on the gel box.
15) In this time you can prepare for the Transfer process. For this-
    i. You need two sponges, 2 filter papers, 1 membrane per gel. Type of membrane can be nitrocellulose membrane (Thermo Scientific Prod #88018) or PVDF membrane (Millipore Prod#IPVH00010). If using the PVDF membrane remember to immerse in methanol for at least 15 seconds so as to activate it before use.
    ii. You need to wet all of these things in Transfer buffer before assembling your sandwich.
    Transfer buffer:
    Glycine 11.6 g
    Tris (base) 23.2 g
    SDS 1.48g
    Methanol 800mL
    Total volume (DI water) 4 L
16) In this time, you can also make TBST pH=8 (WASH buffer).
    TBST pH=8: (Good for two weeks, store covered at 4ºC)

For 2L:	For 1L:	For 500mL (for one memb)
17.5g NaCL	8.75g	4.375g
12.1g Tris base	6.05g	3.025g
2mL Tween-20	1mL	.5g

17) Once the gel is run with complete separation of protein ladder, stop the machine, and take the green cover off. Drain off the running buffer in the sink.
18) Pull the beige tray out and remove the gels out one at a time, so that you know which one is which. Make sure you remember which one came from the front.
19) Using the green gel snapper, slide it between the plastic pieces holding the gel and pull the pieces apart. You want to make sure that you know which side is up on your gel so that you can lay it down correctly. The best way to tell is to make sure the ladder in on the LEFT.
20) Assemble the sandwich using forceps. Keep all components submerged in transfer buffer during assembly. The order of the sandwich is as follows- On the clear side/piece assemble:
    a. Sponge
    b. Filter Paper
    c. Nitrocellulose/PVDF membrane
    d. Gel (With the ladder on the LEFT side)
    e. Filter Paper
    f. Sponge

    Make sure no air bubbles are trapped between the layers. This can be done by constantly pouring transfer buffer (use the sponge) on each layer as you assemble the sandwich. Make sure to mark on the membrane (with pencil) the wells and the gel ID. Then close the sandwich. The current moves from negative to positive (black to red). Always make sure the gel is closest to the black side/piece of the plastic assembly. This ensures the proteins move from the gel to the membrane.
21) In the big plastic box, place a stir bar, and the black and red transfer tray and the ice tray.
22) Once you have assembled your sandwiches, carefully slide them into the black and red transfer tray and fill up the box with transfer buffer. Again check that the black side of the sandwich is closest to the black side of the transfer tray.

23) Add the green cover again on the top of the box (match the red-red and black-black pins). Turn ON the spin plate (check to see that the stir bar is spinning gently), and plug the box back into the machine (red-red and black-black). Once it is plugged in, turn the power on.
24) Proteins can be transferred either overnight (slow transfer) or in one hour (fast transfer). Usually a fast transfer works well. For this set voltage at 100V and run transfer for 60 minutes.
25) During this time prepare the buffer to be used as blocking buffer and for the primary and secondary antibody incubation. This can be a 5% solution of skimmed milk powder in TBST or 5% solution of BSA powder in TBST or a mix of the two. Check the primary antibody product sheet for specfications.
26) Once the transfer is complete, remove the membrane carefully from the assembly and wash once with DI water for 2-3 minutes. The transfer buffer may be re-used as long as it is clear in color (not yellow). Preferably use only 3-4 times as each use tends to concentrate the buffer and a change in the concentration can cause excess heating of the buffer during the run and lack or incorrect transfer.
27) Always make sure the surface of the membrane with the protein ladder is on the top so that it comes in maximum contact with the buffers. Protein transfer can be evaluated using Ponceau S stain. Immerse the membrane in the stain for 5 minutes; keep it on the plate shaker (belly dancer). Remove the stain, wash once (quickly) with TBST and check for protein bands on membrane. Once the transfer is confirmed, wash the membrane with TBST at least 3 times to remove all of the Ponceau S.
28) Drain the TBST and add the Blocking solution. Place the lid on the plastic container and set to rock for 60 min.
29) Once blocking is done, wash quickly twice with TBST and discard in the sink.
30) In a conical tube add appropriate volume of buffer (milk or BSA) and primary antibody. Check the product sheet for antibody dilution specifications. Incubate the membrane in the primary antibody overnight at 4^{o}C on the shaker in the cold room in Dr. Bahr's Lab.
31) Always check the specifics for the blocking and primary as well as secondary antibody incubation time and temperature before starting the experiment. These may vary depending on the type of protein being evaluated and/or the experimental set-up.
32) Once the primary antibody incubation is completed, wash the membrane 3 times for 5 minutes each with TBST buffer.
33) During the last wash prepare your secondary antibody solution. Check the product sheet for specifics. Usually the secondary antibody is used at a 1:5000 - 1:10,000 dilution. Leave it on the shaker in the secondary antibody mixture for 1 hour or as specified in the product sheet/references.
34) Once the secondary antibody incubation is done, wash the membrane 6 times for 5 minutes each with TBST.
35) During the last wash prepare the chemiluminescence solution by mixing equal parts of both solutions in the kit. Be careful that separate pipettes are used for each solution to avoid cross contamination; as this will render the solutions useless for subsequent experiments. Mix well.
36) Prepare a platform laying a clean sheet of Parafilm on the bench top. Once the washes are done, remove the membrane using forceps, drain off excess liquid by touching a tip of the membrane to a paper towel or Kimwipe and place the membrane on the Parafilm platform. Add the chemiluminescence solution on to the membrane making sure the entire membrane is covered (about 1 ml of solution is enough for one membrane). Incubate the membrane in this solution for at least 6 minutes.
37) During this time, go to Dr. Miller's lab and log onto the computer attached to the Image Quant machine. Start the program and set the machine to cool down.
38) Once the 6 minute incubation is done, pick up the membrane with forceps; drain off excess liquid by touching an edge or tip of the membrane to a paper towel/Kimwipe. Place the membrane right side up in a sheet protector packet. Make sure to avoid air bubbles. Label each packet with Gel ID. Keep all such packets with membranes protected from light in the X-ray cassette.

39) Take these to Dr. Miller's lab and image using the Image Quant machine. Set the program to auto exposure as the machine can evaluate the best exposure time for us. Make sure each membrane is set to the same exposure parameters especially when comparison between membranes is required as an experimental endpoint.

Image Quant Instructions

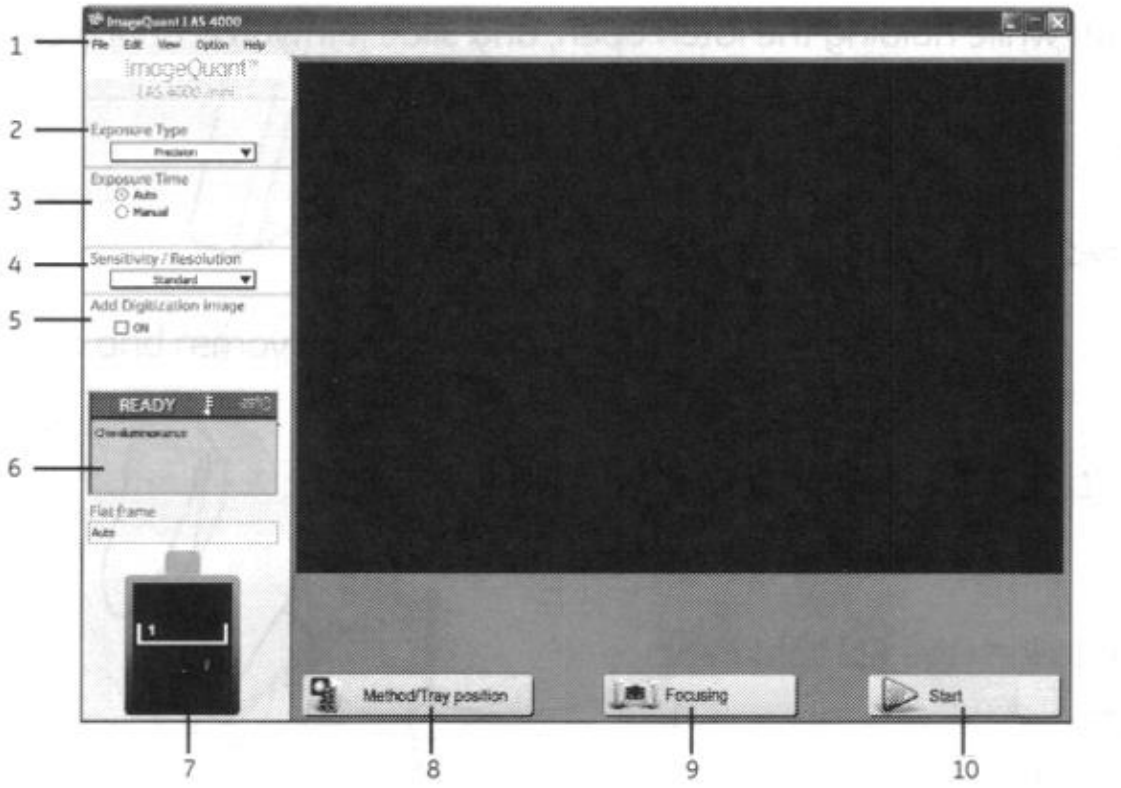

Start up ImageQuant LAS 4000 Control Software

1 – Menu Bar
2 – Exposure Type [Choose Precision, Increment*, Repetition* or Program*]
3 – Exposure Time [Auto or Manual in seconds, minutes, hours]
4 – Sensitivity/Resolution [Choose one, High Resolution and Std are normally used]
See manual for more options
5 – Digitization Image will be exposed simultaneously with chemiluminescence image if checked.
6 – CCD temperature setting displayed. Will display Ready or Not Ready.
7 – The (IDX) Intelligent dark box display
8 – Method/Tray position [Readable area vairies with tray position]
►Small gels use position 1 (closest to camera), biggest gels use position 4.
► Use Epi (Black tray for Chemiluminescence & Fluorescence Epi illumination)
► Use White Trans tray for exposing fluorescent samples with Ethidium Bromide (312nm)
9 – Focusing allows focusing, brightness and adjustment.
10 – Start button
* For Increment, Repetition or Program exposures see manual pgs 59- 69

Placing the Sample: (insert trays with holes facing outwards toward door)

1) For Chemiluminescence & Fluorescence (Epi illuminatiuon) samples place sample directly on Epi (Black) tray.

2) For Gels stained with Coomassie or silver stains use White trans tray. Place a gel sheet (slightly larger than sample) on the tray then place gel on top of sheet.

3) Choose exposure size and tray position
Position 1 = sample size 105mm x 70mm Position 2 = 122mm x 96mm
Position 3 = sample size 180mm x 120mm Position 4 = 210mm x 140mm

4) <u>Exposing Chemiluminescent samples</u>

a. With sample placed on Epi (black) tray
b. Click Method/Tray position button
c. Select CHEMILUMINESCENCE for Method
d. Select TRAY POSITION according to sample size
e. Click OK button
f. Click FOCUSING button [check sample position and focus as needed]
g. Select PRECISION for EXPOSURE TYPE
h. Select AUTO or MANUAL for EXPOSURE TIME
i. Select SENSITIVITY/RESOLUTION
[if unsure select Help:Sensitivity/Resolution to see relation between the two]
j. Click START button
k. Adjust gradations of exposed image, save.
l. Click COMPLETE button
m. Display will return to main screen.

5) <u>Exposing Fluorescence (Epi illumination)</u>

a. Place sample on Epi (black) tray
b. Select FLOURESCENCE [choose marker and light source from pull down menus. Appropriate filters are automatically selected]
c. Select TRAY POSITION
d. Click OK button
e. Click FOCUSING button
f. Click RETURN
g. Select PRECISION for EXPOSURE TYPE
h. Select AUTO or MANUAL EXPOSURE TIME
i. Select SENSITIVITY/RESOLUTION
j. Click START button
k. View image, adjust gradations as desired, then save.
l. Click COMPLETE button

6) <u>Exposing dye stained samples and films (White Epi light)</u>

a. Place sample on White Trans tray.
b. Select DIGITIZATION:TRANS-ILLUMINATION for Method
c. Select TRAY POSITION
d. Click OK button
e. Click FOCUSING button.
f. Confirm the sample position and the focus
g. Click RETURN button.
h. Select PRECISION for EXPOSURE TYPE
i. Select EXPOSURE TIME

j. Select SENSITIVITY
k. Click START button
l. View image, click COMPLETE

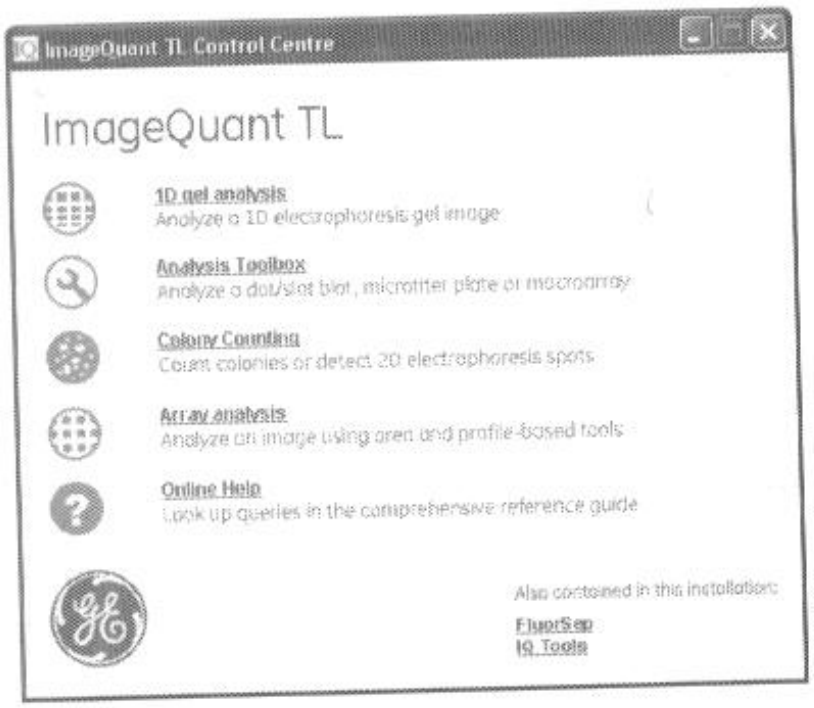

Instructions for using ImageQuant with ethidium bromide stained gel:

ATTENTION IMAGEQUANT USERS!!!
PLEASE REMOVE AT LEAST ONE GLOVE PRIOR TO TOUCHING THE PC AND IMAGEQUANT EQUIPMENT TO AVOID CONTAMINATION OF ETHIDIUM BROMIDE.

1. Remove at least one glove to do the following:
    a. Log on PC using your password, launch ImageQuant application, and turn on ImageQuant machine.
    b. Using one hand **without** glove, open the ImageQuant door and place the **clear tray with the white paper** inside the ImageQuant.
    c. Using the other hand **with** glove, place the gel onto the **clear tray with the white paper (NOTE:** To position the gel correctly under the camera, use one hand **without** glove to open the ImageQuant door and use the other hand **with** glove to **ONLY** move the gel or to move the **white paper** under the gel).
    d. Once the gel imaging is done, use one hand **without** glove to open ImageQuant door. Use the other hand **with** glove to remove the gel.
    e. Using one hand **without** glove, take the **clear tray with the white paper** to the sink and briefly rinse with running water.
    f. Wipe with a paper towel and return the **clear tray with the white paper** to its location.

Scanning slides in the Nanozoomer at IGB

1. Clean and dry slides for 24 hours before scan.
2. 210 slides can be scanned in one batch.
3. Log-in to the IGB system on the Nanozoomer computer.
4. Put in the slides in the slide holders starting from the first slot. Do not leave any slot empty.
5. Open door of the slide holder by pushing on the door (do not use the button).
6. Open NDP.scan2.5.85 (double click).
7. Go into settings → output path – my computer – data part D – users – choose your file – click "apply" then OK.
8. Threshold 5.1-94.9%
9. Choose batch mode when running multiple slides.
10. Profile – choose previous profile set up for you by Donna Epps.
11. Slide Reference – name the order of slides put in the holder.
12. Start batch.
13. Set up scan area → manual – semiautomatic - Choose scan area by click dragging the edge of the box created around your section….bring it as close to the edge of your section as possible so the machine doesn't spend time on unnecessary areas of the slide. For selection of specific points on scan area – right click on various parts of your tissue section which will produce yellow colored "+" signs and the machine will concentrate on these regions.

Sample Preparation for SEM

(At the Microscopy Suite in Beckman Institute.)

1. For each sample, use a 1-in-long piece of glass cut from a clean microscope slide.

2. On each piece of clean glass put a drop (ca. 20 microliters) of concentrated microvesicles in liquid, as prepared.

3. To each drop add the same volume of 2.0% E.M.-grade formaldehyde and 2.5% E.M.-grade glutaraldehyde in 0.1 M sodium cacodylate buffer, pH 7.4.

4. Use a diamond stylus to scratch a circle around each (now larger) drop, and put each piece of slide with its drop of microvesicles/fixative into the refrigerator for 60 to 75 minutes.

5. Put each piece of slide into a small plastic Petri dish and add 0.1 M sodium cacodylate buffer, pH 7.4. Put each small Petri dish on a slowly moving shaker table. The 0.1 M sodium cacodylate buffer is used to rinse the fixative away; change it after a few minutes, for completely new buffer. Never leave the slide exposed to air for long; always have the next change of solution ready when you take the old solution away.

6. After 10 minutes, change the buffer for 37% ethanol (10 minutes), then 67% ethanol (10 minutes), then 95% ethanol (10 minutes), and then three changes of 100% ethanol (10 minutes each).

7. After that, in 100% ethanol, critical-point-dry the samples using the Tousimis PVT-3D critical point dryer, one at a time to avoid cross-contamination. Then mount the samples on a stub and coat them with about 6 nm of gold-palladium. Paint Flash-Dry silver paint onto an edge of each piece of slide while the piece of slide is in the fume hood so the solvent in the paint will not affect the samples. Then do the SEM imaging.

Protocol for using the Ultra-centrifuge machine (Dr. Bahr's lab)

(requires large volume of medium)

1. Cool down takes about 20 minutes so start the machine in advance (won't start if not cool). Vacuum will be at <20 when cool enough.
2. Check and set up parameters for speed, time, temperature and vacuum before starting.
3. Acceleration and deceleration at maximum.
4. When at 4^{o}C press vacuum so you can open the machine.
5. Rotor should be stored at 4^{o}C (cold room Bahr Lab). It has a laser on the bottom so be very careful while fixing it in place in the machine or even while placing it on any surface.
6. Fix rotor in place, spin by hand to check that it is not wobbly. Put in samples and tighten lid well.
7. Press "speed-enter-time-enter-temp-enter" in fast succession and then press start very quickly.
8. Vacuum starts automatically.
9. Once done press vacuum to release pressure and open.
10. Take your samples out of rotor and keep on ice.
11. Mark on the tube the position of the micro-vesicle pellet (usually towards outer side) as it soon becomes clear and not visible to the eye.
12. Remove rotor from machine carefully and place in the cold room again. Don't fix the lid on too tight.
13. Write down the revolution counter details at the end of the run.
14. 40,000rpm at 4^{o}C for 1 hour takes about 1 hour 20 minutes to complete. Plan ahead.

Cell Culture Etiquette

Laminar Flow Biosafety Hood

1.) Air Flow: the air flow needs to be turned on for **at least 15 min** before working in the hood to establish sterile conditions.
2.) UV light: the UV light offers protection from the growth of material (bacterial/fungal/cells) that may be displaced during use of the hood. The UV light needs to be **turned on every night** at the closing of the lab and **turned off every morning** prior to working in near the biosafety hood.
3.) Aspiration: there is a vacuum trap located inside the hood that is connected to a collection trap by plastic tubing. This vacuum is used to aspirate media from cells and therefore needs to be treated with bleach to eliminate the growth of cells in the collection trap. It is important that the trap is never overfilled because the backflow of the fluid into the vacuum line will result in major repair bills. The collection trap should be treated by bleach after every use by EACH lab member. When the trap is $3/4^{th}$ full it should be emptied down the lab drain with running cold water for at least 15 min.
4.) Maintenance: The biosafety hood needs to be sprayed with 70% ethanol and wiped with a Kim wipe prior and after each use. All spills need to be cleaned up immediately. General cleaning should be done 2X/year with mild soap and warm water. NEVER use toxic/halogenic chemicals in the flow hood. This is not a fume hood so please do not treat it as such. All chemicals or toxic substances need to be used in the fume hood. This includes TRIZOL.

CO_2 Incubators

1.) Relative Humidity: Cell lines utilized in the Nowak lab require 99% relative humidity. To create this humidity the incubator is set at 85% relative humidity and we have a pan of DI water in the bottom of the incubator. This pan needs to be checked and filled at least once a week. Only DI water should be used in this incubator; add few drops of the antifungal solution to this DI water in the pan. The incubator also has a water jacket surrounding the cell chamber. The indicator on the incubator will alert us when this water lever is low and needs to be filled.
2.) CO_2 levels: The level of CO_2 in our cell culture is set for 5%. The CO_2 supply tanks are located next to the laminar flow hood (main lab) or next to the door (small cell culture room). The registers on the supply tanks will indicate the level of CO_2 being supplied to the incubator. The pressure of CO_2 supplied to the incubators should be at 15mmHg, anything higher will offset the monitor of the incubator. When the tanks get low it is the responsibility of each lab member to change the tanks and notify the correct personnel of the number of empty tanks so that they can order new tanks. The level of CO_2 within the incubator can be determined by using our FYRITE gauge. This will be checked every week and necessary calibrations will be performed by a specific lab member.
3.) Temperature: Unless otherwise stated the temperature of the incubators should always be set at 37^oC. An internal thermometer should be read with the door is shut to determine the actual internal temperature. The temperature should be calibrated once a week. Chicken cells in culture need a higher temperature of 39^oC.
4.) Cell containers: All cell culture dishes, flasks, plates, etc. should be contained in an autoclaved tray. Cell culture plastic ware should never be placed directly on shelves. This will help prevent spilling of cell culture media and also keep the incubators clean. Once your experiments are complete you can place the tray on the dirty dish cart and it will be cleaned and autoclaved for future use. Clean cell trays are located next to the incubators on top of the freezers and refrigerators.

5.) Maintenance: If we should encounter a contamination, the shelves and water pan need to be removed from the incubator and cleaned/autoclaved. Then the walls of the incubator should be cleaned with warm water and mild soap followed by a 70% ethanol wipe.
6.) General Notes: DO NOT leave the inner door open while using the incubator. DO NOT go into the incubator without first cleaning your gloves with 70% ethanol. If the incubator is alarming DO NOT ignore the alarm or silence the alarm without first taking action to fix the reason for the alarm indication.

Inverted Microscope

1.) Imaging cells: Cell dishes/flasks may be placed on the stage for imaging. Please be sure to clean up the stage after imaging cells, especially if media has been spilled.
2.) Confluency: One of the main reasons for imaging cells is to determine cell growth/confluency. Cell confluency is expressed as a percentage and it is a very subjective measurement of cell growth. Develop your own style and stick with it.
3.) Cell Counts: To determine the number of cells that are in a dish/flask for seeding we perform cell counts using a very special/costly slide called a hemacytometer slide. This slide has a grid etched into the glass slide which you can use to count your cells.

Water Bath

There is a water bath located on the bench by the laminar hood in the main lab. The temperature on this water bath is set to 37^{o}C and should remain at this temperature. It is important that the water bath always have a constant level of water, therefore if you see the water level low then please use DI water ONLY to refill the water bath. The water bath is used to warm media/reagents and also to thaw cells therefore it is critical that the water bath stay clean and free of fungus and bacteria. To clean the water bath please empty all the water and use mild soap and warm water. Following cleaning please spray with 70% ethanol prior to refilling the water bath with DI water. Add antifungal solution to the DI water in the water bath.

1.) Warming up media/reagents: Please make sure that all media/reagent bottles are secured in the water bath. They tend to float so use the weights provided near the water bath to anchor the media bottles. You do not want to use a bottle that has tipped over in the water bath, it is considered contaminated.
2.) Thawing cells: When cells are thawed they need to have a quick thaw. This allows the cells to remain viable by quickly removing the cryoprotectant from inside the cell. Place your cells in a tube flotation device with their caps above water level. Only allow cells to sit in the water bath until halfway thawed, NO LONGER.
3.) When items are removed from the water bath they need to be dried and wiped with 70% ethanol. Please make sure that everything is wiped prior to placing in the hood.

RULES FOR STERILITY

1.) Never open anything that needs to be used for cell culture unless it is in the laminar flow hood. This includes the lids of your dishes/plates/flasks/media.
2.) All media should be made in the hood. All aliquots of cell culture supplies should be prepared in the hood.
3.) For small pipetting only use barrier tips. These tip boxes are located in the hood. These boxes are individually wrapped and should not be used except for RNA/DNA or cell culture work.
4.) For aspirating media use the glass pipettes. The container for these pipettes should be opened in the hood and closed after use by each person. Never leave this open if the blower is not on!!!
5.) For large pipetting use the serological pipettes. These should only be opened in the hood.
6.) When placing items in the hood that are not usually left in the hood… always first wipe the bottom surface with 70% ethanol. This is easily done by spraying Kimwipe with ethanol and then wiping the surface of the container/pipet/pipetaid/rack/etc.

7.) Gloves and a lab coat should be worn at all times when working in the hood/incubator/handling cell dishes. We work in a BSL2 lab and handle human cells. You shouldn't have exposed skin beyond the air barrier in the cell culture hood. This is for your protection as well as to eliminate any disruption of the sterile field. Also as a side note, hair should be worn up or kept out of the face. You don't want to have to brush your hair out of your eyes with your gloved hand or have it bothering you while working at the hood. Do not touch anything (hair, face, mobile phone, ear phone etc.) with your gloved hand.
8.) Do not do any work over the air barrier. As a rule try to keep your elbows on the air barrier so that forces you to do all your work beyond the air barrier. Anything that crosses the air barrier is no longer considered sterile.
9.) Clean up spills immediately so that they don't cause contamination.
10.) Do not let media bottles sit for too long in the water bath. Also do not let media bottles turn over in the water bath.

How to deal with a contamination:

1.) First notify everyone that there is a contamination either in the incubator/water bath/ hood.
2.) Remove all of the contaminated plates and dispose of properly in the biological waste container. This includes aspirating out the contaminated media in the vacuum trap and bleaching the trap.
3.) Remove all trays/shelves/water pans from the incubator and clean with soap and water. Then sterilize equipment by autoclaving in wrapped bags.
4.) Wipe down walls of the incubator with soapy water using a soft sponge or cloth.
5.) Finally spray incubator walls with 70% ethanol to remove any leftover contamination.
6.) Change the HEPA filter according to incubator guidelines.
7.) Allow 48 hours to cycle air and then notify lab personnel that incubator can be used again.

Defined media and supplements

pH

Most cells grow well at pH 7.4 Phenol red is the indicator that is used in most of our cell media. At pH 7.4, phenol red is red, at 7.0 orange, at 6.5 lemon yellow, at 7.6 pink and at 7.8 purple.

CO_2 and bicarbonate

Carbon dioxide interacts with HCO_3 and lowers the pH of the media. For this reason bicarbonates ($NaHCO_3$ or HEPES) are added to the media to stabilize the pH. Without CO_2 cells will not grow. If you have Na pyruvate in your media your cells are less dependent on CO_2 and therefore should be added if cells are to be transported.

Oxygen

Cultured cells often rely on glycolysis for energy production. In many cells this is anaerobic glycolysis instead of respiration. In most incubators the level of oxygen is atmospheric 21%. However, cells can be cultured in normoxic 6% or hypoxic conditions 0.5-2% and still survive. The level of oxygen used for cell culture is highly dependent on oxygen diffusion. For this reason the depth of the media used for cell culture needs to be within the range of 2-5mm for each culture dish/plate/flask.

Osmolarity

Cells should be cultured in media within the osmolarity range of 260-320 mosmol/kg. Once an osmolarity is reached it should not deviate more than 10 mosmol/kg. In this lab we typically use balanced salt solutions that are pre-made to maintain osmolarity.

Amino Acids

Glutamine is an amino acid that is required by most cells for growth and function. In this lab we buy media containing L-glutamine or we add it exogenously. Please note what concentration of glutamine is needed for your particular cell type.

Antibiotics

Antibiotics penicillin and streptomycin are added to all culture media to prevent contamination. We typically use 6mls of Pen/Strep at 10,000IU/ml Pen and 10,000ug/ml Strep for 500 ml bottle of media. Some cell culture experiments (i.e. Transfection of cells) will not use antibiotics in the serum. Please take extra precautions when working with this type of media.

Serum

Serum contains growth factors that are vital to cell growth. In this lab we use Fetal Bovine Serum (FBS), Newborn Calf Serum (NCS), Bovine Calf Serum (BCS), Chicken serum for our serum types. Be sure to know which type and what concentration of serum your cell line needs to grow efficiently.

Depending on the cell line you are working with it may be necessary to add additional components to the media such as, vitamins, mineral, hormones, growth factors, etc. It is important to realize that your cell line can be as individual as you or I so they each have a little variation in how they like to grow. Understanding the needs of your cell type prior to experimental assay will save you a lot of time and effort in the long run.

Please be sure that when you are done working in the hood all of these items are checked!

1.) Laminar hood restocked for
    a. Pipette tips, serological pipettes, dishes, flasks, glass pipettes.
2.) Vacuum flask bleached and if necessary emptied.
3.) Hood sprayed with 70% ethanol
4.) Media put away in appropriate fridge
5.) Pipettes replaced to holder and pipette man plugged in
6.) Glass pipette lid replaced
7.) If the last one to leave then please turn on the UV light and turn off the blower
8.) Check to make sure incubators are not alarming

Thawing Cells

Wear Gloves at all times
Be as gentle and careful as possible throughout the procedure

1.) Place 10% serum containing medium in the water bath.
2.) Remove cryovial containing frozen cells from the liquid Nitrogen tank
3.) Place cryovial in the water bath and observe for thawing. Remove them as soon as they are halfway thawed. (Never leave them in for too long; the DMSO will kill the cells)
4.) Add 5 mL of medium to sterile 15 mL conical tube.
5.) Use P1000 pipette to transfer the thawed cells from the cryovial into the conical tubes. Use the resuspension method to insure that all of the cells are removed.
6.) Spin the cell suspension for 5 minutes at 50-100RCF.
7.) Aspirate out the supernatant and add an appropriate volume of fresh medium to resuspend the cell pellet (depending on number of dishes).
8.) Prepare appropriate number of culture dishes and label them (Cell ID, Passage number, Initials, Date)
9.) To each culture dish, add 1 ml of cell suspension and an appropriate volume of fresh serum containing medium.

Freezing Cells

1.) Trypsinize cells as done for passaging and collect cell suspension in conical tube.
2.) Centrifuge the cell suspension at 50-100RCF for 5 mins. BE SURE to balance the centrifuge.
3.) During this time place freezing media (located in the freezer of the cell culture freezer on the door rack far left) in the 37deg water bath.
4.) After spinning the 15 ml conical – take the conical and look for a cell pellet. Remove the supernatant without disturbing the pellet.
5.) Resuspend pellet in 1.5 ml of freezing media. Mix carefully.
6.) Label a 2 ml cryovial with cell information (cell ID, passage #, date and your initials).
7.) Place cells that are resuspended in the freezing media into the 2ml cryovial and place on ice for 30 mins.
8.) After the 30 minutes place cells/cryovials in the -80 freezer.
9.) Transfer the cryovials from the -80C freezer to the liquid Nitrogen tank after 24 hours. Make a note of the placement in the liquid nitrogen tank Log book.

Protocol for Passaging Cells in Culture

1.) Aspirate out the old media
2.) Add appropriate volume (3-5 ml) of Trypsin EDTA or sterile PBS depending on culture dish and wash over cells
3.) Aspirate out
4.) Add an appropriate volume (3-5 ml) of Trypsin EDTA to the cells
5.) Incubate for 5-6 minutes in the incubator
6.) Check the culture dish under the microscope for detachment of cells. Incubate for longer if needed.
7.) Add 7-10 ml of serum containing culture medium to the culture dish to neutralize the effect of the Trypsin EDTA
8.) Collect this cell suspension in conical tubes and centrifuge at 50-100RCF for 5 minutes (speed depends on cell type)
9.) Aspirate the supernatant and resuspend the cell pellet in an appropriate volume of fresh culture medium depending on number of dishes to be used for expansion of cells (1 ml per dish)
10.) Add 1 ml of cell suspension to each culture dish and an additional appropriate volume of fresh medium depending on type of culture dish being used
11.) Move the culture dish to spread out the cell suspension and place these new dishes into the incubator
12.) Check periodically for cell growth

Reminder

-Use the standard 10% serum containing medium or as needed for specific study
- Place the Trypsin EDTA and medium into the water bath for about 10-15 min prior to passaging
-Make sure all culture dishes are properly labeled with cell ID, passage number, initials, and date of passage
-Try to be as sterile as possible, if in doubt, filter the final product

Counting Cells

1.) Trypsinize cells as done for passaging and collect cell suspension in conical tube.
2.) Centrifuge the cell suspension at 50-100RCF for 5 mins. BE SURE to balance the centrifuge.
3.) Aspirate the supernatant while leaving pellet.
4.) Depending on the size of the cell pellet, add fresh medium and resuspend pellet thoroughly but carefully.
5.) Clean the hemacytometer and coverslip with DI water and then 70% EtOH before and after each use. Dry the counting chamber completely before use.
6.) Place the coverslip on the counting chamber. Add 10ul of the above prepared cell suspension to each side of the hemacytometer under the cover slip.
7.) Place the slide on the microscope stage and focus on to the counting grid using the 10x lens on the inverted microsocope. Both grids on the slide can thus be counted.
8.) Count the number of cells in the 4 corner squares thus counting a total of 16 smaller squares. Make sure the cell suspension is dilute enough to provide a uniform single cell suspension and the cells do not appear too crowded within the grid.
9.) When counting, count only those cells on the lines of two sides of the square to avoid counting cells twice. Decide on which two sides will be included and stick to it throughout the counting process.
10.)The area of each big square is 1mm x 1mm = $1mm^2$ and the depth of each square below the coverslip is 0.1mm. Since $1cm^3$ is equivalent to 1ml, the final volume of each square is $0.1mm^3$ = 0.0001ml.
11.)Divide the total number of cells counted in four large squares by 4 to obtain average count
12.)Cells per ml = average count per big square x 10^4
13.)Total cell count = cells per ml x original volume of media used to resuspend cell pellet

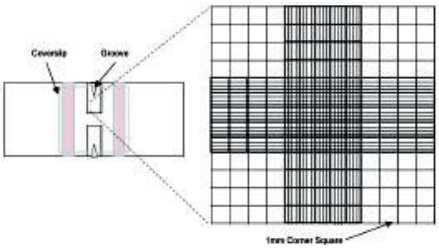

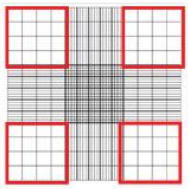

Figure 1: Hemacytometer grid

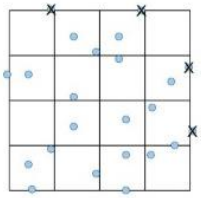

Figure 2: Cell counting guidelines

10X TBE Buffer Recipe (pH 8.3)

108g Tris Base
55g Boric Acid
9.3g EDTA
Add to 800ml MilliQ water. Make up to 1L after everything dissolves.
Add 9L MilliQ water to make 1X solution that we need.

10X PBS (pH 7.4)

80g Sodium Chloride
2g Potassium Chloride
21.6g Sodium Phosphate dibasic heptahydrate ($Na_2HPO_4.7H_2o$)
2.4g Potassium dihydrogen Phosphate (KH_2PO_4)
Dissolve in 1L MilliQ water.